

Dissertation

submitted to the

Combined Faculties for the Natural Sciences and for Mathematics

of the Ruperto-Carola University of Heidelberg, Germany

for the degree of

Doctor of Natural Sciences

presented by

Yi Ni

born in: Fujian, P.R. China

Oral-examination:

Characterization of the infectivity determinants of the envelope proteins of Hepatitis B Virus

Referees: Prof. Dr. Stephan Urban
Prof. Dr. Ursula Klingmüller

Index

Summary.....	1
Zusammenfassung.....	3
1. Introduction.....	5
1.1 Hepatitis B virus biology.....	5
1.1.1 Classification of viruses within the Hepadnavirus family.....	5
1.1.2 Serotypes and genotypes.....	5
1.1.3 Virus structure.....	7
1.1.4 Genome structure and organization.....	7
1.1.5 Primary attachment and receptor mediated binding	9
1.1.6 Fusion with cellular membrane.....	12
1.1.7 Nucleocapsid transportation.....	12
1.1.8 cccDNA formation.....	13
1.1.9 Transcription.....	13
1.1.10 Translation of viral proteins and co/post-translational modification.....	14
1.1.11 Genome replication.....	15
1.1.12 Assembly and virus release.....	15
1.2 The HBV entry inhibitor: Myrcludex B.....	17
1.3 Host and organ tropism of hepadnaviruses.....	19
1.4 Cellular factors needed for infection.....	19
1.5 The HBV envelope and known viral infectivity determinants.....	20
1.6 Animal and cellular models for HBV infection.....	24
1.7 Aim of this work	27
2. Results.....	29
2.1 Optimization of virus production and infection assay.....	29

2.1.1 Optimization the viral production by transfection of complementary expression plasmids.....	29
2.1.2 Kinetics of virus production following co-transfection.....	30
2.1.3 Anti-core IF staining of infected HepaRG cells.....	31
2.1.4 Quantification of the infection by secreted viral marker and the number of infected cells.....	33
2.1.5 Optimization of the infection-the effect of DMSO.....	34
2.1.6 Optimization of the infection-the effect of “spin inoculation”.....	37
2.1.7 Optimization of the infection-the effect of PEG.....	38
2.1.8 Optimization of the infection-the effect of EGTA.....	40
2.1.9 The effect of passage number on HBV infection	41
2.2 The N-terminus of preS1 domain serves a critical function for virus infectivity.....	46
2.2.1 Infectivity of genotypically L-protein pseudotyped HBV particles.....	48
2.2.2 Infectivity of HBV carrying chimeric L proteins from genotypes D and B.....	50
2.2.3 Infectivity of HBV carrying chimeric L protein with His-6 tag.....	52
2.2.4 Infectivity of HBV with different myristoylation motifs	54
2.2.5 Infectivity of HBV carrying chimeric L protein of different genotype.....	56
2.2.6 Characterization of inhibitory peptides bearing mutations in the N-terminus	58
2.2.7 The role of myristoylation in HBV entry.....	64
2.2.8 A possible role of preS aa 49-78 in virus entry.....	67
2.3 Using M protein-free virus to dissect the role of preS2 for assembly and infectivity of Hepatitis B virus	70
2.3.1 M-free system with independent expression of S and L-protein without loss of infectivity.....	70
2.3.2 No specific sequence in preS2/114-163 is needed for virus infectivity but a length dependent linker within this region is important for viral assembly	73

2.3.3 M-protein-deficient HBV with a randomized preS2-sequence in its L-protein properly assembles and is infectious in HepaRG cells and PHH.....	75
2.4 Analysis of the role of the S domain in the L protein and the S protein for assembly and infectivity of HBV.....	79
2.4.1 The effect of cysteine mutations in the S and the L protein on protein expression and virus secretion.....	80
2.4.2 The effect of cysteine mutations in the S and the L protein on virus assembly.....	81
2.4.3 The effect of cysteine mutations in the S and the L protein on HBV infectivity.....	83
2.4.4 The effect of cysteine mutations on the topology of the L-protein.....	85
2.4.5 The heparin-binding activity of the HBV particles with cysteine mutations.....	88
3. Discussion.....	92
3.1 Analysis of different parameters on their effect on HBV infection in HepaRG cells	92
3.2 The role of N-terminus of L-protein in HBV assembly.....	95
3.3 The role of preS2 domain in HBV assembly and infectivity.....	100
3.4 The role of S-domain in HBV entry.....	102
3.5 Model for HBV attachment and receptor binding	104
4. Materials and Methods.....	107
4.1 Materials	107
4.1.1 Instruments, consumables, software, and reagents.....	107
4.1.2 Oligonucleotides.....	111
4.1.3 Plasmids.....	117
4.1.4 Peptides.....	123
4.1.5 Cells.....	124
4.2 Methods.....	125
4.2.1 General Cloning strategy.....	125
4.2.2 Agarose electrophoresis.....	125
4.2.3 Gel exaction of DNA fragments.....	125

4.2.4 Polymerase Chain Reaction (PCR)	126
4.2.5 Competent cells preparation and transformations.....	126
4.2.6 DNA sequencing.....	127
4.2.7 Plasmid preparations.....	127
4.2.8 SDS-PAGE.....	127
4.2.9 Western blot.....	128
4.2.10 Immunoprecipitation.....	128
4.2.11 Cultivation of HuH-7 cells.....	129
4.2.12 Cultivation and infection of primary human hepatocytes and HepaRG cells	129
4.2.13 Transfection of HuH-7 using polyethylenimine.....	131
4.2.14 Production of HBV particles.....	131
4.2.15 Purification and concentration of virus by PEG-precipitation.....	131
4.2.16 CsCl-gradient centrifugation and DNA dot-blot analysis.....	132
4.2.17 Immunofluorescence analyses of HBcAg expression in infected cells.....	132
4.2.18 HBsAg and HBeAg measurement in the supernatants of infected cells.....	132
4.2.19 Heparin binding assay	132
4.2.20 lentivirus production and transduction of HepaRG cells.....	133
References list.....	134
Abbreviations	153
Supplemental.....	156
Assurance of research.....	161
Curriculum Vitae	162
Publications.....	163
Acknowledgement.....	164

Summary

The human Hepatitis B virus (HBV) is a small hepatotropic DNA virus, which consists of a nucleocapsid and an envelope with three membrane-embedded surface proteins (large (L), middle (M), and small (S)). While the S protein is required for budding and is the major component of the envelope, the L protein is crucial for infectivity. Several infectivity determinants have previously been described: (i) The N-terminal myristic acid moiety together with aa 2-48 are indispensable for virus infectivity and specifically bind a yet unknown receptor. Consistent with this, a peptide HBVpreS/2-48^{myr}, composed of a myristoyl group and the N-terminal 47 residues of the L protein, inhibits HBV entry at picomolar concentrations. (ii) Amino acids 49-78 and the first transmembrane domain of the L protein are also required for virus infectivity. However, their function is not clear. (iii) Recently, it has been shown that the S-domain, which is common to all three surface proteins, also contains an infectivity determinant in its antigenic loop. Currently, it is not fully understood how the virion orchestrates these infectivity determinants during entry process and how exactly the preS-derived peptide HBVpreS/2-48^{myr} interferes with virus entry. The major obstacle, restricting such investigations for a long time, was the lack of easily accessible *in vitro* infection systems. A recently established human hepatoma cell line (HepaRG), susceptible for HBV infection upon differentiation *in vitro*, resolved this issue and allowed us to analyze the role of the HBV envelope proteins in virus entry.

In the present work, several approaches were undertaken: (i) systematic optimization of HepaRG cells for HBV infection, (ii) establishment of a reverse genetics approach that allows production of virions with mutated envelope proteins, (iii) an extensive mutation analysis within the L and S protein to determine viral assembly and infectivity, (iv) infection-competition study using preS-derived peptides, and (v) design of membrane-anchored inhibitory peptides by replacing the myristoyl group with a type II transmembrane protein.

With an optimized infection assay, over 30% of differentiated HepaRG cells could be infected. The optimized infection assay facilitated further infectivity analyses of HBV virions generated by complementation, in which the L and S proteins were separately expressed. The following was observed in the present work: (i) Besides acting as a simple myristoylation signal, the N-terminus of the L-protein (aa 2-8) bears a more complex function for virus entry, since the substitution with heterologous myristoylation motifs abolished virus infectivity. This conclusion is strengthened by a complementary approach showing that the inhibitory potential of the peptide was also severely reduced when amino acids 2-8 were deleted or substituted. (ii) Expression of a

membrane-anchored peptide prevents HepaRG cells from HBV infection, probably due to an interference with virus receptor on the plasma membrane. (iii) Amino acids 49-78 of L protein do not tolerate insertions and point mutations at their conserved region, and the peptide comprising aa 49-78 did neither interfere with HBV infection nor inhibit the antiviral activity of HBVpreS/2-48^{myr}. (iv) While the M protein is dispensable for both HBV assembly and infectivity, the preS2 domain as an internal domain of the L protein is needed for virion release in a length-dependent but sequence-independent manner. Notably, HBV with an L protein carrying a mostly scrambled preS2 domain fully supported virion formation and virus infectivity. (v) Cysteine mutations in cytosolic loop-I of L protein drastically reduced virus infectivity, indicating that a properly formed cytosolic loop-I is also required for HBV entry. (vi) The essentiality of the antigenic loops during virus entry is mainly contributed by those in the context of S protein, and is correlated with the binding activity of the virion to heparin.

In summary, this data indicates that the myristoyl chain of the L protein provides an anchor into the hepatocyte membrane thereby allowing the subsequent interaction with a hepatocyte-specific receptor. The N-terminal amino acids 2-8 of the HBV L protein serve as an adapter between the myristoyl moiety and the receptor-binding domain that orients the essential receptor binding site into the right position. The preS2 domain is dispensable for the HBV infectivity *in vitro*.

However, it acts as a linker within the L-protein during virus assembly. The S protein may participate in primary attachment of virion to hepatocytes via the antigenic loop, which is critical for virus infectivity. Last but not the least, the membrane-anchored inhibitory peptide presents a promising approach to identify the virus receptor and may be used in a gene therapy approach against HBV infection.

Zusammenfassung

Das humane Hepatitis B Virus (HBV) ist ein kleines hepatotropisches DNA Virus. Es besteht aus einem Nukleokapsid und einer Hülle mit drei membran-ständigen Oberflächenproteinen (groß (L), mittel (M), und klein (S)). Während das S-Protein Hauptbestandteil der Hülle und für das Budding des Virus notwendig ist, ist das L Protein für die Infektiösität entscheidend.

Verschiedene Infektiösitätsdeterminanten wurden beschrieben: (i) Der N-terminale Myristinsäurerest zusammen mit den Aminosäuren 2-48 sind unverzichtbar für die Virusinfektiösität und binden spezifisch an einen bis jetzt unbekannten Rezeptor auf Hepatozyten. In Übereinstimmung mit diesen Erkenntnissen inhibiert ein HBVpreS/2-48^{myr} Peptid, bestehend aus einer Myristolgruppe und den 47 N-terminalen Aminosäuren des L-Proteins, die Eintritt von HBV bereits in picomolaren Konzentrationen. (ii) Die Aminosäuren 49-78 und die erste Transmembrandomäne des L-Proteins sind für die Infektiösität des Virus ebenfalls essentiell. Der genaue Mechanismus ist jedoch noch nicht geklärt. (iii) Kürzlich wurde gezeigt, dass auch das S-Protein, das in allen drei Oberflächenproteinen vorkommt, eine Infektiösitätsdeterminante im „antigenic loop“ trägt. Bis heute ist noch nicht vollständig verstanden, wie das Virion die verschiedenen Infektiösitätsdeterminanten während des Eintrittsprozesses koordiniert und in welcher Weise das HBVpreS/2-48^{myr} Peptid den Eintritt des Virus behindert. Das Haupthindernis, das solche Untersuchungen für lange Zeit eingeschränkt hat, war das Fehlen eines einfach zugänglichen *in vitro* Infektionssystems. Eine kürzlich etablierte humane Hepatomazelllinie (HepaRG), die nach Differenzierung *in vitro* suszeptibel für HBV Infektionen wird, hat dieses Problem gelöst und erlaubt es die Rolle der HBV Hüllproteine während des Viruseintritts zu analysieren.

In der vorliegenden Arbeit wurden verschiedene Ansätze unternommen: (i) Die systematische Optimierung von HepaRG Zellen für HBV Infektion, (ii) Die Etablierung eines Versuchsmodells, das mit Hilfe von reverser Genetik die Produktion von mutierten Hüllproteinen erlaubt, (iii) eine detaillierte Mutationsanalyse der L- und S-Proteine um den viralen Aufbau und die Infektiösität zu bestimmen, (iv) Studien zur Infektionskompetition mit von preS abgeleiteten Peptiden und (v) die Entwicklung von membran-verankerten inhibitorischen Peptiden bei denen die N-terminale Myristoylgruppe durch ein Typ-II-Transmembranprotein ersetzt wurde.

Durch die Optimierung des Infektionsassays konnten über 30% der differenzierten HepaRG Zellen infiziert werden. Der optimierte Infektionsassay ermöglichte Infektionsanalysen von HBV Virionen die durch Komplementation generiert wurden. Hierfür wurden das L- und das S-Protein getrennt exprimiert. In der vorliegenden Arbeit wurden folgende Beobachtungen gemacht: (i) Neben der Aufgabe als einfaches Myristoylationssignal zu fungieren, hat der N-Terminus des L-Proteins (Aminosäuren 2-8) auch eine Funktion für den Viruseintritt, da die

Substitution mit heterologen Myristoylationsmotiven zu Viren führt, die nicht mehr infektiös sind. Durch einen ergänzenden Ansatz, der zeigt, dass das inhibitorische Potential des HBV preS2-48^{myr} Peptids durch Deletion oder Substitution der Aminosäuren 2-8 stark vermindert wird, konnte diese Beobachtung weiter untermauert werden. (ii) Die Expression eines membranständigen Peptides verhindert die Infektion von HepaRG Zellen mit HBV. Dies geschieht wahrscheinlich durch die Interferenz mit dem Virusrezeptor auf der Plasmamembran. (iii) In der Aminosäuresequenz 49-78 des L-Proteins befindet sich eine konservierte region. Innerhalb dieser Region werden keine Insertionen und Punktmutationen toleriert. Peptide die die Aminosäuren 49-78 enthalten können eine HBV Infektion nicht inhibieren. Diese Peptide beeinflussen die inhibitorische Aktivität von HBVpreS2-48^{myr} Peptiden nicht. (iv) Während das M-Protein für den Viruszusammenbau und für dessen Infektiösität unwesentlich ist, ist die preS2-Domäne, als interne Domäne des L-Proteins, Längen-abhängig aber Sequenz-unabhängig unverzichtbar für die Freisetzung von Virionen. Bemerkenswert ist, dass ein HBV Virus, mit einem L-Protein dass eine beinahe vollständig randomisierte preS2 Domäne aufweist trotzdem keine Defekte bei der Formierung von Virionen oder eine Verminderung der Infektiösität aufweist. (v) Dagegen führen Cysteinmutationen im cytosolischen Loop-I des L-Proteins zu einer drastisch reduzierten Virusinfektiösität. Diese Beobachtung impliziert, dass ein genau geformter cytosolischer Loop-I für die HBV-Eintritt erforderlich ist. (vi) Die Bedeutung der „antigenic loops“ während dem Viruseintritt ist hauptsächlich auf die Loops im S-Protein zurückzuführen und korreliert mit der Bindungsaktivität der Virionen an Heparin.

Zusammenfassend implizieren die vorliegenden Daten, dass die Myristoylkette des L-Proteins einen Anker in die Hepatozytenmembran darstellt und somit die folgende Interaktion mit dem Hepatozyten-spezifischen Rezeptor erlaubt. Die preS2-Domäne nicht essentiell für die Infektiösität von HBV *in vitro*, fungiert aber als ein Linker im L-Protein beim Zusammenbau des Virions. Möglicherweise ist das S-Protein mit seinen für die Infektiösität essentiellen „antigenic loops“ an der Initialen Anlagerung eines Virions an die Hepatozyte beteiligt. Das in dieser Arbeit entwickelte membranständige Peptid, bei dem die N-terminale Myristoylgruppe durch eine Typ-II-Transmembranprotein ersetzt wurde eröffnet neue Möglichkeiten bei der Identifikation des HBV Rezeptormoleküls und eignet sich möglicherweise für die Verwendung in einem gentherapeutischen Ansatz zur Behandlung von chronischen HBV Infektionen.

1. Introduction

1.1. Hepatitis B virus biology

1.1.1 Classification of viruses within the Hepadnavirus family

Hepatitis B virus (HBV) was discovered in the 1960s as a serum agent¹⁻³. It is a DNA virus that requires reverse transcription in its life cycle^{4,5}. HBV belongs to the family of *Hepadnaviridae*, which preferentially infect hepatocytes. Hepadnaviruses are subdivided into two genera, the Orthohepadnaviruses and the Avihepadnaviruses, according to their different host ranges, mammals and birds.

HBV is the prototype virus of the orthohepadnaviruses and is genetically related to other species in this genus, such as woodchuck hepatitis virus (WHV), Ground squirrel hepatitis virus (GSHBV) and woolly monkey hepatitis B virus (WMHBV). Duck hepatitis B virus (DHBV), which is more distantly related, is the prototype virus of avihepadnavirus. Other members of this genus are heron hepatitis virus (HHBV)⁶, Snow goose hepatitis B virus (SGHBV)^{7,8}, Crane hepatitis B virus (CHBV)⁹, and Stork hepatitis B virus (STHBV)¹⁰.

1.1.2 Serotypes and genotypes

HBV was first identified in serum of an individual as “Australian antigen” and has been divided into different serotypes according to their antigenicity for a long time. The different serotypes are defined by antibody recognition sites on the small surface protein. All known hepatitis B virus strains have a common epitope called determinant “a”. Four different serotypes can be distinguished by two pairs of mutually exclusive epitopes, named “d” or “y” and “w” or “r”. Determinant “d” has a lysine at position 122 on the small surface protein, while “y” has an arginine at the same position; “w” has a lysine at position 160 while “r” has an arginine at that position¹¹.

The availability of molecular techniques, such as polymerase chain reaction and DNA sequencing, made it easy to obtain genetic information. This led to the division of HBV into different genotypes according to pair-wise differences greater than 8% and smaller than 17%¹²⁻¹⁴. So far, ten genotypes, A to H, and the newly proposed genotypes I¹⁵ and J¹⁶, have been identified. They can be further divided into subgenotypes and are correlated to the serotypes (Tab. 1). Different genotypes and subgenotypes show distinct geographic distributions (Fig. 1) and possibly distinct clinical behaviors. Previous reports indicate that hepatocellular carcinoma (HCC) is more frequent in the patients infected with genotype C than those infected with genotype B^{14,17}. Treatment with interferon is more effective in patients infected with genotype B

than in those with genotype C (in Asia). The same was observed in patients infected with genotype A, which is more effectively treatable with interferon-alpha than genotype D (in Europe)^{18,19}.

HBV has also been found in chimpanzees^{20,21}, gorillas²², orangutans²³, and gibbons²². The isolates are closely related to human HBV and are considered to be subtypes of HBV.

TAB. 1. Overview of the genotypes and the associated serotypes (modified from Stephen Locarnini²⁴)

Genotype	Serotype	Genome length/nt	preS1/aa	pol/aa	core/aa
A	adw2, ayw1	3221	119	845	185
B	adw2, ayw1	3215	119	843	183
C	adw2, adr, ayr	3215	119	843	183
D	ayw2, ayw3	3182	108	832	183
E	ayw4	3212	118	842	183
F	adw, ayw	3215	119	845	183
G	adw2	3248	108	842	195
H	adw	3215	119	843	183

nt, nucleotides; aa, amino acids; pol, polymerase.



FIG. 1. Geographic distribution of HBV genotypes (from the review by Stefan Schaefer²⁵)

The map shows the geographic distribution of the eight different HBV genotypes (A to H) and subgenotypes (numbers).

1.1.3 Virus structure

HBV is an enveloped DNA virus. The infectious virion (Dane particle) has a diameter of 42 nm²⁶. In addition to Dane particles, sera of HBV-infected patients contain 1000-fold excessive amounts of subviral particles (SVP) that are either 22 nm spheres or 22 nm-diameter filaments with variable lengths. The SVPs do not contain nucleocapsids and are therefore non-infectious.

The nucleocapsid of HBV has an icosahedral structure, with a diameter of ~28 nm. It was assembled by 120 core protein dimers. The nucleocapsid contains one copy of partially double-strand viral DNA genome and probably one polymerase. There is also evidence for the presence of cellular proteins, including one or more serine kinases within the virus^{22,27}.

The nucleocapsid of HBV is surrounded by a virus envelope, which contains three different viral envelope proteins (L, M, and S). These proteins are estimated to be present in the virion with a molecular ratio of 1:1:4 (L:M:S). For subviral particles, this ratio is believed to be different. Spheres contain the M and S proteins in a ratio of about 1:2, but only traces of the L protein²⁸. However, filaments contain approximately equal amounts of the M and L protein.

The membrane topology of the M and S proteins is shown in Fig. 2, whereas the topology of the L protein is still not fully understood. The N-terminal myristoylation of the L protein is required for virus infectivity²⁹. Since myristoylation takes place in the cytosol, the N-terminus of L protein is initially located inside the virion (i-preS). This is consistent with the fact that preS is responsible for binding the viral capsid during the viral assembly. On the other hand, the preS is also responsible for the interaction with the cellular receptors during virus entry. The fact that the virus can be immunoprecipitated and neutralized with antibodies against preS supports the notion that preS is in the outside of virus (e-preS). This paradox is explained by the commonly accepted translocation model for the L proteins: 50% of the L proteins, initially i-preS, translocate to e-preS, the other 50% of preS remain inside and interact with the capsid³⁰. The detailed topology of the two different forms of L proteins is still not fully understood. For example, it is not clear where is the location of trans-membrane domain I (TM-I) in L protein with i-preS conformation.

1.1.4 Genome structure and organization

Coding regions in the genome of hepatitis B virus are organized in a highly efficient manner (Fig. 3). Four overlapping or nested open reading frames (ORFs) are translated to yield seven different viral proteins. In this compact genetic organization, every nucleotide is at least present in one of the ORFs for coding a protein. In addition, crucial elements like a polyadenylation

signal, a packaging signal, two enhancer elements, and two direct repeats, are also present within the coding regions.

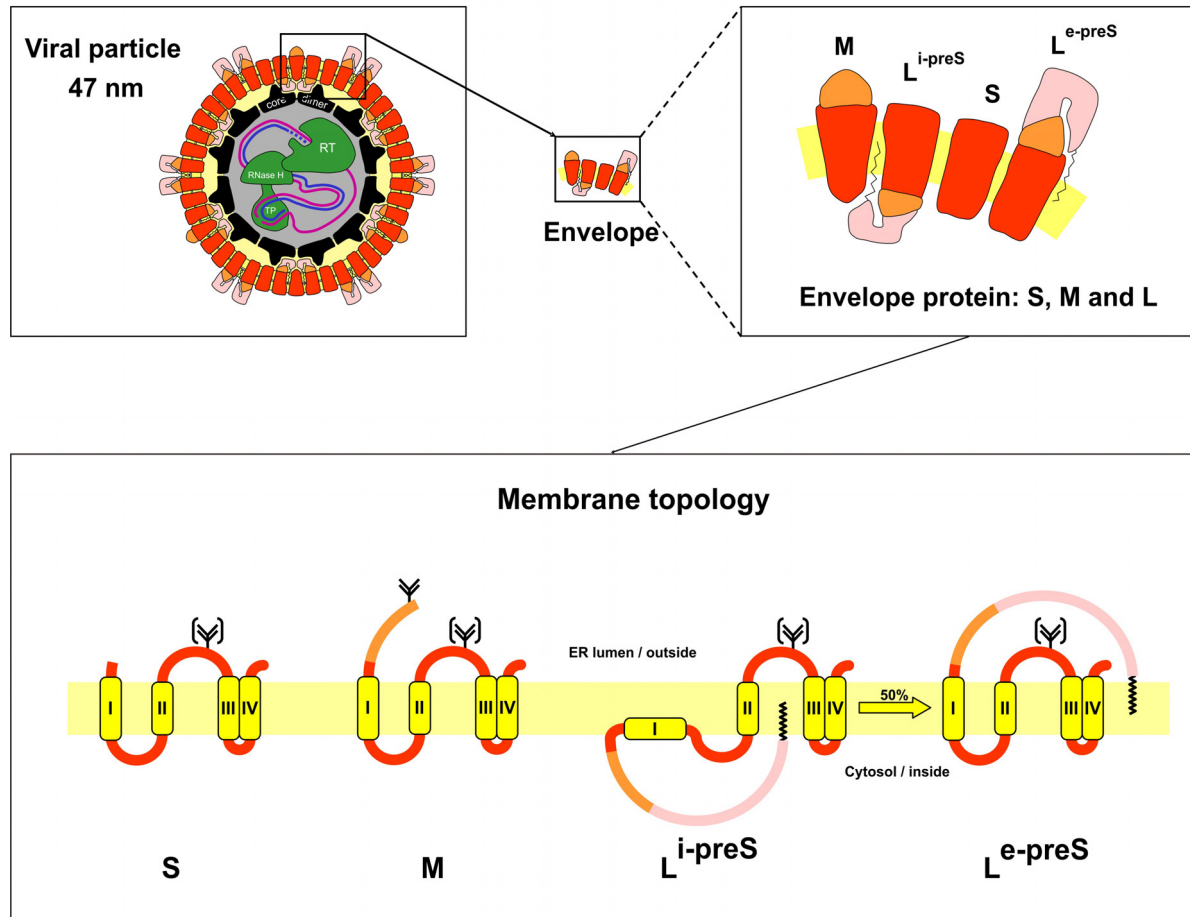


FIG. 2. Schematic diagram of hepatitis B particle (picture kindly provided by Stefan Seitz)

Top left: Illustration of the infectious viral particle of HBV. Capsid, envelope, polymerase, preS1, preS2 and S are labeled as black, green, pink, orange and red respectively. RT, reverse transcriptase; TP, terminal protein.

Top right : The envelope of HBV contains three viral proteins (L, M and S protein). Note that the L protein is thought to have two different topologies (L^{i-preS}, L^{e-preS}).

Bottom: Proposed membrane topology of the three HBV envelope proteins. The preS1, preS2, S region are labeled with pink, orange, red bars. Four transmembrane domains (I, II, III, IV) are shown in yellow box. glycosylation, Y; partial glycosylation, Y~; myristoylation, wavy line.

Within virions, relaxed circular DNA (rcDNA) represents the major form of the viral DNA. In rcDNA the minus-strand is complete, spans the entire genome and is covalently linked to a viral polymerase. In contrast, the plus strand extends to about two-thirds of the genome length and has variable 3' ends^{31,32}. Due to an aberrant plus-strand priming in virus maturation, a small fraction (5%-20%) of virus particles contains double-stranded linear DNA (DSL) instead of rcDNA³³. The virions with DSL DNA are infectious but can lose important sequences from

their ends during initiation of infection and therefore appear to only play a minor role in hepadnavirus replication^{34,35}.

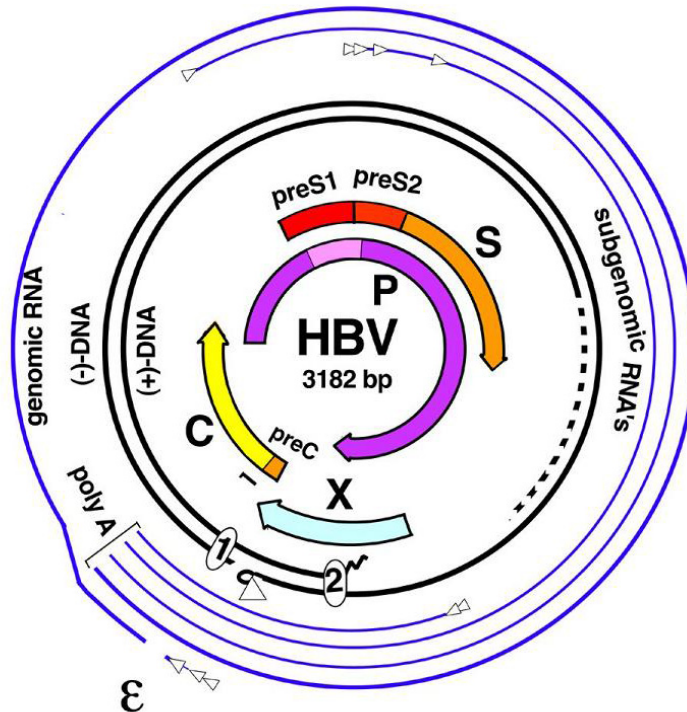


FIG. 3. HBV genome organization (picture kindly provided by Stephan Urban)

The HBV genome consists of a circular partially double-stranded DNA (black bold circles). The (-) strand is associated with the viral polymerase (Δ) and the 5' end of the (+) strand consists of an RNA-oligonucleotide (~~~~~). Two direct repeats (small circles) are located at the ends of the strand. The genome comprises four different ORFs (centre), the preC/C-ORF, preS/S-ORF, the X-ORF and the P-ORF which encodes the pre-core/core protein, the surface proteins, the X-protein and the polymerase, respectively. During transcription, 4 mRNAs (outer lines) are produced with a 5' cap (small triangles) and contain a 3' poly-A- tail. The genomic RNA bears the endcapsidation signal (ε) at the 5' end.

1.1.5 Primary attachment and receptor mediated binding

Identification of virus receptor(s), in most case, is not an easy task and the virus-receptor interactions are often complex. The criteria for identification of virus receptors are quite stringent. Evidence should be provided for direct interaction between receptor and the viral surface protein. Additionally it must be demonstrated that permissive cells gain virus-binding activity and can be infected, if receptor molecules are provided to the cells. Moreover, it is important to show that infection can be inhibited with antibodies or soluble receptors, and that the receptors are expressed on the surface of susceptible cells or organs³⁶.

Virus-host cell interaction is often a process which involves the interaction with multiple receptors with different affinities. This multivalent binding is common in many viruses³⁷. Upon

interaction with the first binding partner, viruses usually bind to a second molecule that mediates a virus-specific interaction. During this scenario, the virus might bind weakly to the abundant first receptor in order to move over the surface of a cell, while the interaction with a second receptor could be more specific, with higher affinity, and induce endocytosis or fusion. This multi-step binding is beneficial for the virus, since the binding to the cell surface allows movements in only two dimensions instead of three. To understand the viral entry process, it is important to distinguish between the abundant receptor with low affinity and the specific receptor with high affinity, both co-existing on the cell surface.

The described scenario could be true for HBV entry. It has been known that the viral infectivity determinant is located in the N terminus of the L protein (preS1). A second epitope involved in cell attachment outside the preS1 region has been suggested. Paran et al. showed that beads conjugated with particles containing the all three surface proteins bind to HepG2 cells better than preS1 alone³⁸. This “second epitope” might interact with heparan sulfate proteoglycans (HSPG), which has been described as the primary attachment site for many virus such as HSV, HIV-1 and flavivirus³⁹⁻⁴¹. Indeed, it also plays an important role in HBV entry. This conclusion is based on the following observation. Heparin can bind specifically to infectious virus particles and prevents virus binding to and infection of susceptible HepaRG cells. Enzymatic removal of defined acidic carbohydrate structures from the cell surface using heparinase I/III inhibits HBV infection and leads to a reduction of virus binding to the cell surface⁴². A recent study using hepatitis delta virus (HDV), a satellite virus of HBV requires envelope proteins to infect hepatocytes, provided evidence that the antigenic loop of the S domain is required for the infectivity of HDV⁴³. However, the binding partner of the antigenic loop has not been linked to HSPG. Nevertheless, it is apparent that HBV contains at least two separate determinants that synergistically act to mediate effective cell attachment.

It is commonly believed that there is a specific receptor for HBV preS1 domain on the surface of hepatocytes, but it has not yet been identified. A lot of candidate receptors have been reported and are summarized in Tab. 2, but all of them were not commonly accepted as the specific receptor of HBV.

TAB. 2. Described binding partners for HBV preS1-domain.

(modified from the review by Dieter Glebe⁴⁴).

Domain	aa	Described interaction partners/binding factors for HBV	Ref.
preS1	10-36	Binding of hepatoma cells HepG2 to HBsAg (subtype ad) can be inhibited by synthetic peptide aa 21-47 and antisera against aa 21-47	45

	16-38	Binding of highly purified virion to plasma membrane extraction of human liver. Inhibition by anti-preS1 aa16-38	46
	10-36	PreS1-peptide binding not limited to liver cells, also on extrahepatic sites	47
	10-36	Partial homology of preS1 aa10-36 with IgA. HBV entry via IgA-binding receptor?	48
	10-21	PreS1 aa10-21 crossreact with IgA alpha-1 chain, IgA and HBV use related receptors?	49
	10-36	PreS1 aa10-36 binding to 31 kDa protein on HepG2 cells	50
	10-36	PreS1-peptide aa10-36 binds to Interleukin 6 (IL6) but not IL3, IL5 and IL7	51
	10-36	CHO cells transfected with IL6 cDNA acquire binding sites for preS1 peptide aa10-36	52
	10-36	Isolation of a 44 kDa protein (HBV-BP) from HepG2 plasma membranes. Homology to SCCA1, human squamous cell carcinoma antigen 1 (human serpin)	53
	preS1-GST	Isolation of p80 binding protein from human hepatocytes. Needs preS1 aa12-20/82-90 for binding. p80 binding also to rat hepatocytes	54
	preS1	Anti-idiotypic antisera of antibody inhibiting binding of HBV to HepG2. 35kDa protein homology to Glycerinaldehyde-3-phosphate-dehydrogenase (GAPDH)	55,56
	preS1/preS2	50 kD serum glycoprotein interferes with binding of preS1 and preS2 mAbs. Soluble form of plasma membrane protein on human hepatocytes	57
	preS1	Yeast two-hybrid assay I: preS1 domain and human liver cDNA library. Isolation of an unidentified protein and a mitochondrial protein.	58
	preS1	Yeast two-hybrid assay II: preS1 domain and human liver cDNA library. Isolation of cytoplasmic "nascent polypeptide-associated complex alpha polypeptide" (NACA)	59
	HBV particles	Asialoglycoproteinreceptor (ASGPR) I: preS1-but not preS2-mabs inhibited binding of HBV to ASGPR. SHBs did not bind to ASGPR	60
	HBV particles	Asialoglycoproteinreceptor (ASGPR) II: HBV uptake by HepG2 and HuH-7 (ASGPR+), but not CHO (ASGPR-)	61
	HBV particles	Asialoglycoproteinreceptor (ASGPR) III: Desialylated HBV only binds to HepG2. Uptake only by susceptible primary human hepatocytes	62
	HBV particles	Asialoglycoproteinreceptor (ASGPR) IV: Increased HBV uptake by HepG2 after desialylation results in HBV infection	63

Numbering of amino acids (aa) is given for HBV genotype D.

1.1.6 Fusion with the cellular membrane

In order to release the nucleocapsid into cytoplasm during virus entry, the enveloped virus has to get rid of its envelope. This is thought to happen by fusion with the cellular membrane.

Depending on where the fusion occurs, two modes of fusion have been described. One is pH-independent fusion mostly happen at the plasma membrane, as the fusion of human immunodeficiency virus (HIV) triggered by association with a second receptor. Another is fusion following endocytosis triggered by acidification in the endosome.

Endocytosis is required for various different functions that are essential for the cells. It is the process by which cells take up material from outside by engulfing them with their cell membrane. It is not surprising that viruses, in order to deliver themselves into cells for replication, take advantage of this process to mediate their entry. Virus binding to receptor is mostly followed by receptor mediated endocytosis. Even the well-accepted dogma for endocytosis independent entry of HIV, had recently been challenged by visualization of the virus movement in living cells⁶⁴.

As an enveloped virus, HBV could also be endosome-dependent for virus entry. The close related virus, DHBV, uses endocytosis for the virus uptake^{65,66}. Infection of duck hepatocytes with DHBV is a slow process that can take up to 16 hours⁶⁷. It hints that internalization rather than binding to the receptor appears to be the rate-limiting step because the binding occur rapidly at 4°C. Additionally, exposure of DHBV particles to low pH was shown to induce a conformational change in the viral large surface protein resulting in increased hydrophobicity of the virus surface⁶⁸. Entry of HBV is thought to be pH independent, but the entry could be inhibited by hyperosmotic medium (supplemented with sucrose) which inactivate endocytosis (Schultz A and Glebe D, unpublished data from). It is not clear which endocytosis pathway the HBV particles take advantage after binding to the receptor.

1.1.7 Nucleocapsid transportation

There is little information on the post-fusion events in HBV entry. It is believed that after uncoating of virions, nucleocapsids have to be transported to the cell nucleus⁶⁹ in order to form cccDNA, a prerequisite for transcription. It has been shown that HBV capsid can be lipid-mediated “transfected” into the hepatocytes and leads to genome expression⁷⁰. Additionally, the core protein contains nuclear localization signals (NLSs) and has been shown to bind the hepatocyte nuclear membrane⁷¹ in a core phosphorylation and importin-dependent manner⁷². Although the mechanism of this process is poorly understood, the transport of nucleocapsids

brings the virions rcDNA to the nucleus, where it is converted into covalently closed circular DNA (cccDNA) to serve as a template for the transcription.

1.1.8 cccDNA formation

Ten hepatitis B virions entering the blood of chimpanzee are enough to establish a chronic infection. However, it is still an open question, how many virions successfully entering the hepatocytes could eventually convert their rcDNA into cccDNA. This is partially due to the lacking of detection methods to quantify both events, i.e., quantification of engulfed viruses and cccDNA at the single-cell level. Referring to the cccDNA as the endpoint of successful entry, uptake of virus particle might lead to “abortive entry”, which is a phenomenon described in viruses like HIV-1⁷³ and HCMV⁷⁴. The kinetics of cccDNA formation shows that the conversion of rcDNA to cccDNA in the liver is established within the first 24 hours post-infection. In DHBV, in a simulating one-step growth kinetics studies, it was determined that internalization and transportation to the nuclear membrane required a period of approximately 4 hours⁷⁵. The subsequent step of uncoating/transfer into the nucleus is measured by the appearance of the cccDNA, which happens within 48 hours. In contrast, by using a sensitive PCR assay selective for the detection of cccDNA derived from input viral DNA and not through replication, it had been shown that transfer into the nucleus required only 20 hours^{65,76}. It is still unclear if the model for DHBV can be applied to that of HBV.

The mechanisms of DNA repair involved in this conversion are also not fully understood, but the rcDNA must be deproteinized to remove the covalently bound polymerase from the 5' end of minor-strand. Consecutively, a capped RNA oligomer present at the 5' end of plus-strand DNA must be removed, while DNA synthesis at the 3' end makes the entire molecule double-stranded. The ends of each strand are then ligated to form cccDNA. It is still a matter of debate whether the viral polymerase plays a role in this process, although most of these modifications are performed by host enzymes.

1.1.9 Transcription

cccDNA serves as the template for all viral transcripts. The initiation of transcription is suggested to be dependent on viral X protein (Kuhn C and Sonnabend J, unpublished results). All transcripts are capped and polyadenylated due to a unique polyadenylation signal in the viral genome, these transcripts have the same 3' end but differed in the 5' end, as found in Northern blot as 3.5, 2.4, 2.1 kb and 0.7 kb length products. These mRNA are called pre-C/C, pre-S, S and X, respectively^{65,76-80}.

Since most of HBV promoters do not contain the TATA box, different products exist with slightly heterogeneous 5' end within each size of mRNA band. For example, the 2.1 kb transcripts actually contain mRNA covering the start codon of PreS2 (the transcript for the M protein) or mRNA only with the start codon of S-ORF (the transcript for the S protein). Another example is the 3.5 kb product, which differs according to the absence or presence of the preC start codon. The longer transcript with the preC start codon is used only for the translation of e-antigen. The short one without the preC start codon can be transcribed into core protein, polymerase and used as the pregenomic RNA (pgRNA)⁸¹. The 5' end of X mRNA is also heterogeneous⁸².

The 3.5 kb RNA product is longer than the circular 3.2 kb cccDNA. Thus, this product has to be transcribed by ignoring the first polyadenylation signal in the viral genome. Studies on DHBV indicated that it is facilitated by a sequence named PET (positive effector of transcription), which is located between the transcription initiation site and the poly(A) signal⁸³.

1.1.10 Translation of viral proteins and co/post-translational modification

The translation of viral proteins is depicted in Fig. 3. In the common scenario, the mRNA is scanned for the first start codon to initiate the translation, except for the translation of the polymerase. The start codon of the Pol ORF is downstream of the core protein together with several other possible start codon. For the translation of the HBV pol, it appears that the ribosome bypasses the upstream start codons by 'leaky scanning'. Another model suggests that ribosomes bind at the 5' end, but are then shunted to the initiation codon of the pol without scanning the codons in between⁸⁴. By any of these mechanisms, much more core proteins are translated than pol, which makes sense for the ratio requirement in the assembly of the virus capsid (240 core proteins and 1 polymerase per nucleocapsid).

Some of the viral proteins undergo a co-translational or post-translational modification. HBeAg is translated from the longer subset of the 3.5 kb mRNAs including the start codon for the preC/C ORF. A signal sequence in the N-terminus of the newly translated product directs the translation of HBeAg to ER membranes. As a consequence, the protein enters the secretory pathway, where it undergoes a second cleavage event, in which the proximal 34 aa from the C-terminus are removed before it is secreted⁸⁵⁻⁸⁹. All three envelope proteins are partially glycosylated in their common antigenic loop. While the preS2 region of the M protein is fully glycosylated, the L protein is not glycosylated in the preS2 region but is myristoylated at the N-terminus. It has been found that myristoylation of L is not required for virus assembly but required for the virus infectivity^{29,90}.

When the L protein is translated, the N terminus is located in the cytosol and gets myristoylated. However, after translation, the N-termini of a portion of the L proteins have to be translocated into the lumen side of ER membrane to form the two distinct topologies. It is not clear when and how this translocation takes place, but it is thought that the cell heat shock protein Hsc70 plays a role in this process via the interaction with the preS1 region of the L protein⁹¹.

1.1.11 Genome Replication

Although cccDNA in the nucleus of infected hepatocytes exists as a mini chromosome, the hepadnavirus uses a unique replication strategy, i.e., transcription of pregenomic mRNA (pgRNA) followed by intracellular reverse transcription to form genomic DNA.

As mentioned above, the 3.5 kb mRNA transcript, which does not contain the start codon of PreC, acts as the template for DNA synthesis. At the same time, it is also used for the translation of the P protein. It has been shown that the polymerase binds to an RNA stem-loop structure (ϵ , epsilon) at the 5' end of the pgRNA, and that this event triggers the packaging of pgRNA and polymerase into RNA-containing capsids^{92,93}. It has also been shown that the polymerase preferentially binds to its cognate mRNAs to ensure the integrity of pgRNA to be packaged.

The genome replication inside the capsid proceeds as the following. Initially a 4-nucleotide minor-strand DNA complementing the ϵ -sequence is synthesized and then transferred to a complementary sequence in DR1 near the 3' end of the pregenome. DNA synthesis continues towards the 5' end of the pregenome template. The RNase H activity of the P protein degrades the pregenome RNA from the RNA/DNA duplex. The RNA is removed except for a remnant of 15–18 bases including the cap. The –OH group at the 3' end of the RNA remnant acts as the primer for the synthesis of the plus-strand DNA. During plus-strand DNA synthesis nucleocapsids can either migrate to the nucleus to increase the pool of cccDNA or undergo maturation that enables it to bud through a membrane containing virus envelope proteins.

1.1.12 Assembly and virus release

To secrete a Dane particle, a nucleocapsid must be formed first. The core dimer forms an isohedral capsid when the polymerase binds to pregenomic RNA. The mature nucleocapsid can thereafter interact with the preS domain of the L protein and also interact with the cytosolic loop of the S protein. This conclusion is supported by two facts: (1) Mutation in a linear stretch of preS domain (aa 93-113) or in the CYL-I of S domain (aa 56-59) do not interfere with subviral particle formation but block virion formation^{94,95}. (2) Synthetic peptides identical to aa 96-116 of the L protein and aa 56-80 of the S protein bind efficiently to core particle in vitro⁹⁶. This

process is believed to happen in a compartment between the endoplasmic reticulum and the Golgi complex. Virions are thought to be transported within vesicles and released from the cell by exocytosis⁹⁷.

A distinguished characteristic of HBV infection is the formation of excessive amount of subviral particles, secreted irrespective of viral nucleocapsid, compared to infectious Dane particle. A similar phenomenon is also found in the foamy virus. It is suggested that the robust self-secretion of subviral particles might use a different pathway compared to the secretion of infectious Dane particles. Patient *et al.* has shown that subviral particles are formed by the S protein self-assembly into branched filaments in hamster kidney cells. This takes place in the lumen of the endoplasmic reticulum and then transported to the ER-Golgi intermediate compartment (ERGIC)⁹⁸. Several study on DHBV or HBV showed that Dane particle are secreted via multi vesicle bodies (MVB) by EM study. By introducing dominant negative form of AIP1 and Vps4B, both of which are MVB protein, Watanabe *et al.* also showed that virions, subviral particles and naked nucleocapsids were released by distinct pathways⁹⁹⁻¹⁰¹.

As a summary, the life cycle of HBV from entry to virus release is depicted in Fig. 4.

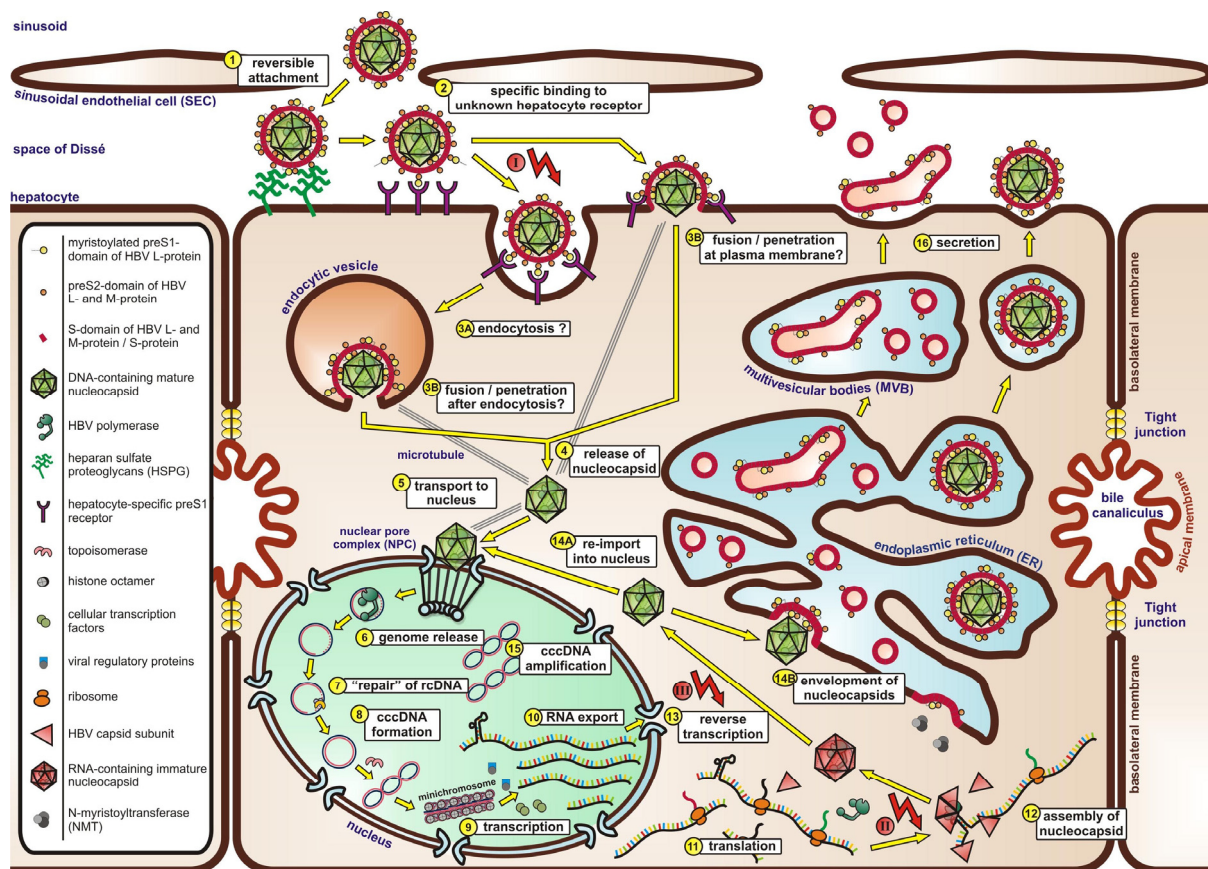


FIG. 4. The replication cycle of hepatitis B virus (adapted from the review of Stephan Urban¹⁰²)

(1) Reversible attachment to HSPG. (2) Specific binding to an unknown hepatocyte-specific preS1-receptor. (3) Two different entry pathways have been proposed: endocytosis or fusion at the plasma membrane. (4) Release of the viral nucleocapsid containing rcDNA. (5) Transport of the nucleocapsid along microtubules. (6) Possible trapping of the nucleocapsid in the nuclear basket and release of rcDNA into the nucleoplasm. (7) “Repair” of the incoming rcDNA: Completion of the plus strand of the rcDNA by the viral polymerase. (8) cccDNA formation by covalent ligation of both DNA strands. (9) Transcription of the subgenomic RNAs which encode the surface proteins and the X-protein and the pregenomic (pg) RNA, which encode the polymerase and the core-protein. (10) All 4 major mRNAs utilize a single common polyadenylation signal. (11) Translation of the pregenomic RNA (pgRNA) to the core protein and the viral polymerase. (12) Complex formation of the pgRNA (via its epsilon stem loop structure) with the core protein and the polymerase and self-assembly of an RNA-containing nucleocapsid. (13) Reverse transcription of the pgRNA followed by plus-strand DNA-synthesis within the nucleocapsid. (14) DNA-containing nucleocapsids can be either re-imported into the nucleus to form additional cccDNA molecules or can be enveloped for secretion. (15) Re-import of nucleocapsids increases the cccDNA population. (16) Compared to virions, spherical and filamentous SVPs are secreted in a 10^3 – 10^6 -fold excess into the blood of infected individuals.

1.2 The HBV entry inhibitor: Myrcludex B

There are 7 FDA approved drugs and several drug candidates in the pipeline for Hepatitis B treatment¹⁰³. According to the different steps they interfere with virus infection, they can be divided into three catalogs: (1) immunomodulating agents like interferon- α , (2) reverse transcriptase inhibitors like nucleoside analogue Lamivudine, (3) Non-nucleoside antivirals interfering with viral protein during replication, e.g., Bay 41-4109. Another drug candidate, Myrcludex B, is coming in the pipeline addressing a different stage of HBV infection. Similar to the Fuzeon against the entry of HIV, Myrcludex B is an entry inhibitor for the HBV and HDV infection. Now it is in the preclinical stage and towards the phase I clinical trials in 2010.

The concept of developing Myrcludex B came from the characterization of a peptide, originally described as HBVpreS/2-48^{myr}, bearing the same sequence and N-myristoylation as the N-terminal 47 residues of the L protein. It potentially inhibits HBV entry *in vitro* and *in vivo* in an efficient and specific manner, and was further optimized with respect to the length, N-terminal modification, and genotype usage¹⁰⁴. To summarize these results, the following characteristics are found: (1) the N terminal modification is necessary since the activity of unmyristoylated peptide decreases 1000-fold *in vitro*; (2) based on the sequence of genotype D, the length of peptide was optimized to the N-terminal 47 aa, since the shorter or longer peptide reduces the potency of inhibition; (3) by comparing the preS1 sequence between genotype C and genotype D, the optimal peptide come from the consensus sequence based on genotype C. Following this observation, a peptide was produced for the clinical trial and was named as Myrcludex B. It has a potent inhibition activity with IC₅₀ of 25-800 pM (unpublished data).

Toxicity tests of Myrcludex B in rats and dogs showed the possibility of this drug to be applied in a high dose. This paves the way towards the Phase I clinical trials. However, the discovery and

characterization of Myrcludex B did not only lead to a promising clinical application, but also gave some hints for the mechanisms of HBV entry.

Firstly, the presence of the peptide during inoculation inhibits the virus entry, and the pre-incubation of the hepatocytes with the peptide also lead to abolishment of the entry event. This indicates that the peptide addresses to a cellular factor, where it interferes with the virus-cell interaction. Apparently, this cellular factor might be the receptor of HBV.

Secondly, an interesting observation is that the peptide at the concentration for 90% inhibition can not inhibit the binding of virus to hepatocytes. Indeed, the HBV infection can be inhibited at extremely low concentration of Myrcludex B (25-800 pM). These facts indicate that either the virus binding to hepatocytes is a multivalent event (see section 1.1.5), or the peptide might not simply compete the binding of virus but interfere with a critical step afterwards. However, it should be taken into account that the unusual efficacy of the peptide might be due to the N-myristoylation, which enhances the membrane association of peptide and facilitate the interaction of the peptide and its binding partner at a two dimension level of cellular membrane. Indeed, *in vitro* data have suggested that the peptide can highly specifically bind to the surface of differentiated hepatocytes, and this binding is myristoylation dependent (Anja Meier, unpublished data).

In addition, the peptide shows a compelling liver tropism *in vivo*. This observation is based on study with radioactively labeled peptide, when subcutaneously injected, quickly addressed to and accumulated in the liver (within 20 minutes) and were retained in the liver for 24 to 48 hours. The C-terminus shortened peptide HBVpreS/2-20^{myr} still showed the liver tropism (Alexa Schieck, unpublished data). These results explained the organ tropism of HBV infection and pinpointed the determinant of liver tropism to the very short sequence in the N-terminus of the L protein. Moreover, it suggested for further applications of Myrcludex B as a vehicle to specifically deliver drug to the liver.

In the end, the essential elements of the peptide were narrowed down to the N-myristoylation and the aa 9-15. Both of them are very critical for the inhibitory activity, hepatocyte binding and liver tropism. Considering that these two elements are very close to each other, it is reasonable that the hydrophobic myristic group and aa 9-15 might form a complex before or during the virus-receptor interaction, and this conformation is crucial for the virus infectivity.

1.3 Host and organ tropism of hepadnaviruses

So far, HBV can only infect primates. The host determinant of HBV has been identified in the preS region. Studies comparing DHBV with HHBV showed that the host determinant of DHBV lies within aa 22-37 of preS region. Similarly, the study comparing the infectivity of WMHBV and HBV in PHH showed that the N-terminal aa 1-30 of the L protein determine the species specificity of WMHBV and HBV¹⁰⁵.

The assumption that the specific host tropism of HBV is due to the specific binding receptor was challenged. It has been shown that mouse hepatocytes, although mice are not susceptible to HBV infection, can very efficiently interact with the peptide HBVpreS/2-48^{myr} (Anja Meier, unpublished data). This peptide has been shown to inhibit HBV infection and is supposed to bind to the unknown receptor on the surface of human hepatocytes. More importantly, this peptide is specifically tropic to the mouse liver *in vivo* (Alexa Schieck, unpublished data). Thus, mice actually bear the preS1-specific receptor but the bound viruses are probably restricted in (one of) the post-binding steps so that they are not able to establish cccDNA in the cell nucleus.

It is believed that some cell types other than hepatocytes could also support viral replication. In DHBV, infection of bile duct epithelial cells of the liver also occurs¹⁰⁶, and studies with primary cell cultures suggest that they may be sites of DHBV reproduction *in vivo*¹⁰⁷. cccDNA and typical DNA replication intermediates, with abundant single-stranded DNA, are found not only in liver, but also in pancreas and kidney of chronically infected ducks¹⁰⁸. Extrahepatic infection has also been studied in chronically infected woodchucks. Typical DNA replication intermediates have only been found in the liver and, at a ~10-fold lower level, in spleen. The evidence of extrahepatic infection in the woodchuck was obtained from studies with peripheral blood lymphocytes (PBLs) of WHV-infected woodchucks. Although WHV did not replicate in PBLs *in vivo*, they produced typical viral DNA replication intermediates and released viruses when stimulated with lipopolysaccharide *in vitro*, and thus appear to be latently infected^{109,110}. Nevertheless, the importance of the “nonhepatocyte infection” on virus pathogenesis is still not clear.

1.4 Cellular factors needed for infection

While a preS-specific receptor of DHBV had been identified as the Duck Carboxypeptidase D (dCPD, gp180), the exploration for the HBV receptor has had limited success. During the last 25 years, numerous reports on a variety of possible cellular preS-binding partners have been published (Tab. 2). They were identified via a variety of approaches, such as biochemical identification of the binding partners from the membrane extracts of hepatocytes, or from phage

display library using the viral particles, subviral particles, or peptides. None of these potential preS-binding partners have so far been convincingly proved to be the receptor of HBV¹¹¹. The most important evidence, which is still lacking, is the conversion of permissive cells to susceptible cells when these candidates are expressed.

The myristoylated peptide, HBVpreS/2-48^{myr}, could prevent the binding of purified preS1-containing subviral particles to PTH, whereas preincubation with the myristoylated preS peptides from avian hepadnaviruses could not¹¹². However, inhibition of the binding required micromolar concentrations of the peptide, rather than picomolar concentrations needed for the inhibition of infection¹¹². This difference suggested the presence of an abundant low-affinity receptor for viral and subviral particles. This low affinity receptor might be heparan sulphate proteoglycans (HSPG). It has been shown that binding of HBV to HepG2 cells and PHH are both inhibited by sulphated polymers¹¹³. Furthermore, HBV binds to heparin *in vitro* and could be purified from the plasma of HBV infected patients by heparin-sepharose columns¹¹⁴. Unfortunately, these two reports could not clarify the relevance of binding to HBV infection. Recently, it has been shown that HBV infection could be specifically blocked by preincubation of purified virus with heparin, or by treatment of PTH and HepaRG cells with heparinase^{42,115}. Since heparan sulphate proteoglycans (HSPGs) are enriched in the liver within the space of Disse, one may speculate that HBV is trapped by liver specific HSPGs, serving as low-affinity receptors similar to the interaction and entry of apolipoprotein E lipoprotein remnants by liver HSPGs¹¹⁶. Specific entry of the virus may subsequently require a yet undefined high affinity receptor(s), which can be blocked by the acylated preS1-derived peptides.

1.5 The HBV envelope and known viral infectivity determinants

If the “virus infectivity determinant” was defined here as the particular sequence in the envelope protein that is necessary for virus infectivity, the following scheme summarizes all the available information so far regarding the preS1 region (Fig. 5). In short, the N-myristoylation, consecutive 5 aa of the N-terminal 77 amino acids of the L protein, are known to be critical for the infectivity of either HBV or HDV.

In line with the finding that preS1 contains critical determinants responsible for virus infectivity, the myristoylated peptide comprising the N-terminal 47 aa of preS1 can inhibit HBV infection. The non-myristoylated peptide can only inhibit HBV infection at >1000-fold higher concentration than the myristoylated one. More interestingly, there are some difference between the sequence requirement of peptides and the infectivity determinants of preS1 (Fig. 5). Generally, the N-terminus of peptide is more important than the C-terminus¹⁰⁴. The essential

elements are the aa 9-15 and the N-terminal myristic group. The peptide containing the aa 49-78 does not increase but weakens the activity^{112,117}, which indicates that aa 49-78 may have a different function compared to aa 2-48.

Besides the information from the study on virus infectivity and inhibitory peptides, some other evidence has suggested preS1-domain contains the receptor binding site. It has been reported that a synthetic preS1 peptide, aa 10-36 (in genotype D) without N-terminal myristoylation, binds to the surface of HepG2 cells and also inhibits HBV binding⁴⁵. Furthermore, antisera raised against this peptide compete with the binding of HBV particles to HepG2 cells. Additionally, the neutralizing activity of monoclonal antibodies (mAb) MA18/7¹¹⁸, KR359¹¹⁹, KR127¹²⁰ with epitopes encompassing the aa 20-23, aa 19-26, aa 37-45 hint that these regions are involved in the entry process. Using an *in vitro* binding assay based on peptide-coupled beads mimicking the virus particle, it could be shown that the aa 18-23, motif QLDPAF, is important for binding to HepG2 cells³⁸.

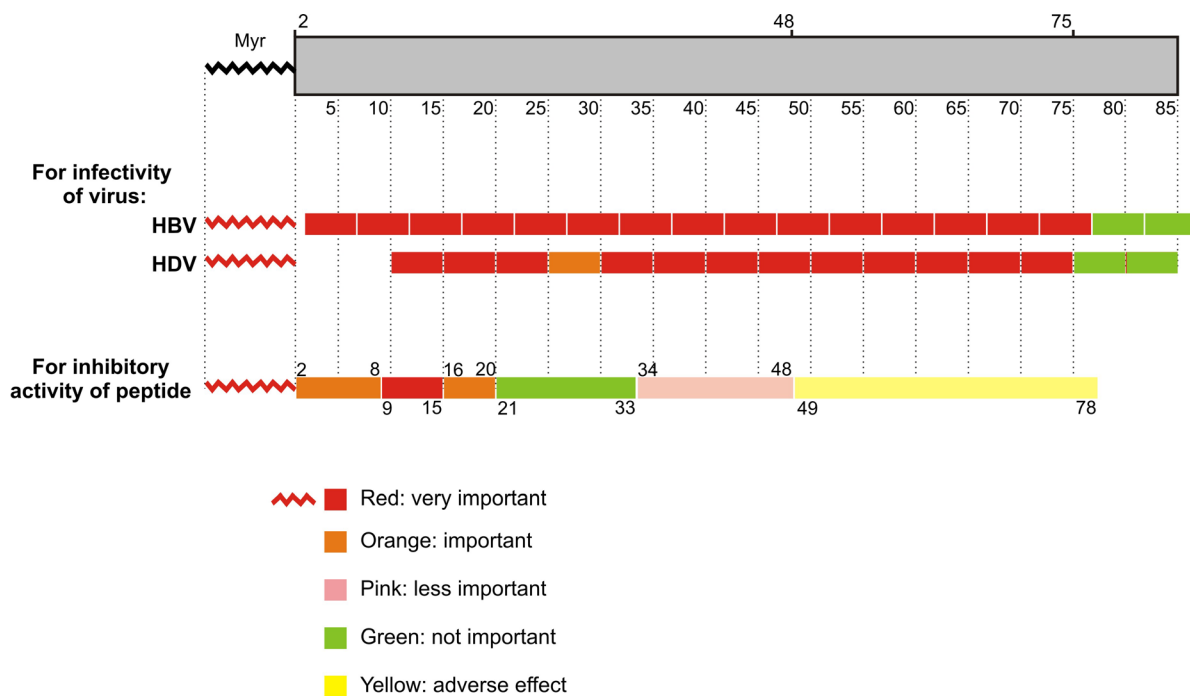


FIG. 5. Schematic illustrations of the infectivity determinants within the N-terminus of preS1 domain

The N-terminus of preS1 is strongly required for the virus infectivity. For HBV, the abolishment of myristoylation or deletion of the consecutive 5 aa in this region completely abrogates the virus infectivity^{29,121}. In consistence, the abolishment of myristoylation or partially substitution of the consecutive 5 aa in the aa 11-75 also abrogates the infectivity of HDV^{43,122}.

The sequence required for the inhibitory peptide derived from the N-terminus of preS1 has been mapped to detail^{104,112,117}. Although the myristoylation (red line) and the aa 9-15 (red bar) are as essential for the peptide as for the virus infectivity, the aa 49-78 do not increase but impair the activity of peptide (yellow bar). While the flanking sequences comprising the aa 2-8 and the aa 16-20 drastically increase the activity of peptide (orange bar), the aa 21-33 do not show significant effect (green bar).

The envelope of HBV contains three envelope proteins, L, M and S, and all three envelope proteins have a common C-terminal S-domain. Beside the preS region, the domain structure of three proteins and the regions necessary for virus infectivity are depicted in Fig. 6. It had been pointed out that some regions are dispensable for the infectivity of HBV or HDV. The C-terminus of preS1 (aa 78-87)¹²¹ and the C-terminus of preS2 (aa 114-163)¹²³ are not important. The matrix-domain critical for HBV assembly⁹⁴ covering aa 87-113 is not important for HDV infectivity, thus is also unlikely involved in HBV entry^{122,124}. The absence of M protein in the virion has no effects on HBV infectivity¹²⁵. A systematic mutation analysis has demonstrated that all assembly-competent HDV with mutation in cytosolic loop-I (aa 24-80 of S domain) are infectious and also minimize a possible role of cytosolic loop-II (aa 193-202) in entry process¹²⁶.

Interestingly, using peptide-coupled beads, the second binding partner in the envelope was identified within the S protein³⁸. In consistence with this result, it was known that the antibodies against the S-domain, generated by current vaccines containing solely S-protein, could neutralize infection *in vivo* and *in vitro*¹²⁷⁻¹²⁹. Moreover, in patients positive for anti-HBs, the presence of escape mutants (commonly found G145R and D144A mutation in the S-domain) also suggests that the antigenic domain is involved in the infection process *in vivo*¹³⁰⁻¹³⁵. The data from HDV infectivity studies *in vitro* confirmed the assumption that S-domain contains an infectivity determinant, which is further narrowed down to the antigenic loop. Virions with the S domain lacking the residues between 119 and 128 showed reduced infectivity on PHHs and HepaRG cells. A further study pinpointed aa 119 to 124 (GPCRTC) as the most important sequence required for HDV infectivity¹³⁶. This domain contains a CXXC motif, known to be the substrate of protein disulfide isomerase (PDI), which catalyzes disulfide-bridge exchanges. For non-enveloped virus like SV40, it has been reported that the isomerase is involved during virus entry to disassemble the viral capsid¹³⁷. For the enveloped virus like murine leukemia virus, the receptor-binding subunit (SU) in the surface proteins contains a CXXC motif that is activated after receptor-binding of the envelope transmembrane (TM) subunit. This leads to isomerisation of SU-TM disulfide bonds and fusion-activation within the TM subunit^{138,139}. All this evidence led to an attractive assumption that CXXC motif in the S domain play a similar role in HBV, i.e., a signal for disassembly. However, the infectivity of HDV was not impaired when the CXXC motif was mutated into CXXXC or CXC motifs that can not be recognized by the PDI. Nevertheless, it could not be ruled out that the S-S disulfide bridge(s) within the AGL plays an important role in HBV entry.

The third infectivity determinant in HBV entry can be ascribed to the first transmembrane sequence of the S-domain, which has a sequence similarity to type I fusion peptides. The replacement of the fusion peptides of influenza virus hemagglutinin (HA) with this first transmembrane sequence of HBV lead to the hemifusion activity of the resulting chimeric HA protein¹⁴⁰. Consistent with this, transmembrane domain I (TM-I) of the L protein but not the S protein is critical for DHBV entry. This scenario might also be applied to HBV because the common putative fusion peptides are found in both viruses¹⁴¹.

A debate was triggered regarding to a so-called translocation motif (TLM) in the preS2 region presenting in both L and M proteins. It was described that a fusion preS2 protein is able to translocate itself into the cell and evenly distributed in the cytosol. Detailed analysis revealed that cell-permeability is mediated by an amphipathic α -helix between amino acids 41 and 52 of preS2, which was named as translocation motif (TLM)¹⁴². Two homologous motifs were found in the preS domain of DHBV, and lacking of these two motif in DHBV lead to the loss of virus infectivity¹⁴³. Therefore, it was suggested that TLM is an essential infectivity determinant for hepadnavirus to translocate virions into cytosol for establishment of productive infection. However, accumulating evidence from the study on HDV and HBV showed that TLM is not necessary for virus infectivity.

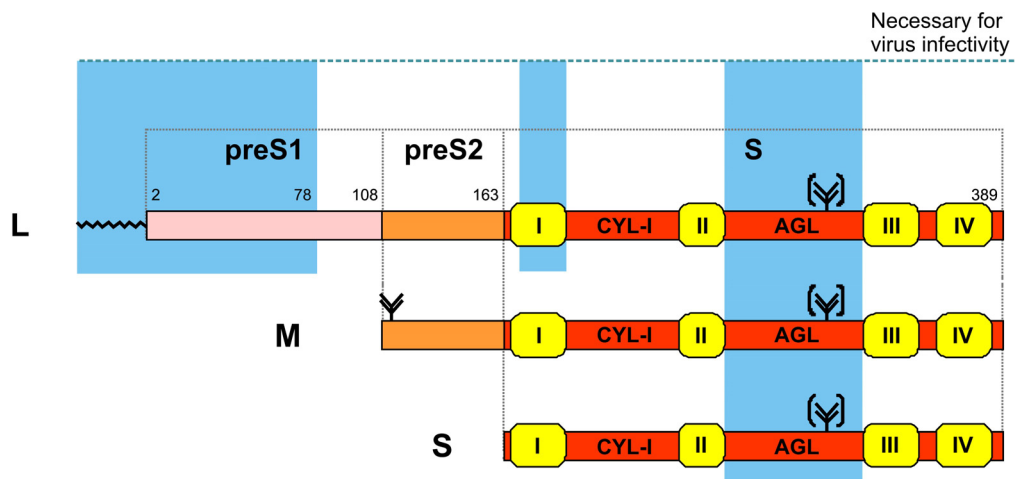


FIG. 6. Schematic representation of the domain structure of the three HBV surface proteins and the regions critical for virus infectivity

The HBV envelope consists of the L, M and S surface proteins. All three proteins are encoded by the nested open reading frame and share the common S-domain (red bar). The hydrophobic S-domain contains four trans-membrane domains (I, II, III and IV; yellow box), that help to form three loop structures in the S-domain, cytosolic loop-I (CYL-I), antigenic loop (AGL) and a small cytosolic loop-II (CYL-II). The M protein consists of an N-terminal extension of S by 55 aa (preS2, orange bar), while L protein (genotype D) contains an additional N-terminal 108 aa (preS1, pink bar). All three envelope proteins are partially glycosylated (Y) in their S-domain. The M protein is fully glycosylated at Asn 4 of preS2, while the L protein is not glycosylated at this site but is myristoylated at the glycine 2 of preS1 domain (~~~~). There are three critical regions for the virus infectivity (underground with blue box): the N-terminal 77 residues of the preS1 domain, the first trans-membrane domain of the L-protein, and the S-domain.

1.6 Animal and cellular models for HBV infection

Due to the strict host tropism, HBV can only infect humans and primates such as chimpanzee, but not the woodchuck (host of WHV) and Duck (host of DHBV). WHV and DHBV are comparable to some extent to the HBV. This led to extensive studies using woodchuck and duck as the animal models. These studies showed the particular advantage of these animal models and brought us invaluable information regarding immune response and viral pathogenesis. The infection of newborn woodchuck by WHV develops chronic infection and presents the most feasible model, so far, to investigate carcinogenesis induced by chronic hepadnavirus infection. Duck is a small animal infection model with ready availability and low expense. Along with the well established primary duck hepatocytes culture for efficient infection and chicken hepatoma cell line for the study of viral replication *in vitro*, DHBV offers the full range of experimental approaches.

Nevertheless, these two animals are not susceptible to HBV infection. Due to poor homology of preS region, WHV and DHBV are very likely to address different cellular receptors compared to HBV. Therefore, in the following text, we prefer to describe infection models on chimpanzee, tree shrews hepatocytes (*Tupaia belangeri*) and the modified mice that can be experimentally infected by HBV.

The chimpanzee, in particular, has been employed periodically to study virus transmission, host response and vaccination. Although the hepatitis in chimpanzee infected by HBV appears to be mild, there are serologic evidences of chronic infection together with persistent liver inflammation^{144,145}. It was shown that inoculation with 1-10 virions could lead to chronic infection, in contrast to that the high dose leads to transient infection and viral clearance. The chimpanzee is not proven as a model for hepatocellular carcinoma but has been used to illustrate the immunological response in the course of viral infection¹⁴⁶⁻¹⁴⁸.

Mice are one of the most commonly used animal models, since they are easy to maintain in the laboratory and have a short breeding cycle. However, mice are not the natural host for HBV and they can neither be experimentally infected by HBV nor other hepadnavirus. Mouse hepatocytes are also not susceptible to HBV infection *in vitro*, but they are competent of HBV replication. Therefore, HBV transgenic mouse has been generated¹⁴⁹. This mouse contains a chromosomally integrated 1.3-mer over-length HBV genome and produces substantial amounts of viral antigens and infectious virions. In contrast to cell lines with integrated HBV genome, such as HepAD38^{150,151}, there is no evidence that the cccDNA, a critical marker for HBV infection, is

formed in mice¹⁵². The transgenic mice are immunologically tolerant to HBV infection, but fundamentally new insights into the immune response against HBV infection have been gained by adoptive transfer of lymphocytes¹⁵³⁻¹⁵⁵. Apparently, the HBV transgenic mice are not suitable for entry studies. It must be mentioned that transgenic mice producing HBV proteins, e.g., HBeAg, core and X, has also been generated to examine the pathologic effects of viral proteins^{156,157}.

Another elegant model is the immuno-incompetent mice, uPA-SCID, xenotransplanted with primary hepatocytes from either humans¹⁵⁸, woodchucks¹⁵⁹, or tupaia¹⁶⁰. These chimeric mice maintain transplanted hepatocytes for a long time and allow the investigation of the full life cycle of HBV infection including the virus entry^{158,161}. As a small animal model, it was used to demonstrate the efficacy of an HBV entry inhibitor *in vivo*¹⁶². The disadvantage of these chimeric animals is the technical difficulty to generate them. Moreover, since these mice are immunodeficient, they are not ideal for immunological investigations.

Since *in vitro* infection systems were not available for long time, several surrogate systems have been established. The ability of certain human hepatoma cell lines, such as HepG2 and HuH-7, to support HBV replication after transfection of cloned HBV DNA, makes them highly valuable tools to investigate replication steps downstream the entry pathway. Most of our current knowledge of HBV replication is derived from these systems. The subsequently developed HepG2.2.15 cells with an integrated HBV genome¹⁶³, and the HepAD38^{112,150,151,164} cells with tet-inducible viral replication are extensively used to investigate reverse transcription, virus assembly, secretion and the sensitivity to RT-inhibitors.

To study the early events of virus infection, or to evaluate the mechanism of HBV entry inhibitors, primary human hepatocytes (PHH) have been used exclusively for a long time. The infection of PHH with HBV was irreproducible and insufficient at the beginning. As shown by immuno-staining, intracellular HBcAg was present in only 2-3% of the PHH post infection¹⁶⁵, 12% of the primary fetal hepatocyte¹⁶⁶ and less than 0.1% of cryopreserved PHH¹⁶⁷. Gripon *et al.* demonstrated that the addition of 1.5% dimethyl sulfoxide (DMSO) to the culture markedly enhanced the infection efficiency¹⁶⁸. Consistent with this observation, the addition of 2% DMSO to the culture of primary duck hepatocytes (PDH) also increases DHBV infection^{67,169}. This effect is contributed by two reasons: (1) DMSO prolongs the susceptibility of PDH to allow the virus spread via repeated cycle of infection. (2) DMSO enhances the expression of core antigen and viral DNA in PDH. In addition, the work from Gripon demonstrated that, besides the adding of 2% DMSO, the infection of PHH could be greatly enhanced by addition of

polyethylene glycol (PEG) during inoculation. This effect is mediated by enhanced attachment of virions to PHH¹⁷⁰. The role of PEG was further suggested to enhance the binding of HBV to cell-surface glycoaminoglycans (GAG)⁴².

Established in 2002, the HepaRG cell line is the first cell line supporting HBV infection. It was obtained from liver tumor tissue of a female patient suffering from hepatitis C virus (HCV) associated hepatocellular carcinoma (HCC)¹⁷¹. Subsequently, HepaRG cells were shown to be HCV-free and to behave as bi-potent progenitor cells that can be differentiated into hepatocyte-like cells and biliary-like cells under a certain condition¹⁷². In similar to primary hepatocytes, HepaRG cells can only be infected by HBV in a differentiated state. The selection procedure for establishment of HepaRG cells was heavily dependent on the combination of hydrocortisone (5×10^{-5} M) and 2% DMSO, two differentiation inducers for hepatocytes. It was observed that the continuous presence of hydrocortisone in culturing cells keeps the phenotypic stability. The adding of DMSO differentiates the cells into hepatocyte clusters and the removal of DMSO trans-differentiates the cells into an active proliferate state¹⁷¹. Therefore, to promote a maximum morphological differentiation level, culture conditions were defined as 2 weeks in the presence of 5×10^{-5} M hydrocortisone followed by 2 weeks of exposure to both hydrocortisone and DMSO. It must be pointed out that HepaRG cells start to differentiate when they reach the confluency, probably due to the presence of hydrocortisone. After seeding, the transcription levels of haptoglobin, albumin and aldolase B on HepaRG cells increase over time in absence of DMSO. However, in the presence of DMSO, the transcriptions of cytochrome P450 (CYP) family, such as CYP 1A2, 2C9, 2E1 and 3A4, are significantly up-regulated¹⁷³. In two independent observations on HepaRG cells, the expression of hepatocyte nuclear factor (HNF)-4 α was drastically increased in the presence of DMSO^{172,174}. HNF-4 α is known to be essential for HBV replication, since knock-down of HNF-4 α has a significant negative effect on pgRNA transcription, intracellular core protein expression, replicative intermediates and even the size of cccDNA pool¹⁷⁴. In similar to infection of PHH, infection of HepaRG cells by HBV is also significantly enhanced by the presence of PEG during virus inoculation¹⁷¹.

In 2001, primary tupaia hepatocytes (PTH) from tree shrews (*Tupaia belangeri*) were shown to be susceptible to HBV and WMHBV infection¹⁷⁵. However, the infection *in vivo* by HBV is mild and self-limited. The cell culture model is useful for investigations on mechanism of HBV entry^{112,164} and studies on the pathogenesis of clinical HBV isolates from patients with fulminant hepatitis¹⁷⁶. However, the optimal culture condition for infection of PTH is quite different from that for the infection of PHH and HepaRG cells. In short, optimal infection on PTH is obtained

in the absence of DMSO, PEG and serum, while the optimal infections on PHH and HepaRG both require the presence of 2% DMSO, 4% PEG and 10% serum. In addition, PEG-precipitated viruses are as infectious as the sucrose-gradient purified virus in PHH and HepaRG cells, but they are significantly less infectious in PTH (Sonnabend J and Glebe D, unpublished data).

1.7 Aims of this work

The mechanism of virus entry is still largely unknown and remains one of the most interesting questions in the field of HBV study. In the present work, HepaRG-cell-based infection system was optimized in order to characterize infectivity determinants of the envelope proteins of hepatitis B virus.

1. HepaRG-cell-based infection system is available in our lab, but with a fluctuated efficiency. Recombinant virion bearing mutation is a useful tool to study the role of viral proteins in virus entry. To test the infectivity of recombinant virion, normally with a low yield, is a technically challenging task. Therefore, we were asking for an optimal infection system and a sensitive read-out for HBV infection. To optimize HepaRG cells with respect to reliable susceptibility and robust virus replication is the first aim in the present study. To this purpose, we defined the HepaRG cell passages with a comparable susceptibility, and systematically study the effect of culture condition including the usage of DMSO, the concentration of PEG, EGTA treatment, spin-down inoculation. In addition, to quantify the infection events, especially those with a low infection rate, we developed a quantitative immunofluorescent method and compare its sensitivity and linearity to commercial assay measuring secreted viral markers.
2. The integrity of the N-terminal 78 amino acids of preS1 is required for the infectivity of Hepatitis B virions. It is known that aa 2-48, with an essential sequence at aa 9-15, is responsible for binding to an unknown virus receptor. However, the role of aa 2-9 and aa 49-78 remains unclear. To answer this question, recombinant virions, bearing mutation in aa 2-9 and aa 49-78 of the L protein, were produced and analyzed for their infectivity. In addition, a panel of preS1-derived peptides was tested for their inhibitory activity against HBV infection.
3. It is still unclear what the role of myristoylation is in viral L protein and in the preS-derived inhibitory peptide. With a hypothesis that myristoyl chain of peptide (and viral L protein) is inserted into cellular membrane during interaction with an unknown receptor, we replaced the myristoyl chain of peptide with a type II transmembrane protein. This

membrane anchored peptide was expressed in differentiated HepaRG cells via lentiviral transduction system and was characterized for its effect on the oncoming HBV infection.

4. The preS2 region in the L protein and the M protein has been shown to be dispensable for virus assembly and infectivity. A so-called TLM motif in the preS2 region triggered the debate on the role of preS2 domain. With a system to produce M-protein-free recombinant virion, we tried to answer the role of preS2 by comprehensive mutations on the preS2 region of L protein.
5. The cysteine residues in the S-domain have been shown to be critical for the infectivity of HDV, a satellite virus carrying envelope proteins of HBV. However, it is not clear if these cysteine residues are also important for the infectivity of HBV. Since the S-domain is present in all three envelope proteins (L, M and S), the importance of S-domain in different envelope proteins is not well-understood. To answer this question, in the present study, we mutated the cysteine residues in the L and S proteins and further determined virus assembly and infectivity. Moreover, a previous work has suggested that HSPG is the primary attachment site for HBV. We tried to correlate the infectivity of viruses bearing cysteine mutation with their binding activity to heparin, and explore the role of the S-domain in virus entry of HBV.

2. Results

2.1 Optimization of HBV recombinant virus production and infection assay

2.1.1 Optimization of the viral production by transfection of complementary expression plasmids

In order to dissect the role of envelope proteins for the virus infectivity, it is important to establish a virus production system that allows production of virus carrying mutated envelope proteins. Since the ORFs of the viral polymerase and envelope genes overlap, mutations introduced into the envelope genes *in cis* change the sequence and possibly the function of the viral polymerase. Complementation is commonly used to avoid such interference through expression of envelope protein(s) from a helper construct.

To produce HBV particles, the *Sac*I fragment (3381bp) of pCHT-9/3091¹⁷⁷ containing 1.1-mer HBV genome (genotype D) was inserted into the pcDNA3.1 zeo(-) vector for introducing the selection marker and some useful restriction sites. This construct is designated HBV (kindly provided by Kerry Mill). Like its parental construct pCHT-9/3091, this plasmid support HBV replication and virus secretion. To prevent the expression of L protein, a point mutation was introduced at the start codon of the L-ORF (ATG to ACG). This construct was designated HBV L⁻ (kindly provided by Kerry Mill). The introduced mutation remains silent in the overlapping reading frame of the viral polymerase. A helper construct was generated by insertion of the L ORF into *Nhe*I-*Hind*III sites of pcDNA3.1/Zeo(-) vector to express the wild type HBV L protein (genotype D), designate as wt L (kindly provided by Kerry Mill).

It has been shown that the N-terminus of L protein contains a retention signal, which retains the S protein in the ER membrane and inhibits the secretion of subviral and viral particles¹⁷⁸. Thus the expression level of the L protein might interfere with virus production. Therefore, the ratio of genomic construct (HBV L⁻) to the helper construct (wt L) has to be optimized for virus production. HuH-7 cells were co-transfected with different ratio of these two plasmids and the supernatants of cell cultures day 3-8 post transfection were applied to the CsCl density gradient centrifugation, and fractions of the gradient were analyzed by HBV specific DNA dot-blot. In addition to subviral particles and virions, free capsids are secreted into the supernatant by an unknown mechanism, but they have a higher density compared to the enveloped capsids, i.e., virus particles. As expected, the lacking of L protein abrogated virus production and the complementation with helper construct rescued virus production. The ratio of 5:1 (genomic : helper) facilitated the virus production up to a level in which the L proteins are intrinsically expressed (Fig. 7).

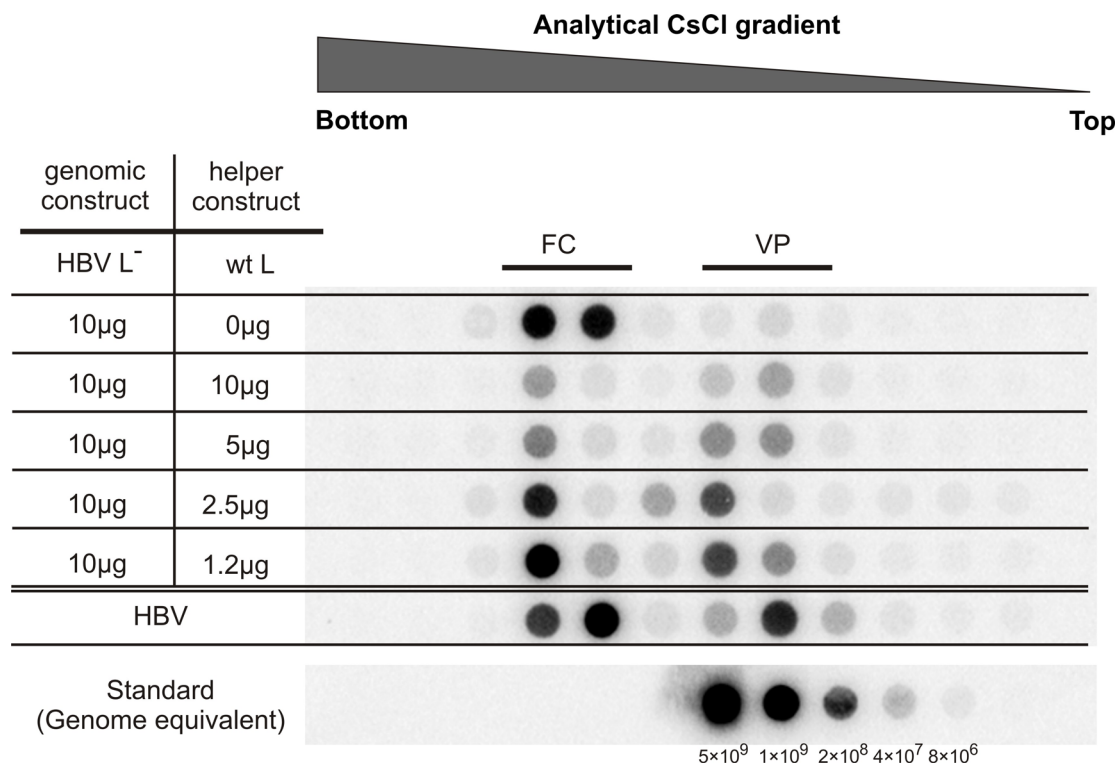


FIG. 7. Titration of the genomic construct and helper construct for complementary viral production HBV-DNA specific Dot-blot of fractions of analytical CsCl density gradients obtained from supernatants of transfected HuH-7 cells, which have been transfected with different ratios of genomic construct (HBV L⁻) and helper construct (wt L). The parental construct (HBV) supporting HBV replication was also included. Linearized pCHT-9/3091 at the indicated copy numbers were used as the standard. Note that transfection with the HBV genomic construct and the helper construct expressing L-protein resulted in secretion of both viral particles (VP) and free nucleocapsids (FC).

Based on the result, in the following experiments, co-transfections were consistently performed with 10μg of genomic construct and 2μg of the helper construct (ratio of 5:1) for a 10-cm dish of HuH-7 cells to produce virus particles.

2.1.2 Kinetics of virus production following co-transfection

To quantify the kinetics of particle production in HuH-7 cells following co-transfection, the supernatant was collected at different time points post-transfection, and virus production was determined by CsCl gradient centrifugation and DNA dot-blot analysis.

As shown in Fig. 8, the production of free capsids dropped more rapidly than the production of virions, which kept relatively constant for 2 weeks. Considering that both constructs are driven by the CMV-promoter, it is possible that the decline of free capsids reflects the kinetics of CMV-promoter-driven transcription of pregenomic RNA and the formation of subsequent capsids. The limiting factor for virus secretion in this scenario could be the L protein, which might accumulate at the ER membrane for a relatively long period.

Based on these result, in the following experiments, the supernatant of days 3-8 (or mixed with supernatant of days 8-13) post-transfection were routinely collected for subsequent quantification of the virus assembly and infectivity.

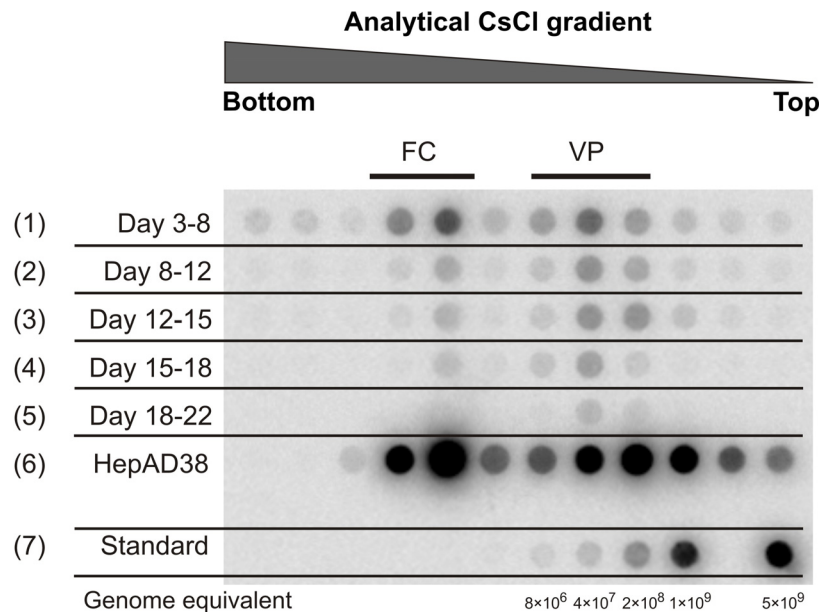


FIG. 8. Kinetics of recombinant viral production

HBV-DNA specific Dot-blot of fractions of an analytical CsCl density gradient of the supernatants of HuH-7 cells transfected with a mixture of genomic construct (HBV L-) and helper construct (wt L) at a ratio of 5:1. These supernatants were collected at different time points post-transfection and concentrated by PEG-precipitation before applying them to a CsCl density gradient (row 1-5). Also included was the supernatants obtained from cultivated HepAD38 cells in the absence of tetracycline (row 6). Linearized pCHT-9/3091 with indicated copy numbers was used as the standard (row 7). FC, free nucleocapsid; VP, viral particle.

2.1.3 Anti-core IF staining of infected HepaRG cells

To detect infection events on the single-cell level, it is important to select an antibody that specifically binds to an intracellular viral marker. Since the recombinant virus is deficient for L protein expression, the anti-core antisera were chosen to perform the IF staining.

Several polyclonal antibodies were tested against the core protein (#158, #312 and H363) for the IF staining (Fig. 9A). All of them were suitable for the IF staining, judged by the following observations: (1) infection could be seen only in a subset of HepaRG cells, i.e., differentiated hepatic cells; (2) the IF signal was specific and in marked contrast to uninfected cells; (3) single-cell-staining patterns showed that the core protein was associated with nuclei and speckle-like structures in the cytoplasm, especially profound with antibody H363. Thus, H363 was used as the antibody for anti-core staining in the following studies, if not specified otherwise.

To optimize the IF assay, the HepaRG cells were infected with a concentrated virus stock from the supernatant of HepAD38 cells. The cells were fixed at different time points and stained for

the presence of the core protein (Fig. 9B). As shown, the overnight inoculation of virus with HepaRG cells led to a strong core-staining (Day 1) although the cells had been intensively washed for 3 times with PBS before the IF staining. The signals were specific but it was hard to distinguish between membrane-associated viral particles and free capsids. Irrespective of this, the signal decreased quickly afterwards and the specific staining of the expressed core protein of infected cells (as mentioned above) emerged and became dominant over time. In the cells with the typical staining patterns as described above, a few infection events were identified at day 4 post-infection. However, the strongest signal from the infected cells was obtained at day 13.

In the following experiments, the IF-staining was routinely performed at day 13 post-infection.

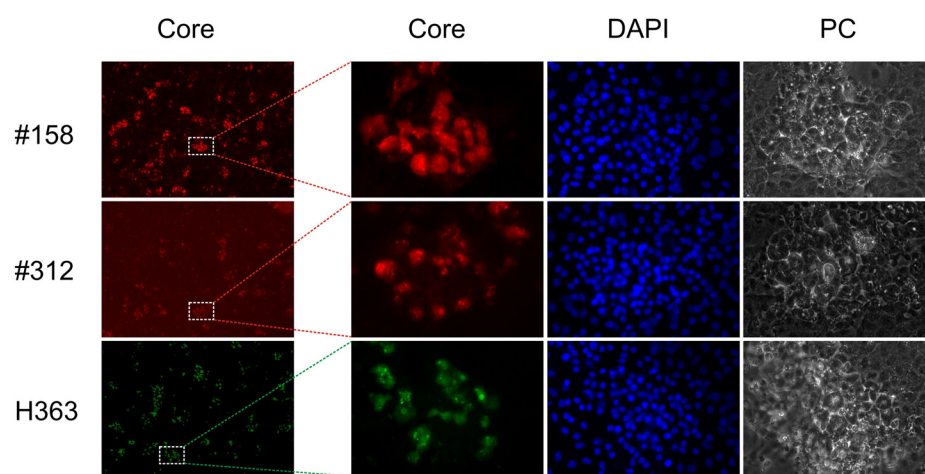
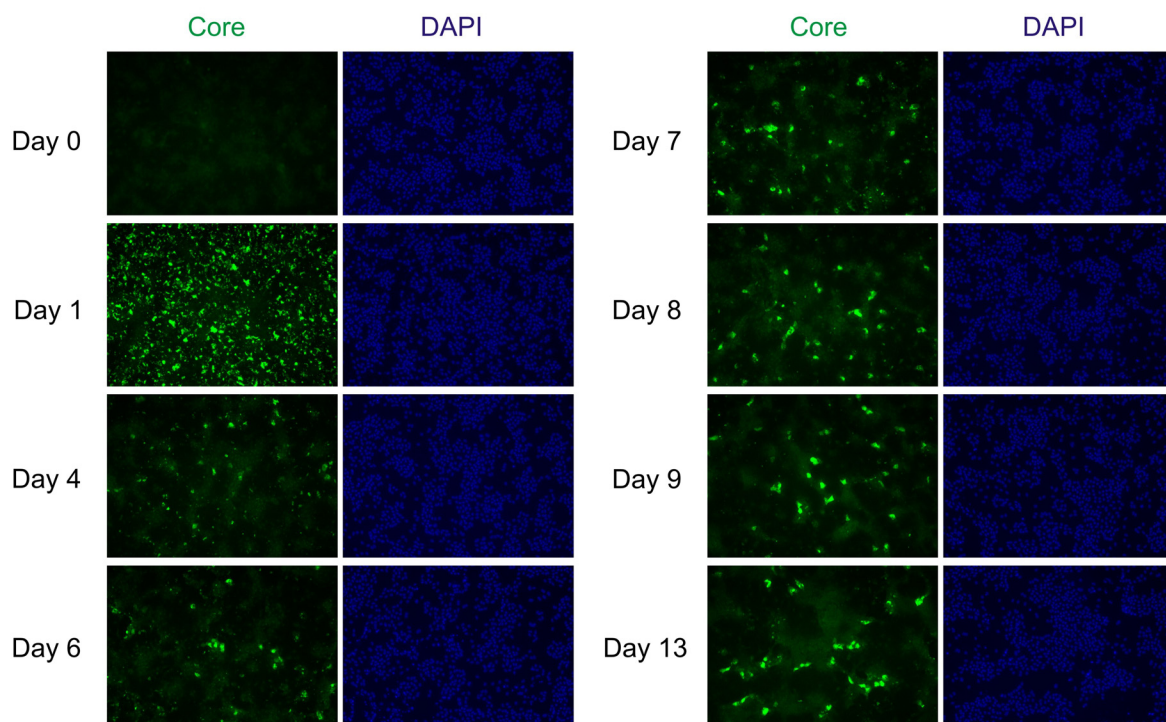
A**B**

FIG. 9. Anti-core immunofluorescence analysis of the HBV infection in the HepaRG cells

A. HepaRG cells 13-days post-infection were stained with the polyclonal rabbit antiserum (H363) or polyclonal mouse antiserum (#158, #312) against HBV core protein (the first column from the left). The higher magnification of the selected region (dashed box) is shown in the second column. The identical regions with nuclei-staining (DAPI, column 3), phase-contrast graph (PC, column 4) and the merged pictures (column 5) are shown as well. B. Kinetic of core-protein expression in HepaRG cells post-infection with virus prepared from HepAD38 cells. HepaRG cells were washed and fixed before the infection (Day 0), or after the infection at the indicated time points (Day 1, 4, 6, 7, 8, 9 and 13). Then the cells were subjected to the IF analysis by polyclonal anti-core antiserum H363 (green) and the cell nuclei were stained by DAPI (blue).

2.1.4 Quantification of the infection by secreted viral markers and the number of infected cells

HBV infection can be quantified by secreted viral proteins such as HBsAg and HBeAg. To explore the possibility to quantify infection by more sensitive IF staining at a single cell level, the number of infected cells was quantified and correlation with the secreted HBsAg and/or HBeAg, which is measured by microparticle enzyme immunoassays (MEIA), was evaluated.

HepaRG cells were infected with a virus stock prepared from HepAD38 cells (Fig. 10A) or virus preparation following co-transfection of HuH-7 cells with HBV L and wt L (Fig. 10B). In addition, the infection was performed in the presence of inhibitory peptide at different concentration (Fig. 10C). In all of the cases, the number of infected cells correlated with the secreted viral marker independent of the source of the virus. This correlation was also observed when the infection was inhibited by the peptide, HBVpreS/2-48^{myr}, in a dose-dependent manner. The anti-core staining of the cells post-infection are also shown in Fig. 10D.

The data indicates that the infection events can be quantified by counting infected cells even when the HBsAg and HBeAg have decreased below the cut-off value of MEIA. Therefore, counting of infected cells after IF staining is a more sensitive method than the commercial HBsAg and HBeAg assay we used.

More importantly, the two read-out of infection based on the number of infected cells and the secreted HBsAg both showed a linear correlation with the virus input in a broad range. This fact demonstrates the possibility to compare the infectivity of virus without infecting cells with the same amount of virions. Instead, both of the read-outs (HBsAg and cell number) can be normalized to the amount of virus input after infection to calculate the specific infectivity.

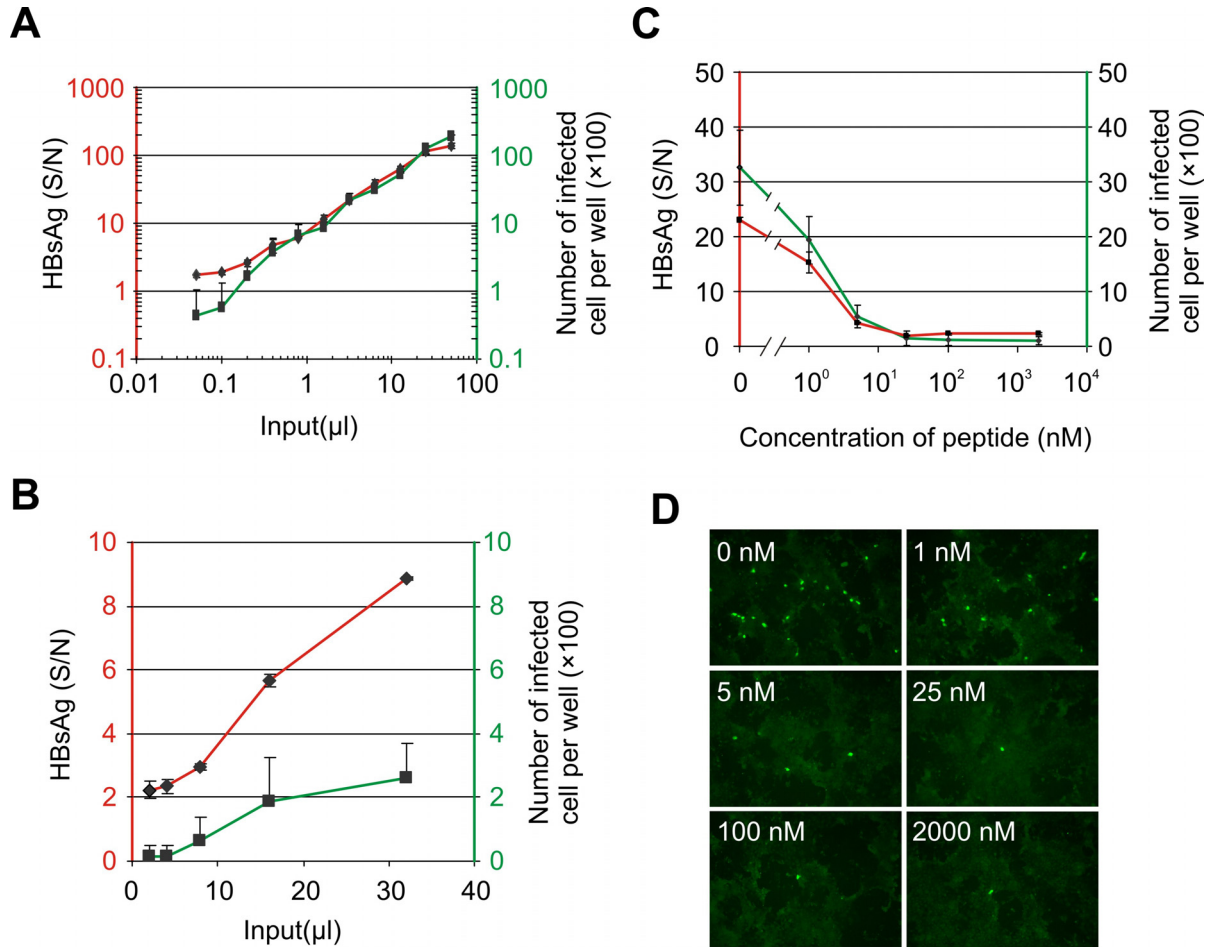


FIG. 10. Correlation of the secreted viral marker and the number of infected cells

A. HBsAg (red line) secreted from day 8-13 post-infection of HepaRG cells with concentrated virus from cell culture supernatants of HepAD38 cells. The amount of virus used for infection varied from 0.05 μl to 50 μl , which resulted in a multiplicity of 10 to 10000 genome equivalents per cell. Quantification on the single cell level was performed by counting HBcAg-positive cells 13 days post-infection (green line).

B. HBsAg (red line) secreted from day 8-13 following infection of HepaRG cells with concentrated virus from cell culture supernatants obtained from HuH-7 cells, which were co-transfected with HBV L₁ and wt L₁. The amount of virus used for infection varied from 2 μl to 32 μl . Quantification on the single cell level was performed by counting HBcAg-positive cells 13 days post-infection (green line).

C. HBsAg (red line) secreted from day 8-13 following infection of HepaRG with concentrated virus from HepAD38 cells in the absence (0 nM) or in the presence of different concentration (1, 5, 25, 100, 2000 nM) of inhibitory peptide. Quantification on the single cell level was performed by counting HBcAg-positive cells 13 days post-infection (green line).

D. HBcAg-specific immunofluorescence (green) of HepaRG cells 13 days post-infection with concentrated virus from HepAD38 cells in the absence (0 nM) or in the presence of different concentration (1, 5, 25, 100, 2000 nM) of the inhibitory peptide, HBVpreS/2-48^{myr}.

2.1.5 Optimization of the infection-the effect of DMSO

It has been shown in DHBV infection assay¹⁶⁹, that the addition of DMSO to the culture medium could maintain the differentiation state of duck hepatocytes and dramatically prolong the susceptibility to DHBV infection. During the cultivation of the HepaRG cells, it has also been shown that DMSO could differentiate the progenitor HepaRG cells into epithelial-like cells and hepatocyte-like cells, which are susceptible to HBV infection. It is recommended that the

HepaRG cells are grown for 2 weeks, and then cultivated with 2% DMSO to be differentiated for additional 2 weeks before they can be used for HBV infection¹⁷¹. Since the concentrations of DMSO have a significant influence on cell differentiation and consequently susceptibility, the effect of DMSO was therefore systematically evaluated to optimize virus infection.

For this purpose, the effect of DMSO on virus infection was evaluated during three different time periods (Fig. 11A), i.e., 2 weeks before the inoculation, the overnight inoculation, and post inoculation. The effect of DMSO on the infection assay 2 weeks before the inoculation was investigated, during which period the DMSO was considered to accelerate the differentiation process. Surprisingly, the absence of DMSO during “differentiation period” yielded a higher HBsAg compared to 2% DMSO, which was recommended (Fig. 11B). Further titrations revealed that constant 0.5% DMSO resulted in the optimal infection (Fig. 11C, Fig. 11D).

Next the effect of DMSO during inoculation was investigated. The HepaRG cells pretreated either with 0.5% or 2% DMSO were infected in the presence of 0, 0.5, 1.0, 1.5 and 2.0% DMSO. Additionally, the necessity of fetal calf serum (FCS) during this period was tested. The results showed that 2% DMSO and the presence of FCS (10%) during the inoculation led to the highest values of secreted HBsAg (Fig. 11E). Finally, the effect of DMSO post-inoculation was investigated. Based on the information from previous results, two batches of HepaRG cells were treated with 0.5% DMSO for 2 weeks prior to infection and then inoculated with virus in the presence of 2% DMSO. The cells were further cultivated in medium with different concentrations of DMSO. The maximal infection was achieved with 2% DMSO post-inoculation (Fig. 11F). The infection of HepaRG cells with an optimized DMSO concentration largely improve the efficacy of infection, as demonstrated by the secreted HBsAg in 1:4 diluted supernatant (S/N: ~100).

To summarize the results, the optimized DMSO recipe for the infection assay is the following: The HepaRG cell should be grown for 2 weeks without DMSO, and further treated with 0.5% DMSO for 2 weeks, and then the cells should be infected and further cultivated in the presence of 2% DMSO.

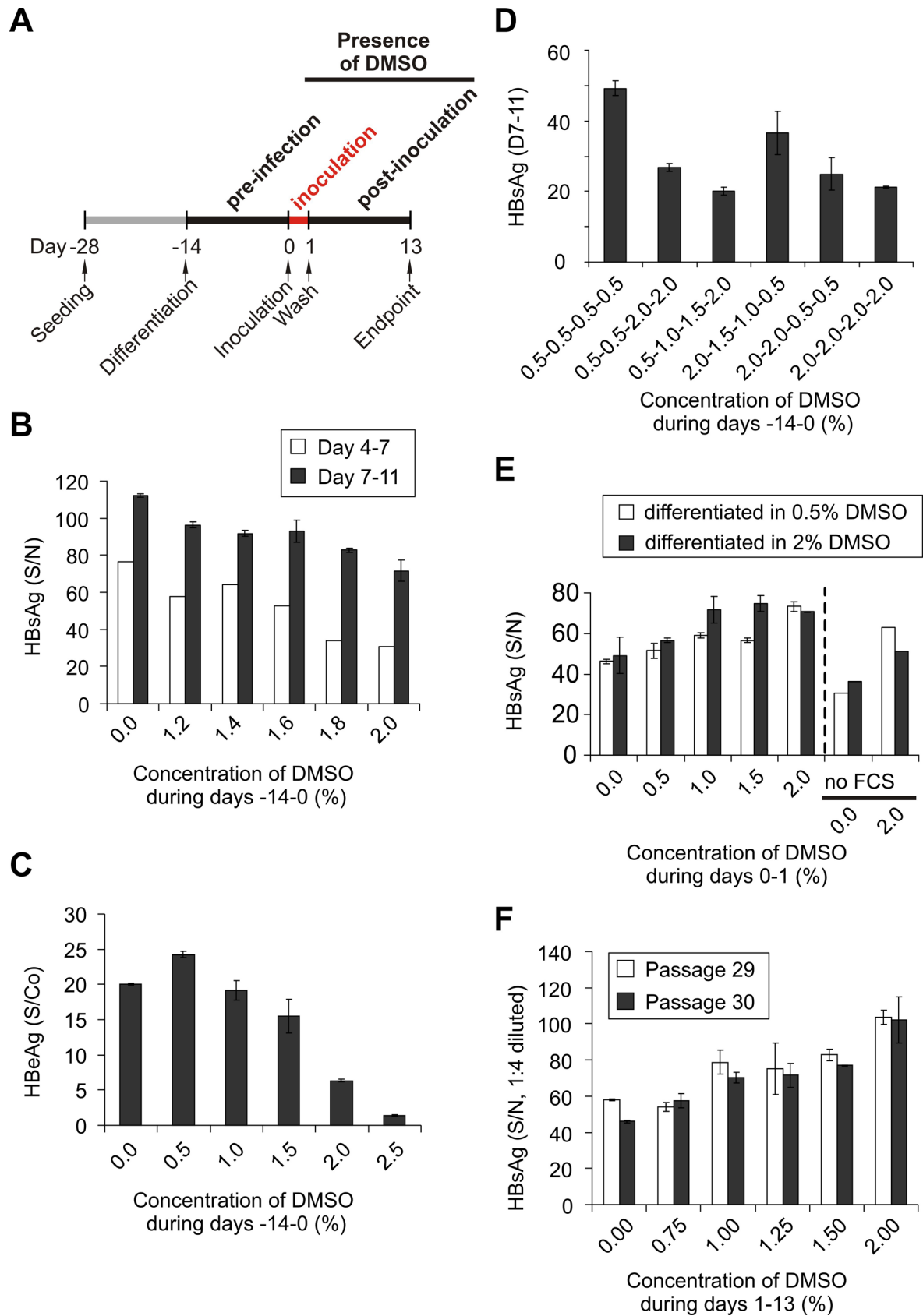


FIG. 11. The effect of DMSO on HBV infection of HepaRG cells.

A. Schematic illustration of the cultivation and the infection of HepaRG cells. The detailed procedure is described in the "Material and Methods". Note that DMSO is present in three periods defined as pre-infection, inoculation and post-inoculation.

B-D. The influence of DMSO during the pre-infection period on infection. During the pre-infection period of 2 weeks, HepaRG cells were treated with 0%, 1.2%, 1.4%, 1.6%, 1.8% or 2% DMSO (B), or with 0%, 0.5%, 1%, 1.5%, 2% or 2.5% of DMSO (C). In addition, the cells were treated with gradually increased concentration of DMSO from 0.5%, 1.0%, 1.5% to 2% (0.5-1.0-1.5-2.0) or from 0.5%, 0.5%, 2.0% to 2% (0.5-0.5-2.0-2.0) during this period. Similarly, gradually decreased or constant concentration of DMSO (2.0-2.0-0.5-0.5, 2.0-1.5-1.0-0.5, 0.5-0.5-0.5-0.5, 2.0-2.0-2.0-2.0) were used during this period (D). Infection was performed using standard procedure. The supernatant of cells were collected at the indicated time points and the amount of HBsAg or HBeAg was determined.

E. The influence of DMSO during inoculation on HBV infection. HepaRG cells were treated with 0.5% or 2.0% DMSO for two weeks before infection. During the overnight inoculation period, indicated amount of DMSO (from 0% to 2.0%) were presented. The supernatant of cells between day 7-11 post-infection were collected and the amount of HBsAg was determined.

F. The influence of DMSO post-inoculation on HBV infection. HepaRG cells were treated with 0.5% DMSO before infection and incubated with virus in the presence of 2.0% DMSO. After infection, the cells were further cultivated at the indicated concentration of DMSO. The diluted cell supernatant (1:4) of days 7-11 post-infection were analyzed for the amount of HBsAg. For this experiment, two different passages, P29 (white bar) and P30 (black bar), of HepaRG cells were used.

2.1.6 Optimization of the infection-the effect of “spin inoculation”

It has been shown that heparan sulfate proteoglycans (HSPG) on the surface of hepatocytes can facilitate the attachment of HBV to the cells and the addition of PEG during the inoculation improves the infection by increasing the primary attachment via HSPG⁴². Based on these observations, HBV infection strongly relies on a close contact between the virus and cells. Spin inoculation has been used for some viruses, such as the lentivirus, to improve the efficiency of infection¹⁷⁹. Thus, next question was: does the centrifugation also improve the infection of HBV in HepaRG cells?

To answer that, HepaRG cells was inoculated with virus and subsequently centrifuged at different speeds and for different periods. Fig. 12 A showed that efficiency of infection was enhanced slightly in an input-dependent and specific manner when centrifugation was performed at 280g for 5 minutes. When the speed and time of centrifugation was increased, the efficiency of infection was further elevated. A maximal elevation of 50% was observed when the virus/cells were centrifuged at 1200g for 90 minutes (Fig. 12). Indeed, the HepaRG cells tolerate these centrifugation procedures.

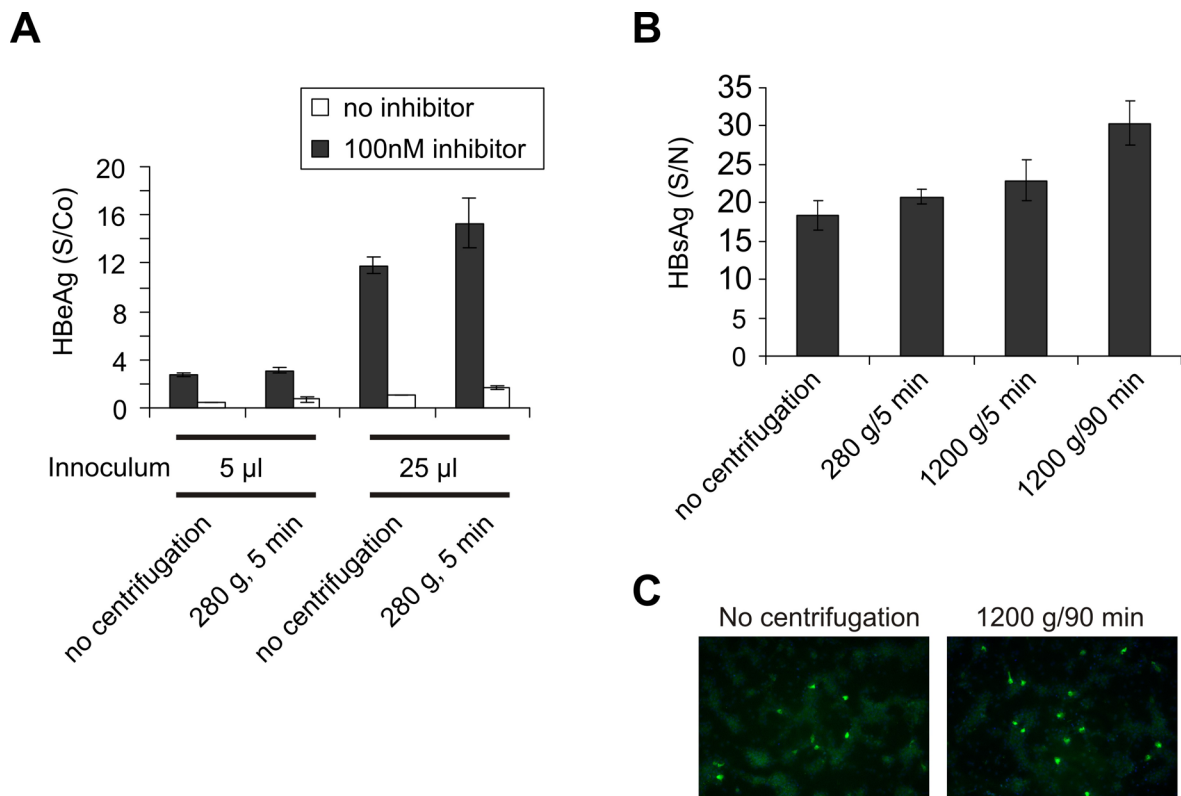


FIG. 12. The influence of centrifugation on the infection assay

A. HBeAg secreted from day 4-7 following infection of HepaRG cells by 5 µl or 25 µl virus stock without (no centrifugation) or with spin-inoculation. For spin-inoculation, HepaRG cells with inocula were centrifuged at 280 g for 5 minutes immediately after the inoculation (280 g/5 min). To control the specificity of infection, virus inoculation was performed in the absence (black bars) or presence of 100 nM HBVpreS/2-48^{myr} (white bars).

B. HBsAg secreted from day 8-13 following infection of HepaRG cells by virus stock without (no centrifugation) or with spin-inoculation at different parameter (280 g/5 min, 1200 g/5 min, 1200 g/90 min).

C. Immunofluorescence staining 13 days following infection of HepaRG cells without or with spin-inoculation (1200 g/90 min). The infected cells were visualized by staining with polyclonal rabbit antiserum (H363) against HBV core protein (green).

2.1.7 Optimization of the infection-the effect of PEG

For in vitro infection of primary human hepatocytes (PHH) and HepaRG cells, PEG was commonly added during the inoculation with HBV to increase the efficiency.

To infect HepaRG cells, the viral inoculum diluted in culture medium were mixed with PEG (final concentration of 4%) before it was incubated with the cells. In order to investigate the stability of virus inoculum in the presence of PEG, the mixture of virus with PEG was immediately used to inoculate the cells or was incubated for different time periods before the inoculation. There is no significant difference on infection (Fig. 13A), suggesting that inoculum containing PEG is quite stable for at least 6 hours.

Furthermore, two concentrations of PEG commonly used for the HBV/HDV infection assay were compared. Two batches of HepaRG cells were infected in the presence of 4% or 5% of PEG, there is no significant difference as shown by IF staining (Fig. 13B).

In summary, the virus inoculum containing PEG is quite stable, and 4% or 5% of PEG can both be used for HBV infection.

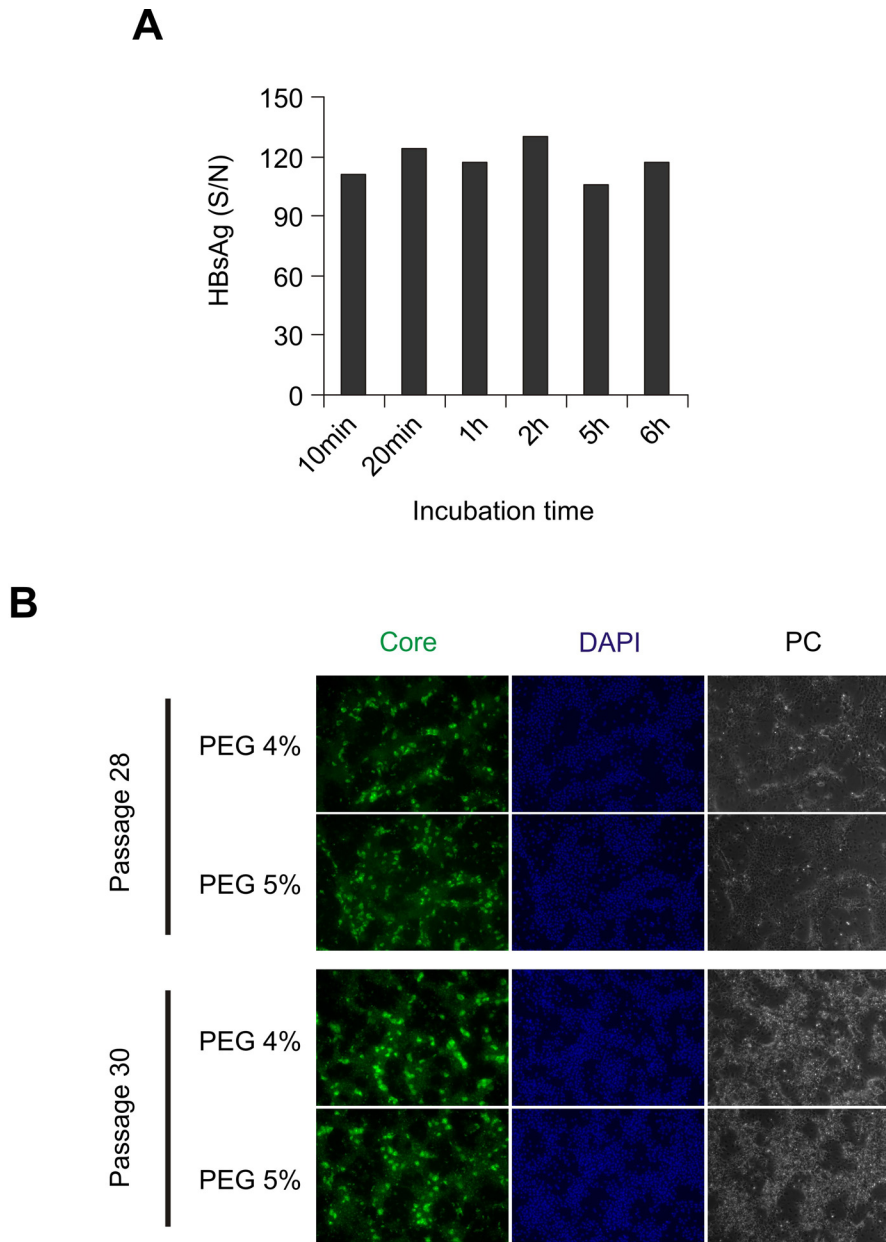


FIG. 13. The influence of PEG on the infection assay

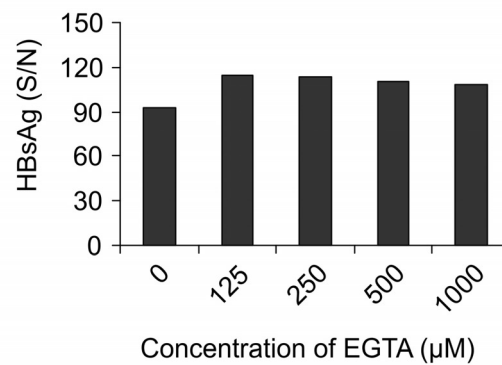
A. HBsAg (day 7-11) secreted from HepaRG cells post-infection. Concentrated virus from HepAD38 cells were mixed with 4% PEG for the indicated time periods before the incubation with HepaRG cells.

B. HBcAg-specific immunofluorescence of HepaRG cells 13 days post-infection. Concentrated virus from HepAD38 cells was inoculated with two different passages of HepaRG cells (Passage 28 and Passage 30) in the presence of 4% or 5% PEG. The infected cells were stained with polyclonal rabbit antiserum (H363) against HBV core protein. The identical region with nuclei-staining (DAPI), or phase-contrast (PC) is shown as well.

2.1.8 Optimization of the infection-the effect of EGTA

The previous results in our lab (Kerry Mills and Andreas Schulze, unpublished results) showed that EGTA treatment of HepaRG cells could enhance the infection, and suggested that EGTA treatment might open the tight junction between cells and make a subset of differentiated cells accessible and thus susceptible to virus infection. Here this observation was confirmed again in the optimized infection procedure.

A



B

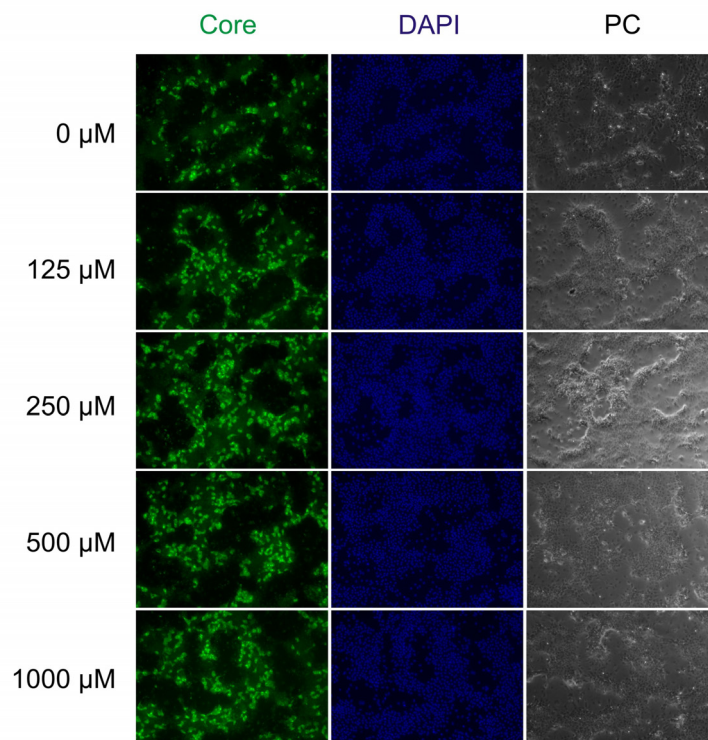


FIG. 14. The influence of EGTA on the infection assay

A. HBsAg secreted from day 7-11 following infection of HepaRG cells with concentrated virus from HepAD38 cells. Prior to infection, the HepaRG cells were treated with EGTA of indicated concentration (0, 125, 250, 500, 1000 μM) for 5 minutes.

B. Immunofluorescence staining 11 days following infection of HepaRG cells pre-treated with EGTA as described in (A). The infected cells were visualized by staining with polyclonal rabbit antiserum (H363) against HBV core protein (the left column). The identical regions with nuclei-staining by DAPI (the middle column), phase-contrast graph (PC, the right column) are shown as well.

The HepaRG cells were treated with the optimized DMSO recipe as mentioned above, and then treated with different concentrations of EGTA for 5 minutes. The virus inoculum was incubated with HepaRG cells and then centrifuged at 1200 g for 90 minutes. The EGTA treatment slightly increases the infection as shown by secreted viral markers (Fig. 14A) or IF staining of cells (Fig. 14B). However, the enhancement of infection was not concentration-dependent at least in the tested range.

With all the optimized procedures tested so far, the infection efficiency of HBV on HepaRG cells can be significantly increased to achieve ~30% infection of differentiated cells (Fig. 14B).

2.1.9 The effect of passage number on HBV infection

The HepaRG cell line derived from a patient with hepatocellular carcinoma. Interestingly, these cells exhibit an undifferentiated morphology (characterized by active dividing) when seeded at low density, and after having reached confluence they formed typical hepatocyte-like colonies surrounded by epithelial-like cells^{172,173,180}. Similar phenomenon was observed in the present study that the cells formed hepatocyte-like and epithelial-like cells one week after seeding in the absence of DMSO. This hinted that they already differentiated to some extent when they reach confluence. However, when they were passaged at low cell density, they again acquired the undifferentiated morphology and divided actively as described¹⁷². The reversible differentiation raised a question: how often they can be differentiated and dedifferentiated during the cell passaging without loss of their susceptibility to perform the infection assay.

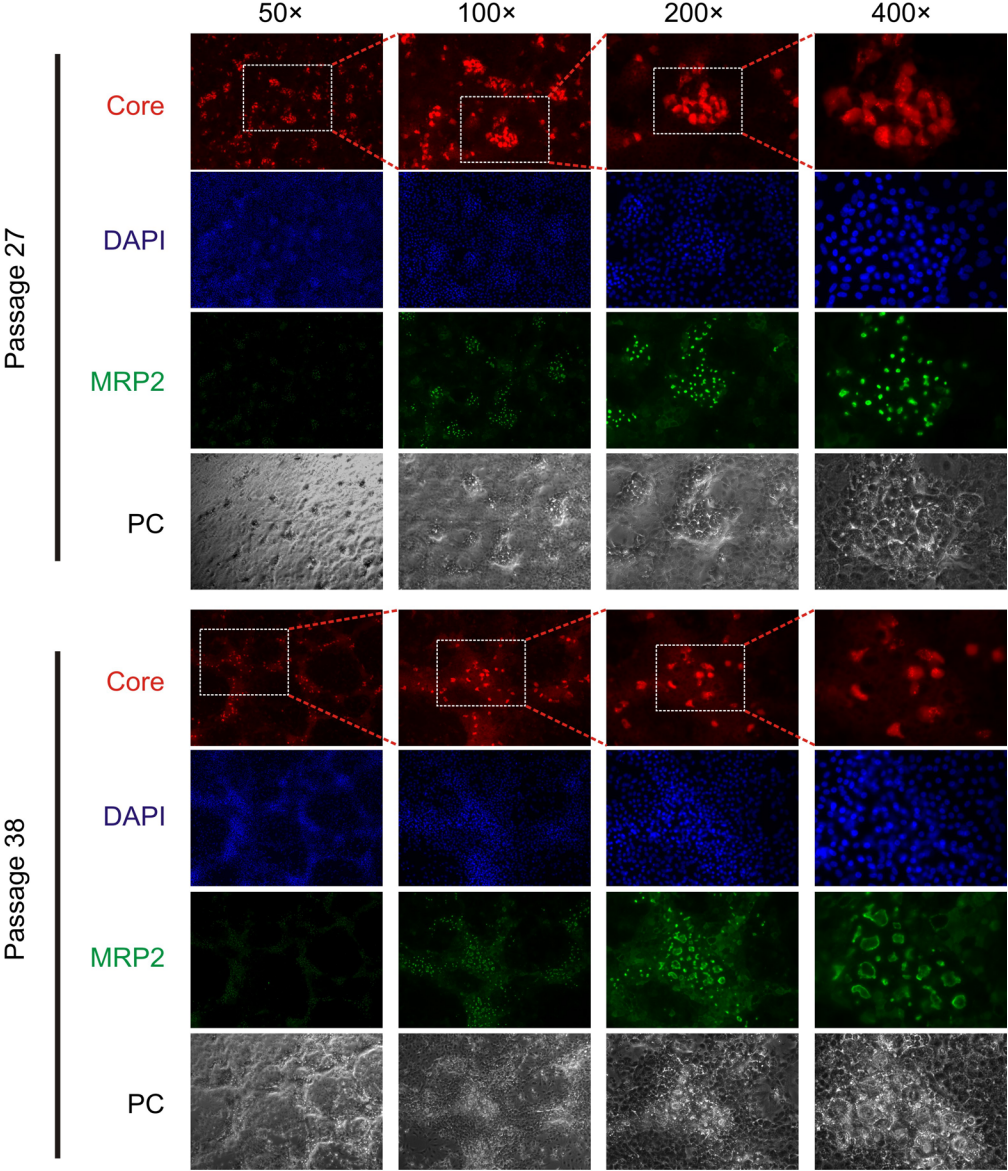
To answer the question, HepaRG cells with two different passage numbers, passage 27 (P27) or 38 (P38), were seeded and further differentiated. The same amount of inoculum was used to infect the cells at the same time and the secreted viral markers were measured at day 11.

Additionally, the cells were stained for the core protein (d13 post-infection) and a differentiation marker, multidrug resistance-associated protein 2 (MRP2). MRP2 has been characterized as an ATP-dependent membrane transport protein, which is responsible for the biliary excretion of a diverse range of substrates, including glutathione and organic anions. It is located exclusively on the canalicular membrane (apical membrane) of the hepatocytes¹⁸¹ and, thus, is a marker for differentiation and polarization. The morphologies of two passages of HepaRG cell were different. While P27 cells displayed small but abundant hepatocyte islands, the older passage (P38) formed large but connected hepatocyte region. The patterns of MRP2 staining also

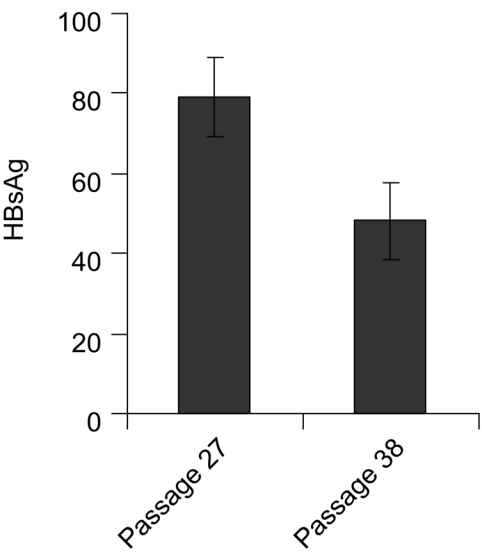
support their different morphology (Fig. 15A). In both cases, only the hepatocyte regions were infected, although the infection on the early passage (P27) was slightly higher than on the late one (P38) (Fig. 15B). The anti-core staining and different cell morphologies were also shown in a higher magnification (Fig. 15C). As observed previously (Kerry Mills and Andreas Schulze, unpublished data), most infected HepaRG cells were well-polarized as shown by the MRP2 staining.

Collectively, the HepaRG cells can be cultivated, differentiated and dedifferentiated extensively for a long time without loss of their susceptibility to HBV infection. For most of the following experiment, infection assay was performed with HepaRG cells between passage 27 and 38.

A



B



C

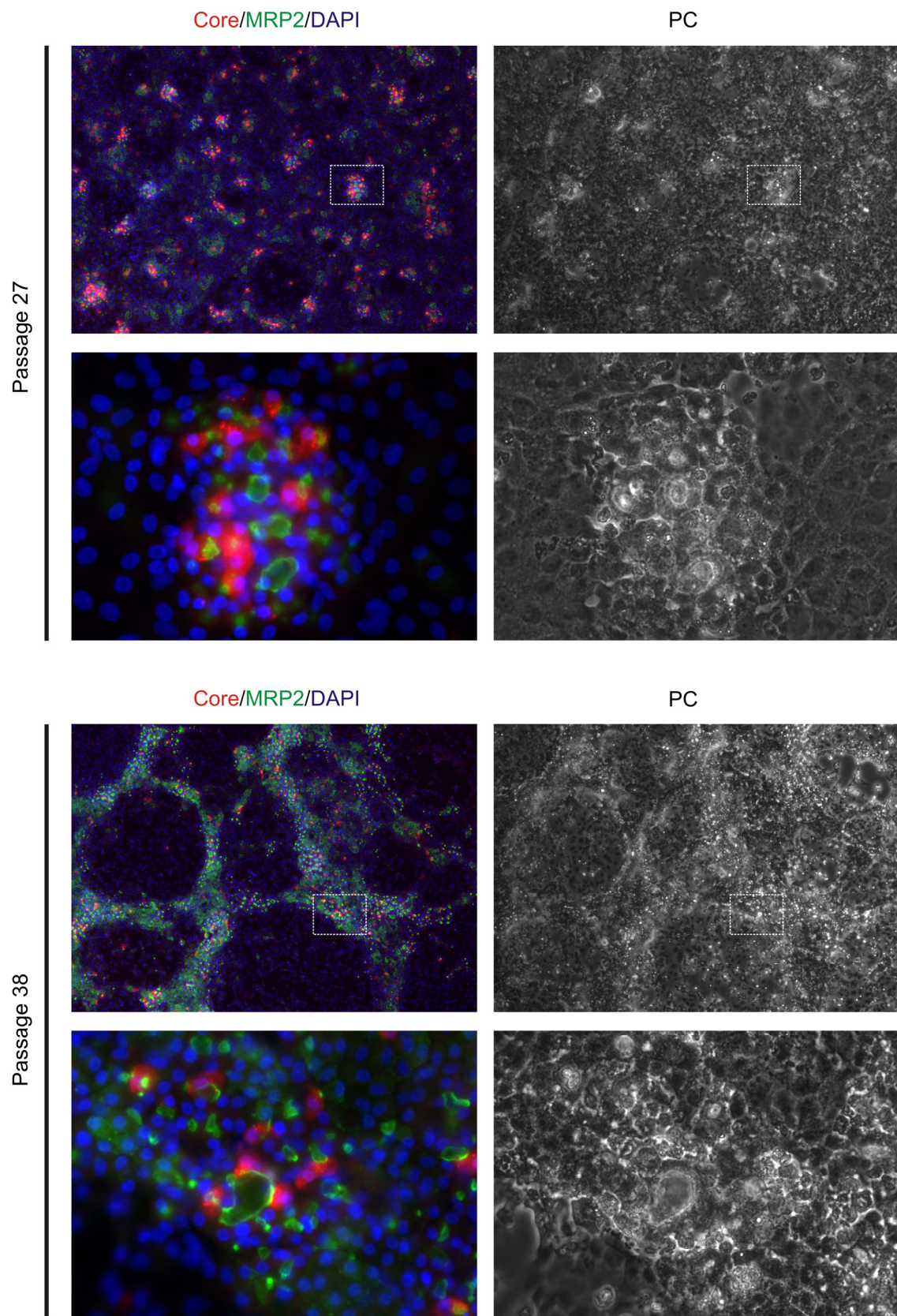


FIG. 15. The effect of passage number on the infection assay

A. Two passages of HepaRG cells (Passage 27 and Passage 38) 13-days post-infection were stained with mouse anti-core antiserum (Core) and rabbit anti-MRP2 antiserum (MRP2). The identical regions with nuclei-staining (DAPI)

and phase-contrast graph (PC) are shown as well. The higher magnification of the selected regions (dashed box) is showed in next column to the right.

B. HBsAg secreted from day 7-11 following infection of two passages of HepaRG cells (Passage 27 and Passage 38).

C. Staining pattern and morphology of two passages of HepaRG cells (Passage 27 and Passage 38). For each passage, the staining of core protein (red), MRP2 (green) and nuclei (blue) are merged in the left column, while the phase contrast graph (PC) was shown in the right. The higher magnification of selected regions (dashed box) is shown below.

2.2 The N-terminus of preS1 domain serves a critical function for virus infectivity

It has been shown that the preS1 domain of the L protein play different roles in the HBV life cycle. Present inside of the virus particle, the preS1 domain contains elements crucial for virus assembly⁹⁴, and other activities such as binding to heat shock proteins, of which the biological function remains unclear⁹¹. The preS1 is also known to be important for virus infectivity when it is present outside of the virus particle¹²¹. The region critical for virus infectivity is located within the N-terminal ~77 amino acids of preS1 domain (numbered according to genotype D). Mutagenesis analyses within this region in both HBV and HDV showed that deletion or substitution of 5 amino acids in this region abrogated virus infectivity^{121,122}. This region consists of three distinguishable elements, which is summarized according to currently available knowledge in Fig. 16. The first is the myristoyl group, which is covalently linked to the second amino acid (glycine) of preS1 domain. Secondly, concluded from characterization on inhibitory peptide, the N-terminal 47 amino acids of preS1 with essential region (aa 9-15) and accessory region (aa 28-48) are responsible for the binding of L protein to an unknown hepatocyte-specific receptor. The third is a region encompassing aa 49-78, which is also required for virus infectivity.

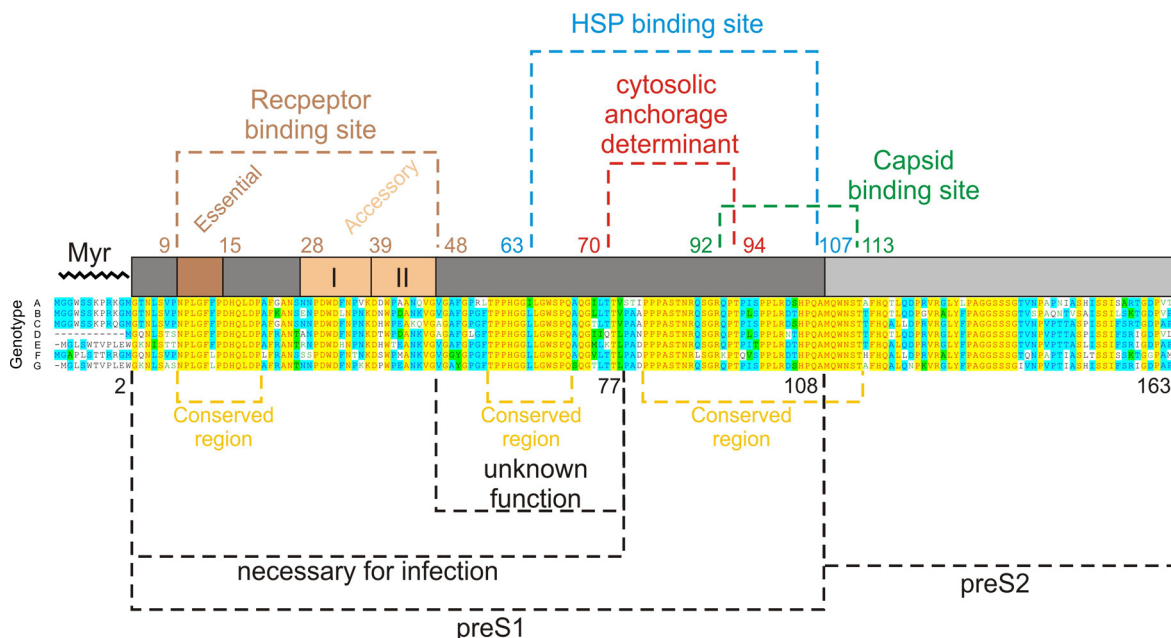


FIG. 16. Schematic representation of preS-domains from different genotypes

The HBV L-protein is myristoylated (Myr) at Gly-2 of the N-terminus of the preS domain. The potential receptor binding site (brown dashed line) within the preS1-domain is shown with an essential region (aa 9-15) and two accessory regions (aa 28-39 and 39-48). The cytosolic anchorage determinant (red dashed line), HSP (Hsc70) binding site (blue dashed line), capsid binding site (green dashed line) are indicated as well. The sequence is numbered according to genotype D (108 aa), in comparison with other genotypes (alignment produced with Vector NTI 11.0, highly conserved residues are labeled with yellow background). The preS1 and preS2 domains are

indicated (black dashed line below). Three conserved regions are shown (yellow dashed line below). aa 2-77 are known to be necessary for viral infection (black dashed line below), but aa 49-78 have an unknown function (black dashed line below).

The role of myristoylation is not fully understood. Although unmyristoylated preS1-derived peptide binds to hepatocytes to some extent (e.g. aa 2-48¹¹², aa 10-36⁴⁵, and the QLDPAF motif³⁸), the modification with myristic acid drastically increases the binding activity of HBVpreS/2-48^{myr} to hepatocytes (Anja Meier, unpublished results) and confer the peptide an inhibitory activity at nM concentrations. It seems that the myristoyl group plays a role by increasing the hydrophobicity of the N-terminus of L-protein, since the inhibitory activity of peptide are correlated with the length of hydrocarbon chain (C18,C16>C14>C8>c5)¹¹⁷. Thus it is reasonable to assume that the myristoyl group might increase the affinity of virus to the unknown receptor in a hydrophobicity-dependent manner. What the exact role of myristoylation is in the viral L protein and in the inhibitory peptide is one of the questions we address in this section.

Myristoylation is a post-translational modification processed by the cellular N-Myristoyltransferase (NMT) during or early after protein synthesis via recognition of the myristoylation motif, which is located in the N-terminus of the L-protein. The well known motif for N-myristoylation is MGXXXS/T¹⁸², which is present in the L proteins of all genotypes of HBV irrespective of their diverse N-terminal sequences. The diversity of N-terminal residues suggested that the sequence of aa 1-8 might just function as provider for a myristoylation signal. This is consistent with the loss of virus infectivity when 5 amino acids within this region are deleted¹²¹. Since a myristoylated peptide made up of aa 2-8 can not inhibit HBV infection, the suggestion from this observation is that aa 2-8 are not important for inhibitory peptide¹¹². However, our following studies showed that the activity of peptide, HBVpreS2-48^{myr}, was more drastically impaired when it was truncated at the N-terminus than at the C-terminus¹⁰⁴. This observation raised one of the questions that we want to answer in this section: do aa 1-8 just serve as myristoylation signal or are they required for virus infectivity?

Beside the well-defined binding site within the N terminus of preS1, the role of residues 49-78 is still enigmatic. Although it is apparently that aa 49-77 is also critical for virus infectivity^{121,122}, the peptide encompassing this region, HBVpreS/2-78^{myr}, has a reduced inhibitory activity compared to HBVpreS/2-48^{myr}¹¹⁷. This difference indicates that aa 49-78 may have a different function other than binding. The alignment of preS1 domain with L proteins from different genotypes shows that there is a conserved sequence as 57-TPPHGGIGWSPQ-68 within aa 49-78, beside the other two conserved regions in the receptor binding site (9-NPLGFFP-15) and capsid

binding region respectively (Fig. 16). Therefore, mutation analysis and infection-inhibition assay were also described in this section to address a possible role of aa 49-78.

2.2.1 Infectivity of genotypically L-protein pseudotyped HBV particles

As mentioned above, there are several conserved sequences in the viral L proteins of different genotype. Diverse regions can also be found, especially in the N-terminus of preS1 domain. The preS1 domain of genotype D encodes 108 aa while genotypes A, B and C encode 11 additional residues (MGGWSSKPRKG) in the N-terminus. The preS1 of genotype F also encodes 11 residues (MGAPLSTTRRG), while genotype E and G encode only 10 additional residues (MGLSWTVPLE) and the downstream methionine is substituted with tryptophan (M1W). Therefore, the first question was: can L proteins from other genotypes replace the function of genotype D L protein.

To answer this question, the L-ORF of genotype B, E and G were inserted into the NheI-HindIII site of pcDNA3.1 Zeo(-) vector. The difference in their N-terminus is shown (Fig. 17A). These constructs were verified by DNA sequencing (data not shown) and the L protein expressions were confirmed by Western blot (Fig. 17B). HuH-7 cells were co-transfected with L-deficient genomic construct, HBV L, (genotype D) without or with genotypically different helper constructs in order to produce pseudotyped virus. As shown, all these L proteins can rescue virus production as efficient as the L protein of genotype D (Fig. 17C). The infectivity of these pseudotyped viruses was quantified by measuring the secreted HBsAg and counting of infected cells. It was evident that the infectivity of these L-protein pseudotyped viruses was similar to the authentic genotype D virus. Moreover, in the presence of genotype-D derived peptides, HBVpreS/2-48^{myr}, the infections were inhibited to a comparable level (Fig. 17D-F).

A

L proteins		SEQUENCE in the N termini	Assembly	Infectivity
Genotype	D	MGQNLSTSNPLGFFPDHQLDPAFRANTAN ·····	+	+
	B	MGGWSSKPRKGMGTNLSVPNPLGFFPDHQLDPAFKANSEN ·····	+	+
	E	MGLSWTVPLEWGKNISTTNPLGFFPDHQLDPAFRANTRN ·····	+	+
	G	MGLSWTVPLEWGKNLSASNPLGFLPDHQLDPAFRANTNN ·····	+	+

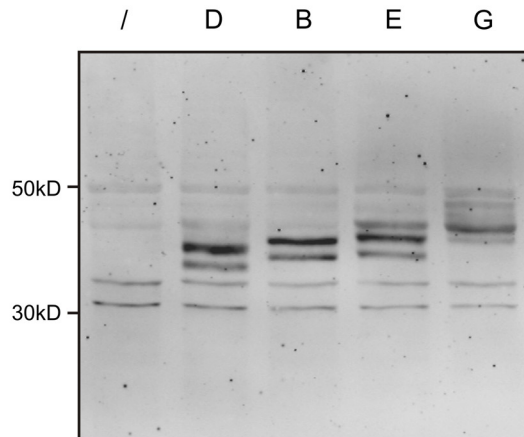
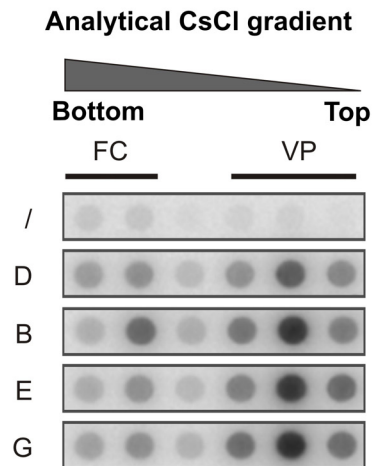
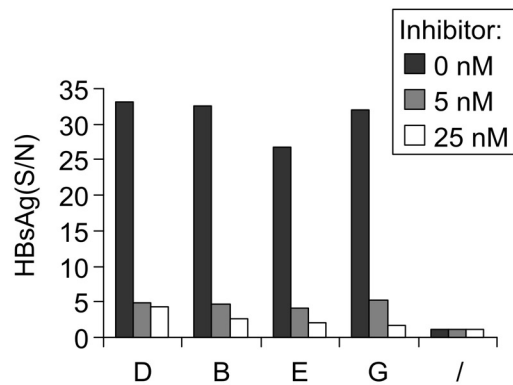
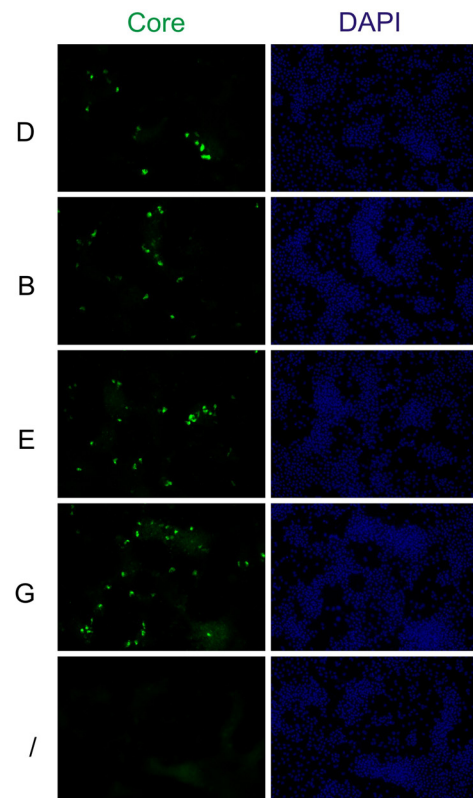
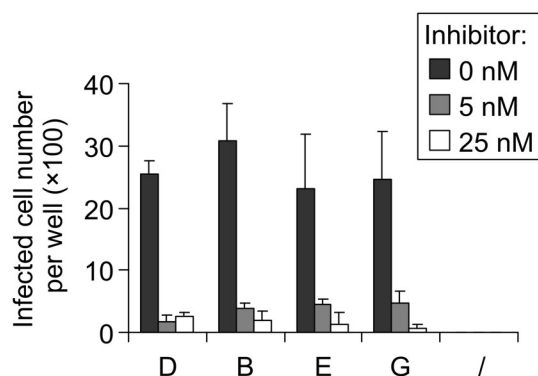
B**C****D****F****E**

FIG. 17. Assembly and infectivity of pseudotyped genotype-D virus carrying genotype-specific L proteins
A. Amino acid sequences of the N-terminus of L proteins of genotypes D, B, E, and G. The letters in red indicate the aa that differ from genotype D. The assembly and infectivity of virus with these L proteins are summarized on the right.

B Western blot of cellular extracts of HuH-7 cells 2 days post-transfection without (/) or with the genotype-specific L expression constructs (D, B, E and G).

C. Analysis of assembly and secretion of the pseudotyped virus bearing genotype-specific L proteins post-transfection. HBV-DNA specific Dot-blot of fractions of an analytical CsCl density gradient was obtained from concentrated supernatants of HuH-7 cells, which were transfected with a mixture of the genomic construct (HBV L₁) and helper constructs expressing genotype-specific L-proteins (D, B, E and G). As a control, the HuH-7 cells transfected without the helper expressing L-protein (/) was included.

D. HBsAg secreted from HepaRG cells day 8-13 p.i. by the pseudotyped virus bearing genotype-specific L protein. The concentrated supernatant was obtained from HuH-7 cells transfected with a mixture of genomic construct (HBV L₁) and helper constructs expressing genotype-specific L-proteins (D, B, E and G). To test their sensitivity against inhibitory peptide, virus inoculation was performed in the absence (black bars) or presence of 5 nM (grey bars) or 25 nM (white bars) HBVpreS/2-48^{myr}. As a negative control, the concentrated supernatant from HuH-7 cells transfected without the helper (/) was also incubated with HepaRG cells.

E. Quantification on the single cell level was performed 13 days post-infection by counting HBcAg-positive HepaRG cells infected with pseudotyped virus as described in (D).

F. HBcAg-specific immune fluorescence (green) of HepaRG cells 13 days post-infection with pseudotyped virus. Identical regions with nuclei-staining (DAPI) are shown in the right column.

This data demonstrates that L proteins from other genotypes can replace that of genotype D without losing viral assembly and infectivity. Because the envelope of these pseudo-particles is a mixture of genotypically different S- and L-protein, it can be concluded that neither genotype-specific interaction between L and S protein is required for both viral assembly and infectivity. Finally, the cross-inhibition of these pseudotyped viruses with a genotype-D derived peptide suggests that the peptide could be clinically used as an entry inhibitor for all genotypic HBV infections.

2.2.2 Infectivity of HBV carrying chimeric L proteins from genotypes D and B

Since the chimeric envelope (mixture of genotypically different S- and L-protein) does not interfere with virus assembly and infectivity, it is interesting to examine the influence of chimeric L proteins on assembly and infectivity. Although no genotype-specific interactions between L and S proteins are required, as shown previously, a possibility for interactions within L proteins still exists, e.g., interaction between that the preS and the S domain. If this interaction does exist and is genotype-specific, the chimeric L protein could become nonfunctional for assembly or infectivity.

Helper constructs expressing a panel of chimeric L proteins of genotype D and B (Fig. 17A) were produced according to the sequence alignment of these two L proteins. These constructs were verified by DNA sequencing and protein expressions were confirmed by Western blot (data not shown). The virus assembly was then determined by CsCl density gradients of concentrated virus obtained from transfected HuH-7 cells (Fig. 17B). The virus infectivity was tested in HepaRG cells (Fig. 17C). None of the chimeric L proteins interfered with virus assembly. Most chimeric L proteins did not impair the virus infectivity, suggesting that there is no genotype-specific interaction required between preS and S domain, and between preS1 and preS2 domain.

Intriguingly, the N-terminal 11 amino acids of genotype-B L-protein fused to that of genotype-D (B11-D) abolished viral infectivity to the background level. In contrast, 8 amino acid longer replacements (B19-D) restored the virus infectivity. Therefore, it is possible that, to keep the virus infectious, the additional N-terminal 11 amino acids of L protein of genotype B (numbering as aa -11/-1) have to be adjacent to its own downstream 8 amino acids. This result argued that there is a genotype-specific interaction within the N-terminus, i.e., between the N-terminal 11 amino acids and the following 8 amino acids.

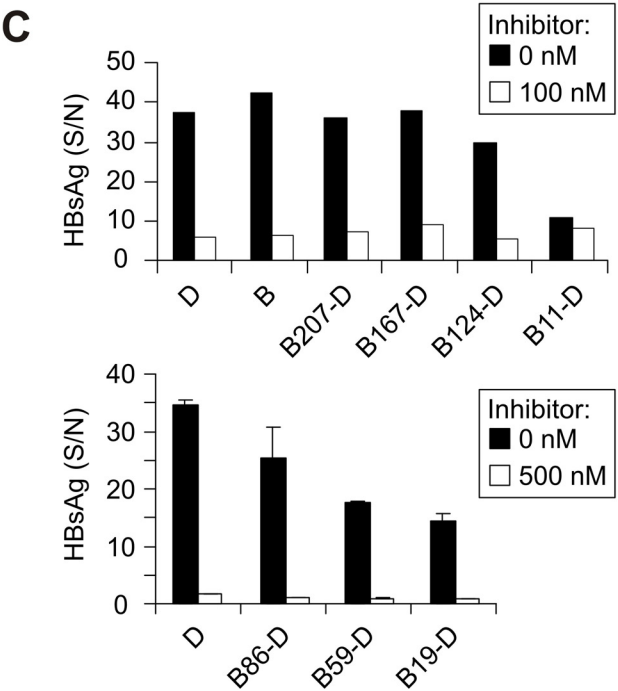
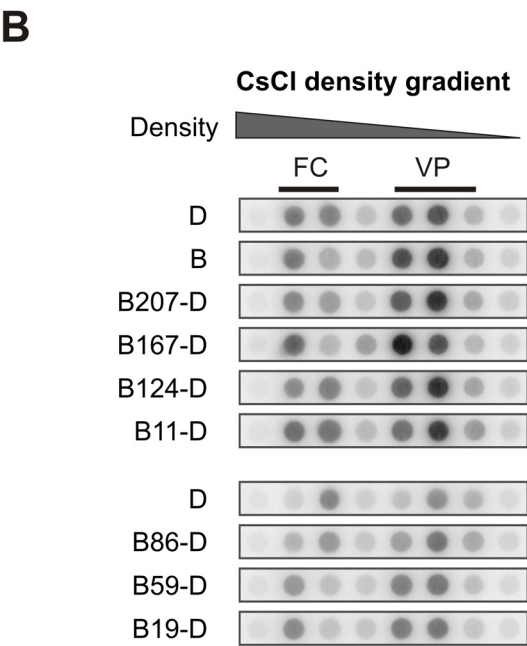
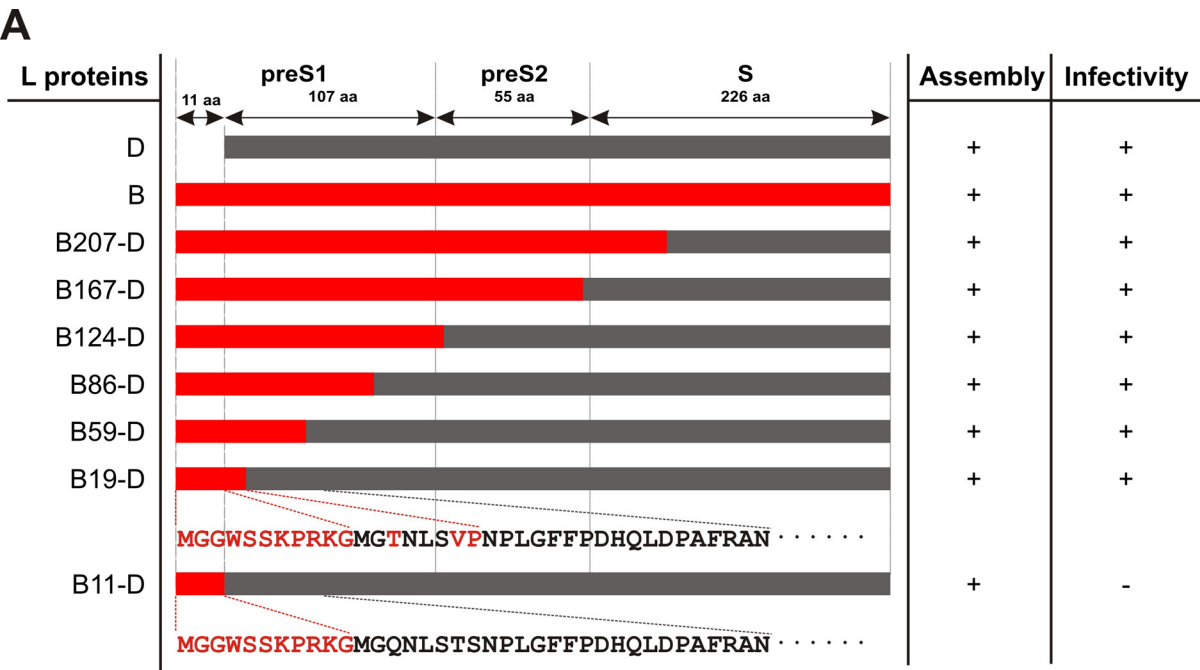


FIG. 18. Assembly and infectivity of pseudotyped virus carrying chimeric L proteins of genotype D and B

A. Schematic illustration of the L proteins from HBV genotypes D (black) and B (red), and the produced chimeras. The assembly and the infectivity of the pseudotyped viruses with these L proteins are summarized on the right. To highlight the differences between B11-D and B19-D, the N-terminal residues are depicted below, in which the genotype-B specific amino acid are shown in red. Note that three residues differ between the N-terminus of B11-D and B19-D and result in different virus infectivity.

B. Analysis of assembly and secretion of the chimeric pseudotyped virus. HBV-DNA specific Dot-blot of fractions of an analytical CsCl density gradient were obtained from supernatants of HuH-7 cells, which were transfected with a mixture of L-deficient genomic construct and helper constructs expressing L proteins of genotype D (row 1 and 7), genotype B (row 2), or the chimeras (row 3-6 and row 8-10).

C. HBsAg secreted from day 8-13 following infection of HepaRG cells with the pseudotyped virus bearing L proteins of genotype D, genotype B, or the chimeras. The infection was performed in the absence (black bars) or presence of 100 or 500 nM HBVpreS/2-48^{myr} to block the preS1-receptor-mediated entry pathway of HBV (white bars).

It is noteworthy to point out that these 8 amino acids of genotype-B L protein (aa 1-8) are not responsible for the myristoylation, but the corresponding sequence in genotype-D L-protein is commonly thought as myristoylation recognition signal. This raised a question: what is the role of these 8 amino acids in the L protein?

2.2.3 Infectivity of HBV carrying chimeric L protein with His-6 tag

To further confirm that this 8 amino acids are critical for the virus infectivity, the His-6 tag (HHHHHH) was used to partially substitute this region (Fig. 18A, gt B/14H6) in the context of genotype-B L protein, together with other substitutions in near positions (gt B/8H6, gt B/11H6).

The results clearly showed that three chimeric L proteins were correctly expressed (Fig. 19B), did not interfere with virus assembly (Fig. 19C), but abolished virus infectivity (Fig. 19D).

Therefore, it can be confirmed that these 8 amino acids (aa 1-8) are critical for virus infectivity in genotype-B L proteins, although they are not used as a myristoylation signal. It is likely that the conformation of N-terminus is changed when these amino acids are replaced by His-6 tag, which subsequently abolishes virus infectivity by interfering with the receptor-binding.

A

L mutants	SEQUENCE in the N termini	Assembly	Infectivity
D	MGQNLSTSNPLGFFP ·····	+	+
B	MGGWSSKPRKGMGTNLSVPNPLGFFP ·····	+	+
8H6	MGGWSSKHHHHHTNLSVPNPLGFFP ·····	+	-
11H6	MGGWSSKPRKHHHHHSVPNPLGFFP ·····	+	-
14H6	MGGWSSKPRKGMGHHHHHNPLGFFP ·····	+	-

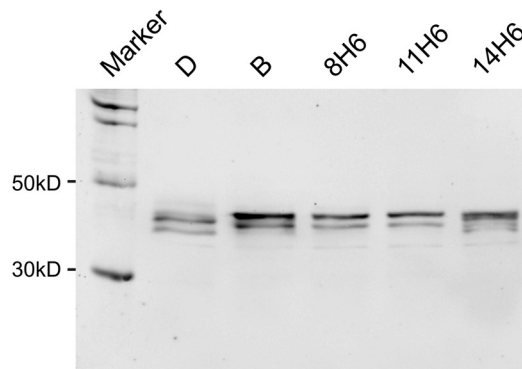
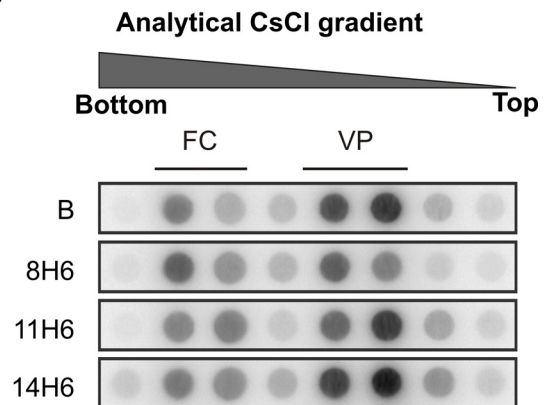
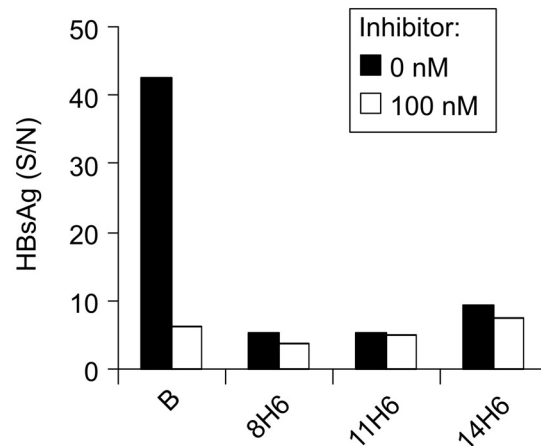
B**C****D**

FIG. 19. Assembly and infectivity of pseudotyped virus carrying L proteins with substituted His-6 tag at the N-terminus

A. N-terminal sequences of L proteins from genotype-D (D), genotype-B (B), and the mutants with substitutions with His-6 tag (8H6, 11H6, 14H6). The letters in red indicate aa that differ from genotype D. The assembly and infectivity of virus with these L proteins are summarized on the right.

B. Western blot of cellular extracts of HuH-7 cells 2 days post-transfection with helper constructs expressing the wild-type (genotype D and B) or the mutant L-proteins as shown in (A).

C. DNA Dot-blot analysis of assembly and secretion of the pseudotyped virus bearing mutated L proteins. The HBV-DNA specific Dot-blot of fractions of an analytical CsCl density gradient were obtained from supernatants of HuH-7 cells, which were transfected with a mixture of L-deficient genomic construct and helper constructs expressing L proteins of genotype B (row 1), or the mutated L protein bearing His-6 tag at different position (row 2-4).

D. HBsAg secreted from days 8-13 following infection of HepaRG cells by the virus bearing L proteins of genotype B, or the mutants. The infection was performed in the absence (black bars) or presence of 100 nM HBVpreS/2-48^{myr} (white bars).

2.2.4 Infectivity of HBV with different myristoylation motifs

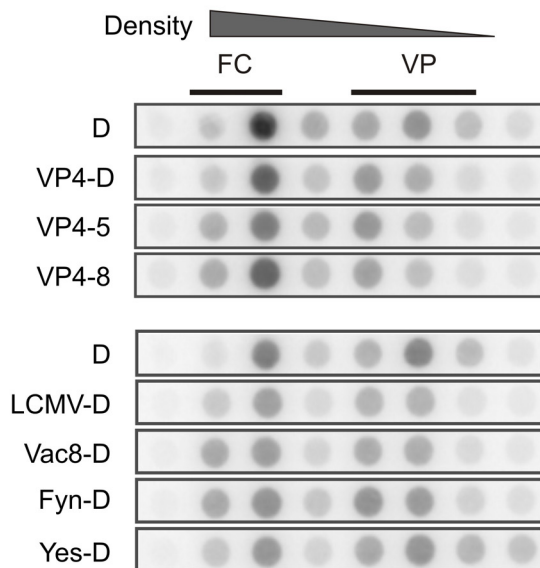
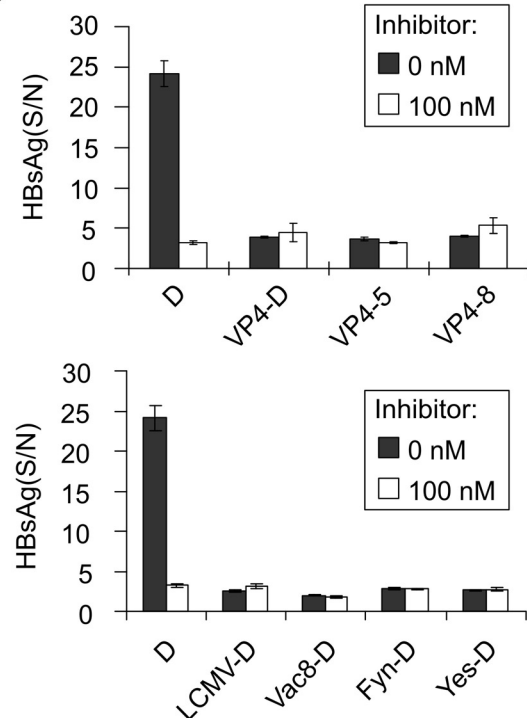
In the genotype-B L protein, aa 1-8 are important for virus infectivity. It is therefore reasonable to assume that the corresponding sequence in genotype-D L-protein also serve an specific function aside from being a myristoylation recognition signal, i.e. the sequence itself is also a determinant for virus infectivity. If this hypothesis held true, heterologous myristoylation motifs should not be able to replace this region although N-myristoylation occurred. The N-terminal 9 amino acids (MGAQVSSQKV) of poliovirus VP4 protein is a well-defined myristoylation motif. It has been demonstrated that these 9 amino acids are sufficient to confer the myristoylation of green fluorescence protein (GFP) when it was fused to the N-terminus of GFP¹⁸³. Therefore, the VP4 myristoylation motif was used to replace aa 1-8 of HBV L protein (Fig. 20A, VP4-8), together with some replacements shown in Fig. 14 (VP4-5, Vp4-D). Assembly and infectivity of pseudovirus with these chimeric L proteins were determined (Fig. 20B-C, upper panels). These chimeras did not interfere with the virus assembly, but the all the pseudoviruses including VP4-8 lost its infectivity, supporting the hypothesis that aa 1-8 of genotype-D L-protein does not simply serve as myristoylation motif. Interestingly, the VP4-D, in which the VP4 myristoylation motif was fused N-terminally to Gly-2 of the L protein, did also abolish virus infectivity. This result is similar to our previous observation that the myristoylation motif of L protein of genotype B (within the N-terminal 11 amino acids) has to be adjacent with its own downstream 8 amino acids in order to keep virus infectivity (Fig. 18, mutants B19-D and B11D).

To strengthen the previous finding, the myristoylation motifs of other well-defined myristoylated protein were fused to the N-terminus of D-genotype L protein (Fig 20A, lower panel). These myristoylation motifs include the N-terminus of LCMV μ 1 protein (LCMV), Vac8p, Fyn and Yes protein^{184,185}. The correctness of the depicted constructs was verified by DNA sequencing and the protein expression was confirmed by Western blot (data not shown). All chimeric L proteins can be expressed, did not interfere with viral assembly, but abolished the virus infectivity (Figure 20B and C, lower panels). Apparently, although aa 1-8 were intact, the infectivity of virus was lost when the aa 1-8 were N-terminally fused to other myristoylation signals, suggesting that a highly strict sequence in the N-terminus is required for virus infectivity.

In conclusion, the 8 amino acids at the N-terminus of D-genotype L protein serve not only as a myristoylation signal, but might also be directly involved in virus entry. These results suggest a highly strict sequence requirement within the N terminus of L protein for virus infectivity.

A

L proteins	SEQUENCE in the N-termini	Assembly	Infectivity
D	MGQNLSTSNPLGFFP ·····	+	+
VP4-D	MGAQVSSQKV ^{red} GQNLSTSNPLGFFP ·····	+	-
VP4-5	MGAQVSSQKV ^{red} LSTSNPLGFFP ·····	+	-
VP4-8	MGAQVSSQKV ^{red} SNPLGFFP ·····	+	-
LCMV-D	MGQIVTMFEALPHI ^{red} IDEV ^{red} GQNLSTSNPLGFFP ·····	+	-
Vac8-D	MGSCCSCLKD ^{red} GQNLSTSNPLGFFP ·····	+	-
Fyn-D	MGCVQCKDKEAAK ^{red} L ^{red} GQNLSTSNPLGFFP ·····	+	-
Yes-D	MGCIKSKENKSPA ^{red} IK ^{red} GQNLSTSNPLGFFP ·····	+	-

B**DNA dot-blot of CsCl density gradient****C****FIG. 20. Assembly and infectivity of pseudotyped virus carrying L proteins with heterologous myristoylation signals.**

A. N-terminal preS1 sequences of chimeric L proteins with myristoylation signal from Poliovirus VP4 protein (VP4-D), μ 1 protein of LCMV (LCMV-D), Vac8 (Vac8-D), Fyn (Fyn-D) and Yes (Yes-D). The letters in red indicate the heterologous myristoylation signals. Assembly and infectivity of the respective viruses with these chimeric L proteins are summarized on the right.

B. Analysis of assembly and secretion of the pseudotyped viruses. HBV-DNA specific Dot-blots of fractions of analytical CsCl density gradients were obtained from supernatants of HuH-7 cells, which were transfected with a mixture of L-deficient genomic construct and helper constructs expressing L proteins of genotype D (row 1 and 5), or the chimeras (row 2-4 and row 6-9).

C. Infectivity of the pseudotyped viruses in the presence or absence of the inhibitory peptide. Infectivity of the pseudotyped viruses was measured by quantification of secreted HBsAg day 11 p.i.. The infection was performed in the absence (black bars) or presence of 100 nM HBVpreS/2-48^{myr} (white bars).

2.2.5 Infectivity of HBV carrying chimeric L protein of different genotypes

Apparently, aa -11-1 of genotype-B L-proteins can not be fused N-terminally to the genotype-D L-proteins. However, compared to L-protein of genotype-B, the genotype E and G contain 10 additional aa (MGLSW^TTVPLE) that differ from genotype B, while the genotype F has different 11 aa (MGAPLST^TTRRG). In addition, there is isolated HBV genome of genotype C in which preS1 only encode 108 aa, i.e., naturally truncation of N-terminal 11 aa¹⁸⁶. These diverse 10 or 11 amino acids triggered our interest to look into the compatibility of the N-termini of different genotypes.

A set of helper plasmids expressing mutant L protein with chimeric N-terminus were constructed (Fig. 21A), including fusion of genotype-D L protein with the N-terminal 10 aa of the genotype E or G (E/G10-D), 11 aa of genotype F (F11-D), as well as the G2A mutation to prevent the myristoylation (D G2A). A truncated genotype-B L protein (B^t), or further fused with 10 aa from the genotype E or G (E/G10-B^t) were also included. As a control, the VP4 myristoylation motif was fused to the truncated genotype-B L protein (VP4-B^t).

The sequence of these constructs were verified by DNA sequencing (data not shown) and the protein expression was confirmed by Western blot (Fig. 21B). None of these chimeric L proteins interferes with viral assembly (Fig. 21C). However, the infectivities of viruses were different (Fig. 21D). The F11-D mutation abolished virus infectivity similar to the previously shown B11-D and the myristoylation-deficient control (D G2A). E/G10-D partially remained infectivity. Interestingly, B^t showed a higher infectivity compared to the that of genotype D, although they have the same length of preS1 (108 aa). The fusion of additional 10 amino acids from genotype E/G showed also an increased infectivity (E/G10-B^t). In contrast, when it was fused to the heterologous VP4 myristoylation motif, virus infectivity was abolished (VP4-B^t).

Taken together, these results suggest that the genotype D L-protein can hardly be prolonged with N-terminal sequence, while the corresponding sequence from genotype B (B^t) seems more tolerable except for the heterologous myristoylation signal. These results confirm again that a stringent sequence is required in the N-terminus of L protein and further indicates that this sequence is genotype-dependent.

A

L proteins	SEQUENCE in the N termini	Assembly	Infectivity
D	MGQNLSTSNPLGFFPDHQLDPAFRANTAN	+	++
D G2A	MAQNLSTSNPLGFFPDHQLDPAFRANTAN	+	-
B11-D	MGGWSSKPRKGMGQNLSTSNPLGFFPDHQLDPAFRANTAN	+	-
E/G10-D	MGLSWTVPLEWGMGQNLSTSNPLGFFPDHQLDPAFRANTAN	+	+
F11-D	MGAPLSTTRRCMGQNLSTSNPLGFFPDHQLDPAFRANTAN	+	-
B ^t	MGTNLSVPNPLGFFPDHQLDPAFKANSEN	+	+++
E/G10-B ^t	MGLSWTVPLEWGTNLNSVPNPLGFFPDHQLDPAFKANSEN	+	+++
VP4-B ^t	MGAQVSSQKVGTDNLNSVPNPLGFFPDHQLDPAFKANSEN	+	-

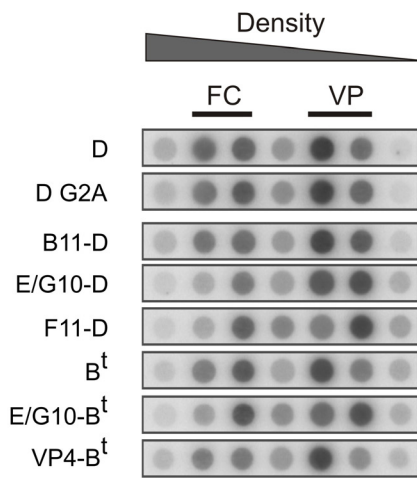
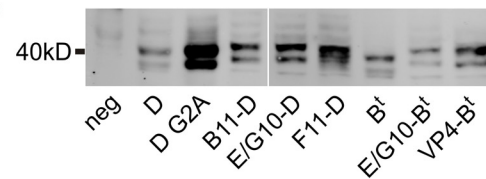
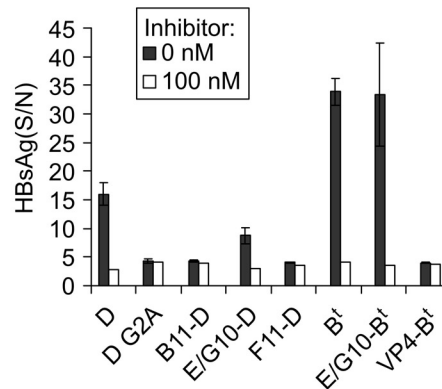
C**B****D**

FIG. 21. Assembly and infectivity of pseudotyped virus carrying L-proteins with chimeric N-termini of different genotypes

A. N-terminal sequence of L proteins with chimeric N-termini. The N-termini of the L proteins of different genotypes, i.e., 11aa from genotype B, 10aa from genotype E or G, 11aa from genotype F were fused to the N terminus of the genotype D L-protein as depicted as B11-D, E/G10-D, F11-D respectively. As a control, the G2A mutation to prevent the N-myristoylation of L protein was also included. In addition, The L proteins of genotype B with the 11 aa truncation or further fused with the N-terminal 10 aa from genotype E/G or with VP4 myristoylation motif were depicted as B^t, E/G-B^t, VP4-B^t, respectively. The letters in red indicate aa that differ from genotype D. The assembly and infectivity of virus with these L proteins are summarized on the right.

B. Western blot of cellular extracts of HuH-7 cells 2 days post-transfection with helper constructs expressing the L-proteins of genotype D, or the chimeric L proteins as described in (A).

C. Analysis of assembly and secretion of the pseudotyped virus bearing chimeric L proteins. HBV-DNA specific Dot-blot of fractions of an analytical CsCl density gradient were obtained from supernatants of HuH-7 cells, which were transfected with a mixture of L-deficient genomic construct and helper constructs expressing L proteins of genotype D (row 1), or the chimeric L proteins as described in (A) (row 2-8).

D. HBsAg secreted from days 8-13 following infection of HepaRG cells by the virus bearing L proteins of genotype D, or the mutated L proteins as described in (A). The infection was performed in the absence (black bars) or presence of 100 nM HBVpreS/2-48^{myr} (white bars).

2.2.6 Characterization of inhibitory peptides with mutations in the N-terminus

To summarize all the mutagenesis analyses of pseudovirus, the N-terminal sequence, between the myristoyl group and the downstream receptor binding site, is highly critical in the following manner. (1) In genotype D, this sequence is relatively short (aa 1-8) but has a dual function as a myristoylation motif and an infection determinant. It does not tolerate N-terminal fusion with foreign myristoylation sequence. (2) In genotype B, it consists of two short sequences: the additional aa -11/-1 and the following aa 1-8. The aa -11/-1 can be deleted but can not be replaced by heterologous myristoylation signal either, and the sequence needs to be adjacent to its own downstream sequence aa 1-8.

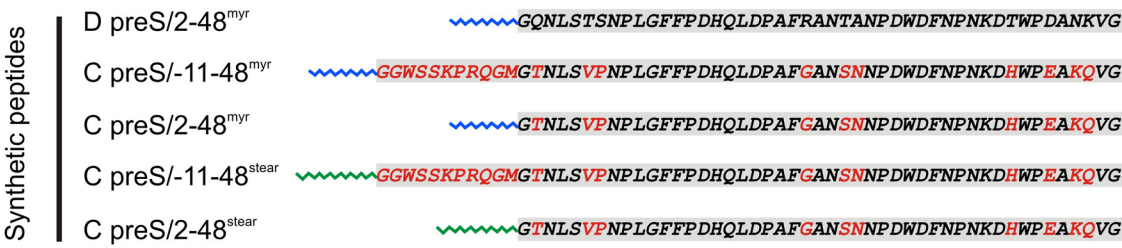
Based on these results, it could be proposed that this short sequence in the N-terminus acts as an “adapter” to connect its N-terminal essential myristic group and C-terminal receptor binding domain. Instead of being flexible, this sequence should be able to form a special secondary structure, which coordinates two essential groups in both ends to implement receptor binding. In order to prove this hypothesis, reconstruction of the 3D-structure of the preS1 domain is extremely valuable. Unfortunately, the preS1 domain is a natively unstructured protein without a unique tertiary structure¹⁸⁷, and the X-ray crystallographic structure of the preS1 domain has not been successfully studied yet.

However, to test the hypothesis that a very short stretch of the N-terminus of the L protein acts as an “adapter”, the inhibitory peptides derived from HBV preS1 provide a complementary tool to the infectivity assay of HBV mutants. The preS1 derived peptides can inhibit virus infection by interference with receptor-binding. This conclusion is supported by the following facts. (1) Pre-incubation of susceptible cells with peptide for 30 minutes inhibits virus infection. (2) The peptide has been visualized to specifically bind to the surface of differentiated hepatocytes¹¹⁷. (3) The mutated peptide without essential aa 11-15 or lacking of N-myristoylation lost their activity to bind with hepatocytes and inhibit virus infection. The virus carrying single-point mutations in this region lost their infectivity¹⁸⁸. Considering these strong correlations between the activity of peptide and the infectivity of virus, the characterization of the peptides bearing N-terminal mutation would be an additional method to test our hypothesis, at least to estimate the binding of preS to the virus receptor. This approach also has some intrinsic advantages. (1) It is technically easy to introduce mutations during the peptide synthesis. (2) The peptides can be N-myristoylated regardless of the presence of NMT recognition motif. (3) More important, its inhibitory activity is useful to estimate the binding of preS1 to the virus receptor.

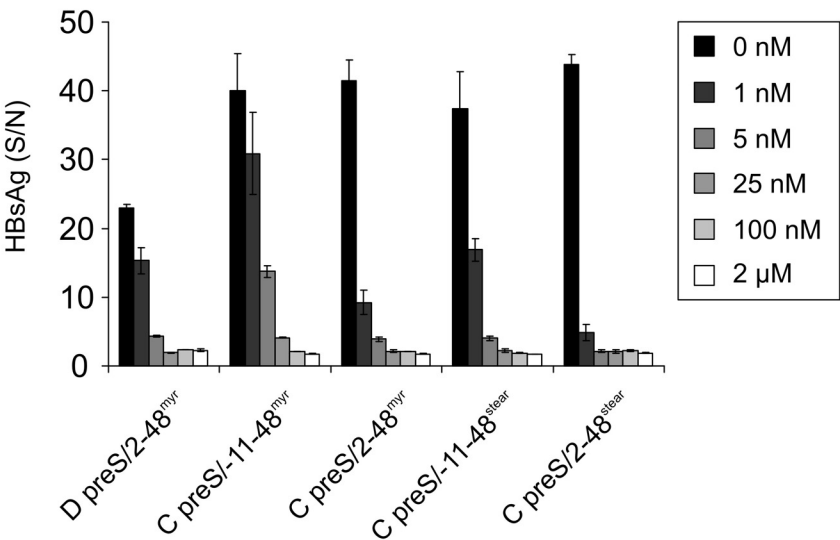
Peptides with two types of modification (N-myristoylation or N-stearoylation) derived from the genotype C (C preS/-11-48^{myr}, C preS/-11-48^{stear}) and its truncated mutant (C preS/2-48^{myr}, C preS/2-48^{stear}) were synthesized (Fig. 22A). Since the peptide derived from genotype D can inhibit the infection of virus pseudotyped with different genotypic L-proteins (Fig. 17), it was also interesting in a *vice versa* experiment to compare the activity of peptides derived from different HBV genotypes. More important, since the virus with N-terminal 11 aa truncated genotype-B L-protein was more infectious than that with genotype-D L-protein (Fig. 21), it would be interesting to compare the activity of intact with N-terminally shortened peptide. According to the “adapter” hypothesis, it could be possible that the truncated peptide form a better secondary structure to coordinate two essential groups in its two ends to implement receptor binding. If this scenario hold true, the genotype C derived peptide (the preS1 sequence of genotype A, B and C are actually quite similar as shown in Fig. 16) truncated at the N-terminal 11 aa should inherit this better conformation. Thus it can bind to the receptor and inhibit virus infection more profoundly than that of genotype D.

To test that, these 4 peptides were incubated at different concentration with virus inoculum during infection to measure their inhibitory activity (Fig. 22). Consistent with previous results¹¹⁷, the stearoylated peptides showed an enhanced inhibitory activity compared to the myristoylated peptides. Moreover, the genotype-C derived peptides were more competent than those of genotype D. When the N-terminal 11 aa of genotype-C derived myristoylated peptides were truncated, it was more active for inhibition of HBV infection, with an IC₅₀ less than 1 nM. This phenomenon can also be observed by comparing stearoylated peptides. The similarity of inhibitory activity of peptide and the infectivity of virus bearing the same N-terminal truncation demonstrated that the “adapter” sequence, when truncated at aa -11/-1, is more efficient in coordinating two essential groups in both ends to bind to virus receptor and thus implement virus entry.

A



B



C

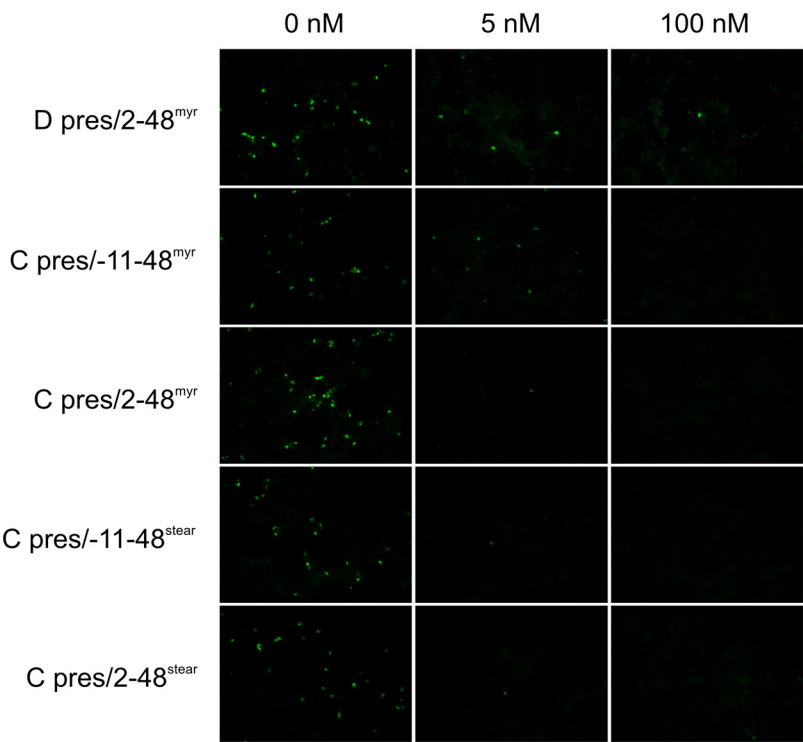


FIG. 22. Inhibition of genotype D HBV entry by genotype C derived peptides

A. Peptide sequences used for the inhibition assay. The letters in red indicate the amino acids that differ from genotype D. All the peptides are either myristoylated (blue zigzag line) or stearylized (green zigzag line) at the N-terminus.

B. HBsAg secreted from day 8-13 following infection of HepaRG cells in the absence (0nM) or in the presence of increasing concentration (1, 5, 25, 100, 2000 nM) of the peptides shown in (A).

C. HBcAg-specific immunofluorescence (green) of HepaRG cells 13 days post-infection in the absence (0 nM) or in the presence of different concentrations (5 nM and 100 nM) of inhibitory peptides shown in (A).

Second, to get an insight into the role of downstream aa 1-8, deletions and substitutions within this region was introduced. These mutant peptides include gradually truncations of N-terminal aa 1-8 or substitutions with alanines to keep the overall length of peptide (Fig. 23A). Their inhibitory activities were measured on the susceptible HepaRG cells infected with HBV.

In contrast to the deletion of aa -11/-1, which increases the peptide activity, the length-increasing N-terminal truncation of aa 1-8 resulted in a progressive loss of the inhibitory activities. Since those peptides were highly purified and fully myristoylated in the absence of myristoylation motif, they provide invaluable information that virus might also gradually lose its infectivity with N-terminally deleted L protein. This can not be tested by introducing the corresponding mutations into virus particle because it would abolish the myristoylation.

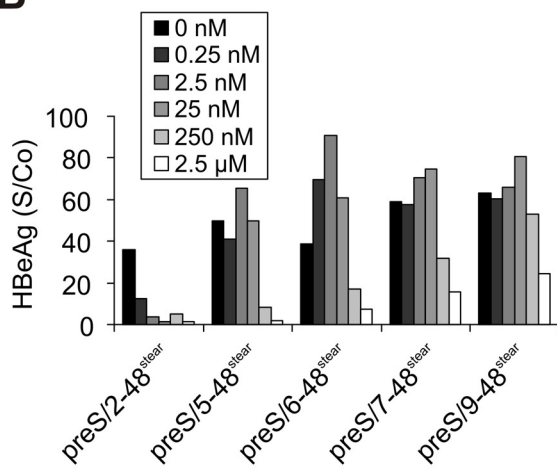
When aa 1-8 were deleted (preS9-48^{stea}), the activity of the peptides decreased by about 1000-fold. This again proves the conclusion that aa 1-8 is not solely a myristoylation signal. Instead, the presence of this sequence is fundamental to maintain the activity of peptide, thus, is also fundamental for the binding of myristic group and receptor binding site to the unknown receptor.

The loss of activity by the N-terminal deletions can not be rescued by introducing alanines to keep the length of N-terminus (preS/A2-8/9-48^{stea}). This indicates that aa 1-8 do not serve as a spacer, coinciding with previous results showing the loss of infectivity of VP4-8 mutant (Fig. 20). Furthermore, the substitution of Asn9 (preS/A2-9/10-48^{stea}) results in a complete loss of inhibitory activity, suggesting that Asn9 is an essential residue for the binding of the peptide to the virus receptor.

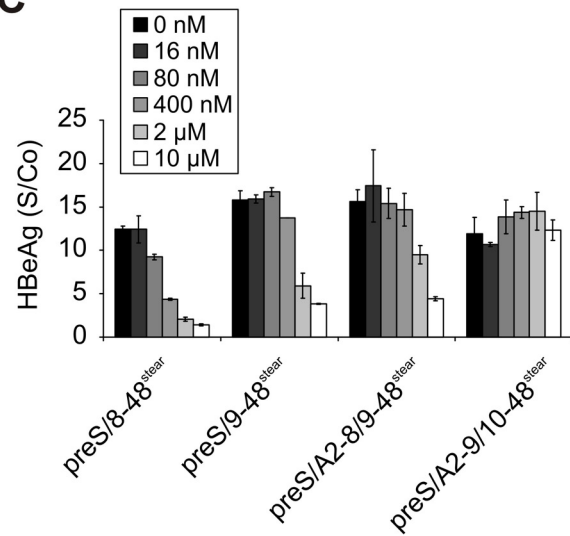
A



B



C



D

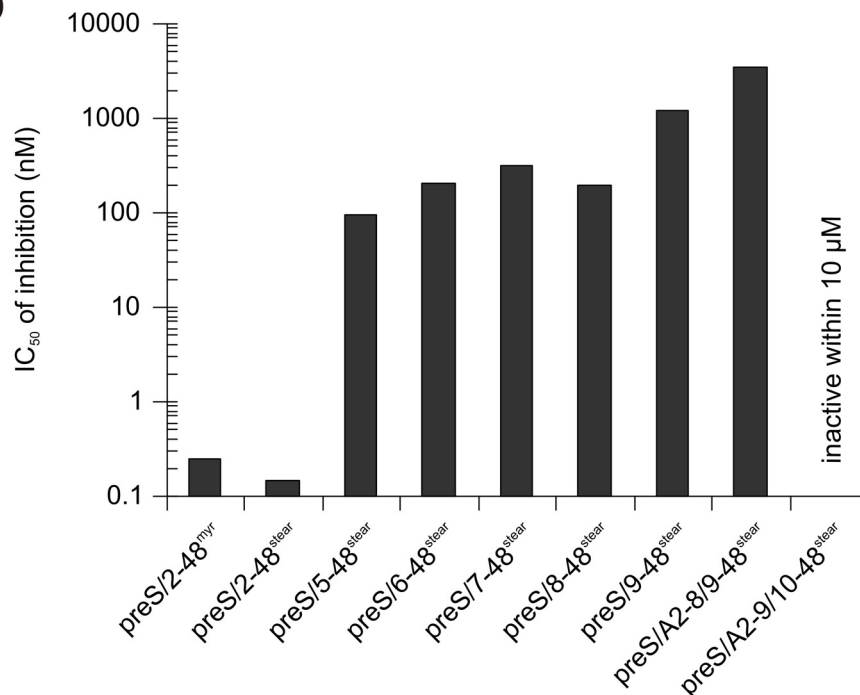


FIG. 23. Inhibition of HBV infection by preS peptides with N-terminal truncations or substitution

A. Schematic illustration of the sequence of peptides used for the inhibition assay. The letters in red indicate the amino acids that differ from genotype D. All the peptides are steaoylated (green zigzag line) at the N-terminus.



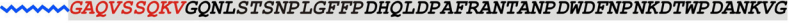
B-C. HBeAg secreted from day 4-7 following infection of HepaRG cells with concentrated virus in the absence (0 nM) or in the presence of indicated concentration of inhibitory peptides described in (A).

D. The IC_{50} (concentration of substance lead to 50% reduction of virus infection) of inhibitory peptides

Previous results indicate that L proteins with chimeric N-termini have a profound influence on the virus infectivity. It was therefore interesting to test the inhibitory peptides consisting of the same chimeric N-termini. We selected two mutants that result in lost infectivity, B11-D and VP4-D, and synthesized the corresponding chimeric peptides, B-D^{myr} and VP4-D^{myr} (Fig. 24). HepaRG cells were infected with virus in the presence of these two peptides at varying concentrations in order to determine their inhibitory activities.

Indeed, the inhibitory activities of both peptides were drastically reduced. Compared to the wild-type peptides (IC_{50} of ~5nM), the IC_{50} of peptide B-D^{myr} is 25-fold higher (~125 nM). Moreover, the peptide VP4-D^{myr} can not inhibit HBV infection in concentration up to 125nM, which is consistent with our observation that the myristoylation signal from VP4 strongly abolishes both genotype-B and genotype-D L protein (VP4-D and VP4-B¹) mediated infection when it is fused to the N terminus (Fig. 20 and Fig. 21).

A

Synthetic peptides	SEQUENCE(with myristoylation in the N-termini)	Inhibitory activity
D preS/2-48 ^{myr}		++
B-D ^{myr}		+/-
VP4-D ^{myr}		no inhibition up to 125nM

B

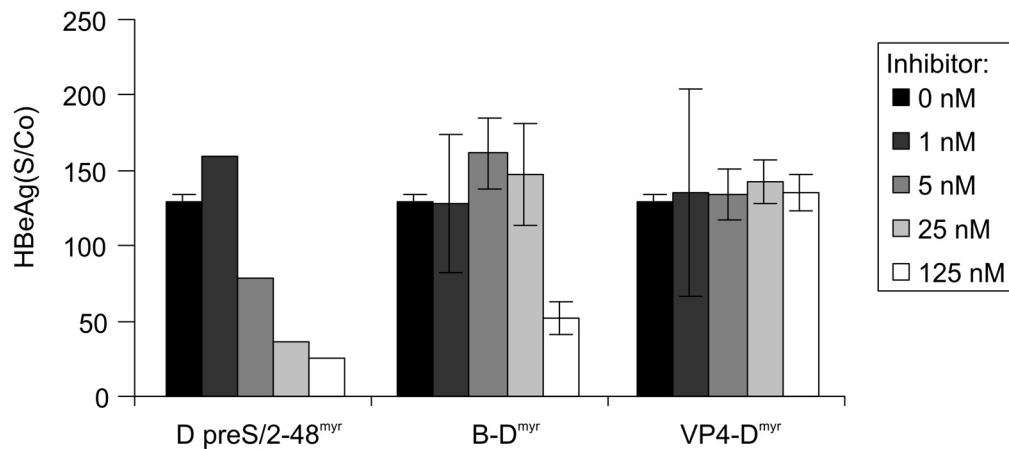


FIG. 24. The inhibitory activities of myristoylated peptides with chimeric N-termini

A. Sequence of peptides used for the inhibition assay. The letters in red indicate the amino acids from genotype-B L-protein or VP4. All the peptides are myristoylated (blue) at the N-terminus. The inhibitory activities of these peptides against HBV infection were summarized at the right.

B. HBeAg secreted from days 4-7 following infection of HepaRG with concentrated virus in the absence (0nM) or presence of inhibitory peptides described in (A) at different concentration (1, 5, 25, 125nM).

Taken together, variations in the N-terminus of the peptide have a significant effect on their inhibitory activities. This effect is correlated with the infectivity of virus carrying corresponding mutations. This complementary evidence from myristoylated peptide minimize the possibility that the lost infectivity of virus with N-terminal chimera of preS1 (e.g. B11-D, VP4-D) is due to the interruption of myristoylation signal. Last but most important, these results show that the N-terminus of the L protein (aa-11/-1 and aa 1-8) was a subtle but critical function for virus infection, which is probably mediated by the interference of the binding of preS to the virus receptor.

2.2.7 The role of myristoylation in HBV entry

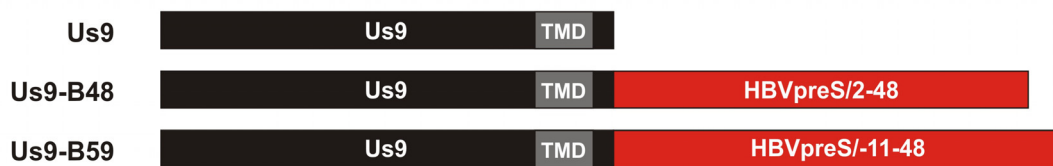
The myristoyl moiety of L protein is critical for HBV entry. G2A mutation of L protein abolishes the myristoylation and also abolishes HBV/DHBV infection. Consistently, the non-myristoylated HBV preS-derived peptide can only inhibit infection at a much higher concentration (>1000 fold). While the presence of myristoyl group is known to be important for several years, the role of myristoylation is still unknown. The most commonly described function of myristoyl group is the targeting of modified proteins to membranes by inserting the hydrophobic C14 carbon chain into the lipid bilayer from the cytoplasmic side¹⁸⁹. We ask if the myristoyl chain of HBV particle or the peptide, from the outside, addresses to and even inserts into the cellular membrane during interaction with receptor. If that is the case, one could speculate that the myristoyl chain of peptide could be functionally replaced by a transmembrane domain, which anchors the peptide and orientates the N-terminus of peptide to the membrane.

To test this possibility, a type-II transmembrane protein (Us9) was fused to the N-terminus of HBV preS2-48. The Us9 protein is derived from pseudorabies virus and well characterized with respect to its trafficking and function. It is located in both trans-Golgi network (TGN) region and plasma membrane¹⁹⁰. When GFP is fused to the C-terminus of US9 (US9-GFP), topology of the fusion protein keeps identical to that of Us9 (single-pass transmembrane protein with an extracellular C-terminus)¹⁹¹. Since the size of HBV preS2-48 is much smaller than GFP, one could speculate that the fusion of preS2-48 to the C-terminus of US9 do not change the topology either. Considering that the important “adapter” sequence between the myristoylation group and receptor binding site might be important for such a fusion peptide, we chose aa 2-48 and aa -11-48 of the preS from genotype B to construct fusion peptides Us9-B48 and US9-B59 respectively (Fig. 25A). The preS sequence of genotype B was used because pseudotyped virus with wide-type and truncated L protein from genotype B are both infectious (Fig. 17 and Fig. 21).

Moreover, the peptide B-preS/2-48^{myr} and B-preS/-11-48^{myr} are both active to inhibit HBV infection (data not shown). The Us9 protein alone was used as a control. All these three proteins were introduced into a lentivirus transduction system, where GFP is co-expressed with the target protein.

First, lentiviruses expressing these three membrane-anchored peptides were produced, and used to transduce differentiated HepaRG cells. Three days post-transduction, the expression of Us9-B48 and US9-B59 was analyzed by IF against HBV preS. An unspecific staining was observed in the control (Us9), but it is not localized in the transduced cell (expressing GFP). In comparison, the staining of Us9-B48 and US9-B59 is mostly localized in the transduced cells. More important, the fusion protein is mainly expressed on the plasma membrane and trans-Golgi compartment-like structures, which is consistent with the described localization pattern of Us9 and US9-GFP fusion protein^{191,192}.

A



B

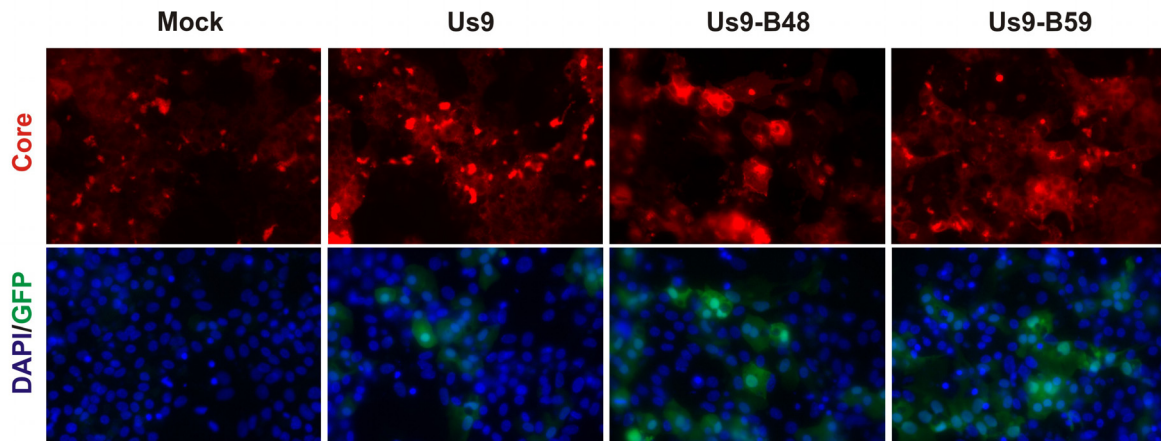


FIG. 25. Design of membrane anchored peptides and their expression in HepaRG cells

A. Schematic illustration of the membrane anchored peptides. The aa 2-48 and aa -11-48 (red bars) of L protein from genotype B were fused to the C-terminus of Us9 protein (black bar), which contain a transmembrane domain within its C-terminus (TMD). The Us9 protein alone was also included as a control.

B. Expression of membrane anchored peptides in differentiated HepaRG cells. 3 days post transduction, the expression of Us9-B48 and Us9-B59 was analyzed by IF with an anti-preS antibody as shown in the upper panel (red). The expression of GFP in transduced cell (green) and nuclei (blue) are shown in the lower panel. Lentiviral production in the absence of transfer vector was also used for the transduction (mock).

In order to investigate the influence of fusion peptides on oncoming HBV infection, the differentiated HepaRG cells were transduced 4 days prior to HBV infection. Indeed, there was a clear drop of infection when Us9-B48 and US9-B59 were expressed (judged by secreted HBsAg) (Fig. 26A). Since the hepatocytes were apparently not fully transduced, it was important to analyze at a single-cell level if the transduction could inhibit HBV infection. Therefore, IF was performed to identify HBV-infected cells (anti-core staining) and transduced cells (anti-GFP staining). It is clear that the Us9-B48 and US9-B59-transduced cells did not allow for a following HBV entry, showing an exclusive red core-staining in the single-cell level. In comparison, there are significant superinfection events (red core-staining co-existed with green GFP-expression in the same cell) in Us9 transduced cell (Fig. 26B).

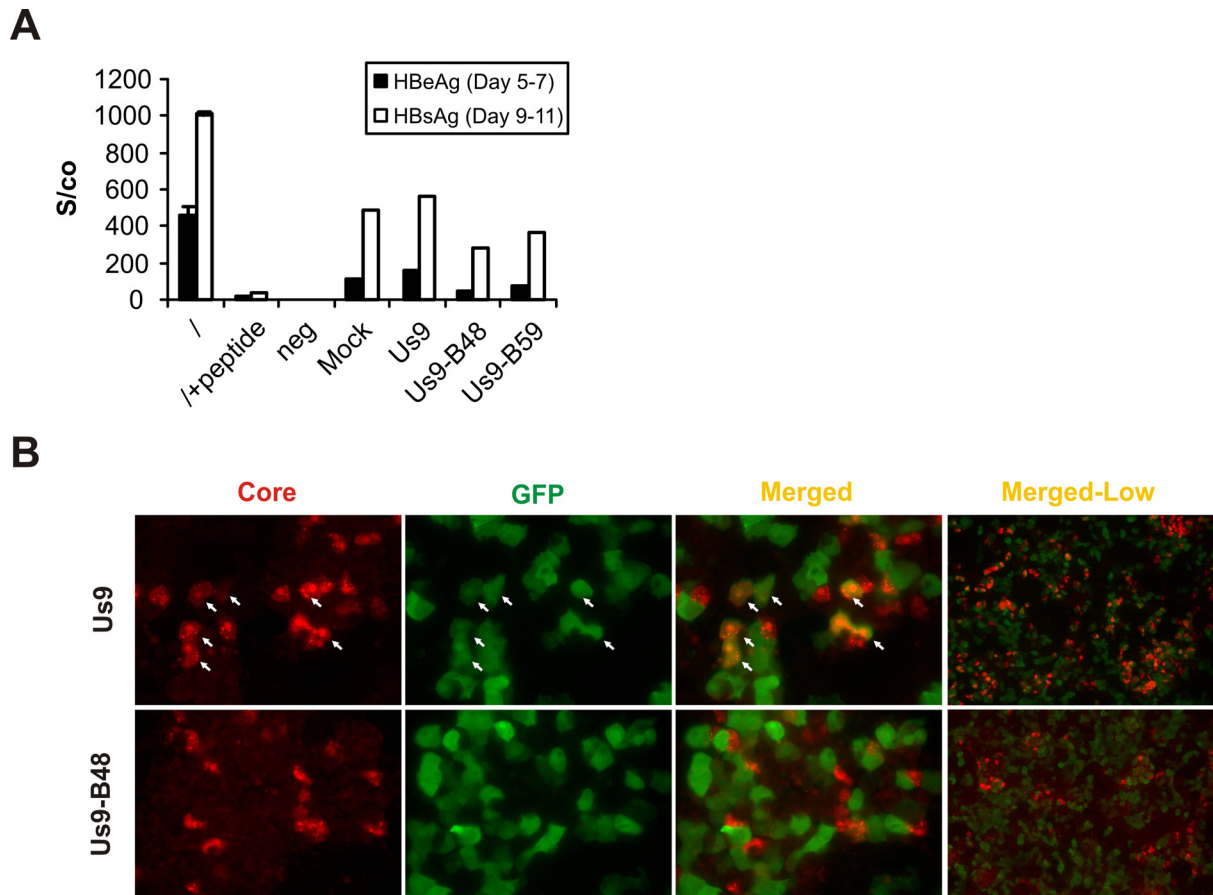


FIG. 26. Infection of HepaRG cells transduced with lentivirus expressing membrane-anchored peptide
 A. Secreted viral markers following infection of transduced HepaRG cells. Non-transduced HepaRG cells were infected with HBV in the absence (/) or presence (/+peptide) of 500 nM HBVpreS/2-48^{myr}. HepaRG cells 4 days post-transduction were also infected with HBV (Us9, Us9-B48, Us9-B59). Lentiviral production in the absence of transfer vector (mock) and the HepaRG cells without transduction and infection (neg) were included. At the indicated time points, the secreted viral markers in the supernatant of HepaRG cells were determined by MEIA.
 B. IF analysis of transduced and infected HepaRG cells. Us9 and Us9-B48 transduced HepaRG cells were infected with HBV 4 days post-transduction. The infected cells are showed in red (Core) and the transduced cells are shown in green (GFP). The merged pictures are shown (Merged). The cells both transduced and infected are indicated with arrow. The merged pictures with low magnification (Merged-Low) are representative of four randomly selected pictures.

In summary, functional membrane-anchored inhibitory peptides were designed by fusion of N-terminal preS to a type-II transmembrane protein. These fusion peptides obviously do not contain myristoyl group, but remarkably inhibit HBV infection. The effectiveness of these fusion peptides indicates that the myristoyl chain of HBVpreS/2-48^{myr} play its role by insertion into cellular membrane. Moreover, it illustrates the topology of HBVpreS/2-48^{myr} during inhibition: the N-terminus towards the cellular membrane. Apparently, this interaction scenario could be applied to the L protein during its interaction with the cellular receptor.

2.2.8 A possible role of preS aa 49-78 in virus entry

As mentioned before, the role of aa 49-78 is still unclear during virus infection. However, this region is required for the infectivity of HBV and HDV. Interestingly, there are antibody responses to both conserved regions in the infectivity-determining region in some patients recovered from the hepatitis B infection (Abd EI Wahed, unpublished data, Gottingen), indicating that these could be neutralizing antibodies. Both sequences must be exposed on the surface of virus particle so that it is able to induce antibody responses. To explore the possible role of this region, mutations were introduced into this conserved region and the infectivity of these mutants were determined (Fig. 27). Firstly the two prolines in the conserved sequence (57-TPPHGGLLGWSPQ-69) were substituted with alanines, PP58/59AA, and this mutant was compared to a substitution of proline outside this region, P36A. In contrast to P36A, the mutant PP58/59AA lost virus infectivity, indicating that proline within this conserved region indeed plays an indispensable role in virus entry. Secondly, two additional repeats were inserted into this conserved region leading to a triple aa57-67 (Tri 57-67). The triple conserved sequence introduced into L protein did not increase but again abolish virus infectivity.

If this region (aa 49-78) in viral L protein contains a cellular binding site critical for virus infection, a synthetic peptide comprising aa 49-78 might interfere with HBV infection.

Additionally, if aa 49-78 in viral L protein interact with upstream aa 2-48 during virus entry, a synthetic peptide aa 49-78 might also impair the activity of HBVpreS/2-48^{myr}. Therefore, this peptide was synthesized (HBVpreS/49-78), and its influence on HBV infection and inhibitory peptide HBVpreS/2-48^{myr} was further determined.

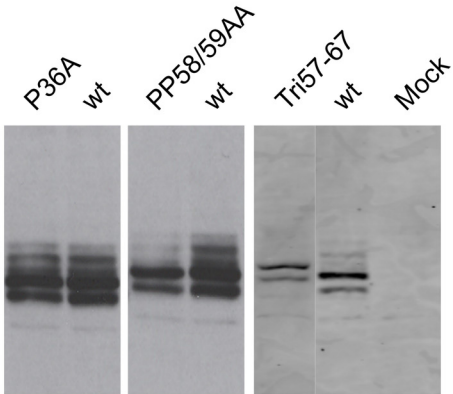
The result clearly showed that it does not have an influence on HBV infection and the activity of preS2-48^{myr} up to a concentration of 10 μ M. This result again suggests that this region is probably not involved in receptor binding, and it does not interact with the upstream aa 2-48 directly (Fig. 28).

This data is not sufficient to make a conclusion about the role of aa 49-78, but it supports the notion that this region does not function as a binding site and that this region is not able to directly interfere with the upstream region, aa 2-48.

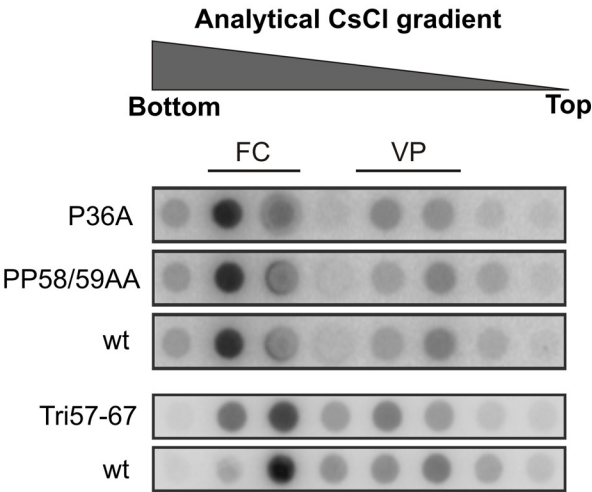
A

L mutants	SEQUENCE
	<div>conserved motif</div> <div>5769</div>
wt	...PDWDFNPNKDTWPDANKVGAGAFGLGFTPPHGGLLGWSPQAQGIL...
P36A	...PDWDFNANKDTWPDANKVGAGAFGLGFTPPHGGLLGWSPQAQGIL...
PP58/59AA	...PDWDFNPNKDTWPDANKVGAGAFGLGFTAAHGGLLGWSPQAQGIL...
Tri57-67	...PDWDFNPNKDTWPDANKVGAGAFGLGFTPPHGGLLGWSTPPHGGLLGWSTPPHGGLLGWSPQAQGIL...

B



C



D

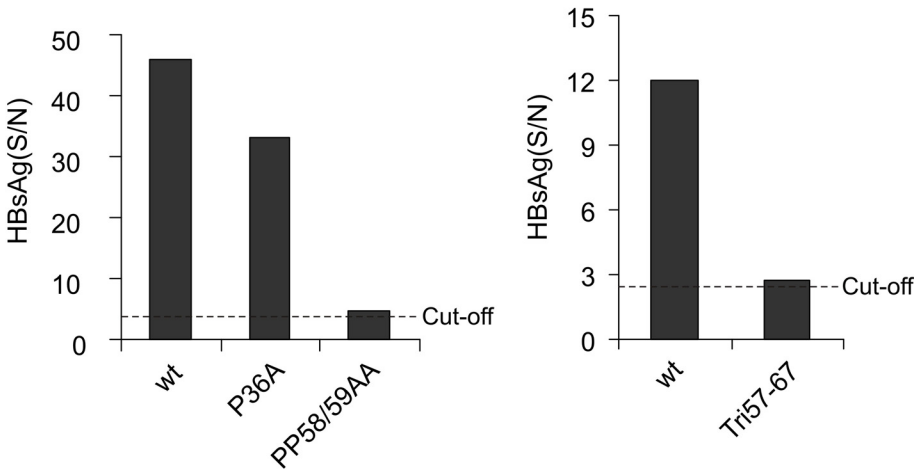


FIG. 27. Expression, assembly and infectivity of pseudotyped virus carrying L-proteins mutated in conserved region (aa 57-69)
A. Schematic illustration of the N-terminal sequence of chimeric L proteins carrying indicated mutation. The letters in red indicate the amino acids that are different from that of genotype D.
B. Western blot of cellular extracts of HuH-7 cells 2 days post-transfection with helper constructs expressing the L-proteins of genotype D (wt), or the mutant L proteins as described in (A).
C. Analysis of assembly and secretion of the pseudotyped virus bearing chimeric L protein. HBV-DNA specific Dot-blot of fractions of an analytical CsCl density gradient were obtained from supernatants of HuH-7 cells, which

were transfected with a mixture of L-deficient genomic construct and helper constructs expressing L proteins of genotype D (row 3 and 5), or the mutant (row 1, 2 and 4).
D. HBsAg secreted from day 8-13 following infection of HepaRG cells by the virus bearing wild type genotype-D L proteins (wt) or the mutant (P36A, P58/59A, Tri57-67).

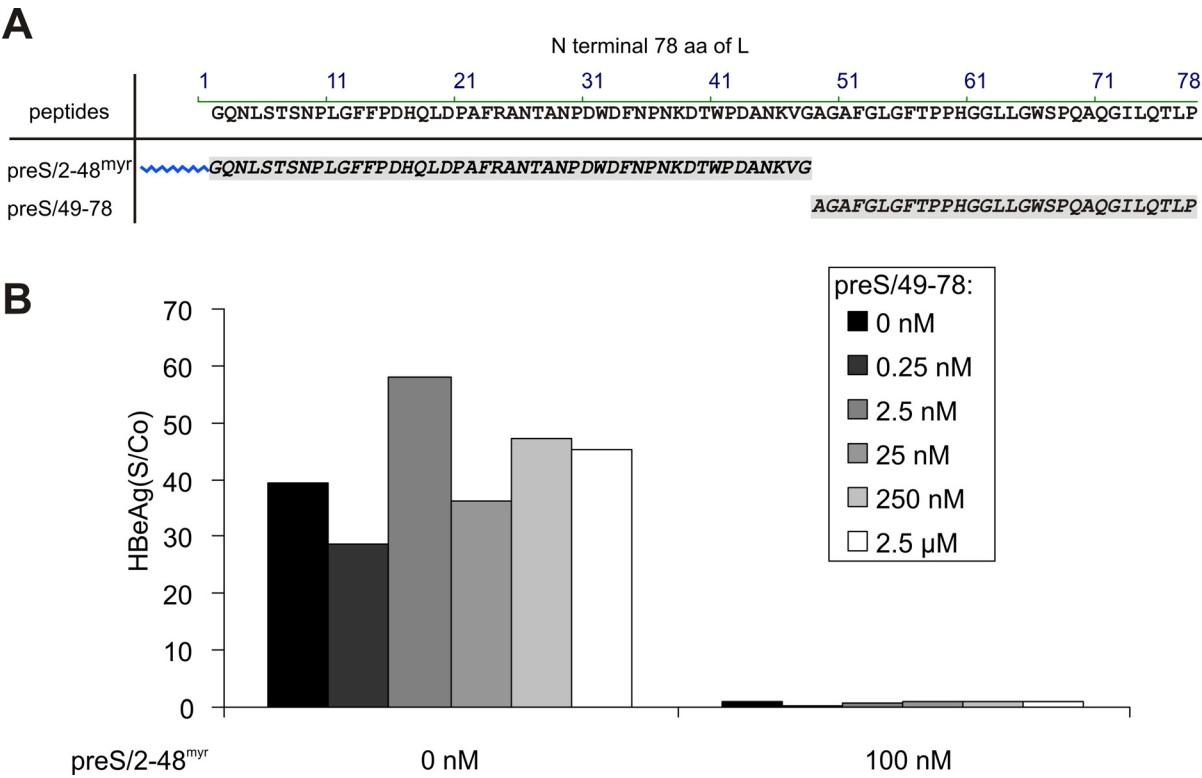


FIG. 28. The activity of peptides HBVpreS/49-78 on infection and the inhibitory peptide
A. Sequence of HBVpreS/49-78 and HBVpreS/2-48^{myr} in compared to the N-terminus of L protein. These peptides are myristoylated (blue zigzag line) at the N-terminus.
B. HBeAg secreted from days 4-7 following HBV infection of HepaRG in the presence of synthetic HBVpreS/49-78 at indicated concentrations without (0 nM) or with 100 nM HBVpreS/2-48^{myr} (100 nM).

2.3 Using M protein-free virus to dissect the role of preS2 for assembly and infectivity of Hepatitis B virus

Due to the overlapping ORFs, the preS2 domain is present in both the L and M protein. It has been demonstrated that the M protein and the preS2 domain of the L protein are not essential for both assembly and infectivity^{123,125,193}. However, a so-called translocation motif (TLM) was found in the preS2 domain, which could permeabilize cells and translocate protein into cytosol¹⁴². The following study suggested the translocation is a critical step during HBV entry, with the evidence that the deletion of TLM in DHBV led to the loss of virus infectivity. In contrast, different approaches from independent groups demonstrated that the absence of TLM in the viral envelope does not impair with infectivity of HBV and HDV^{122,124,194}. Nevertheless, it is still not clear what the role of preS2 is in HBV life cycle. To answer this question, a systematic mutation analysis in preS2 of L protein in an M protein-free system is desirable.

Therefore, M-protein free viruses were produced in this study where the L protein is separately expressed by the helper constructs. A panel of deletion or substitution was introduced to the preS2 domain of L protein, and viral assembly and infectivity of these mutants were further determined.

2.3.1 M-free system with independent expression of S and L-protein without loss of infectivity

To knock out M-protein in virion, we constructed a plasmid termed HBV L⁻M⁻, which derived from parent plasmid HBV L⁺, allowing the transcription of all known viral factors except for the L and M proteins. In this construct, expression of the L and M proteins are suppressed by mutations in the start codons of the preS1 and preS2 ORF respectively (Fig. 29A). These point mutations remain silent for the overlapping polymerase. Indeed, shown by L-protein Western blot and HBsAg assay, HBV L⁻M⁻ do not express L protein but still allow secretion of HBsAg as its parent plasmid HBV L⁺ (Fig. 29B). Similar to previous approach, HBV L⁻M⁻ was complemented with the helper construct wt L, which express wild-type L protein (Fig. 29B) under the CMV promoter. When the helper plasmid was co-transfected with HBV L⁻M⁻, virus assembly and secretion was determined by DNA dot blot analysis of CsCl gradients. As expected, the complementation of HBV L⁻M⁻ with wt L was enough to rescue the viral production (Fig. 29D), indicating that the M protein is not essential for viral assembly.

To exclude the possibility that the S-protein might also be expressed by the helper construct wt L, which contains an intact S ORF, we co-transfected a previously characterized construct (data

not shown), HBV L⁻M⁻S⁻, which cannot express any of the envelope proteins (L, M and S) but allows the assembly and secretion of free capsid (Fig. 29A, 29B, 29C), together with the helper wt L. Then we measured the secreted HBsAg post-transfection, and quantify the assembly of secreted viral particle. There is no detectable HBsAg of day 3 to day 5 post transfection (Fig. 29B, HBV L⁻M⁻S⁻+L), suggesting that the S-protein can not be expressed by the helper construct wt L. This conclusion can be further supported by DNA dot blot showing that no detectable viral particles were secreted (Fig. 29D, HBV L⁻M⁻S⁻+L).

To exclude the possibility that the M-protein was expressed by the helper construct wt L, we introduced a point mutation into the start codon of PreS2 ORF (ATG to ACG) in the helper construct, designated L^{M109T} (Fig. 29A). Then the expression of L^{M109T} was confirmed by Western blot (Fig. 29B). The ability to rescue viral secretion was determined by DNA dot blot, which showed reduced but profound virus particle secretion (Fig. 29D). The reduction might be due to the substitution of the first amino acid (methionine with threonine) of the preS2 domain of the L-protein, which is located in the capsid-binding region. Nevertheless, this result demonstrates that the M-protein is not necessary for viral assembly.

To quantify the infectivity of these recombinant viruses, we inoculated the HepaRG cells with the concentrated virus from transfected or co-transfected HuH-7 cells as quantified in Fig. 29C. For HBV, HBV L⁻M⁻+L, HBV L⁻M⁻+ L^{M109T}, equal genome equivalents of viral particles (ranging from 22-185 μ l) were used for inoculation. For HBV L⁻M⁻, HBV L⁻M⁻S⁻ and HBV L⁻M⁻S⁻+L that only produce free capsids but not viral particles, 185 μ l preparation of concentrated supernatant was used for inoculation. We then collected the supernatant from day 7 to day12 post infection to quantify HBsAg and then fixed the cells for the subsequent immunofluorescence staining against HBV core protein. The secreted viral marker and the number of infected cells (Fig. 29D) both clearly showed that HBV L⁻M⁻+L, HBV L⁻M⁻+ L^{M109T} were infectious, indicating that M-protein is not essential for viral infectivity. The inoculation of HepaRG cells with HBV L⁻M⁻, HBV L⁻M⁻S⁻ or HBV L⁻M⁻S⁻+L did not result in any infection, even judged by the sensitive IF staining (Fig. 29E). The results demonstrate the potency of the infection assay and confirm that the infectivity of M-free virus is not impaired.

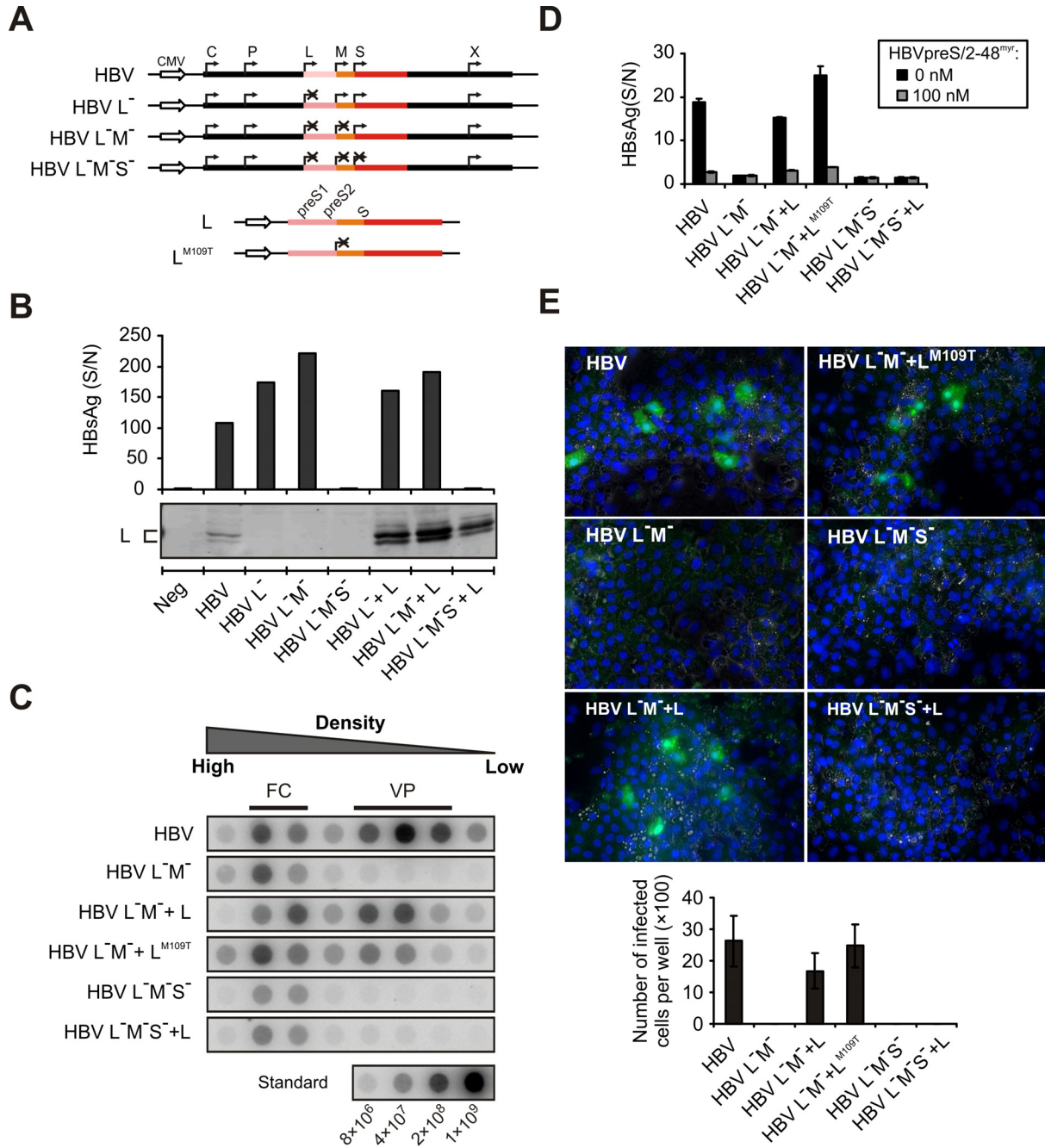


FIG. 29. Expression, assembly and infectivity of M-protein-deficient hepatitis B viruses

A. Schematic illustration of the genomic (HBV, HBV L⁻, HBV L⁻M⁻ and HBV L⁻M⁻S⁻) and the subgenomic plasmids (L, L^{M109T}) used for the production of M-protein deficient HBV. Start codons of the viral proteins (C = core protein, P = polymerase, L = L-protein, M = M-protein, S = S-protein, X = X-protein) are marked by arrows. The preS1-, preS2- and the S-domains of the L-protein are highlighted in pink, orange and red, respectively. The positions of point mutations introduced to abolish initiation of translation of L-, M-, and S-protein are depicted by a cross.

B. Analyses of secreted HBsAg (MEIA of supernatant from day 3-5) and intracellular L-protein (Western Blot at day 2 using mAb Ma18/7) post-transfection of HuH-7 cells with the plasmids indicated below. Note that despite the fact that endogenous promoter driven expression of L-protein (HBV) is significantly lower than ectopic co-expression controlled by the CMV-promoter (L), HBsAg secretion remains similar.

C. HBV-DNA specific Dot-blot of fractions (indicated 2-9) of an analytical CsCl density gradient obtained from concentrated supernatants of transfected HuH-7 cells. Note that transfection with the HBV genomic construct with L expression *in cis* or *in trans* both result in secretion of viral particles (VP, fractions 6-8) and free nucleocapsids (FC, fractions 3-4). Constructs lacking either L- or S-expression only form free nucleocapsids.

D. Infection of HepaRG-cells with comparable amounts concentrated cell culture supernatants of HuH-7 cells after transfection/co-transfection with HBV, HBV L-M, HBV L-M + L, HBV L-M + L^{M109T}, HBV L-M-S and HBV L-M-S + L. HBsAg secreted during day 7-11 post-infection was determined (black bars above). A control infection was performed in the presence of 100 nM HBVpreS/2-48^{myr} to block the preS1-receptor-mediated entry pathway of HBV (grey bars above).

E. HBcAg-specific immunofluorescence (green) and nuclei specific DAPI-staining (blue) of HepaRG cells 13 days post-infection with the concentrated cell culture supernatants of transfected HuH-7 cells indicated in the picture. Quantification of the number of HBcAg-expressing HepaRG cells (bar chart below) was done by single cell counting. The number of HBcAg-positive cells correlates to the secreted HBsAg depicted in Fig. 1D.

2.3.2 No specific sequence in preS2/114-163 is needed for virus infectivity but a length dependent linker within this region is important for viral assembly

The established M-protein-free viral production and infectivity assay endow us the capacity to investigate the role of preS2 of L-protein in the in the absence of M-protein. Considering the fact the preS2 might function in a length dependent but not sequence dependent manner, we constructed serial mutants to dissect the role of preS2 in the context of L-protein. In brief, we cloned the mutant L-protein expression construct as following: (1) the serial deletion started from aa 114 with increasing length, (2) shift mutations keeping the overall length of preS2 but substituting the residues with the corresponding ORF of polymerase which overlaps with the PreS2 ORF, (3) direct deletion of the TLM motif or the 20 residues in the carboxyl terminal region of preS2 which contains the TLM motif along with a control construct delete the first 20 amino acids of the S domain in the L-protein (Fig. 30A). Again, the protein expression (Fig. 30B), viral assembly (Fig. 30C) and virus infectivity (Fig. 31) were examined.

We show that a deletion of 20 amino acids of the N-terminus of preS2 is tolerated for the assembly. However, a deletion of longer than 30 amino acids completely abolishes viral assembly. Interestingly, substituting these 30 amino acids with the exactly corresponding part of the polymerase sequence rescues the assembly, suggesting that the first 30 amino acids in preS2 are important for viral assembly in a length dependent but not sequence specific manner. Meanwhile, the longer substitutions of 50 or 70 amino acids again abolished the assembly, but that was reasonable due to the marginal L-protein expression of S114-163 and undetectable expression of S114-183. The difference between the expression level of S114-143 and S114-163 does not come to the conclusion that the last 20 amino acid are crucial for the L-protein expression, since the deletion of last 20 amino acid do not harm the L-protein expression and viral assembly, but suggest that the corresponding sequence in the polymerase probably lead to unstable conformation of L-protein, which might be degraded quickly.

The last, we showed that the TLM is not necessary for the HBV infectivity since the deletion of TLM (Δ 149-160), even a longer deletion of the last 20 amino acid (Δ 144-163) do not impair viral

infectivity. In contrast, the deletion of 20 aa in the S domain of L-protein completely abolish the infectivity since it destroy the first trans-membrane domain (TM-I). This result shows the role of preS2 for the virus is not for their infectivity but for the viral assembly in length-dependent but not sequence specific manner.

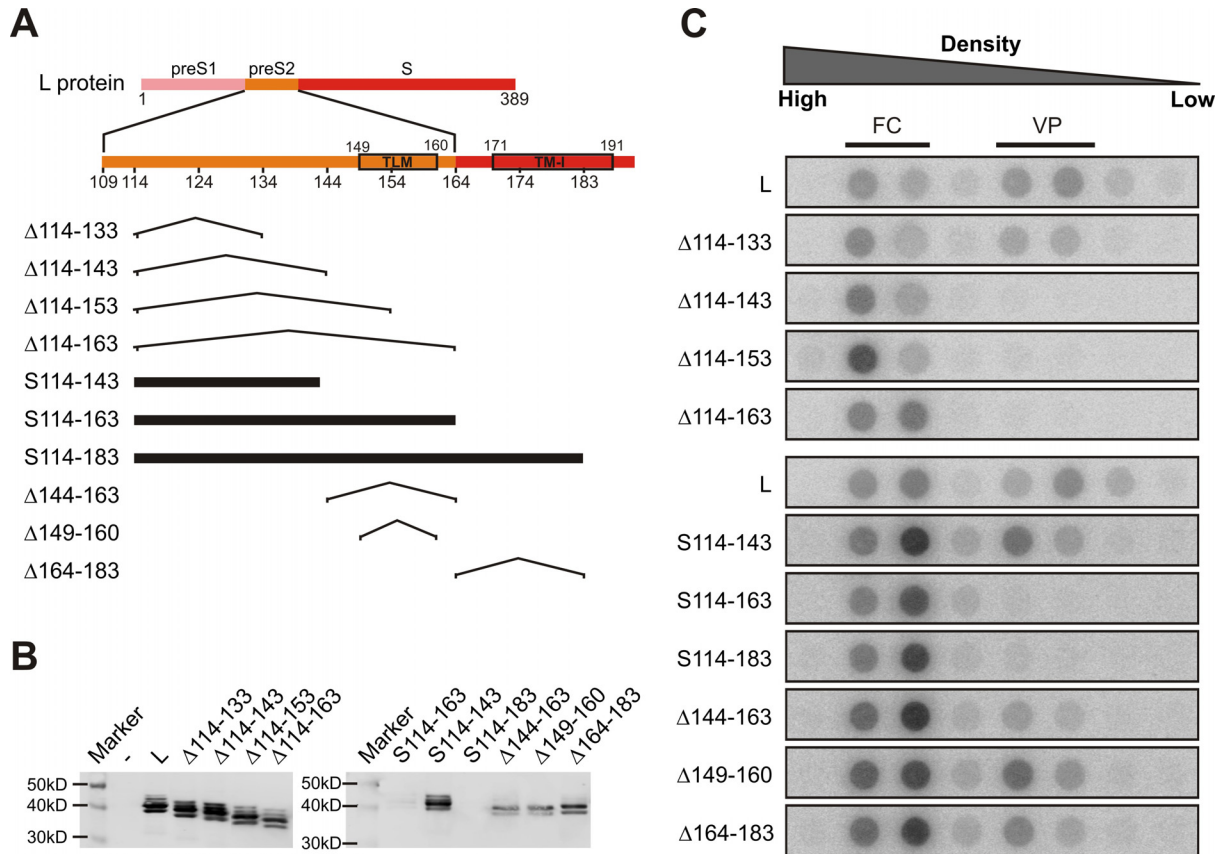


FIG. 30. Protein expression and assembly competence of M-protein-deficient HBV with deletions and frame shift mutations in the preS2-domain of the L protein.

A. Schematic illustration of the HBV L-protein (top) with its preS1- (pink), preS2- (orange) and S- (red) domains and the enlarged preS2/TM-I-domain (below). The numbers in the line drawings refer to the amino acid positions of the beginning and the end of the deletions (thin lines) and the onset and the ending of the polymerase frame-shift (thick lines). The trans-location motif (TLM) mapped to amino acids 149-160¹⁴² and the first transmembrane domain (TM-I, amino acids 171-191) of the S-domain are boxed.

B. Western blots of cellular extracts of HuH-7 cells 2 days post-transfection with the different preS2-deletion L-constructs. Note that the L-protein mutants encoding the two longest polymerase frame-shifts (S114-163 and S114-183) are barely or even not expressed while all other mutants show the unglycosylated and the mono-glycosylated forms at the expected molecular weights.

C. HBV-DNA specific Dot-blot of fractions of analytical CsCl-density gradients of the concentrated supernatants of HuH-7 cells which have been co-transfected with the genomic construct HBV L-M⁻ and the respective deletion/frame-shift mutation indicated at the left. Fractions containing the non-enveloped nucleocapsids are labeled FC, virions are labeled VP.

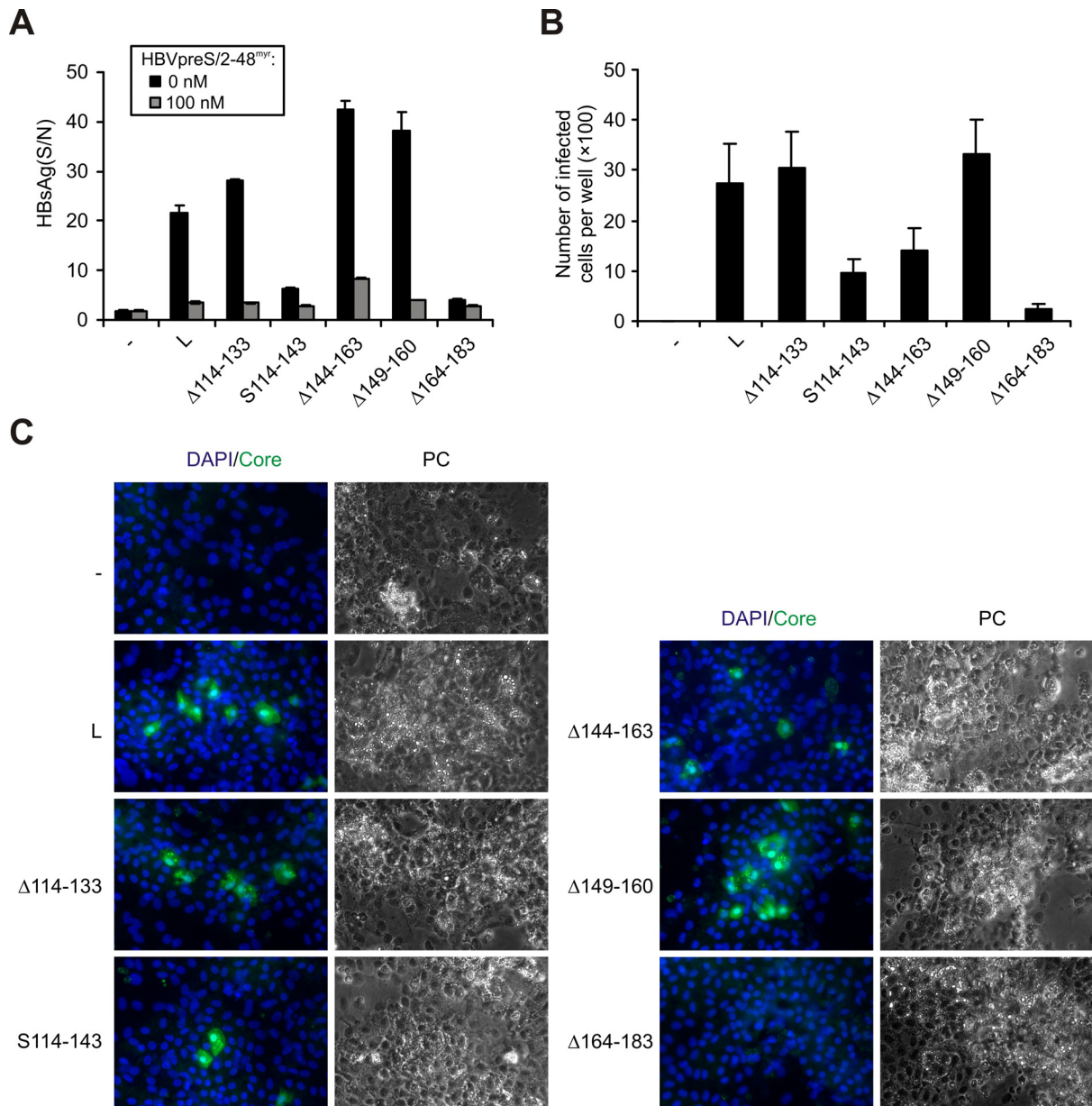


FIG. 31. Infectivity of M-protein-deficient HBV with mutations in the preS2-domain of the L-protein

A. HBsAg secreted from day 7-11 following infection of HepaRG cells with concentrated virus from cell culture supernatants of transfected HuH-7 cells. Equal genome equivalents (as judged from the CsCl-density gradient) of M-deficient viral particles containing wild type L (L) or the L- mutations Δ114-133, S114-143, Δ144-163, Δ149-160 and Δ164-183 were used (black bars). To control specificity of infection virus inoculation was also performed in the presence of 100 nM HBVpreS/2-48^{myr} (white bars).

B. Single cell analysis of infection by the respective M-protein free L-mutants by quantification of HBcAg-expressing HepaRG cells.

C. HBcAg-specific immunofluorescence (green) and nuclei specific staining (blue) of HepaRG cell 13 days post-infection with the M-protein-deficient HBV mutants L, Δ114-133, S114-143, Δ144-163, Δ149-160 and Δ164-183.

2.3.3 M-protein-deficient HBV with a randomized preS2-sequence in its L-protein properly assembles and is infectious in HepaRG cells and PHH

In the previous results we showed that the most of preS2 is not needed, since both the first 20 amino acid deletion and the last 30 amino acid substitution did not abolish the viral assembly and

infectivity. However, S114-163 could not be expressed well, which might be due to the instability of L-pol chimeric protein. To strengthen the notion that the majority of preS2 act solely as linker between the preS1 and trans-membrane region, we tried to replace aa 114-163 with scrambled amino acids instead of the sequence from pol. We synthesized overlapping oligos encoding scrambled amino acid sequence of preS 114-163 but kept the codon usage except for an introducing of a Pst I site in the 3' end of PreS2 (Fig. 32A). This mutated L-protein (114-163^{Scramble}) could be expressed although with a decreased amount (Fig. 32B). Importantly, this mutant supports viral assembly as well as the wild-type L protein (Fig. 32C).

Since this mutant allows a functional L-protein expression and viral assembly, we are interested to explore the infectivity of recombinant virus. Firstly, the HepaRG cells were used to determine the infectivity of 114-163^{Scramble}. The infectivity is marginally affected as demonstrated by the secreted HBsAg post-infection and the number of infected cells (Fig. 32D). The infectivity of this pseudovirus was further illustrated using PHH, which is a more authentic infection system. The result is highly in line with that from the HepaRG cells (Fig. 32E). The increasing amount of secreted HBsAg and HBeAg indicates an ongoing viral replication, which could be visualized by the IF staining (Fig. 32F). Importantly, the specificity of infection could be well manifested by co-inoculation the pseudovirus with the myristoylated inhibitory peptide. This result clearly showed that virtually the entire preS2 in the L-protein act solely as a linker for assembly. Since this M-protein-free mutant, 114-163^{Scramble}, is almost as infectious as the wild-type, it again excludes any sequence-specific role of preS2 in HBV entry, such as translocation or fusion.

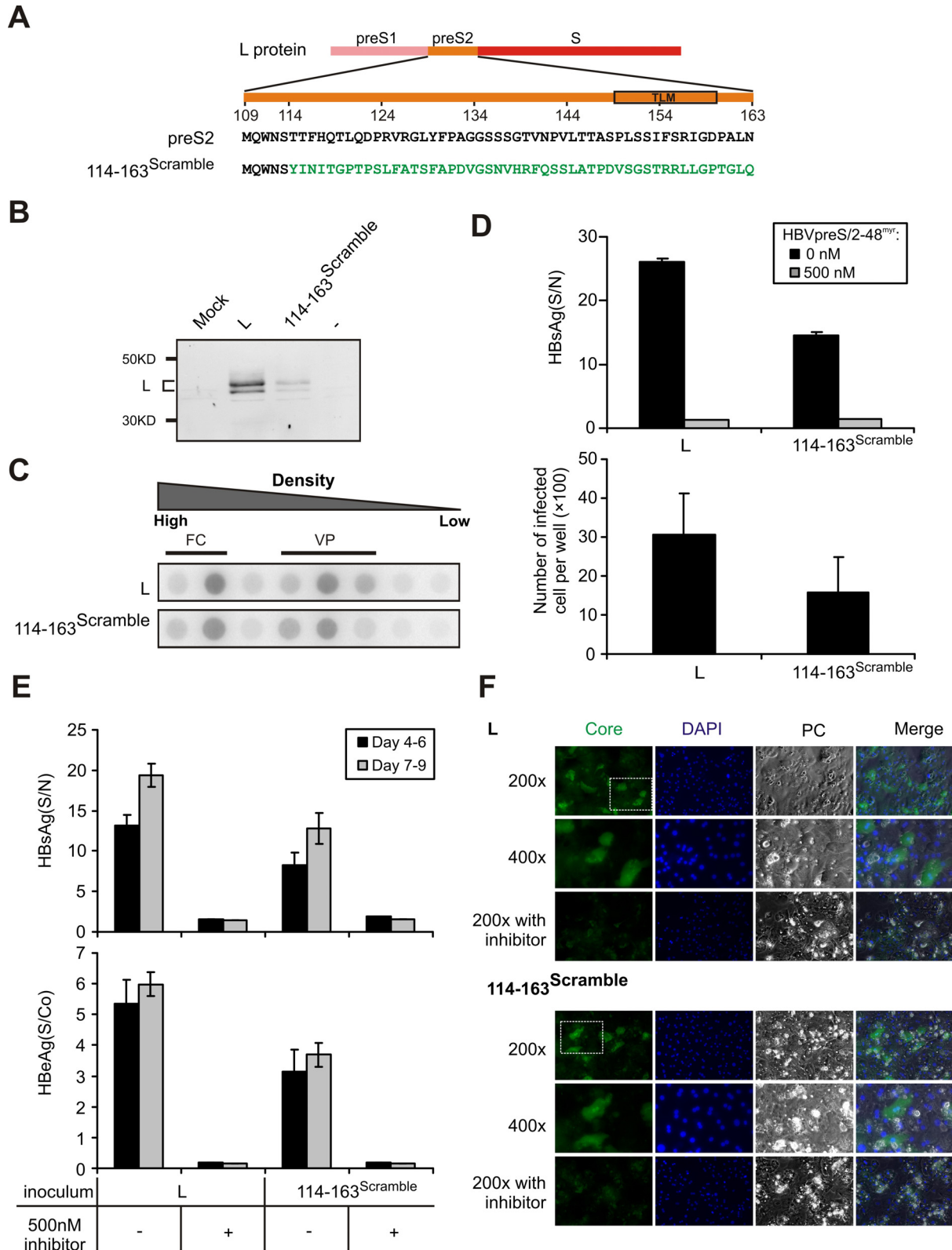


FIG. 32. Analysis of assembly and infectivity of an HBV-mutant containing a scramble preS2 sequence.

A) Sequence of the HBV preS2-domain (genotype D) as part of the L-protein (top) and the scrambled preS2 sequence encompassing amino acid 114-163 (below). Note that the very N-terminal five amino acids remained unchanged in order to sustain nucleocapsid envelopment. The algorithm for scrambling amino acids 118-163 (YINI) differed from the one used to randomize amino acids 114-117 (YINI).

B) HBV-preS1-specific Western blot (mAb Ma18/7) of cellular extracts of HuH-7 cells transfected with wide-type L and 114-163^{Scramble}.

C) HBV-DNA specific Dot-blot of fractions from analytical CsCl-density gradients of the concentrated supernatants of HuH-7 cells after co-transfections with HBV L:M + L and HBV L:M + 114-163^{Scramble}. Fractions containing non-enveloped nucleocapsids are labeled FC, fractions containing virions are labeled VP. Note that although expression the preS2-scrambled L-protein was lower, virion formation was virtually unaffected.

D). Infection of HepaRG cells using comparable amounts of concentrated virus preparation obtained from HuH-7 cells, co-transfected with HBV L:M + L and HBV L:M + 114-163^{Scramble}. HBsAg (above) secreted between day 7-11 post-infection was quantified by MEIA (black bars). Quantification on the single cell level was performed by counting HBcAg-positive cells 12 days p.i. (below). Control infections were performed in the presence of 500 nM HBVpreS/2-48^{myr} (white bars above).

E) Infection of PHH using equivalent amounts of concentrated virus preparation obtained from HuH-7 cells, co-transfected with HBV L:M + L and HBV L:M + 114-163^{Scramble}. HBsAg (above) and HBeAg (below) secreted between day 4-6 and day 7-9 were quantified. Control infections were performed in the presence of 500 nM HBVpreS/2-48^{myr}.

F) HBcAg-specific immune fluorescence (green) of PHH 9 days post-infection with the concentrated virus preparation obtained from HuH-7 cells co-transfected with HBV L:M + L (left panels designated with L) and HBV L:M + 114-163^{Scramble} (right panels designated with 114-163^{scramble}). Note that infection by both viruses is blocked by 500 nM HBVpreS/2-48^{myr}.

2.4 Analysis of the role of the S domain in the L protein and the S protein for assembly and infectivity of HBV

As mentioned above (1.1.3), both the S and L protein, bearing the S-domain, are present in the envelope of Dane particle and dispensable for virion morphogenesis. The S-domain contains four trans-membrane domains (TM) and three loop structures, designated cytosolic loop-I (CYL-I), antigenic loop (AGL), and cytosolic loop-II (CYL-II).

The short N- and C-terminus of the S protein, as well as the 60-aa AGL, the main recognition site for the antibody response, intrude into the ER lumen and are thus present at the outside of the virus particle (Fig. 2). The two cytosolic loops (CYL-I and CYL-II) face toward the cytosol and are present in the inside of the virus particle.

The S-domains in the S and the L protein have different topologies and functions. The CYL-I of the S-protein but not of the L protein is important for virus assembly, due to its interaction with the HBV capsid⁹⁶. Whereas, the first trans-membrane domain (TM-I) of L protein probably does not cross the membrane and acts as a fusion peptide¹⁴¹.

It has been shown that three cysteine residues (C48, C65 and C69) in the CYL-I are required for the SVP and virus secretion¹²⁶. It has also been shown that the importance of these cysteine residues on the viral assembly is due to its context in the S protein, since the substitutions in the S protein abolish the secretion of 22nm spherical particle¹⁹⁵. Except for these cysteine residues, virtually all residues in the CYL-I can be substituted without interference with the infectivity of HDV¹²⁶. It is noteworthy to point out that these introduced substitutions affected all three envelope proteins, and it is still unclear whether the three cysteine residues in the context of CYL-I of L protein affect the viral assembly and infectivity.

It has been shown that the AGL in the S-domain is required for the infectivity of HDV¹³⁶. Further mutation analysis showed that the cysteine residues (C121, C124, C137, C138, C139, C147 and C149) in the AGL are essential for the infectivity of HDV. Again, since these introduced mutations were present in all three envelope proteins, it is not clear in which context of envelope protein the mutation interfere with virion infectivity. The underlying mechanism remains unclear since a possible role of protein-disulfide isomerase (PDI) as a cellular factor is excluded by modification of the PDI-recognition motif (see 1.4)⁴³. Thus, the following questions were addressed in this study: (1) Is the AGL required for the infectivity of HBV? (2) Do the AGLs in the L protein and the S protein actually play different roles? (3) What is the role of AGL in the HBV entry?

Two advantages we have, as shown in the previous section, enable us to answer these questions. First, we have shown that the M protein is not important for infection. Since we have set up a method for the production of M-free virus, we can focus solely on the L and S protein. Second, in the envelope of the M-free virus, we showed that the L and S protein can be expressed separately by two different constructs, which enable us to selectively introduce mutations into the L or the S protein. Based on these advantages and the previous results shown in the HDV system, cysteine residues of CYL-I or AGL were substituted independently in either the S or the L protein to determine the viral assembly and infectivity. As the preS-outside topology and the HSPG-binding activity of virus particle are considered as prerequisites for the virus infectivity, the topology of L protein and heparin-binding activity of mutant virus were analyzed correspondingly.

2.4.1 The effect of cysteine mutations in the S protein and the L protein on protein expression and secretion

To dissect the role of cysteine residues, we selectively addressed three cysteine residues (C48, C65, and C69) in the CYL-I of L or S and three cysteine residues (C124, C139 and C149) in the AGL of L or S. these cystenies were known to be important for viral assembly and infectivity respectively. In the CYL-I, these cysteine residues were individually substituted with alanines (C48A, C65A, and C69A), and in the AGL, the cysteine residues were individually substituted with serines (C124S, C139S, and C149S). All the mutations were introduced either into the helper construct (expressing the L protein) or genomic construct (expressing the S protein) (Fig. 33A).

To check the expression of the L protein, HuH-7 cells were transfected with wild-type or mutant helper constructs, and the cells were lysed 2 days post-transfection. All the L-proteins (p39/gp42) were detectable by Western blot using the preS1-specific monoclonal antibody mAb Ma18/7 (Fig. 33B). Although the expression level of CYL-I mutated L-protein was considerably lower compared to the wild-type L-protein, the glycosylation pattern of both proteins was similar (p39 and gp42).

To check the secretion of S-protein, the HuH-7 cell were transfected with genomic and helper constructs at a ration of 5:1 as established before. The supernatants of cell culture at day 3-5 post-transfection were collected to quantify HBsAg by MEIA. Compared to the transfection with S-protein expression constructs, the co-transfection of S and L protein expression constructs resulted in 50% reduction of secreted HBsAg, which is probably due to the retention potency of the L protein. Nevertheless, secreted HBsAg after co-transfection with all mutant L-

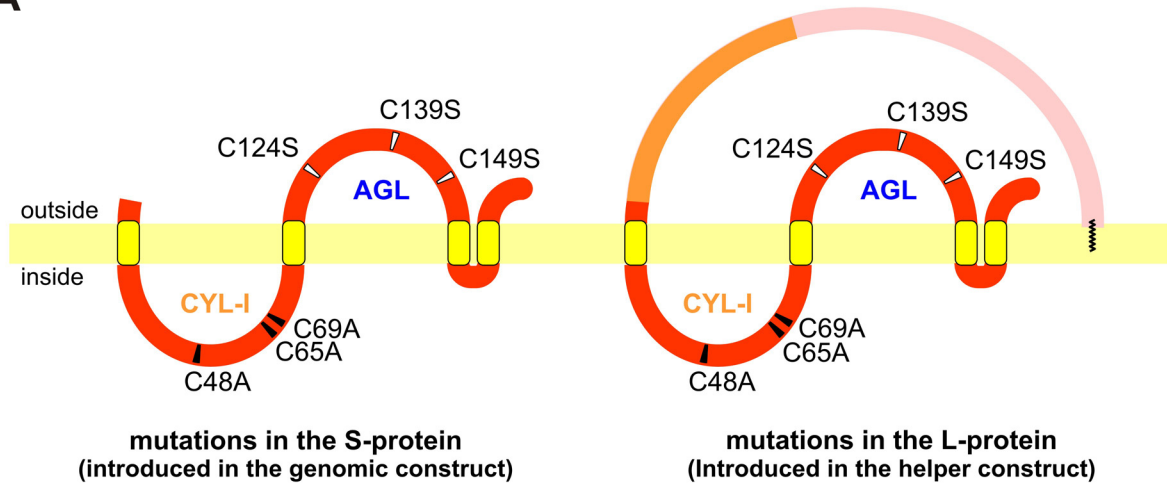
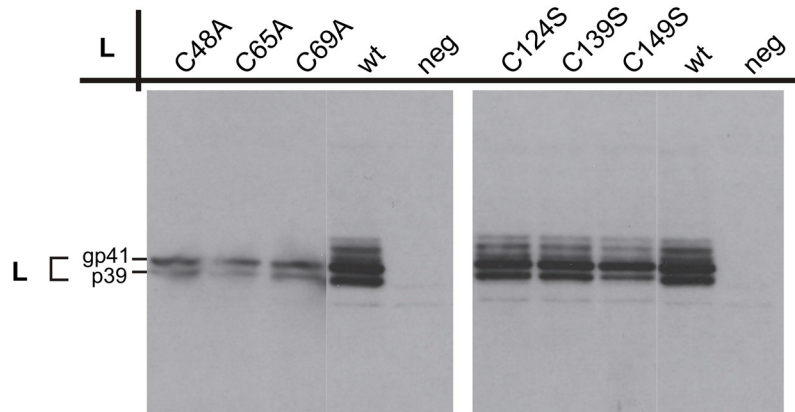
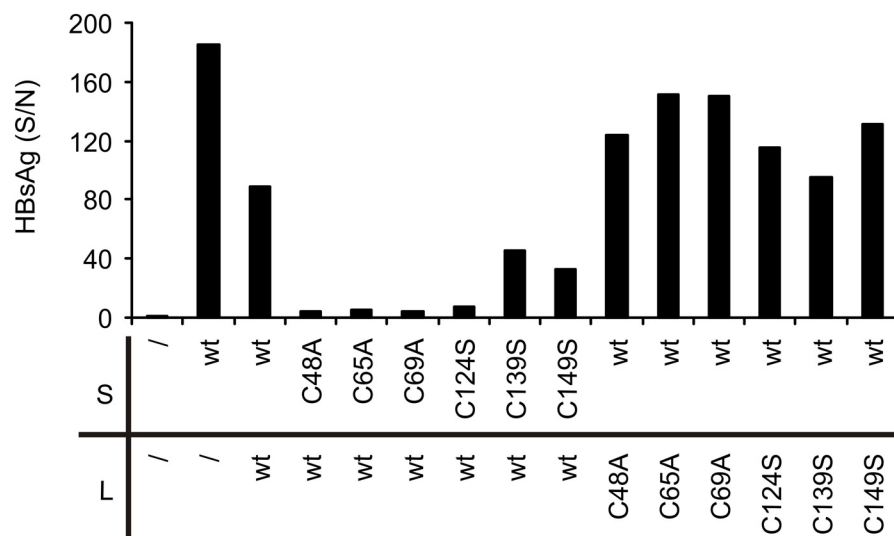
proteins was comparable to that with wild-type L-protein, suggesting that these mutant L proteins allowed subviral particle secretion as efficiently as the wild-type L protein. As expected, the cysteine mutation introduced into CYL-I of S protein abolished the S-protein secretion, which is consistent with previous data¹⁹⁶. However, we could not evaluate the secretion of HBsAg when the cysteines in AGL of S protein were substituted with serine, since the commercial HBsAg test against antigenic loop probably also can not detect these mutants as described previously⁴³.

2.4.2 The effect of cysteine mutations in the S protein and the L protein on virus assembly

To answer the question whether the cysteine residues in either L protein or S protein have different influence on HBV assembly, HuH-7 cells were co-transfected with the respective genomic and helper constructs as described before. The virus present in the culture supernatant was concentrated for DNA dot-blot analysis of viral assembly.

Substitution of one of the cysteines in the CYL-I (C48, C65 and C69) of the S protein resulted in a completely abolished assembly (Fig. 34). This is consistent with the observation that these mutations also abolished the secretion of HBsAg (Fig. 33C), suggesting that the CYL-I is crucial for the interaction between S proteins to form the viral envelope as it was shown previously¹⁹⁶. Notably, the corresponding mutation, when selectively introduced into the L protein context, did not significantly reduce the level of viral formation and secretion. This indicates that the interaction between L and S proteins for the envelope formation might be distinct from interactions between S proteins.

In contrast, all the cysteine mutations introduced into the AGL of the S proteins did not diminish viral secretion, although there is a considerable difference (e.g. ~5 fold decrease in the case of the C149S mutant) with regarding to the amount of secreted particle judged by DNA dot-blot (Fig. 34). The corresponding mutations introduced into the context of L protein did not lead to significant difference in the viral assembly.

A**B****C****FIG. 33. Expression of the L and S protein bearing cysteine mutations**

A. Schematic illustration of introduced cysteine mutations in the envelope of M-free virus. The 6 cysteine residues (C48, C65, C69, C124, C139, C149) in the CYL-I or AGL of the S protein (left) were individually substituted by alanine or serine as indicated. The corresponding cysteine in the L protein was also individually substituted by alanine or serine as indicated (right). The AGL and CYL-I are assumed to be located on the outside and inside of the virus particle respectively. The preS1-, preS2- and the S-domains are highlighted in pink, orange and red. Note that the L protein with “preS-outside topology” was shown.

B. Western blots of cellular extracts of HuH-7 cells 2 days post-transfection without (neg) or with the wild-type L-constructs (wt), or with L construct bearing mutation in the CYL-I (C48A, C65A, C69A) or AGL (C124S, C139S, C149S).

C. Analyses of secreted HBsAg (MEIA of supernatants from day 3-5) post-transfection of HuH-7 cells with the plasmids indicated below.

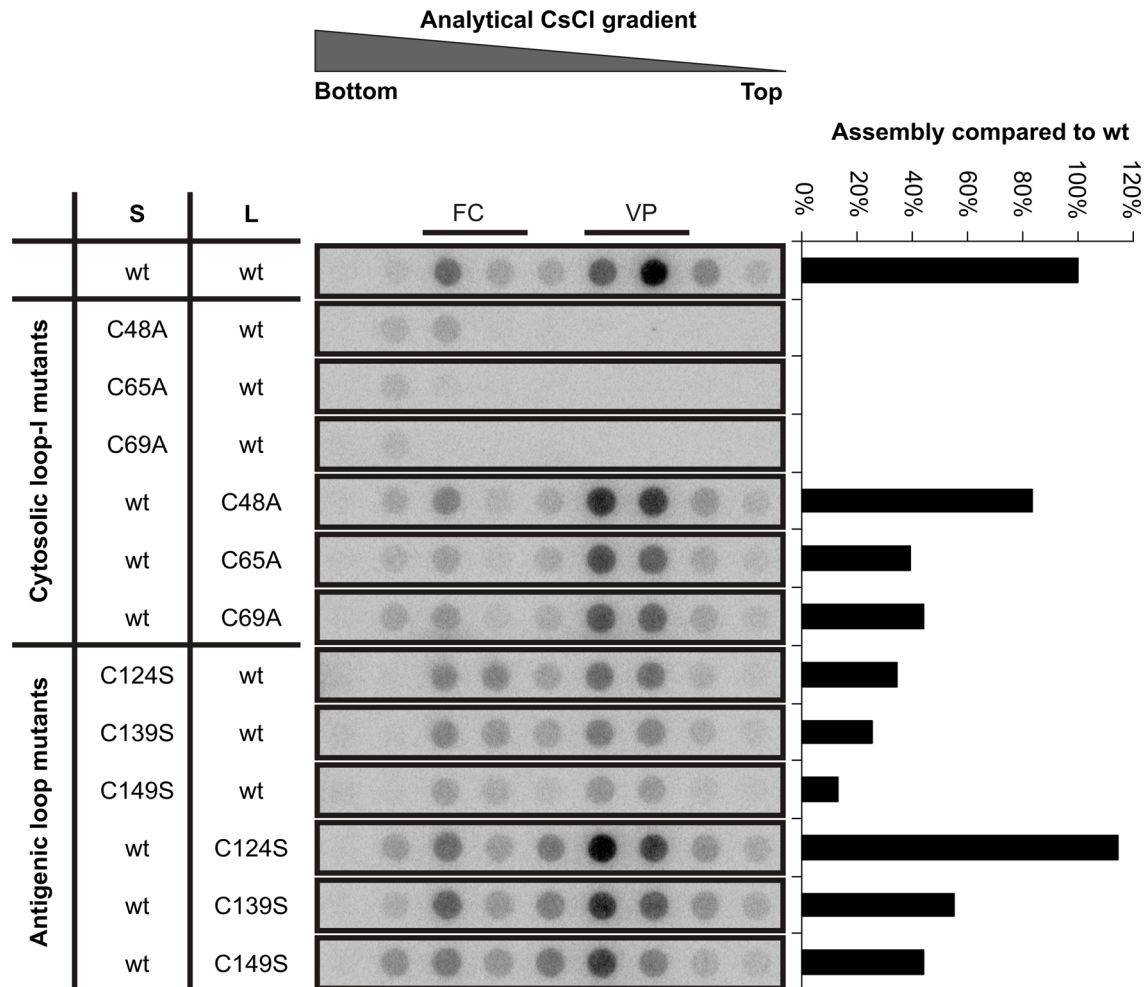


FIG. 34. Analysis of assembly and secretion of M-protein-free HBV with mutated cysteines in either the S or L protein

HBV-DNA specific Dot-blots of fractions of analytical CsCl density gradients obtained from supernatants of HuH-7 cells, which have been transfected with a mixture of L and M-deficient genomic construct expressing S protein, and helper constructs expressing L proteins. These M-protein-free viruses contain wild-type S and L protein, or the indicated mutated cysteines in the CYL-I in S proteins or L proteins, or mutated cysteine in the AGL of S proteins or L proteins. Virus production was quantified using Quantity One, and the relative production compared to the wild-type is shown in the right panel with horizontal black bars.

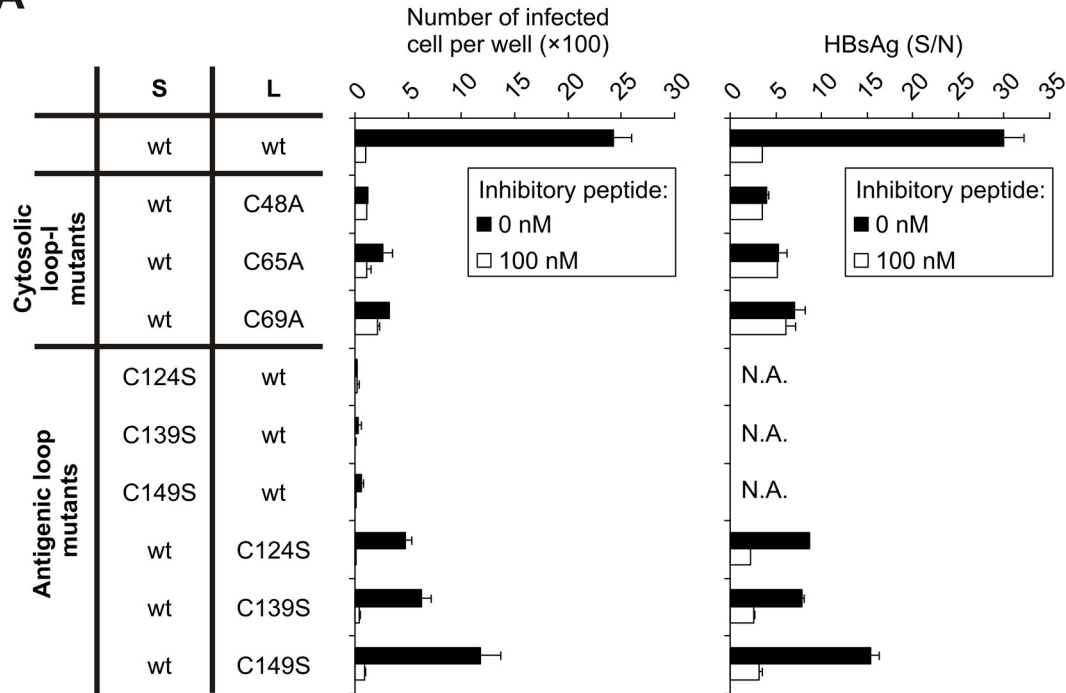
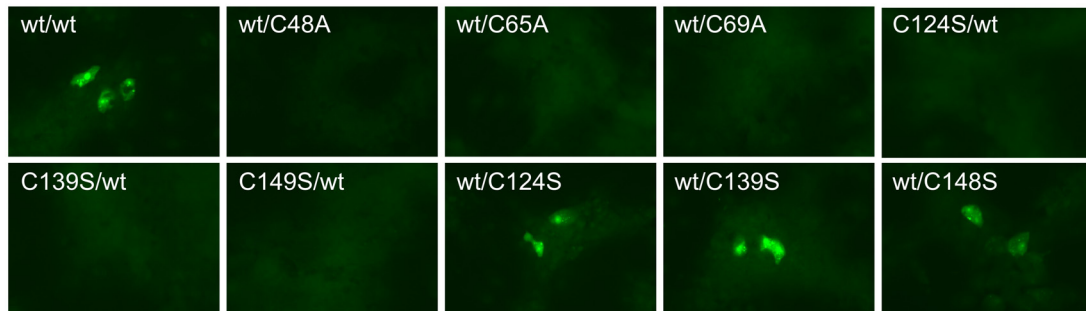
2.4.3 The effect of cysteine mutations in the S and the L protein on HBV infectivity

The nine assembly-competent mutant viruses with mutation in the CYL-I or AGL allowed us to investigate the impact of individual cysteine substitutions in the S and L protein on virus infectivity. HepaRG cells were infected with comparable genome equivalents of the mutants, and the infection was quantified by the secreted viral marker or the number of infected cells (Fig. 35).

When any of 3 cysteines in the CYL-I of L protein was substituted, the virus infectivity was drastically lost, as judged by the secreted viral marker and the number of infected cells. This indicates the existence of an infectivity determinant in the CYL-I of L protein. Since cysteines are important for the formation of disulfide bonds, it is probably not the cysteine residue *per se* but the conformation of CYL-I formed by inter or intra-molecular disulfide bonds¹⁹⁷, which is critical for the virus infectivity.

When the mutation was introduced into the AGL of the S protein, but not into the L protein, HBV infectivity was drastically reduced to the background level judged by co-incubation with 100nM inhibitory peptide HBVpreS/2-48^{myr}. This indicates that HBV infection relies largely on the AGL of the S protein as HDV. It must be mentioned that the infectivity of viruses with mutated cysteine in the S-protein is not suitable for the MEIA of secreted HBsAg, since the commercial HBsAg test relies on the antibody recognizing the wild-type AGL.

The data above demonstrates the distinct roles of the CYL-I and AGL in the S and L proteins of HBV for infection. The CYL-I in the L protein but not S protein allows proper viral assembly but severely impairs the infectivity of virions. The cysteines in the AGL of the S protein, but not of the L protein are critical for HBV infectivity, suggesting that the observed impact of the AGL on HDV infectivity⁴³ might also be resulted from the AGL in the S protein.

A**B****FIG. 35. Infectivity of M-protein free HBV with cysteine mutations in either S or L protein**

A. Infectivity of the cysteine mutants on HepaRG cells. The infectivity was determined by the number of infected cells and the amount of secreted HBsAg into the supernatant between days 8-13 post-infection. The infection was performed in the absence (black bars) or presence of 100 nM HBVpreS/2-48^{myr} (white bars).

B. IF staining of HepaRG cells using the HBcAg-specific antibody 13 days post-infection. Infected cells with virus containing cysteine mutations (S/L) were visualized by staining with polyclonal rabbit antiserum (H363) against HBV core protein (green).

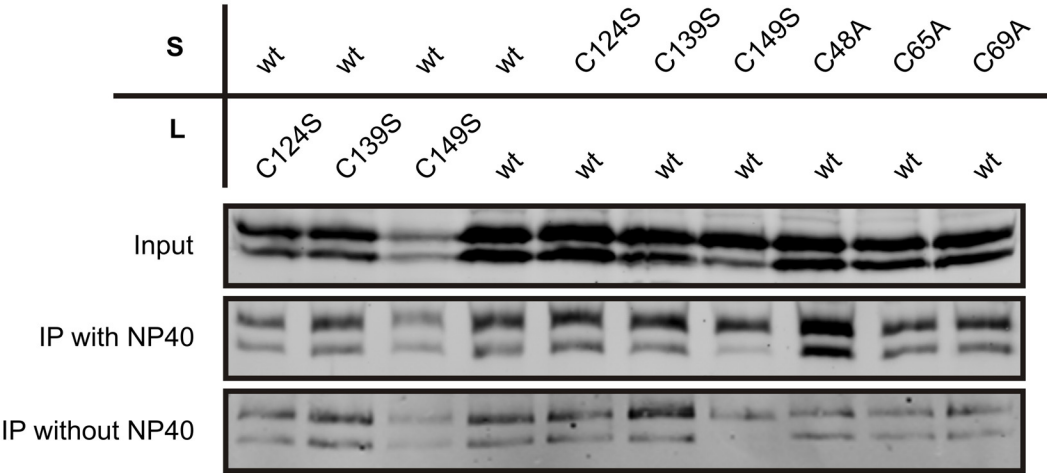
2.4.4 The effect of cysteine mutations on the topology of the L protein

It was important to understand the mechanism that the virus assembly and infectivity differ when the mutations were differentially introduced into the S protein and the L protein. It is thought that the L protein have two different topologies. In one of the topology, preS is inside and is necessary for nucleocapsid binding, while another with preS outside is critical for receptor interaction. We next asked whether these mutations introduced into the CYL-I of the L protein, and the AGL of S protein and L protein affect the L-protein topology during virus assembly.

Two techniques were used to analyze the L protein topology. One is based on the assumption that the anti-preS antibody can only recognize viral and subviral particles with preS orientated outside. An rabbit polyclonal antiserum was raised against the myristoylated N-terminal 47 residues of the L protein, HBVpreS/2-48^{myr}. Therefore this antibody was used to immunoprecipitate both viral and subviral particles from the supernatant of co-transfected HuH-7 cells in the presence or absence of 0.5% NP-40. As a control for efficiency of the IP, the same amount of material was precipitated with PEG. Western blot analysis was performed with all three precipitates to determine the amount of L protein. Our result showed that the L protein-enriched particles can be precipitated in the absence of NP-40, suggesting that all mutant viruses bear the preS1-domain accessible on the surface of virus particle. The use of NP-40, which disrupts virus membrane and increase the accessibility of the preS-inside L protein, increase the efficiency of IP to some extent, supporting the model of two topology of the preS-domain. More importantly, the amount of L protein-enriched particles correlated to the total amount, the PEG-precipitate (Fig. 36A), indicating that mutant viral particles and subviral particles were recognized by the anti-preS antibody as efficiently as the wild-type. This suggests that the introduced mutations in the envelope protein do not significantly change the preS-outside topology of the L protein in viral and subviral particles. Change in their infectivity therefore did not result from a changed preS-accessibility.

A trypsin digestion assay was used as the second method to quantify the ratio of preS-inside and preS-outside L protein (Fig. 36B). This method was established in previous study since trypsin can only hydrolyze the arginine or lysine residues in the preS domain on the outside the virus particle¹⁹⁸. As a control, NP-40 was added to expose the inside preS and makes them accessible to trypsin digestion. Therefore, the PEG-precipitated virus was treated with trypsin in the presence or absence of NP-40. Following trypsinization, L protein was detected by Western blot with Ma18/7. Our result showed that when wild-type S and L proteins are present in the particle, a proportion of L protein is trypsin-resistant compared to the undigested control. The results favored the two topologies of L protein and validated the used digestion assay. As the wild-type, all cysteine mutants showed a similar trypsin-digestion pattern, supporting again the notion that the L proteins in the mutant viruses are topologically arranged as the wild-type.

A



B

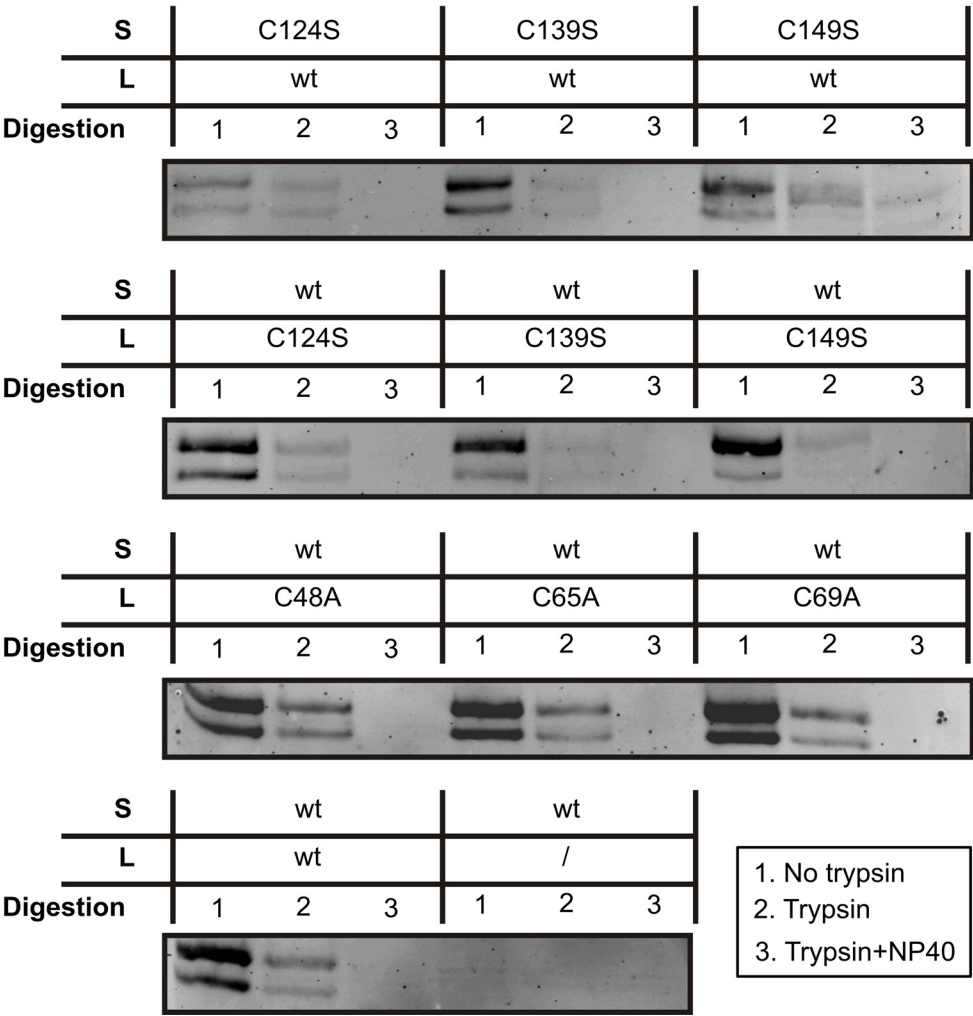


FIG. 36. The topology of the L protein in cysteine mutants of HBV
A. IP analysis to resolve the L protein topology. 1 ml supernatant of transfected HuH-7 cells with plasmid producing the indicated mutant viruses were subjected to IP by the polyclonal anti-preS1 antiserum (Rabbit anti-Myrcludex B) in the presence or absence of 0.5% NP-40. As a control, the same amount of supernatants was PEG-precipitated (input). Precipitates were analyzed by Western blot (using mAb Ma18/7) to detect the L protein.

B. Trypsin digestion analysis of L protein topology. The supernatant of transfected HuH-7 cell producing the indicated mutant virus was concentrated by PEG-precipitation. Following incubation with trypsin in the absence (2) or presence (3) of 0.5% NP40, Western blot analysis was performed (using mAb Ma18/7) to determine the remaining L protein. As a control for the amount of input, the untreated viruses (1) were also subjected to the Western blot analysis.

2.4.5 The heparin-binding activity of the HBV particles with cysteine mutations

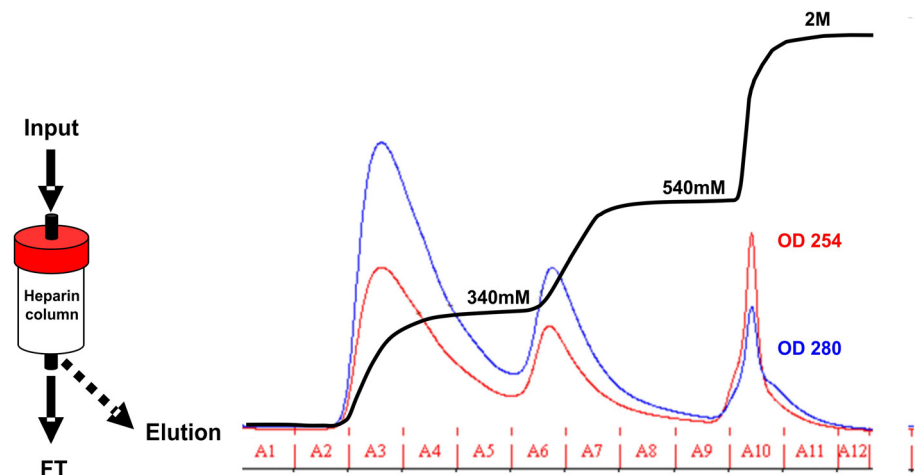
As demonstrated above, the lost or reduced infectivity of cysteine mutant do not result from a changed preS-topology. Previous studies have demonstrated the importance of heparan sulfate glycosaminoglycans (HSPG) during HBV infection and it was suggested that HSPGs are responsible for primary attachment during HBV entry^{42,115}. I therefore asked if the cysteine mutants interfere with virus infectivity at the primary attachment step, i.e., the interaction of virus particles to heparan sulfate. To answer this question, a heparin binding assay was set up in order to quantify the percentage of virus that can specifically bind to heparin, which has a similar structure to heparan sulfate (Fig. 37A). Supernatants of HuH-7 cells between day 3 and day 8 post-transfection were applied to a heparin affinity column, and the bound viral particles were eluted with increasing concentrations of sodium chloride. Unbound particles in the flow-through and the eluted fraction were quantified by DNA-dot blot assay of the CsCl density gradients.

Virions containing wild-type S and L protein bound to the heparin column with ~85% yield. The binding capacity of the heparin column was not saturated, since a 5-fold higher amount of input did not change the ratio of bound virus to unbound virus. This also suggests that a portion of virions are unable to bind heparin, as well as the majority of nonenveloped capsids (Fig. 37B). Furthermore, fine characterization of the eluate by three-step increasing concentration of sodium chloride showed that the majority of the bound virions could be eluted at 340 nM, while some bound virions could only be eluted at 540nM. The 2 M eluate mainly contained marginal free capsids (Fig. 37B). Using this binding assay, cysteine mutants were evaluated with respect to their binding capacity. The CYL-I mutant in the L protein with impaired infectivity did not show remarkable change of heparin binding. However, mutants containing cysteine mutations in the AGL of the S protein, which lead to a loss of infectivity, also lost their ability to bind heparin. In contrast, the AGL cysteine mutations in the L protein did not significantly reduce the capability of binding to heparin. This coincides with their remained infectivity. The bound virus can also be visualized in the overall elution (Fig. 37C) and the elution at 340 nM (data not shown).

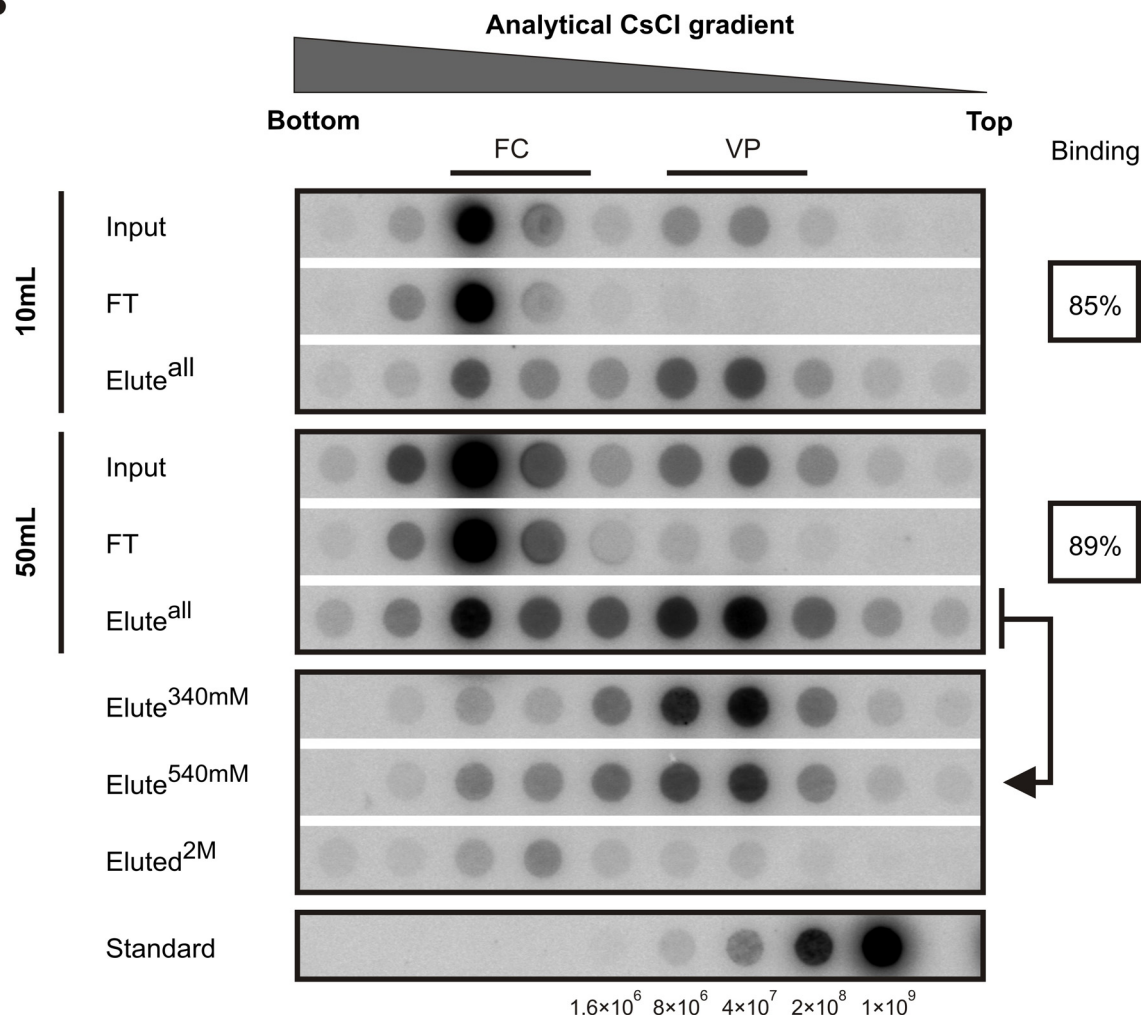
In conclusion, There is a correlation between virion infectivity and the heparin-binding activity when the mutations were introduced into the AGL of S and L, indicating that the AGL of S is the main determinant involved in the virus interaction with HSPG, which is proposed to mediate primary attachment during virus entry. The reduced infectivity of the cysteine mutants in the

CYL-I of L protein do not correlate with the heparin-binding activity leaving the underlying mechanism unsolved.

A



B



				Analytical CsCl gradient												
				Bottom					Top							
		S	L			FC					VP					
Cytosolic loop-I mutants	wt	wt	Input											85%		
			FT													
			Elute ^{all}													
	wt	C48A	Input											63%		
			FT													
			Elute ^{all}													
	wt	C65A	Input											62%		
			FT													
			Elute ^{all}													
wt	C69A	Input											64%			
		FT														
		Elute ^{all}														
Antigenic loop mutants	C124S	wt	Input											4%		
			FT													
			Elute ^{all}													
	C139S	wt	Input											~0%		
			FT													
			Elute ^{all}													
	C149S	wt	Input											~0%		
			FT													
			Elute ^{all}													
Antigenic loop mutants	wt	C124S	Input											69%		
			FT													
			Elute ^{all}													
	wt	C139S	Input											71%		
			FT													
			Elute ^{all}													
	wt	C149S	Input											76%		
			FT													
			Elute ^{all}													

FIG. 37. Heparin-binding activity of viruses with cysteine mutations in the S or L protein

A. Schematic illustration of heparin binding assay. Supernatants of HuH-7 cells containing cysteine mutants were applied to the heparin column. The flow-through (FT) was collected and the bound material was eluted in 12 fractions by 3 steps of increasing concentration of sodium chloride (340mM, 540mM and 2M). The eluted fractions consist of three peaks as visualized by the blue (OD_{254}) and the red lines (OD_{280}).

B. Characterization of the heparin-binding capacity and the elution profile of recombinant HBV virions. HBV-DNA specific Dot-blot of fractions of an analytical CsCl density gradients were obtained from the input, flow through and elution fractions of heparin column. 10 ml supernatant of HuH-7 cells, which was transfected with HBV L-M⁻ and wt L, was diluted to final volume of 50 ml, applied to the column and eluted by three-step increasing concentration of sodium chloride as described in (A). 4% of input (Input), 4% of flow through (FT) and 16% of elution (Elute^{all}) were applied to the CsCl density gradient and DNA dot-blot analysis was performed (row 1-3). Dot-blot of row 4-6 was obtained as same as row 1-3 except that 50 ml undiluted supernatant of HuH-7 cells was used. The three peak virus-containing fractions (Elute^{340mM}, Elute^{540mM}, Elute^{2M}) were individually applied to the analytical CsCl density gradient and HBV-DNA Dot-blot analysis (row 7-9). Linearized pCHT-9/3091 with indicated copy numbers was used as the standard (the lowest row). The virus containing fraction was further quantified using software Quantity One, and the percentage of bound virus was calculated and shown in the box.

C. The binding capability of cysteine mutants in the L and S protein. 10-50 ml of supernatant of HuH-7 cell post-transfection was applied to the column. 4% of input and flow through were subjected to analytical CsCl gradient as well as 16 % of the overall elution (Elute^{all}). The percentage of bound virus are quantified, calculated and shown in the box.

3. Discussion

3.1 Analysis of different parameters on their effect on HBV infection in HepaRG cells

The HepaRG cell line was obtained from liver tumor tissue of a female patient suffering hepatitis C virus (HCV) associated hepatocellular carcinoma (HCC)^{171,173}. This cell line was shown to be HCV-free and has the potential to differentiate into hepatocyte-like cells in the presence of DMSO and hydrocortisone. The differentiated HepaRG cells are susceptible to HBV, which was prepared from the culture supernatant of HepG2.2.15 cells¹⁷¹. HBV infection of HepaRG cells has rarely been reported so far with particles produced after transient transfection, e.g. HuH-7 cells transected with replication-competent plasmid. In contrast, HDV particles produced by transient transfection have been used to infect HepaRG cells to investigate the infectivity determinant of viral envelope^{43,122,126}. In the present study, we intended to set up an improved infection assay to systematically investigate infectivity determinants of HBV on HepaRG cells with simple and visible read-outs. The specificity of infection was ensured by use of a competing peptide. Our effort consists of several critical steps.

First, in order to produce sufficient amount of virus particles to support in vitro infection, we optimized virus preparation. The viruses were produced by co-transfection of HuH-7 cells with L-deficient over-length genomic construct and a helper construct. The complementation enables us to conveniently introduce mutations into envelope proteins without interfering with overlapping polymerase. The HuH-7 cells were co-transfected with these two plasmids using polyethylenimine (PEI). The PEI-mediated transfection on HuH-7 cells achieved transfection efficiency of ~30%, judged by the paralleled transfection with the GFP-expressing plasmid using the same expression vector (pcDNA3.1/Zeo) as the over-length HBV genomic construct. The efficiency of PEI-mediated transfection is ~5 fold higher than the transfection mediated by calcium phosphate (data not shown). Viruses produced in the supernatant could reach $5\text{--}10 \times 10^7$ GE/ml, as determined by DNA-dot blot analysis of the virus-fractions of a CsCl-gradient (Fig. 8). This method allows the separation of enveloped virions from free capsids, which are also produced for a still unknown reason. The virus concentration in the supernatant is an important factor for a successful infectivity assay on HepaRG cells. In previous studies, where viruses were harvested from the a stable cell line HepG2.2.15, virus concentrations in the supernatant could reach 1×10^7 /ml in stationary culture¹⁹⁹, 1.4×10^8 /ml with optimized protocol²⁰⁰, and 8×10^7 /ml for the infection of HepaRG cells¹⁷¹. Nevertheless, the viruses in the supernatants have to be concentrated by precipitation with 6% PEG and resuspension in $1/100^{\text{th}}$ of the original volume. Generally, $\sim 2 \times 10^8$ GE virus particles (suspended in $<100\mu\text{l}$) were used to infect $\sim 10^6$ HepaRG

cells (1 well of a 12-well plate). In contrast, the viruses in the supernatant of HepAD38 cells were apparently much more abundant (Fig. 8). When concentrated with PEG, virus concentration could reach 5×10^{11} GE/ml, infect 30% of HepaRG cells (Fig. 14B) and 90% of PHH (data not shown) of a multiplicity of 10^4 GE/cell.

The second step was to optimize HepaRG cells. In the current study, we validated cell passages (from passage 27-38) for comparable susceptibilities and enhanced the infection by optimizing DMSO concentrations. The most significant difference compared to previous reports^{171,201} was the usage of 0.5% DMSO for cell differentiation. Cell death (apoptosis) of HepaRG cells differentiated in the presence of 0.5% DMSO was less pronounced when compared to 2% DMSO. Therefore, low-dose DMSO might increase the overall number of susceptible cells. Considering the fact that the concentration of DMSO has to be 2% during and post inoculation, it is surprising that HepaRG cells treated with increasing DMSO concentration from 0.5% to 2%, or with decreasing DMSO concentration from 2% to 0.5% during this period, were less susceptible than those treated with constant 0.5% DMSO (Figure 10). This supports the notion that low concentration of DMSO (0.5%) is sufficient to differentiate HepaRG cell into a susceptible status for HBV infection. However, 2% DMSO resulted in the highest values of secreted viral marker in the following period (inoculation and post inoculation). Three possibilities can explain this observation. (1) High concentration of DMSO helps to accelerate post-entry process of the virus, e.g., endocytosis, intracellular transport of virus, or conversion of viral rcDNA to cccDNA. (2) High concentration of DMSO during infection enhances the viral replication rather than increases the number of infected cells, as previous observation showed that the presence of DMSO increased the replication of HBV and DHBV^{169,200,202}. Comparing the number of infected cells under different DMSO concentration would help to clarify this possibility. (3) High concentration of DMSO could enable or increase the rate of virus spread, i.e., infection of naïve cells by progeny viruses. However, this explanation is contradicted by our observation that the progeny viruses produced by infected HepaRG cells were ~100-fold less abundant than the inoculated viruses (data not shown). Nevertheless, application of entry inhibitors to HepaRG cells after infection, such as inhibitory peptide and neutralizing antibody, might clarify this possibility.

As last point, we intended to establish a sensitive single-cell-based read-out for quantifying HBV infection. In addition to determining the secreted viral marker (HBsAg/HBeAg), IF-analysis with a rabbit polyclonal anti-core antibody was developed to visualize the infected cells. The HBcAg-specific IF staining was quantified by counting infected cells. The number of infected cells is linearly correlated to the amount of virus input and the secreted HBsAg in a broad range

(Fig. 9). Moreover, even if the value of HBsAg assay (AxSYM, Abbott) goes below the cut-off due to low percentage of infection, the infection can still be quantified by the number of infected cells. Therefore, this new method can help us investigate infection events when the assembly or infectivity of virus is severely reduced.

At the time point we performed IF (day 11-13 p.i.), core-proteins in the infected HepaRG cells were predominantly stained in the nucleus, along with some speckle-like structures in the cytoplasm. In contrast, the S-protein stained by a sheep anti-HBsAg antibody exhibited diffused staining pattern throughout the cytoplasm (data not shown). It is not clear if this anti-core antibody predominantly binds capsids or core proteins, and it is also not clear if the stained core/capsids are enveloped, because the Triton-100 was used to permeabilize the cell for the intracellular staining. This permeabilization could expose enveloped capsids to the antibody recognition as well. Studies have suggested that HBV virions, subviral particles, and unenveloped nucleocapsids might be released by distinct pathways^{99,101}. Lambert *et al.* has proposed that HBV virion bud through late endosomal multivesicular bodies (MVB) based on the fact that Vps4 (Vacuolar protein sorting 4) is colocalized with viral protein, and that dominant negative Vps4 mutant blocks viral secretion¹⁰¹. Thus, the core-positive speckle in our study could be the late endosomal class E compartments as observed by Lambert. With our contribution to reaching high-levels of infection, the HepaRG cells might present a better model to investigate the viral assembly than non-susceptible cells, because it support the entire virus life cycle from entry to release.

Another aspect related to endosomal trafficking is the entry process of HBV. Although DHBV infection has been suggested to be mediated by endocytosis^{65,66}, it is still poorly understood whether endocytosis is required for HBV entry. However, endocytosis seems to be favored to play a role because inhibition of endocytosis by hypertonic medium also blocks HBV entry (Schulze A., personal communication; Glebe D., unpublished results). The involvement of endosomes in both pathways for virus entry and assembly raises interesting questions: do the incoming viruses and newly formed viruses actually “see” each other in a common compartment, and what is the influence on HBV life cycle?

The inoculation of HepaRG cells with virus for 2 to 4 hours is not sufficient to reach the plateau of infection, but inoculation overnight significantly increases the infection (data not shown)¹¹². Concentration rather than MOI dependent infection was observed in HBV infection (personal communication with Stephan Urban). Increasing ratios of virus-to-cell (from 10 to 10000 GE/cell) during inoculation did not result in a saturation of infection with regarding to the

number of infected cells (Fig. 9). The infection can be further enhanced by spin-down-inoculation (Fig. 11). For retroviral infection, the spin-down procedure increases the reversible binding of virus to the cells and counteracts forces of diffusion¹⁷⁹. We also observed that the HBV particles bound to the surface of HepaRG cells were significantly increased after spin-down inoculation (data not shown). All these data suggest that a low-affinity binding process is a prerequisite step to establish a productive entry. This phenomenon also suggests that HBV infection can only be established when substantial amounts of virus particles are bound on the cell surface, and that post-entry processes might be critical for the HBV infection, i.e., only a small portion of incoming/uptaken virus could successfully convert their rcDNA into cccDNA. In almost fully-infected PHHs (unpublished observation), the early kinetics of uptaken virus DNA and the cccDNA formation could be helpful to elucidate this process.

An interesting observation is that infected HepaRG cells are mostly found with a canaliculus staining. This indicated the infected HepaRG cell is polarized similarly to primary human hepatocyte, where the membrane toward canaliculus forms an apical membrane. One explanation is that those cells forming canaliculus allow robust virus assembly and secretion. However, this explanation is contradicted to the well-known fact that HuH-7 and HepG2 cell well support HBV replication even the canaliculi are poorly formed in those cells. The second explanation is that the canaliculus membrane is the main entry site for HBV in cultivated HepaRG cells. The last explanation is that the formation of canaliculi represents a fully-differentiated state of hepatocytes, which allows virus entry from the side of basal membrane. The visualization of virus entry would be helpful to distinguish these possibilities.

3.2 The role of the N-terminus of the L protein in HBV infection

It has been assumed for a long time that the N-terminus of the L protein plays an important role in receptor binding during HBV infection. The first study to pinpoint this site was published by Neurath *et al.*, who highlighted aa 10-36 (referred to as Neurath's site) from the preS1 domain as the specific binding site using a synthetic peptide in a HepG2 cell-binding assay⁴⁵. Since more than 20 years, this conclusion has not been undermined. Instead, using Neurath's site, many following studies identified several receptor candidates on hepatocyte, e.g., the IL-6, SCCA-1, IgA receptor, or 31 kD protein on HepG2 cells (summarized in 1.1.5). However, there is almost no functional data connecting these proteins to infectivity studies.

Other studies kept narrowing down the receptor binding site on the viral envelope protein using different methods. In 1992, Sominskaya *et al.* used a known neutralizing mAb, Ma18/7, to

underline the receptor binding site at aa 20-23^{118,203}. Studies on other neutralizing antibodies also underlined aa 25-32 with mAb 5a19^{119,204} and aa 26-34 with mAb KR127^{119,120}. In 2001, Paran *et al.* identified aa 18-23 as the receptor-binding viral epitope using protein-coupled beads³⁸. Collectively, all these studies showed that the central or C-terminal Neurath's site is the receptor-binding site.

Grippon *et al.* and Bruss *et al.* identified the N-myristoylation of L protein and Le Seyec *et al.* defined the N-terminal 78 aa of L protein as the essential infectivity determinant with experiments analyzing the virus infectivity instead of binding^{29,121,205}. A great idea coming from these studies was to synthesize and characterize the peptide comprising aa 2-78 with a N-myristoylation. Surprisingly, this peptide is highly active in inhibiting HBV infection and also exhibits binding activity to hepatocytes. Compared to the previous findings, studies on the peptide revealed that the N-terminal region (aa 9-15) of the Neurath's site is essential for binding to differentiated hepatocytes^{104,112,117}. The different results on mapping the receptor-binding site are apparently resulted from the fact that these peptide studies used N-myristoylated peptide and addressed to infectivity rather than binding. Thus, when the N-terminal myristoyl moiety is taken into account, the receptor-binding site of L protein is strongly dependent on aa 9-15, the N-terminal region of Neurath's site.

A nearby sequence to the binding site, aa 2-8, was analyzed to details in this study. We show the peptide with serial deletion in this region drastically lost its activity. Furthermore, the substitution with alanines and the elongation with foreign sequence, such as myristoylation motif of VP4, severely deteriorate the function of inhibitory peptide. As a complementary approach, we show that the very N-terminus of L protein, aa 2-8 and aa -11-1, do not just confer the N-myristoylation recognition site, but these sequences themselves are also strictly needed for virus infectivity. This seems to contradict the diverse N-terminal sequences of L proteins in different genotypes. However, it should be pointed out that aa 2-8 of L protein are relatively conserved among all genotypes, implying that it plays a critical function. One can speculate that, during the evolution of HBV, the N-terminus of L protein selectively chose some residues that enable myristoylation but also kept its critical function as an adapter. Considering that the aa -11-1 in some genotypes are dispensable for virus assembly and infectivity, one might ask why these residues are still present, and do they play a role in other aspects like viral pathogenesis.

It should be pointed out that, beside as a myristoylation motif, the strict and extraordinary short sequence (aa 2-8) connects two critical elements for HBV infection, receptor-binding site and the N-myristoyl group. Therefore, I propose that this motif additionally acts as a bridge to render

the two infectivity determinants in a proper position to further interact with the cellular binding partner. As long as the receptor of HBV is still unknown, the proposed cooperation between the N-myristoyl group and the receptor binding site cannot be illustrated in detail. However, this notion is consistent with our unpublished observation that myristoylation and the following aa11-15 need to be present in the same molecule of L protein (Supplemental, Fig. S4).

To get insight into how this linker plays its role, we have to understand how the myristoyl group, in general, interacts with its partner. The most commonly described function of myristoyl group is the targeting of modified proteins to membranes by inserting the hydrophobic C14 carbon chain into the lipid bilayer from the cytoplasmic side¹⁸⁹. It affects the protein's localization and increases the affinity of soluble proteins for membranes, and thus enables the further interactions between the modified proteins and its interaction partner. HIV Nef is one of the well-known examples for this kind of interaction²⁰⁶. Until now, to my knowledge, there is no single reported case, in which the myristoyl group of one protein could interact with another protein. Thus it could be assumed that, in the case of HBV, virions also use the myristoyl group to interact with cellular membrane rather than directly with the receptor. This assumption is supported by the following observations of our laboratory. First, the myristoylated peptide, HBVpreS/2-48^{myr}, have been visualized to interact with the cell surface of hepatocytes. When the peptide is present at μM concentration, this interaction becomes sequence-independent (Anja Meier, unpublished results). Second, in a liposome-leakage assay, the pore-formation activity was only observed when the peptide was N-myristoylated (Caroline Gähler, unpublished results). In the present study, this assumption is validated by successful replacing the myristoyl group of the inhibitory peptide with a type II trans-membrane protein (Us9-B48). Our results also demonstrate the topology of the peptide to execute inhibition. Moreover, Us9-B48 provides us an alternative to inhibit HBV entry: gene transfer of membrane anchored peptide. It is noteworthy to mention that, to inhibit the early event of HIV infection, a similar strategy to anchor inhibitory peptide on the cellular membrane has been adopted. Hildinger *et al.* firstly showed that membrane-associated C46 blocks HIV entry²⁰⁷. Following studies reveal that it interferes with the fusion event, as the soluble C46, by binding to the N-terminal domain of gp41 and preventing formation of the six-helix bundle^{208,209}. Moreover, the delivery of membrane-associated C46 via foamy virus vector has proved to be successful to block HIV replication²¹⁰. A liver-specific gene delivery thus is desirable for the possible application of Us9-B48 as an entry inhibitor of HBV infection.

Since the myristoyl group itself is not sufficient to confer permanent anchoring²¹¹, stable binding to lipids is often mediated by other means, such as subsequent palmitoylation of nearby cysteine

residues, or the presence of clusters of basic amino acids near the myristoyl group to allow the interactions with negatively charged lipids. The L protein of HBV apparently does not have any of those properties. However, since the receptor-binding site is so close to the N-myristoyl group, it is rational to assume that interaction between the receptor and aa 9-15 of L protein stabilizes the anchoring of the myristoyl group. In return, the anchoring of the myristoyl group could also stabilize the sequence-specific receptor-binding.

A more important inference from the vicinity of viral receptor-binding site and N-myristoyl group is that the interaction site on cellular receptor must be close to the membrane (or the receptor has a very small ectodomain). If this scenario holds true, it could be similar to the model of recoverin proposed by Valentine *et al.*, who determine the structure of myristoylated recoverin bound to lipid bilayers by solid-state NMR. They demonstrated that membrane binding by recoverin is achieved primarily by insertion of the myristoyl group into the membrane bilayer with apparently little rearrangement of the protein structure. The N-terminal region of recoverin points toward the membrane surface allowing an exposed crevice, near the membrane surface, to serve as a potential binding site for rhodopsin kinase²¹². The close virus-binding site of HBV receptor near the membrane surface might also explain why the preS region are mostly unstructured¹⁸⁷, since a flexible preS region could stretch to the membrane when the virion is bound to HSPG^{42,115}.

Nevertheless, several questions remain to be addressed with respect to the cooperative interaction between the myristoyl group and receptor-binding site. The first question is: Where is the myristoyl group initially located in virion? It is commonly thought that the myristoyl group is closed to the virus envelope. However, we could not exclude the possibility that preS or AGL, which is in the outside of viral particle, might form hydrophobic pocket to accommodate the myristoyl group.

The second question is: What triggers the myristoyl switch to the cellular membrane? In some proteins, the myristoyl group is sequestered inside the molecule, but is exposed after an appropriate signal has been received. Several myristoyl switch triggers have been characterized, such as the binding of calcium^{213,214}, the hydrolytic switch of the ARF1 GTPase²¹⁵, and the autoinhibitory switch of c-Abl tyrosine kinase²¹⁶. Myristoyl switch of HIV-1 matrix protein is regulated by entropic modulation of a pre-existing equilibrium²¹⁷. In some cases, conversion between myristoyl group-exposed and -sequestered states is accompanied by conformational changes of protein structure. For example, in a soluble state, the myristoyl group of PKA is bound to a hydrophobic pocket in the C-terminal lobe. In the membrane-associated form, the

N-terminus extends its helical conformation, thus exposing the myristoyl group to the solvent and/or membrane²¹⁸. Interestingly, the NMR study on the preS modified by N-myristoylation suggested that the conformational transition induced by fatty acylation is important for efficient attachment of virus to cell receptors²¹⁹. One might speculate that the receptor-binding or the downstream aa 49-78 of L protein could be involved in the myristoyl switch of HBV.

The third question is: Whether the N-terminus plays a role in later fusion events? For enveloped viruses, fusion is mediated by viral fusion protein, which contains a small hydrophobic sequence termed fusion peptide. Upon appropriate triggering, the fusion peptide interacts with the target membrane and undergoes a conformational change that drives the membrane fusion. Actually, the putative fusion peptide of HBV has been described at the N-terminus of S domain²²⁰ and a synthetic peptide comprising this predicted fusion region was shown to interact with membranes, and destabilize liposomes in a pH-dependent manner²²¹. Interestingly, this year, Nunez *et al.* from the same lab reported that preS domains are also able to insert themselves into the hydrophobic core of bilayer. Moreover, the insertion resulted in a conformational change of preS1 which increased the helical content²²². Notably, the preS was not myristoylated in the study of Nunez. As a well-known fact, the myristoylation at the N-terminus of peptide can significantly enhance its membrane binding activity. Therefore, it could be expected that the authentic preS, with myristoylation, is more potent for inducing the lipid mixing or leakage assay. Thus, a study of our laboratory was initiated to measure the activity of the peptide, HBVpre/2-48^{myr}, in inducing membrane-leakage of liposomes. At a concentration around 70 μ M, the genotype D-derived peptide penetrates the liposome in a sequence- and myristoylation-dependent manner (unpublished result of Caroline Gähler). Furthermore, the myristoylated peptide comprising the N-terminus of different genotypes or chimeric genotypes were synthesized and their membrane-leakage activity were determined (Supplemental, Fig. S5). Although the membrane activity of peptide was not well correlated with the infectivity of virus, it appeared to be highly dependent on the N-terminal residues of L protein. For example, the peptides of genotype E and the chimera E10-D, drastically increased the membrane-leakage activity, while the genotype B exhibited slow kinetics. If the N-terminus of L protein can be further confirmed to act as a fusion peptide, it might represent a different model compared to the commonly accepted class-I and class-II fusion protein²²³. It must be pointed out that the hydrophobic fusion peptide of HIV can be substituted by fatty acid in lipid merging and fusion²²⁴, indicating the intrinsic fusion activity of myristoyl chain. A similar case might come from the reovirus fusion-associated small transmembrane (FAST) proteins, which has been shown to be myristoylated in the ectodomain, capable of inducing efficient membrane fusion under physiological conditions. The reovirus

FAST proteins are small proteins, containing a moderately apolar N-proximal region, termed the hydrophobic patch. Corcoran *et al.* synthesized a myristoylated peptide comprising the hydrophobic patch of p14 of reptilian reovirus (Fig. 38), and demonstrated that it is mostly disordered in solution but mediated extensive lipid mixing in a liposome fusion assay in a myristoylation- and sequence-dependent manner. Thus they proposed that p14 ectodomain is composed of a fusion peptide motif which depends on myristoylation for the membrane fusion activity²²⁵.

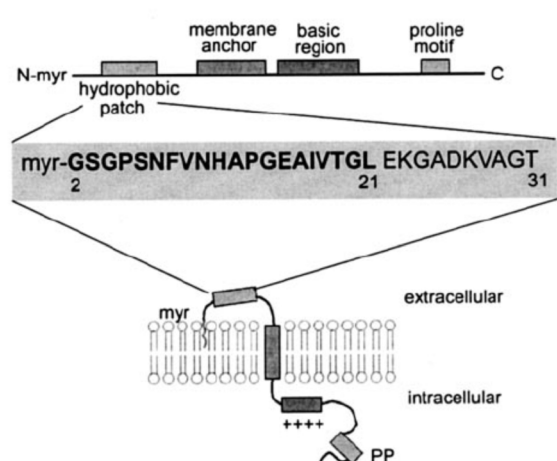


FIG. 38. p14 contains a hydrophobic patch in its ectodomain (modified from Jennifer A. Corcoran²²⁵). The locations of the myristoylation consensus sequence, hydrophobic patch, transmembrane anchor, polybasic region, and polyproline region are indicated in structural models of p14. The p14 hydrophobic patch (residues 2–21, *boldface*) is located within the small 38-residue ectodomain of p14. The p14 hydrophobic patch peptide (myr-30HP) included residues 2–31 with the N-terminal myristic acid modification on Gly2.

Our preliminary investigation on aa 49-78 elicit great interest about its function. Since it is apparently not involved in binding to cellular receptor, it might be worth looking into if it behaves as a switch (as mentioned above) to help the conformational changes when the N-terminal region binds to a cellular receptor. It must be pointed out that the conserved sequence PHGGLLGWSPQ is close to a motif (PHGGGWGQ) in the prion protein, which constitute a pH-dependent folding site²²⁶. In the present study, we showed that two proline residues in this domain, compared to the proline outside this domain, are highly important for virus infectivity. Proline residue has an exceptional conformational rigidity compared to other amino acids. It is often found in a hinge or a kink and acts as a disruptor of alpha helices and beta sheets. Interestingly, HBV preS is a proline-rich sequence (18 prolines out of 108 residues), and this structure might provide the flexibility of preS domain to interact with receptor.

3.3 The role of preS2 in HBV assembly and infectivity

In this work, the whole preS2 region except 5 aa in the N-terminus was mutated in a comprehensive manner, and the effect of mutations were further characterized with respect to virus assembly and infectivity. Le Seyec *et al.* have shown that consecutive 10 amino acids in this

region can be deleted without interference with virus assembly and infectivity¹²³. In complementary to their work, we show that larger deletions, exceeding 30 amino acids (Δ 114-143), lead to an abolished virus assembly. However, substitution of these 30 amino acids (S114-143) rescued the viral assembly and partially infectivity. This indicates that aa 114-143 is required for virus assembly in a length-dependent but not sequence-dependent manner.

We also showed that 20 aa in the C-terminal part of preS2 can be deleted (Δ 144-163) with marginal effect on assembly and no effect on infectivity. Therefore, it is rational that whole 50 aa actually serve as a spacer. The entire 50 amino acids of preS2 were thus substituted with overlapping pol-ORF. Due to inefficient expression of the L-protein, the virion secretion can not be detected. The substitution of the entire 50 amino acids with a scrambled sequence finally clarify that the preS2 domain is only required as a spacer for virus assembly. There is also an interesting question: if the spacer function of preS2 are also required during virus entry.

In consistent to the result from Le Seyec *et. al.*, we also observed an increased secretion when the amino acids 114-123 were deleted from the preS2 of the L-protein (data not shown). Moreover, we showed that the 20 amino acids deletion was still tolerated. Indeed, HBV isolates from patients reveal that the naturally occurred deletion in the preS2 region is mostly located within aa 114-133²²⁷⁻²²⁹. So far, to my knowledge, no HBV isolate has been reported with a larger preS2 deletion than 20 amino acids. This fact fits to the observation that 30 amino acids deletions abrogate viral assembly. It is noteworthy to point out that there is a conserved sequence “AGGSSSG” within aa 134-143, which might providing a flexible connection between capsid binding region and transmembrane domain of L protein.

Consistent with several independent works^{122,124,194}, we show that the deletion of so-called TLM motif (aa 149-160) does not interfere with virus infectivity. Collectively, these data rule out the possibility for TLM to play a role during virus entry, such as translocation of the virion into cytosol or fusogenic activity¹⁴³. On the other hand, a deletion of a nearby region (Δ 164-183) constitutive of TM-I abolishes virus infectivity. This is consistent with recently published data, which showed that deletion of a small hydrophobic cluster (aa 175-178) at TM-I is enough to abolish HBV infectivity²⁰¹. It has been supposed that TM-I might act as fusion peptide^{141,220}. However, two elements related to fusion event, PEST sequence (aa 157-169) and heptad repeat motif, are both dispensable for virus infectivity. The role of TM-I during virus infection is still unclear.

3.4 The role of S-domain in HBV entry

Heparan sulfate proteoglycans (HSPGs) have been described as primary attachment site or receptor for many viruses. In the present study, we showed that, for the first time, the AGL in the S protein determine HBV infectivity and further correlate the role of AGL to HSPG-binding activity.

A previous study from our lab shows that HBV entry in hepatocytes depends on the interaction with cellular HSPG and further suggests that the preS domain in the L protein is involved in HSPG-binding⁴² based on the following observation. (1) Heparin-binding activity was lost when the viral particle was digested with trypsin to remove preS. (2) HBsAg bound much weaker to heparin than virion. In view of this data, we initially expected that a reduced heparin-binding activity might be observed in the virions with CYL-I-mutated L protein, since these mutants exhibited a reduced infectivity and the mutation in CYL-I might change the topology of preS in the L protein. Unexpectedly, it turned out that these mutants did not change their preS topology and did not lose their heparin-binding activity. However, the AGL mutants lost their heparin-binding activity without changing the preS topology.

The discrepancy between the present study and the previous work can be explained by two possibilities: (1) The preS domain and the antigenic loop, of which both are exposed on the surface of virion, cooperatively bind to the heparin column. (2) The antigenic loop exclusively binds to heparin, but that fact that virus digested by trypsin fail to bind heparin is due to an interrupted antigenic loop caused by trypsin digestion.

In most cases, the interaction between cell surface HSPG and its ligands is thought to be nonspecific and probably based on electrostatic attractions between the highly charged sulfated proteoglycans and basic residues. The linear sequences XBBXB_X, XBBBXXB_X, TXXBXXTBXXXTB_B (B is Arg or Lys and T define a turn) are common HSPG binding motifs found in proteins, such as interleukin-8, and fibroblast growth factors²³⁰. Some viruses also use clustered basic residues for their interactions with HSPG. These interactions provide initial attachment sites and concentrate viruses in the proximity of the cell surface to facilitate interactions with specific receptors²³¹⁻²³⁵. Two HSPG binding motifs of pseudorabies virus (PRV) glycoprotein gC, SRRKPPRN and AHGRKRI, were found in the N-terminus of the protein²³⁶. The HSPG binding domain of HIV-1 gp120 was mapped to three sequences, RGKVQK, RPNNNTRKRIR and KAKRR²³⁷. A basic motif of KKTK was found in the fiber shaft of

human adenovirus type 5 to interact with HSPGs²³⁸. A Loop in DENV-2 envelope protein, which contains three Lys residues (KFKIVK), constitutes the HSPG binding site.

Unlike the known HSPG-binding motifs in the viruses mentioned above, most basic residues in the envelope proteins of HBV are not clustered. In the genotype-D virus, there are 17 arginine or lysine residues in the L protein consisting of 389 amino acids. They are R24, K38, K46, R88, R92, R102, R124, R126, R156, R187, R236, R241, R242, R285, K304, K323 and R332. Among them, only 6 residues are located in the infectivity-determining region. Since the other residues can be either deleted or substituted without interfering with virus infectivity, they should not be the critical residues responsible for HSPG-binding. Among these 6 residues, 3 of them are located in aa 2-78 (R24, K38 and K46). When compared with amino acid sequences from different genotypes, only K38 is conserved among these three residues. R24 and K46 were often replaced with glycine and glutamine. In contrast, the other 3 residues located in the AGL (R285, K304 and K323) are highly conserved. Since these residues are also present in the S-protein, they are often numbered as S-R122, S-K141, and S-K160 according to their positions in the S-protein. These highly conserved basic residues in the S-domain indicate that they are likely more important for virus-HSPG interaction than those in the preS domain.

It is noteworthy to mention that two of the three basic residues in AGL (S-R122 and S-K160) could be exclusively replaced with lysine and arginine in different virus serotypes. These changes constitute two pairs of epitopes defined by antibody recognition, named “d” or “y” and “w” or “r”. Determinant “d” has a lysine at the position 122, while “y” has an arginine at the same position; “w” has a lysine at position 160 while “r” has an arginine at that position (see 1.1.2). The accessibility of these residues to antibody recognition shows that they are exposed in the out surface of viral particle and, thus, should be also accessible to HSPG-binding.

The notion that AGL is responsible for HSPG-binding is supported by an observation: A point mutation at S-R122 leads to decreased heparin-binding activity and loss of HDV infectivity (Sureau C., personal communication). The decreased heparin-binding activity by single-point mutation suggests that the affinity between AGL and HSPG is quite weak. However, since the protein content of HBV envelope is rather high and the AGL is present in all envelope proteins, the avidity between virus particle and heparin could still be high enough to support a stable interaction.

It should also be kept in mind that the majority of HBsAg do not bind to heparin column in contrast to virions. This fact seems contradict to our conclusion that AGL is responsible for binding with HSPG. This contradiction could be explained by two possibilities. The first is that

some basic residues in the preS region also contribute to the binding with HSPG. However, since the 20 nm sphere particles are the main component of HBsAg and the 42 nm virions apparently contain more envelope proteins per particle, the second explanation is that the avidity but not affinity of virion to HSPG are higher than that of sphere particle solely due to the abundance of envelope proteins. One could deduce that filament, apparently with more abundant envelope protein, could bound to HSPG more tightly than virion and sphere particle. Indeed, it is the case according to an unpublished observation (Caroline Gähler, unpublished data).

It is demonstrated that the lost infectivity of C121 or C124 mutants is not related to a typical PDI activity⁴³. However, treatment of hepatitis delta virion with reducing agents leads to the loss of virus infectivity. This argues that proper-formed disulfide bridges in the envelope are critical for virus infectivity. Although it can not be excluded that atypical recognition sites rather than CXXC motif are utilized by PDI or other enzyme, there is a simple explanation for the loss of infectivity when the virus bears mutation at cysteine residue of AGL or is treated with reducing agents. The mutations or treatments change the conformation of AGL, which might disable the interaction between the basic residues and the heparan sulfate.

In view of the role of AGL we proposed, the following questions are interesting and should be further investigated. (1) Do the neutralizing antibodies induced by commonly used vaccine, which only contain S protein, play their role by preventing the S-domain from binding to HSPG? (2) Do the two well-known escape mutants, S-G145R (introduction of a positively charged residue) and S-D144A (removal of a negatively charged residue), not only disable antibody recognition but also result in a higher affinity between the virion and HSPG? (3) Can the abolished infectivity of AGL mutant described in the present work be rescued by introduction of positively charged residues or the HSPG-binding motifs with high affinity?

3.5 Model for HBV attachment and receptor binding

According to the information obtained from this works and the published dataa, I propose here a model for a multi-step interaction between virion and hepatocyte during the attachment and receptor-mediated binding (Fig. 39).

To enable the initial attachment, both the S-protein and the S-domain of L-protein interact with the HSPG via (one of) the three basic residues in the AGL (Sureau C., unpublished results). Since the S-protein is much more abundant than L-protein on the surface of virus particle, the main contribution to viral attachment is from the AGL of S-protein and the role of L protein in this process would be marginal (concluded from Chapter 2.4). At this time point, the N-terminal

myristoyl group of L protein is still associated with the virus membrane for the free virus and the HSPG-associated virus. Meanwhile, the interaction site of virus receptor with preS1 is in a close proximity to the membrane, or simply that virus receptor is a molecule with small ectodomain, (concluded from Chapter 2.2, the inhibitory activity of shorter peptide preS/2-48^{myr} is higher than preS/-11-48^{myr}). During the specific interaction, aa 2-48 of preS1 domain of L protein are involved. The aa 49-78 act as a switch to project the viral membrane associated N-terminus (speculation from Chapter 2.4). Afterwards, the interaction between the essential binding site and the virus receptor occurs. The affinity of this interaction is greatly enhanced by the insertion of myristoyl group into cellular membrane. The adapter sequence, aa 2-8, is critical to enable this close cooperation between the myristoyl group and essential binding site (concluded from Chapter 2.2, aberrant aa 1-8 impairs the activity of peptide and abolishes the infectivity of virus).



- (1) During virus attachment, both L and S protein on the virus membrane attach to HSPG via the AGL, but the S protein is the main contributor to the attachment due to its high abundance on the viral envelope.
- (2) Prior to the preS-mediated receptor binding, the myristoyl chain is hidden while the essential binding site (aa9-15) and aa 49-78 are exposed.
- (3) Conformational change of preS (via aa 49-78?) switches the N-terminus to the cellular membrane.
- (4) The viral receptor-binding site interacts with a specific receptor in proximity of the membrane.
- (5) The myristoyl group inserts into the membrane, consolidating the interaction between the preS1 and its receptor.
- (6) The atypical linker (aa 2-8) enables the cooperation of myristoyl group and receptor binding site.

4. Materials and Methods

4.1 Materials

4.1.1 Instruments, consumables, software and reagents

Instruments and consumables	Supplier
ABI PRISM 7000 Gene Analyzer	Applied Biosystems
Autoclaver, 5050 ELV	Tuttnauer Systec
Incubator (37°C)	Heraeus
Ice machine	Scotsman
Electrophoresis plates	Amersham Pharmacia (Hoefer)
Electrophoresis chambers	EMBL86 (V150), Amersham Pharmacia (Hoefer): „Mighty Small“
Filter paper	Whatman
Fraction collector	Beckman
Cell culture flask (75 bzw. 25 cm ²)	Greiner
Cell culture dish (60mm x 1,5cm ;145mm x 2cm)	Greiner
Centrifuge J2-21M/E (JA-14/JA-20)	Beckman
Cryo-tube	Greiner
Refrigerators (4°C/-20°C)	Liebherr
Microscope, Axiovert25	Zeiss
Microscope, DM IRB	Leica
Cell culture plate (6, 12, 24-well)	Greiner
Mixer	Thermomixer compact, Eppendorf
Parafilm	Pechiney Plastic Packaging
Pasteur Pipet	WU Mainz
Thermocycler	Thermo Hybaid
pH-Meter	Metrohm
Photometer (DNA/Proteine)	Eppendorf, Amersham Pharmacia
Photometer OD600nm (DU 7400)	Beckman
Pipeter	Gilson
Pipet helper	Hirschmann, Integra Biosciences
Polystyrene reaction tube (15 or 50ml)	Falcon
Power Supply	Monacor, LKB Brumma, Amersham Pharmacia
Reaction tube 0,5 ml, 1,5 ml, 2 ml	Eppendorf, Sarstedt
Film	Kodak
Sample mixer (rotation)	NeoLab
Shaker (30°C), Certomat BS-1	B.Braun Biotech International
Shaker (RT/ 4°C)	GFL, Heidolph
Shaker for Bacterial culture (37°C)	GFL, Infors
Biosafety Cabinet, NapFlow,	NapCo
0.2µm and 0.45µm sterile filters	Fisherbrand

Sterile filter bottles (500ml/Nalgene)	Nalge Nunc
Sterile plastic pipettes	Sarstedt
Nitrogen tank, Cry300	Thermo Forma
TC-Plate 6-well	Greiner
Freezer –80°C	Nap Coil
Trans-Blot SD, Semi-Dry Transfer Cell	Bio-Rad
Vacuum Hand Control	Vacuubrand
Vortexer	Bender + Hobein AG, Neolab
Water bath	Medingen, Braun
Cell Counter	IVO
Centrifuge, Biofuge	Heraeus
Centrifuge, Multifuge3 S-R	Heraeus
Nitrozellulose-Membran (0,2µm, 0,4µm)	Schell und Schleicher
Parafilm	Serva
PVDF-Membrane	Schleicher & Schüll
Sterile filter	Schleicher & Schüll
Softwares	Supplier
Vector NTI	InforMax, Invitrogen
Quantity One	Biolab
Chemical reagent	Supplier
Acrylamid/Bisacrylamid mixture, 29:1	Roth
3-Amimophthalhydrazid	Sigma
Agarose	Gibco
Ammonium acetate	AppliChem
Ammonium peroxodisulfate (APS)	Roth
Ammonium sulfate	Gerbu
Ampicillin	Sigma
Aqua ad iniectabilia	Braun
Bacto-Agar	Difco
Bacto-Trypton	Difco
Bacto-Yeast Extract	Difco
Big Dye	Applied Bioscience
β-Mercaptoethanol	Merck
BSA (Bovine serum albumin)	Roth
Cesium chloride	Sigma
Coomassie brilliant blue G250	Sigma
Coomassie brilliant blue R250	Sigma
p- Coumaric acid	Sigma
Cyanbromid	Sigma
deoxyribonucleoside triphosphate	Sigma

Di-Kaliumhydrogenphosphat	Merck
Di-Natriumhydrogenphosphat (Na ₂ HPO ₄)	J.T.Baker
DMSO (Dimethylsulfoxid)	Merck
dNTP Mix	Roche
DMEM (Dulbecco`s modified Eagles medium)	Invitrogen
DTT	Biovectra
ECL Reagent	Amersham Pharmacia, or home-made solution
EDTA-Dihydrate	Roth
Acetic acid	Roth
Ethanol absolute	Riedel de Haen
Ethanol 99%	Chemikalienlager
Ethidium bromide	Sigma
FCS (fetal calf serum)	Invitrogen
FCS (fetal calf serum)	Biochrom
Formaldehyd, 37%	J.T. Baker
Glutamin-solution (200mM)/Cell culture	Gibco
Glutamin	Invitrogen
Glycerin 99,5%	J.T.Baker
Glycin p.a. min. 99% Glykokoll	AppliChem
Hydrocortison	Sigma
pH indicator paper	Merck
Insulin	Sigma
Isopropanol	AppliChem
Calcium acetate	Roth
Calcium chloride	Sigma
Calciumdi hydrogen phosphate	Gerbu
Milk powder	Roth
Methanol 100%	Chemikalienlager
Sodium acetate	J.T. Baker
Sodium bicarbonate-solution (NaHCO ₃ / 7.5%)	Gibco
Sodium carbonate, water free	AppliChem
Sodium deoxycholate	Sigma
Sodium chloride	Grüssing
Sodium dihydrogenphosphate (NaH ₂ PO ₄)	Merck
Sodium hydroxide	J.T. Baker
NP40	Sigma
Orange G	Sigma
PEG 8000	Sigma
Protease inhibitor Cocktail	Roche
Rainbow colored protein molecular weight markers	Amersham Pharmacia

SDS (sodium dodecyl sulfate)	Serva
Silver Nitrate	AppliChem
Sucrose, D(+)	Roth
TEMED (N,N,N',N'-Tetramethylethyldiamin)	Roth
Tris	Roth
Triton X100	Serva
Tween 20	Roth
William's E Medium	Invitrogen
Dulbecco's Modified Eagle Medium	Invitrogen
William's E Medium	Invitrogen
Enzymes	Supplier
Deep Vent Polymerase (exo+)	New England Biolabs (NEB)
Calf Intestine Phosphatase	New England Biolabs (NEB)
T4 DNA Ligase	New England Biolabs (NEB)
Klenow Fragment	Roche
DNase I	Roche
Shrimp Alkaline Phosphatase (SAP)	New England Biolabs (NEB)
RNase A	Boehringer
Trypsin	Gibco
Antibiotics	Supplier
Ampicillin	Sigma
Chloramphenicol	Sigma
Kanamycin	Serva
Penicillin	Sigma
Streptomycin	Sigma
Primary antibodies	Supplier
Ma18/7	hybridoma kindly provided by W.H. Gerlich, Giessen
Rabbit anti MRP2	gift from Keppler O, University of Heidelberg
Rabbit anti core H363	gift from Schaller H, ZMBH, Heidelberg
Mouse anti core #312	gift from Schaller H, ZMBH, Heidelberg
Mouse anti core #158	gift from Schaller H, ZMBH, Heidelberg
Secondary antibodies	Supplier
Goat-anti-Rabbit peroxidase	Dianova
Goat-anti-Mouse peroxidase	Dianova
Mouse-anti-Goat peroxidase	ImmunoResearch Laboratories

Goat anti-Mouse IgG Alexa 488	Invitrogen
Goat anti-Mouse IgG Alexa 546	Invitrogen
Goat anti-Rabbit IgG Alexa 488	Invitrogen
Goat anti-Rabbit IgG Alexa 546	Invitrogen
Goat anti-Mouse Alexa 680	Invitrogen
Goat anti-Mouse Alexa 800	Invitrogen
Goat anti-Rabbit Alexa 680	Invitrogen
Goat anti-Rabbit Alexa 800	Invitrogen
Kits	Supplier
Plasmid Maxi and Midi kit	Qiagen
Terminator-cycle Sequencing kit	ABI
Gel exaction kit	Qiagen
Fastplasmid Mini kit	Eppendorf

4.1.2 Oligonucleotides

No.	Name of primer	Sequence(5'-3')	bp
55	MfeI-Pres-down	GCAAT [*] TGATTATGCCTGCCA	20
56	XhoI-PreS-up	GGTCCCCAATCCTCGAGAAG	20
57	1279stop-down	GCCATGCAGTAGAAT [*] TCCACA	21
58	1279stop-up	TGTGGAATTCTACTGCATGGC	21
59	1279stop-down-2	TGCAGTAGAAT [*] TCCACAACCT	21
60	XhoI-PreS-up-2	GCAACATACCT [*] TGATAGTCCA	21
61	L muta S	GTAGGCGTGTACGGTGGGAGGT	22
62	L 114/123 AS	GCCTCTCACTCTGGAAT [*] TCCACTGCATGGCCTGA	34
63	L 114/123 S	CAGTGGAAT [*] TCCAGAGTGAGAGGCCTGTAT [*] TCC	34
64	L 114/133 AS	TGAACTGGAGCCGGAAT [*] TCCACTGCATGGCCTGA	34
65	L 114/133 S	CAGTGGAAT [*] TCCGGCTCCAGT [*] TCAGGAACAGTAA	34
66	L 114/143 AS	GGCAGTAGTCAGGGAAT [*] TCCACTGCATGGCCTGA	34
67	L 114/143 S	CAGTGGAAT [*] TCCCTGACTACTGCCTCTCCCTTAT	34
68	L 114/153 AS	AATCCTCGAGAAGGAAT [*] TCCACTGCATGGCCTGA	34
69	L 114/153 S	CAGTGGAAT [*] TCCTTCTCGAGGATTGGGGACCCTG	34
70	L 114/163 AS	GATGT [*] TCTCCATGGAAT [*] TCCACTGCATGGCCTGA	34
71	L 114/163 S	CAGTGGAAT [*] TCCATGGAGAACATCACATCAGGAT	34
72	L 114/173 AS	CACGAGAAGGGGGGAAT [*] TCCACTGCATGGCCTGA	34
73	L 114/173 S	CAGTGGAAT [*] TCCCCCTTCTCGTGT [*] TACAGGCGG	34
74	L 114/183 AS	TCTTGTCAACAAGGAAT [*] TCCACTGCATGGCCTGA	34
75	L 114/183 S	CAGTGGAAT [*] TCCTTGT [*] TGACAAGAATCCTCACAA	34
76	L 114/193 AS	CGAGTCTAGACTGGAAT [*] TCCACTGCATGGCCTGA	34
77	L 114/193 S	CAGTGGAAT [*] TCCAGTCTAGACTCGTGGTGGACTT	34
78	L 114/203 AS	TCCCCCTAGAAAGGAAT [*] TCCACTGCATGGCCTGA	34

79	L 114/203 S	CAGTGGAATTCCTTCTAGGGGGAACTACCGTGT	34
80	L 114/213 AS	CTGCGAATTTTGGGAATTCCTACTGCATGGCCTGA	34
81	L 114/213 S	CAGTGGAATTCCTCAAAATTCGCAGTCCCCAACCT	34
82	L 114/223 AS	AGAGGTGGTGAGGAATTCCTACTGCATGGCCTGA	34
83	L 114/223 S	CAGTGGAATTCCTCACCAACCTCTTGTCTCCAA	34
84	L 114/233 AS	CCAGCGATAACCGGAATTCCTACTGCATGGCCTGA	34
85	L 114/233 S	CAGTGGAATTCGGTTATCGCTGGATGTGTCTGC	34
86	L 114/243 AS	GAGGAAGATGATGGAATTCCTACTGCATGGCCTGA	34
87	L 114/243 S	CAGTGGAATTCATCATCTTCCTCTTCATCCTGC	34
88	L 114/253 AS	CAAGAAGATGAGGGAATTCCTACTGCATGGCCTGA	34
89	L 114/253 S	CAGTGGAATTCCTCATCTTCTTGTGGTTCTTC	34
90	L muta AS	TGGCTGGCAACTAGAAGGCACA	22
91	MS muta S	AAGGTAGGAGCTGGAGCATTCG	22
92	M(-) T1273C AS	AATTCCTACTGCGTGGCCTGAGGATGAG	27
93	M(-) T1273C S	TCATCCTCAGGCCACGCAGTGGAATTC	27
94	S(-) T1438C AS	TGTGATGTTCTCCGTGTTACAGCGCAGG	27
95	S(-) T1438C S	CGCTGAACACGGAGAACATCACATCAG	27
96	MS muta AS	GAGGTGGTGAGTGATTTGGAGG	22
114	pcDNASEQ-F	CCCCTGCTTACTGGCTTATCG	22
115	pcDNASEQ-R	GATGGCTGGCAACTAGAAGGCACAG	25
116	HuL1240 InsA S	ATGCAGTGGAATTCACAACCTTCCACCAA	31
117	HuL1389 DelC AS	ATGTGATGTTCTCCATTTACAGCGCAGGGTCC	31
118	HuL1389 DelC S	GGACCCTGCGCTGAAATGGAGAACATCACAT	31
119	HuL1329 DelT AS	AGAGGCAGTAGTCAGACAGGGTTTACTGTTTC	31
120	HuL1329 DelT S	AACAGTAAACCCTGTCTGACTACTGCCTCTC	31
121	HuL1449 DelC AS	TTGTCAACAAAAAAACCCCGCCTGTAACACG	31
122	HuL1449 DelC S	GGCGGGGTTTTGTGTTGACAAGAATCCTCA	31
123	L 144/163 AS	GATGTTCTCCATAACAGGGTTTACTGTTCTGAA	34
124	L 144/163 S	GTAAACCCTGTTATGGAGAACATCACATCAGGAT	34
125	L 164/183 AS	TCTTGTCAACAAGTTCAGCGCAGGGTCCCCAATC	34
126	L 164/183 S	CCTGCGCTGAACTTGTGACAAGAATCCTCACAA	34
127	L 149/160 AS	CATGTTACAGCGCAGAGGCAGTAGTCAGAACAGGG	34
128	L 149/160 S	ACTACTGCCTCTGCGCTGAACATGGAGAACATCA	34
129	HPreS2 WoS AS	TGATGGTGACATGTTACAGCGCAGGGTCCCCAATC	34
130	HPreS2 WoS S	CCTGCGCTGAACATGTCACCATCAAGTCTCCTAG	34
131	WoS HBV AS	TTTGTAGGGTTTAAATGTATACCCAAATCAAG	34
132	WoS HBV S	GTATACATTTAAACCCTAACAAAACAAAGAGATG	34
133	HBV WoPreS AS	GTGTTGCCCATGCTGTAGATCTTGTTCCTCAAGA	34
134	HBV WoPreS S	AAGATCTACAGCATGGGCAACAACATAAAAGTCA	34
135	WPreS2 HuS AS	GATGTTCTCCATCTCCGGTGACAGTGACAGGGTCC	34

136	WPreS2 HuS S	CTGTCACCGGAGATGGAGAACATCACATCAGGAT	34
137	SphI AS	GCAAAACAAGCGGCTAGGAGTT	22
138	W21H2L AS	AAGATTCTGCCCCACTGCAGGCCACCATGCTGCT	34
139	W21H2L S	TGGCCTGCAGTGGGGCAGAATCTTTCCACCAGCA	34
165	NheI HuL B S	GTGCGCTAGCATGGGAGGTTGGTCTTCCAAAC	32
166	NheI HuL C2 S	GTGCGCTAGCATGCAGTTAATCATTACTTCAA	32
167	NheI HuL E/G S	GTGCGCTAGCATGGGGCTTTCTTGGACGGTCC	32
182	Bst XI S	CTCTATGGAAGGCGGGTAT	19
183	C124S AS	GTAGTCATGGAGGTCCGGCATGGTCCC	27
184	C124S S	GCCGGACCTCCATGACTACTGCTCAAG	27
185	C139S AS	GGTTTGGTAGAGCAACAGGAGGGATAC	27
186	C139S S	CCTGTTGCTCTACCAAACCTTCGGACG	27
187	C149S AS	ATGGGAATAGAGGTGCAATTTCCGTCC	27
188	C149S S	ATTGCACCTCTATTCCCATCCCATCAT	27
189	Bst XI AS	CCACTGAACAAATGGCACTA	20
192	Nhe HuL G2A S	GTGCGCTAGCATGGCCCAGAATCTTTCCACC	31
193	Nhe HuS E2G S	GTGCGCTAGCATGGGGAACATCACATCAGGAT	32
194	C211A AS	TGGCCAAGAGCCACGGTAGTTCCCCCTA	28
195	C211A S	ACTACCGTGGCTCTTGGCCAAAATTTCGC	28
196	C228A AS	GTGAGGAGCAGAGGTTGGTGAGTGAT	28
197	C228A S	CCAACCTCTGCTCCTCCAACCTTGTCTG	28
198	C232A AS	TAACCAGGAGCAGTTGGAGGACAAGAGG	28
199	C232A S	CCTCCAACCTGCTCCTGGTTATCGCTGGA	28
200	P36A AS	CCTTGTGTTGGCATTGAAGTCCCAATCTG	27
201	P36A S	GACTTCAATGCCAACAAAGGACACCTGG	27
202	P42A AS	TGGCGTCTGCCCAGGTGTCCTTGTGTTGG	27
203	P42A S	GACACCTGGGCAGACGCCAACAAAGGTA	27
204	PP58/59AA AS	CTCCGTGCGCTGCGGTGAAACCCAGCCCCGA	30
205	PP58/59AA S	GGTTTCACCGCAGCGCACGGAGGCCCTTTTG	30
206	LG11/12MN AS	GGGAAAGAAATTCATAGGATTGCTGGTGGAAA	32
207	LG11/12MN S	AGCAATCCTATGAATTTCTTTCCCGACCACCA	32
208	LG11/12RE AS	GGAAAGAATTCCCGAGGATTGCTGGTGGAA	30
209	LG11/12RE S	GCAATCCTCGGGAATTTCTTTCCCGACCACC	30
210	L 16/48 AS	ATGCTCCAGCGGGAAAGAATCCCAGAG	27
211	L 16/48 S	ATTCTTTCCCGCTGGAGCATTCGGGCT	27
212	L 49/75 AS	CTGGCAAAGTTCTTACCTTGTGTCGT	27
213	L 49/75 S	CAAGGTAGGAACCTTGCCAGCAAATCC	27
214	L 16/75 AS	CTGGCAAAGTGGGAAAGAATCCCAGAG	27
215	L 16/75 S	ATTCTTTCCCACTTTGCCAGCAAATCC	27
216	L 11/15 AS	ACTGGTGGTCAGGATTGCTGGTGGAAA	27
217	L 11/15 S	CAGCAATCCTGACCACCAGTTGGATCC	27
218	L 41/45 AS	CTCCTACCTTGGTGTCTTGTGTTGGGAT	27

219	L 41/45 S	CAAGGACACCAAGGTAGGAGCTGGAGC	27
220	L 71/75 AS	CTGGCAAAGTAGCCTGAGGGCTCCACC	27
221	L 71/75 S	CCCTCAGGCTACTTTGCCAGCAAATCC	27
222	pVL seq-F	AAATGATAACCATCTCGC	18
223	pVL seq-R	GTCCAAGTTTCCCTG	15
224	Flu FP2 S1	GAAGGAATGATAGATGGTTGGTATGGTTTCGGG CAGAATCTTTCCACC	48
225	Flu FP2 S2	CAATAGCAGGGTTTCATAGAAAACGGATGGGAAG GAATGATAGATGGTTG	49
226	Flu FP2 AS	TCTATGAACCTGCTATTGCACCGAACAGACCC ATGCTAGCCAGCTTGG	49
227	HIV FP2 S1	GCAGCAGGAAGCACTATGGGCGCAGCCTCAGGG CAGAATCTTTCCACC	48
228	HIV FP2 S2	ATAGGAGCTTTGTTCCTTGGGTTCCTTGGGAGCA GCAGGAAGCACTATG	48
229	HIV FP2 AS	CCAAGGAACAAAGCTCCTATTCCCCTGCCATG CTAGCCAGCTTGGGT	48
230	Ras-HuL9 S	CAGGTTTCATCACAGAAAGTGAATCCTCTGGGA TTCTTTCCCG	43
231	Ras-HuL10 S	CAGGTTTCATCACAGAAAGTGCCTCTGGGATTC TTTCCCGACC	43
232	Ras-HuL11 S	CAGGTTTCATCACAGAAAGTGCTGGGATTCTTT CCCGACCACC	43
233	Ras-HuL AS	CACTTTCTGTGATGAAACCTGAGCACCCATGCT AGCCAGCTTGGGTC	47
234	Tri 57 S1	CTCCACATGGTGGGCTGCTTGGCTGGAGTCCTC AGGCTCAGGGCATAAC	48
235	Tri 57 S2	TCATGGGGGACTGCTCGGATGGTCCACACCTCC ACATGGTGGGCTGCT	48
236	Tri 57 AS	ATCCGAGCAGTCCCCCATGAGGTGGAGTGCTCC ACCCCAAAGGCCTC	48
237	Vp4 2 S	CAGGTTTCATCACAGAAAGTGGGGCAGAATCTT TCCACCAGCA	43
238	Vp4 5 S	CAGGTTTCATCACAGAAAGTGCTTTCCACCAGC AATCCTCTGG	43
239	Vp4 8 S	CAGGTTTCATCACAGAAAGTGAGCAATCCTCTG GGATTCTTTC	43
240	LCMV S1	CTGCCTCACATCATCGATGAGGTGGGGCAGAAT CTTTCCACCAGC	45
241	LCMV S2	CAGATTGTGACAATGTTTGAGGCTCTGCCTCAC ATCATCGATGAG	45
242	LCMV AS	CTCAAACATTTGTCACAATCTGACCCATGCTAGC CAGCTTGGGTCT	45

243	adw S	TGGTCTTCCAAACCTCGAAAAGGCGGGCAGAAT CTTTCACCAGC	45
244	adw AS	TTTTCGAGGTTTGGAAGACCAACCTCCCATGCT AGCCAGCTTGGGTCT	48
245	vac8 S	TCATGTTGTAGTTGCTTGAAAGATGGGCAGAAT CTTTCACCAGC	45
246	vac8 AS	TTTCAAGCAACTACAACATGAACCCATGCTAGC CAGCTTGGGTCT	45
247	fyn14 S	CAATGTAAGGATAAAGAAGCAGCGAAACTGGGG CAGAATCTTTCACCA	49
248	fyn14 AS	TGCTTCTTTATCCTTACATTGCACACAGCCCAT GCTAGCCAGCTTGGGT	49
249	yes S	AAGTAAAGAAAACAAAAGTCCAGCCATAAAAGG GCAGAATCTTTCACC	49
250	yes AS	GACTTTTGTTTTCTTTACTTTTAATGCAGCCCA TGCTAGCCAGCTTGGG	49
251	psd95 S	CTCTGTATAGTGACAACCAAGAAATACGGGCAG AATCTTTCACCAGC	48
252	psd95 AS	CTTGGTTGTCACTATACAGAGACAGTCCATGCT AGCCAGCTTGGGTCT	48
253	Gap43 S	ATGAGAAGAACCAAACAGGTGAAAAGAATGGG CAGAATCTTTCACCA	49
254	Gap43 AS	AACCTGTTTGGTTCTTCTCATACAGCACAGCAT GCTAGCCAGCTTGGGT	49
255	B-D S	TGGTCTTCCAAACCTCGAAAAGGCATGGGGCAG AATCTTTCACCAGC	48
257	E-D S	TCTTGGACGGTCCCTCTCGAATGGGGGCAGAAT CTTTCACCAGC	45
258	E-D AS	TTTCGAGAGGGACCGTCCAAGAAAGCCCCATGCT AGCCAGCTTGGGTCT	48
259	F-D S	CCTCTCTCAACGACAAGAAGGGGCATGGGGCAG AATCTTTCACC	45
260	F-D AS	CCTTCTTGTCGTTGAGAGAGGTGCTCCCATGCT AGCCAGCTTGGGTCT	48
261	Nhe Short B S	GCTGGCTAGCATGGGGACAAATCTTCTGTCCCC	34
263	B-D withW S	TGGTCTTCCAAACCTCGAAAAGGCTGGGGGCAG AATCTTTCACCAGC	48
266	B-D G2A AS	TTTTCGAGGTTTGGAAGACCAACCGGCCATGCT AGCCAGCTTGGGTCT	48
267	B-D G12A S	TGGTCTTCCAAACCTCGAAAAGGCatgGCCAG AATCTTTCACCAGCA	49
269	E short B S	TCTTGGACGGTCCCTCTCGAATGGGGGACAAAT CTTCTGTCCCC	45

271	VP4 Short B S	GCTCAGGTTTCATCACAGAAAGTGGGGACAAATCTTCTGTCCCC	45
272	VP4 Short B AS	TTTCTGTGATGAAACCTGAGCACCCATGCTAGC CAGCTTGGGTCT	45
273	I S	ATCCTCAGGCCATGCAGTGGAAATTCCTATATCA ACATTACTGGCCCCACTCCTAGTCTGTTCGCTA CTTCTTTCGCCCCCGATGTGGGCTCCAACGTAC ACAGGTTCCAATCGTC	110
274	II AS	CCTAGGAATCCTGATGTGATGTTCTCCATCTGC AGCCCTGTAGGACCTAACAGTCTTCTGGTTCGAT CCTGAAACGTCAGGTGTGCCAGTGACGATTGG AACCTGTGTACGTTGG	110
275	III S	AGAACATCACATCAGGATTCCTAGGACCCCTTC TCGTGTTACAGGCGGGGTTTTCTTGTGACAA GAATCCTCACAATACCGCAGAGTCTAGACTCGT GGTGGACTTCTCTCAA	110
276	YINI Sense	ATCCTCAGGCCATGCAGTGG	20
277	YINI Asense	TTGAGAGAAGTCCACCACGA	20
278	8H6 AS	TGTATGGTGATGGTGATGGTGTTTGGAAGACCA ACCTCCCATGCT	45
279	11H6 AS	AGAATGGTGATGGTGATGGTGTTTTCGAGGTTT GGAAGACCAACC	45
280	14H6 AS	ATTATGGTGATGGTGATGGTGCCCCATGCCTTT TCGAGGTTTGGA	45
281	8H6 S	AAACACCATCACCATCACCATACAAATCTTTCT GTCCCCAATCCA	45
282	11H6 S	AAACACCATCACCATCACCATTCTGTCCCCAAT CCACTGGGATTC	45
283	14H6 S	GGGCACCATCACCATCACCATAATCCACTGGGA TTCTTCCCGAT	45
284	EcoRI AS	GGTCGAATTCCACTGCATGGCCTGAGGAT	29
285	XhoI AS	AGTCCTCGAGAAGGTTGACGATATGGC	27
286	XbaI AS	CGACTCTAGACTCTGTGGTATTGT	24
287	XhoI S	CCTTCTCGAGGACTGGGGACCCTGTACCGAACAT	34
288	BstXI AS	AAGCCCAAGATGATGGGATGGGAAT	25
289	B(-11-10)D AS	AAAGAATCCCAGTGGATTGGGGACAGAAAGATTT	34
290	B(-11-10)D S	GTCCCCAATCCACTGGGATTCTTTCCCGACCACC	34
291	B(-11-48)D AS	GAATGCTCCAGCTCCACCTTGTGGCATCCGGC	34
292	B(-11-48)D S	AACAAGGTGGGAGCTGGAGCATTCGGGCTGGGTT	34
293	B(-11-75)D AS	TGCTGGCAAAGTAGTTGTGAGTATGCCCTGAGCC	34
294	B(-11-75)D S	ATACTCACAACACTTTTGCCAGCAAATCCGCCTC	34

4.1.3 Plasmids

For each construct, the cloning strategy was summarized below (refer to the description in 4.2.1).

No.	Name of the constructs	Note	Abbreviation
HBV genome expression:			
Wild-type			
26	pcDNA3.1/Zeo(-) HBV1.1 constructed by Kerry Mill	containing 1.1-mer over-length HBV genome	HBV 1.1
Envelope-deficient			
2	pCHT HBV1.1-L(-)-949 constructed by Kerry Mill	silence of start codon at 949 by ATG→ACG	/
27	pcDNA3.1/Zeo(-) HBV1.1-L(-)-949 constructed by Kerry Mill	silence of start codon at 949 by ATG→ACG	HBV L ⁻
6	pCHT HBV1.1 LM(-)-949/Stop1279 55/60-(55/58-P2+59/60)#MfeI/XhoI→P2	silence of start codon at 949 and introducing of stop codon at 1279	/
33	pcDNA3.1/Zeo(-) HBV1.1 LM(-)-949/Stop1279 6-BstXI→P33	silence of start codon at 949 and introducing of stop codon at 1279	HBV L ⁻ M ⁻
35	pcDNA3.1/Zeo(-) HBV1.1 LMS(-)-949/Stop1279/1453 constructed by Christina Damra	silence of start codon at 949 and introducing of stop codon at 1279/1453	HBV L ⁻ M ⁻ S ⁻
With cysteine mutation			
201	pcDNA3.1/Zeo(-) HBV1.1 LM(-)-949/Stop1279 C124S 182/189-(182/183-P33+184/189-P33)#BxtXI→P33	cysteine 124 of S was substituted by serine	S C124S
202	pcDNA3.1/Zeo(-) HBV1.1 LM(-)-949/Stop1279 C139S 182/189-(182/185-P33+186/189-P33)#BxtXI→P33	cysteine 139 of S was substituted by serine	S C139S
203	pcDNA3.1/Zeo(-) HBV1.1 LM(-)-949/Stop1279 C149S 182/189-(182/187-P33+188/189-P33)#BxtXI→P33	cysteine 149 of S was substituted by serine	S C149S
204	pcDNA3.1/Zeo(-) HBV1.1 LM(-)-949/Stop1279 C211A 182/189-(182/194-P33+195/189-P33)#BxtXI→P33	cysteine 48 of S was substituted by alanine	S C48A
205	pcDNA3.1/Zeo(-) HBV1.1 LM(-)-949/Stop1279 C228A 182/189-(182/196-P33+197/189-P33)#BxtXI→P33	cysteine 65 of S was substituted by alanine	S C65A

206	pcDNA3.1/Zeo(-) HBV1.1 LM(-)-949/Stop1279 C232A	cysteine 69 of S was substituted by alanine	S C69A
	182/189-(182/198-P33+199/189-P33)#BxtXI→P33		
L protein expression:			
Wild-type			
21	pcDNA3.1/Zeo(-) HuL	wild-type L protein of genotype D	wt L or D
	constructed by Kerry Mill		
138	pcDNA3.1/Zeo(-)-HuL(GT-B)	L protein of genotype B	B
	165/109-P131#NheI/HindIII→P23		
139	pcDNA3.1/Zeo(-)-HuL(GT-C2)	L protein of genotype C	C
	166/109-P132#NheI/HindIII→P23		
140	pcDNA3.1/Zeo(-)-HuL(GT-E)	L protein of genotype E	E
	167/109-P133#NheI/HindIII→P23		
141	pcDNA3.1/Zeo(-)-HuL(GT-G)	L protein of genotype G	G
	167/109-P134#NheI/HindIII→P23		
With preS2 mutation			
37	pcDNA3.1/Zeo(-) HuL-M(-)-1226	silence of internal M-ORF by ATG→ACG	L ^{M109T}
	61/96-(61/92-P21+93/96-P21)#NheI/EcoRI→P21		
40	pcDNA3.1/Zeo(-) mHuL 114/123	deletion of aa 114-123	Δ114-123
	61/96-(61/62-P21+63/96-P21)#EcoRI/XbaI→P21		
41	pcDNA3.1/Zeo(-) mHuL 114/133	deletion of aa 114-133	Δ114-133
	61/96-(61/64-P21+65/96-P21)#EcoRI/XbaI→P21		
42	pcDNA3.1/Zeo(-) mHuL 114/143	deletion of aa 114-143	Δ114-143
	61/96-(61/66-P21+67/96-P21)#EcoRI/XbaI→P21		
43	pcDNA3.1/Zeo(-) mHuL 114/153	deletion of aa 114-153	Δ114-153
	61/96-(61/68-P21+69/96-P21)#EcoRI/XbaI→P21		
44	pcDNA3.1/Zeo(-) mHuL 114/163	deletion of aa 114-163	Δ114-163
	61/96-(61/70-P21+71/96-P21)#EcoRI/XbaI→P21		
85	pcDNA3.1/Zeo(-) HuL-S114/163	aa 114-163 were shifted to corresponding residues of pol	S114-163
	116/96-(116/117-P21+118/96-P21)#EcoRI/XbaI→P21		
86	pcDNA3.1/Zeo(-) HuL-S114/143	aa 114-143 were shifted to corresponding residues of pol	S114-143
	116/96-(116/119-P21+120/96-P21)#EcoRI/XbaI→P21		
87	pcDNA3.1/Zeo(-) HuL-S114/183	aa 114-183 were shifted to corresponding residues of pol	S114-183
	116/96-(116/121-P21+122/96-P21)#EcoRI/XbaI→P21		
88	pcDNA3.1/Zeo(-) HuL-Del144-163	deletion of aa 144-163	Δ144-163

	61/96-(61/123-P21+124/96-P21)#EcoRI/XbaI→P21		
89	pcDNA3.1/Zeo(-) HuL-Del164-183	deletion of aa 164-183	Δ164-183
	61/96-(61/125-P21+126/96-P21)#EcoRI/XbaI→P21		
90	pcDNA3.1/Zeo(-) HuL-Del149-160	deletion of aa 149-160 (TLM)	Δ149-160
	61/96-(61/127-P21+128/96-P21)#EcoRI/XbaI→P21		
266	pcDNA3.1/Zeo(-) HuL-Scramble 114/163	aa 114-163 were scrambled	114-163 ^{Scramble}
	276/277-(273/274-Ø+275/277-Ø)#EcoRI/XbaI→P21 Ø: no template is needed for the amplification		
With cysteine mutation			
211	pcDNA3.1/Zeo(-) HuL C124S	cysteine 124 of S-domain was substituted by serine	L C124S
	110/109-(110/183-P21+184/109-P21)#EcoRI/HindIII→P21		
212	pcDNA3.1/Zeo(-) HuL C139S	cysteine 139 of S-domain was substituted by serine	L C139S
	110/109-(110/185-P21+186/109-P21)#EcoRI/HindIII→P21		
213	pcDNA3.1/Zeo(-) HuL C149S	cysteine 149 of S-domain was substituted by serine	L C149S
	110/109-(110/187-P21+188/109-P21)#EcoRI/HindIII→P21		
214	pcDNA3.1/Zeo(-) HuL C211A	cysteine 48 of S-domain was substituted by alanine	L C49A
	110/109-(110/194-P21+195/109-P21)#EcoRI/HindIII→P21		
215	pcDNA3.1/Zeo(-) HuL C228A	cysteine 65 of S-domain was substituted by alanine	L C65A
	110/109-(110/196-P21+197/109-P21)#EcoRI/HindIII→P21		
216	pcDNA3.1/Zeo(-) HuL C232A	cysteine 69 of S-domain was substituted by alanine	L C69A
	110/109-(110/198-P21+199/109-P21)#EcoRI/HindIII→P21		
With N-terminal variation			
92	pcDNA3.1/Zeo(-)-W(1-21)H(2-389)-L	N-terminal 21 amino acids of WHV L protein was fused to aa 2 of wt L	WHV 21
	97/96-(97/138-P55+139/96-P21)#NheI/EcoRI→P21		
217	pcDNA3.1/Zeo(-) HuL G2A	G2A mutation to abolish the myristoylation	G2A
	192/56-P21#NheI/EcoRI→P21		
218	pcDNA3.1/Zeo(-) HuL G2A/L11R	combination of G2A and L11R mutation	G2A/L11R
	192/56-P186#NheI/EcoRI→P21		
219	pcDNA3.1/Zeo(-) HuL G2A/L11R Del164/183	combination of G2A, L11R mutation and deletion of TM1	G2A/L11R ΔTM1
	192/56-P21#NheI/EcoRI→P89		

220	pcDNA3.1/Zeo(-) HuL P36A 61/56-(61/200-P21+201/56-P21)#NheI/EcoRI→P21	proline 36 was substituted by alanine	P36A
222	pcDNA3.1/Zeo(-) HuL PP58/59AA 61/56-(61/204-P21+205/56-P21)#NheI/EcoRI→P21	prolines 58/59 were substituted by alanines	PP58/59AA
223	pcDNA3.1/Zeo(-) HuL LG11/12MN 61/56-(61/206-P21+207/56-P21)#NheI/EcoRI→P21	LG at aa 11-12 was substituted by MN	LG11/12MN
224	pcDNA3.1/Zeo(-) HuL LG11/12RE 61/56-(61/208-P21+209/56-P21)#NheI/EcoRI→P21	LG at aa 11-12 was substituted by RE	LG11/12 RE
225	pcDNA3.1/Zeo(-) HuL Del16-48aa 61/56-(61/210-P21+211/56-P21)#NheI/EcoRI→P21	deletion of aa 16-48	Δ16-48
226	pcDNA3.1/Zeo(-) HuL Del49-75aa 61/56-(61/212-P21+213/56-P21)#NheI/EcoRI→P21	deletion of aa 49-75	Δ49-75
227	pcDNA3.1/Zeo(-) HuL Del16-75aa 61/56-(61/214-P21+215/56-P21)#NheI/EcoRI→P21	deletion of aa 16-75	Δ16-75
228	pcDNA3.1/Zeo(-) HuL Del11-15aa 61/56-(61/216-P21+217/56-P21)#NheI/EcoRI→P21	deletion of aa 11-15	Δ11-15
229	pcDNA3.1/Zeo(-) HuL Del41-45aa 61/56-(61/218-P21+219/56-P21)#NheI/EcoRI→P21	deletion of aa 41-45	Δ41-45
230	pcDNA3.1/Zeo(-) HuL Del71-75aa 61/56-(61/220-P21+221/56-P21)#NheI/EcoRI→P21	deletion of aa 71-75	Δ71-75
241	pcDNA3.1/Zeo(-) HuL Flu24 to2 61/56-[61/226-P21+225/56-(224/56-P21)]#NheI/EcoRI→P21	fusion peptide of fluenza virus was fused to aa 2 of wt-L	Flu24-L
242	pcDNA3.1/Zeo(-) HuL HIV23 to2 61/56-[61/229-P21+228/56-(227/56-P21)]#NheI/EcoRI→P21	fusion peptide of HIV gag was fused to aa 2 of wt L	HIV23-L
243	pcDNA3.1/Zeo(-) HuL Tri57-67 61/56-[61/236-P21+235/56-(234/56-P21)]#NheI/EcoRI→P21	Triplication of aa 57-67	Tri57-67
244	pcDNA3.1/Zeo(-) HuL aa9 to9 61/56-(61/233-P21+230/56-P21)#NheI/EcoRI→P21	VP4 myristoylation cassette was fused to aa 9 of wt L	VP4-9
245	pcDNA3.1/Zeo(-) HuL aa9 to10 61/56-(61/233-P21+231/56-P21)#NheI/EcoRI→P21	VP4 myristoylation cassette was fused to aa 10 of wt L	VP4-10
246	pcDNA3.1/Zeo(-) HuL aa9 to11	VP4 myristoylation cassette was fused to aa 11 of wt L	VP4-11

	61/56-(61/233-P21+232/56-P21)#NheI/EcoRI→P21		
247	pcDNA3.1/Zeo(-) HuL aa9 to2	VP4 myristoylation cassette was fused to aa 2 of wt L	VP4-L
	61/56-(61/233-P21+237/56-P21)#NheI/EcoRI→P21		
248	pcDNA3.1/Zeo(-) HuL aa9 to5	VP4 myristoylation cassette was fused to aa 5 of wt L	VP4-5
	61/56-(61/233-P21+238/56-P21)#NheI/EcoRI→P21		
249	pcDNA3.1/Zeo(-) HuL aa9 to8	VP4 myristoylation cassette was fused to aa 8 of wt L	VP4-8
	61/56-(61/233-P21+239/56-P21)#NheI/EcoRI→P21		
250	pcDNA3.1/Zeo(-) lcmv-HuL	myristoylation cassette of LCMV was fused to aa 2 of wt L	LCMV-L
	61/56-[61/242-P21+241/56-(240/56-P21)]#NheI/EcoRI→P21		
251	pcDNA3.1/Zeo(-) adw(B-D without M)-HuL	N-terminal 11 aa of L protein of genotype B was fused to aa 2 of wt L	B11-D M1(-)
	61/56-(61/244-P21+243/56-P21)#NheI/EcoRI→P21		
252	pcDNA3.1/Zeo(-) vac-HuL	N-terminal myristoylation motif of Vac8 protein was fused to aa 2 of wt L	Vac8-L
	61/56-(61/246-P21+245/56-P21)#NheI/EcoRI→P21		
253	pcDNA3.1/Zeo(-) fyn14-HuL	N-terminal myristoylation motif of Fyn protein was fused to aa 2 of wt L	Fyn-L
	61/56-(61/248-P21+247/56-P21)#NheI/EcoRI→P21		
254	pcDNA3.1/Zeo(-) yes-HuL	N-terminal myristoylation motif of Yes protein was fused to aa 2 of wt L	Yes-L
	61/56-(61/250-P21+249/56-P21)#NheI/EcoRI→P21		
255	pcDNA3.1/Zeo(-) psd95-HuL	N-terminal myristoylation motif of psd95 protein was fused to aa 2 of wt L	psd95-L
	61/56-(61/252-P21+251/56-P21)#NheI/EcoRI→P21		
256	pcDNA3.1/Zeo(-) gap43-HuL	N-terminal myristoylation motif of Gap43 protein was fused to aa 2 of wt L	Gap43-L
	61/56-(61/254-P21+253/56-P21)#NheI/EcoRI→P21		
257	pcDNA3.1/Zeo(-) B11-D	N-terminal 11 aa of L protein of genotype B was fused to aa 1 of wt L	B11-D
	61/56-(61/244-P21+255/56-P21)#NheI/EcoRI→P21		

258	pcDNA3.1/Zeo(-) E10-D 61/56-(61/258-P21+257/56-P21)#NheI/EcoRI→P21	N-terminal 10 aa of L protein of genotype E was fused to aa 1 of wt L	E10-D
259	pcDNA3.1/Zeo(-) F-D 61/56-(61/260-P21+259/56-P21)#NheI/EcoRI→P21	N-terminal 11 aa of L protein of genotype F was fused to aa 1 of wt L	F11-D
260	pcDNA3.1/Zeo(-) B-D with W 61/56-(61/264-P21+263/56-P21)#NheI/EcoRI→P21	N-terminal 11 aa of L protein of genotype B was fused to aa 1 of wt L with M1W mutation	B11-D M1W
261	pcDNA3.1/Zeo(-) B-D-G2A 61/56-(61/266-P21+265/56-P21)#NheI/EcoRI→P21	N-terminal 11 aa of L protein of genotype B was fused to aa 1 of wt L with G(-10)A mutation	B-D G-10A
262	pcDNA3.1/Zeo(-) B-D-G12A 61/56-(61/244-P21+267/56-P21)#NheI/EcoRI→P21	N-terminal 11 aa of L protein of genotype B was fused to aa 1 of wt L with G2A mutation	B-D G2A
263	pcDNA3.1/Zeo(-) Short B 261/109-P138#NheI/HindIII→P21	N-terminal 11 aa of L protein of genotype B was deleted	B ^t
264	pcDNA3.1/Zeo(-) E-B 61/109-(61/258-P138+269/109-P138)#NheI/HindIII→P21	N-terminal 10 aa of L protein of genotype E was fused to aa 1 of B ^t	E10-B ^t
265	pcDNA3.1/Zeo(-) N-VP4-short B 61/109-(61/272-P138+271/109-P138)#NheI/HindIII→P21	VP4 myristoylation cassette was fused to B ^t	VP4-B ^t
267	pcDNA3.1/Zeo(-) gtB-8H6 61/286-(61/278-P138+281/286-P138)#NheI/XbaI→P21	aa 8-13 of L protein of genotype B were replaced by His-6 tag	8H6
268	pcDNA3.1/Zeo(-) gtB-11H6 61/286-(61/279-P138+282/286-P138)#NheI/XbaI→P21	aa 11-16 of L protein of genotype B were replaced by His-6 tag	11H6
269	pcDNA3.1/Zeo(-) gtB-14H6	aa 14-19 of L protein of genotype B were replaced by His-6 tag	14H6

	61/286-(61/280-P138+283/286-P138)#NheI/XbaI→P21		
270	pcDNA3.1/Zeo(-) B-PreS1-D	N-terminal 124 residues of L protein of genotype B was fused to corresponding site of genotype D	B124-D
	165/284-P138#NheI/EcoRI→P21		
271	pcDNA3.1/Zeo(-) B-PreS2-D	N-terminal 167 residues of L protein of genotype B was fused to corresponding site of genotype D	B167-D
	165/285-P138#NheI/XhoI→P21		
272	pcDNA3.1/Zeo(-) B-AGL-D	N-terminal 207 residues of L protein of genotype B was fused to corresponding site of genotype D	B207-D
	165/286-P138#NheI/XbaI→P21		
274	pcDNA3.1/Zeo(-) B-21-D	N-terminal 19 residues of L protein of genotype B was fused to corresponding site of genotype D	B19-D
	61/56-(61/289-P21+290/56-P21)#NheI/EcoRI→P21		
275	pcDNA3.1/Zeo(-) B-59-D	N-terminal 59 residues of L protein of genotype B was fused to corresponding site of genotype D	B59-D
	61/56-(61/291-P21+292/56-P21)#NheI/EcoRI→P21		
276	pcDNA3.1/Zeo(-) B-86-D	N-terminal 86 residues of L protein of genotype B was fused to corresponding site of genotype D	B86-D
	61/56-(61/293-P21+294/56-P21)#NheI/EcoRI→P21		

4.1.4 Peptides

Name	Sequence	Modification
D preS/2-48 ^{myr}	Myr-GQNLSTSNPLGFFPDHQL DPAFRANTANPDWDFNPNKD TWPDANKVG-OH	N-myristoylation
C preS/-10-48 ^{myr}	Myr-GGWSSKPRQGMGTNLSVPN PLGFFPDHQLDPAFGANSNNP DWDNFNPNKDHWPQAKQVG-OH	N-myristoylation

C preS/2-48 ^{myr}	Myr-GTNLSVPNPLGFFPDHQL DPAFGANSNNPDWDFNPNKD HWPEAKQVG-OH	N-myristoylation
C preS/-10-48 ^{Stear}	Stear-GGWSSKPRQGMGTNLSVPN PLGFFPDHQLDPAFGANSNNP DWDFNPNKD HWPEAKQVG-OH	N-Stearoylation
C preS/2-48 ^{Stear}	Stear-GTNLSVPNPLGFFPDHQL DPAFGANSNNPDWDFNPNKD HWPEAKQVG-OH	N-Stearoylation
preS/2-48 ^{Stear}	Stear-GQNLSTSNPLGFFPDHQL DPAFRANTANPDWDFNPNKD TWPDANKVG-OH	N-Stearoylation
preS/5-48 ^{Stear}	Stear-LSTSNPLGFFPDHQL DPAFRANTANPDWDFNPNKD TWPDANKVG-OH	N-Stearoylation
preS/6-48 ^{Stear}	Stear-STSNPLGFFPDHQL DPAFRANTANPDWDFNPNKD TWPDANKVG-OH	N-Stearoylation
preS/7-48 ^{stear}	Stear-TSNPLGFFPDHQL DPAFRANTANPDWDFNPNKD TWPDANKVG-OH	N-myristoylation
preS/8-48 ^{stear}	Stear-SNPLGFFPDHQL DPAFRANTANPDWDFNPNKD TWPDANKVG-OH	N-Stearoylation
preS/9-48 ^{stear}	Stear-NPLGFFPDHQL DPAFRANTANPDWDFNPNKD TWPDANKVG-OH	N-Stearoylation
preS/A2-8/9-48 ^{stear}	Stear-AAAAAANPLGFFPDHQL DPAFRANTANPDWDFNPNKD TWPDANKVG-OH	N-Stearoylation
preS/A2-9/10-48 ^{stear}	Stear-AAAAAAAAPLGFFPDHQL DPAFRANTANPDWDFNPNKD TWPDANKVG-OH	N-Stearoylation
B-D ^{myr}	Myr-GGWSSKPRKGMGQNLSTSN PLGFFPDHQLDPAFRANTANP DWDFNPNKDTWPDANKVG-OH	N-myristoylation
VP4-D ^{myr}	Myr-GAQVSSQKVGQNLSTSN PLGFFPDHQLDPAFRANTANP DWDFNPNKDTWPDANKVG-OH	N-myristoylation
Myrcludex B	Myr-GTNLSVPNPLGFFPDHQL DPAFGANSNNPDWDFNPNKD HWPEANKVG-OH	N-myristoylation

4.1.5 Cells

Cells	Description	Suppliers
HuH-7	Human hepatoblastoma cell line ²³⁹	Lab

HepaRG	HBV susceptible hepatoma cell line ¹⁷¹	Grippon
HepAD38	Inducible human hepatoblastoma cell line harbors a integrated tetracycline responsive 1.2 fold HBV genome (serotype ayw, genotype D) ¹⁵⁰	T. Block
DH5 α	<i>E. Coli</i> adjusted for molecular cloning purposes. <i>E. coli</i> (Escherichia coli) DH5 α ²⁴⁰ : SupE44, Δ (lacZYA-argF)U169, Φ 80dlacZ Δ M15, recA1, endA1, gyrA96, thi-1, relA1, hsdR17(rk-, mk+), deoR	BRL

4.2. Methods

4.2.1 General Cloning strategy

The cloning strategy for most of the mutants is based on PCR-amplification of two or several overlapping fragments located upstream and downstream of the mutation site. Taken the plasmid Δ 114-123 as an example, for the first fragment primers 61 and 62 were used to amplify the target sequence from plasmid P21, and this step was noted as 61/62-P21. The second fragment was generated from plasmid P21 using the primers 63 and 96, and this step was noted as 63/96-P21. After purification by extraction of the fragments from agarose gels, these two PCR-products were mixed and subjected to a second round of amplification using the primers 61 and 96, and this step was noted as 61/96-(61/62-P21+63/96-P21). The final PCR product with expected size were purified, hydrolyzed with EcoRI and HindIII and inserted into the EcoRI-HindIII-digested P21 vector. Therefore, the whole cloning strategy was noted as 61/96-(61/62-P21+63/96-P21)#EcoRI/HindIII \rightarrow P21. The correctness of sequences generated by PCR was verified by DNA sequencing.

4.2.2 Agarose electrophoresis

DNA was analyzed by agarose gel electrophoresis. Agarose was dissolved in TAE buffer by heating. 0.1 μ g/ml ethidium bromide was added to the liquid agarose before it was casted into an electrophoresis tray. The density of the gel used was dependent on the expected DNA size. The samples were loaded with 1x agarose gel sample buffer and separated by electrophoresis at 50-120 V. The fragment sizes were compared to molecular weight markers.

4.2.3 Gel exaction of DNA fragments

When it is necessary to separate the DNA from the raw PCR products or digestion product, the sample were loaded on agarose gels of the suitable percentage procedure. After proper separation of the fragments, DNA was visualized under a low energy UV source and cut out of

the gel using a clean blade. DNA fragments were then purified from the gel with the Gel exaction kit (Qiagen) according to the manufactures protocol. Purity and yield of the DNA was determined by agarose gel electrophoresis and UV spectroscopy.

4.2.4 Polymerase Chain Reaction (PCR)

A gernal PCR recipe is the following (for a 50 μ l reaction volume):

RNase free Water	38 μ l
Deep vent Polymerase buffer with magnese (10 \times)	5 μ l
dNTP mixture (25mM each)	0.5 μ l
Deep vent Polymerase (5U/ μ l)	0.5 μ l
Sense primer (100pMl)	0.5 μ l
Antisense primer (100pM)	0.5 μ l
Template	5 μ l

The templates are either 10ng/ μ l plasmid or purified DNA fragment from Gel exaction kit eluted in 50 μ l water (2.5 μ l each for the overlapping PCR).

The parameter of thermocycling is the following:

Step1,	95°C,	5 minutes
Step2,	95°C,	20 seconds
Step3,	54°C,	20 seconds
Step4,	72°C,	varied time, 1min/800bp product
Go to Step2 for 35 cycles		
Step5,	72°C,	7 minutes
Step6,	4°C,	hold

4.2.5 Competent cells preparation and transformations

A single colony from a E .coli DH5 α strain was grown over-night in 2 ml LB medium with 0.02 M MgSO₄/ 0.01 M KCl with vigorous shaking (~300 rpm). It was diluted 1:10 into fresh medium with the same constituents and grown for 90 min, at 37°C to an OD₆₀₀ of 0.45. Cultures were incubated on ice for 10 min after which the cells were pelleted by centrifugation at 6000 rpm at 4°C for 5 min. Cells were resuspended in TFB I (30 ml/ 100 ml culture), incubated

5 min on ice, pelleted again by centrifugation at 6000 rpm at 4°C for 5 min and finally resuspended in TFB II (4 ml per 100 ml culture). 100 µl aliquots of the competent bacteria were frozen at –80°C.

TFB I:

30 mM KOAc, 50 mM MnCl₂, 100 mM RbCl₂, 10 mM CaCl₂, 15% w/v glycerin, pH 5.8

TFBII

10 mM MOPS, pH 7.5, 75 mM CaCl₂, 100 mM RbCl₂, 15% w/v glycerin

Both the solutions were sterilized and stored at 4°C.

4.2.6 DNA sequencing

All constructs generated were verified by sequencing. The sequencing is performed either by a commercial vendor (GATC, Constanze) or using the ABI Prism® BigDye™ Terminator Cycle Sequencing Ready Reaction Kit (PE Applied Biosystems) and performed as described in the product manual. Shortly, template DNA (0.5 µg), the respective primer (10 pmol) and 2 µl Big Dye™ terminator ready reaction mix were combined in a total volume of 10 µl and the sequencing reaction was carried out as follows: 25x (96°C, 30 sec; 50°C, 15 sec; 60°C, 4 min). Sequencing was done on an automated sequencer.

4.2.7. Plasmid preparations

For a middle or large scale plasmid preparation for transfection, Plasmid midi or max kit (Qiagen) were used and performed according to the product manuals.

For a fast and small scale plasmid preparation for cloning, the Fastprep mini kit (Eppendorf) was used and performed according to the product manual.

4.2.8 SDS-PAGE

This method separates a protein mixture dependent on its molecular weight (MW) composition. It was performed as described in standard protocols [Ausubel, et al., 2004]. The polymer density of the separation gel depends on the expected MW of the target protein (MW < 30 kDa = 15 % (w/v) PAGE gel, MW > 30 kDa = 12 % (w/v) PAGE gel). Proteins are denaturated in SDS-PAGE sample buffer by 5 min heat denaturation at 95 °C prior to electrophoresis in SDS-PAGE buffer at 80-120 V.

4.2.9 Western blot

After SDS-PAGE, proteins were transferred to PROTRAN nitrocellulose membrane using a semi-dry blotting chamber. The gel was placed in contact to a nitrocellulose membrane, and was sandwiched with two sheets of Whatmann paper in both side. The proteins migrate from the gel onto the membrane in an electric field of 1.3 mA/cm² for 20 minutes. Membranes were blocked with PBS/5% milk powder/ 0.05% Tween 20 at room temperature for 1 h. Antisera/antibodies was diluted in blocking buffer. Bands were visualized with enhanced chemiluminescence (ECL) substrate or with an Odyssey Infrared Imaging System (LI-COR).

Home-made ECL Solution I:

0.5 ml luminol stock (A), 0.22 ml coumaric acid stock (B), 5 ml 1 M Tris HCl pH 8.5, 45 ml distilled water.

Home-made ECL Solution II:

32 microlitres 30% hydrogen peroxide, 5 ml 1 M Tris HCl pH 8.5, 45 ml distilled water.

Stock A (250 mM Luminol in DMSO):

dissolve 0.8858g Luminol (Sigma #09253, MW, 177.16) in 20 ml DMSO, aliquot to 0.5ml/tube, labeled as A.

Stock B (90 mM coumaric acid in DMSO):

dissolved 0.2955g coumaric acid (Sigma #9008, MW, 164.16) in 20ml DMSO, aliquot to 0.22ml/tube, labeled as B.

4.2.10 Immunoprecipitation

To analyse the preS topology of HBV particle, 1ml supernatant of transfected HuH-7 cells were mixed with 5µl polyclonal anti-preS1 antiserum (Rabbit anti-Myrcludex B) in the absence or presence of NP40 (0.5 % v/v). The incubations were performed overnight for about 18-24 hours at 4°C under rotation. 20µl of protein G-Sepharose (1:1 in suspension buffer) was washed by PBS and subsequently added to bind the immunoprecipitates, and the samples were incubated for a further hour at 4°C while shaking. The beads were then collected by centrifugation at 500g for 3 minutes. Beads were washed three times with the extraction buffer and analyzed together with their corresponding supernatants on the SDS-PAGE followed by Western blot.

4.2.11 Cultivation of HuH-7 cells

HuH-7 cells were passaged every 3-4 days by trypsinization and split at the ratio 1:5. The cells were grown in DMEM medium supplemented with 10% fetal calf serum (FCS), 2 mM L-Glutamin, 100 U/ml penicillin and 100 µg/ml streptomycin.

4.2.12 Cultivation and infection of primary human hepatocytes and HepaRG cells

HepaRG cells were passaged weekly by trypsinization. 2×10^6 HepaRG cell were left in one T-75 flask and supplemented with 10-15 ml Growing medium. For infection assay, 2×10^5 HepaRG cells are seeded in one well of 12-well-plate for 2 week and differentiated in Low differentiation or High differentiation medium for another 2 weeks. Then HepaRG cells are ready for the infection.

For the preparation of PHH, tissue samples were obtained and experimental procedures were performed according to the guidelines of the charitable state controlled foundation HTCR, with the informed patient's consent²⁴¹. PHH were seeded at 1.6×10^5 cells per cm^2 with PHH-1 medium. 4 hours and 1 day post-plating, the PHH was refreshed with PHH-2 medium. Then the PHH was further cultivated less than 3 days before the starting of infection.

For infection, cells of a 12-well plate were inoculated with 500 µl of medium containing 4% PEG 8000 and concentrated virus. To ensure that HBV-entry proceeds via the authentic preS1-mediated pathway, or to test the inhibitory activity of peptides, the peptide stock was added to the inoculum to desired concentration. Virus incubation took place overnight at 37°C.

Afterwards cells were washed three times with PBS and subjected to further cultivation for 11 days. Hepatitis B surface antigen (HBsAg) and e antigen (HBeAg) secreted into the culture supernatant was determined by Abbott AxSYM® HBsAg or HBeAg assay (Abbott Laboratories).

Growing medium:

- Williams E medium 500ml
- + 50ml FCS (Biochrom)
- + 5ml Pen/Strep Stock (penicillin, 10000 U/ml; streptomycin 10 mg/ml)
- + 250µl Hydrocortison [50µM]
- + 250µl Insulin [5µg/ml]

Low differentiation medium:

Williams E medium 500ml
+ 50ml FCS (Biochrom)
+ 5ml Pen/Strep Stock (penicillin, 10000 U/ml; streptomycin 10 mg/ml)
+ 250µl Hydrocortison [50µM]
+ 250µl Insulin [5µg/ml]
+ 2.75ml DMSO

High differentiation medium:

Williams E medium 500ml
+ 50ml FCS (Biochrom)
+ 5ml Pen/Strep Stock (penicillin, 10000 U/ml; streptomycin 10 mg/ml)
+ 250µl Hydrocortison [50µM]
+ 250µl Insulin [5µg/ml]
+ 11ml DMSO

PHH-1 medium:

Williams E medium 500ml
+ 50ml FCS (Biochrom)
+ 5ml Pen/Strep Stock (penicillin, 10000 U/ml; streptomycin 10 mg/ml)
+ 250µl Hydrocortison [50µM]
+ 250µl Insulin [5µg/ml]
+ 200mM L-glutamine

PHH-2 medium:

Williams E medium 500ml
+ 50ml FCS (Biochrom)
+ 5ml Pen/Strep Stock (penicillin, 10000 U/ml; streptomycin 10 mg/ml)
+ 250µl Hydrocortison [50µM]
+ 250µl Insulin [5µg/ml]
+ 200mM L-glutamine

+ 2.75ml DMSO

Insulin Stock [5µg/ml]

100mg Insulin I1882 (Sigma) were dissolved with 10ml Braun H₂O and 100µl Essigsäure versetzen, sterile filtered, aliquot to 250µl and stored at -20°C.

Hydrocortison Stock [100mM]

1g Hydrocortison H4881 (Sigma) were dissolved with 20ml Braun H₂O, sterile filtered, aliquot to 250µl and stored at -20°C

4.2.13 Transfection of HuH-7 cells using polyethylenimine

The human hepatoblastoma cell line HuH-7²³⁹ was transfected with appropriate mixtures of expression plasmids using the polyethylenimine-procedure²⁴¹. Shortly, 4×10⁶ cells (in a 10-cm-dish) were incubated for 6 hours with the mixture of 75 µg polyethylenimine and 10 or 12 µg plasmid DNA. The cells were refreshed and further cultivated in Dulbecco's Modified Eagle Medium supplemented with 10% FCS, 2 mM L-glutamine, 100 U/ml penicillin and 100 µg/ml streptomycin.

PEI stock solution (100mg/ml):

In 50ml Falcon tube, 5g PEI (Polyethylenimine, MW-22,000; Cat. No.408727, Aldrich) was dissolved with Braun-water to final volume of 50ml then was sterilized with 45µm filter. Aliquots of 500ul per tube were frozen at -20°C.

PEI working solution (1mg/ml):

In 50ml falcon tube, 1 tube of PEI stock solution (100mg/ml, 500ul) was diluted with Braun-water to final volume of 50ml and stored at 4°C.

4.2.14 Production of the HBV particle

HBV particles were obtained by co-transfection of HuH-7 cells with a mixture of a 1.1-fold over-length HBV plasmid (HBV L⁻, or HBV L⁻M⁻, or HBV L⁻M⁻S⁻) and a helper construct providing the L-protein. Medium was collected between days 3-8 (and days 8-13) post-transfection.

4.2.15 Purification and concentration of virus by PEG-precipitation

Virions in the supernatant of transfected HuH-7 cells were precipitated overnight at 4°C with 6% polyethylene glycol 8000 (PEG 8000, Sigma) and subjected to a centrifugation (12,000 g, 60

min, 4°C). After suspension in 1/50th to 1/100th of the volume of PBS/10% FCS, the preparation is centrifuged (8,000rpm, 5min) again and the supernatant is frozen at -20°C.

4.2.16 CsCl-gradient centrifugation and DNA dot-blot analysis

2 ml cell culture supernatant or 30-50 µl concentrated virus were loaded onto a cesium chloride gradient ranging from 1.4 g/cm³ to 1.2 g/cm³. Fractions of ~200µl were collected from the bottom of the tube and spotted onto a nitrocellulose membrane. After denaturation the samples were hybridized overnight at 68°C using a HBV specific ³²P-labeled DNA probe. The blot was washed twice at 68°C with SSC-buffer (150 mM NaCl, 15 mM sodium citrate, pH 7.0). Signals were quantified using a PhosphorImager and the Quantity One® software (Bio-Rad).

4.2.17 Immunofluorescence analyses of HBcAg expression in infected cells

11-13 days post-infection HepaRG cells or PHH were washed with PBS, fixed with 4% paraformaldehyde (20 minutes) and permeabilized with 0.25% (v/v) Triton-X-100 (30 minutes) in PBS. After removal of the detergent, the HBcAg or MRP2-specific polyclonal antibody was added (1:1000 dilution in PBS containing 5% skim milk powder). Following 2 h incubation at 4°C, cells were washed three times and incubated in the dark for 1 h at room temperature with the 1:500 diluted Alexa488-conjugated secondary Mouse-anti-Rabbit antibody (Invitrogen, Molecular Probes) in PBS containing 5% skim milk powder. After washing three times with PBS, cells were incubated for 30 min with 1 µg/ml DAPI. Cells were then washed twice with PBS. Images were acquired using the inverted fluorescence microscope Leica DM IRB. All images of one set of experiments were taken and handled under identical conditions. To quantify infection, positive cells in 4-8 fields under 100-fold magnification were counted. The counted numbers were converted to the whole well according the real area under the microscope.

4.2.18 HBsAg and HBeAg measurement in the supernatants of infected cells

The HBsAg and HBeAg were measured by the Abbott Axym test and performed by the Diagnostics Center of University of Heidelberg.

4.2.19 Heparin binding assay

The binding and elution of HBV particle are depicted in the Fig. 37. In short, 50ml of supernatant containing HBV particles was applied to the Heparin column (1ml) equilibrated with 1×TN buffer, and then the column was wash with 50ml 1×TN buffer. Virus bound to the column was eluted at a stepwise concentration of 340nM TN buffer, 540nM TN buffer, and 2M TN buffer respectively. For each concentration, the eluate is collected in 4 tubes (1ml/tube). The OD260 and OD254 are measured by the AKTA system automatically.

1×TN buffer:

50nM Tris, 150nM NaCl

340nM TN buffer

50nM Tris, 340nM NaCl

540nM TN buffer

50nM Tris, 540nM NaCl

2M TN buffer

50nM Tris, 2M NaCl

4.2.20 Lentivirus production and transduction of HepaRG cells

Lentivirus production was generated by the PEI-based co-transfection of 293T cells. In short, 4×10^6 293T cells were seeded in 10-cm-diameter plates 1 day before transfection with 3 µg of envelope protein expression construct pczVSV-G²⁴², 9 µg of HIV-Gag-Pol expression construct pCMVΔR8.74²⁴³, and 9 µg of the lentiviral vector pWPI²⁴⁴. The medium was replaced overnight after transfection. Supernatants containing the pseudoparticles were harvested 48 h later and filtered through 0.45µm filter. The pseudoparticles were concentrated by ultracentrifugation using a SW-28 rotor at 20,000 rpm, RT for 2 hours. The supernatant was aspirated and the precipitated pseudoparticles were dissolved in 1/50 of original volume.

The HepaRG cells in 12-well-plate were transduced overnight with 100µl concentrated virus per well in the presence of 4% PEG. Then lentivirus pseudoparticles were removed, and HepaRG cells were washed once with PBS and further cultivated for 4 days prior to HBV infection.

Reference List

1. **Blumberg, B. S., B. J. Gerstley, D. A. Hungerford, W. T. London, and A. I. Sutnick.** 1967. A serum antigen (Australia antigen) in Down's syndrome, leukemia, and hepatitis. *Ann. Intern. Med.* **66**:924-931.
2. **Blumberg, B. S., A. I. Sutnick, and W. T. London.** 1968. Hepatitis and leukemia: their relation to Australia antigen. *Bull. N. Y. Acad. Med.* **44**:1566-1586.
3. **Blumberg, B. S., H. J. ALTER, and S. VISNICH.** 1965. A "NEW" ANTIGEN IN LEUKEMIA SERA. *JAMA* **191**:541-546.
4. **Bartenschlager, R., M. Junker-Niepmann, and H. Schaller.** 1990. The P gene product of hepatitis B virus is required as a structural component for genomic RNA encapsidation. *J. Virol.* **64**:5324-5332.
5. **Summers, J. and W. S. Mason.** 1982. Replication of the genome of a hepatitis B--like virus by reverse transcription of an RNA intermediate. *Cell* **29**:403-415.
6. **Sprengel, R., E. F. Kaleta, and H. Will.** 1988. Isolation and characterization of a hepatitis B virus endemic in herons. *J. Virol.* **62**:3832-3839.
7. **Guo, H., W. S. Mason, C. E. Aldrich, J. R. Saputelli, D. S. Miller, A. R. Jilbert, and J. E. Newbold.** 2005. Identification and characterization of avihepadnaviruses isolated from exotic anseriformes maintained in captivity. *J. Virol.* **79**:2729-2742.
8. **Chang, S. F., H. J. Netter, M. Bruns, R. Schneider, K. Frolich, and H. Will.** 1999. A new avian hepadnavirus infecting snow geese (*Anser caerulescens*) produces a significant fraction of virions containing single-stranded DNA. *Virology* **262**:39-54.
9. **Prassolov, A., H. Hohenberg, T. Kalinina, C. Schneider, L. Cova, O. Krone, K. Frolich, H. Will, and H. Sirma.** 2003. New hepatitis B virus of cranes that has an unexpected broad host range. *J. Virol.* **77**:1964-1976.
10. **Pult, I., H. J. Netter, M. Bruns, A. Prassolov, H. Sirma, H. Hohenberg, S. F. Chang, K. Frolich, O. Krone, E. F. Kaleta, and H. Will.** 2001. Identification and analysis of a new hepadnavirus in white storks. *Virology* **289**:114-128.
11. **Nicholas H. Acheson.** 2009. *Fundamentals of molecular virology.* John Wiley and Son.
12. **rauz-Ruiz, P., H. Norder, B. H. Robertson, and L. O. Magnius.** 2002. Genotype H: a new Amerindian genotype of hepatitis B virus revealed in Central America. *J. Gen. Virol.* **83**:2059-2073.
13. **Norder, H., A. M. Courouce, and L. O. Magnius.** 1994. Complete genomes, phylogenetic relatedness, and structural proteins of six strains of the hepatitis B virus, four of which represent two new genotypes. *Virology* **198**:489-503.
14. **Fung, S. K. and A. S. Lok.** 2004. Hepatitis B virus genotypes: do they play a role in the outcome of HBV infection? *Hepatology* **40**:790-792.

15. **Olinger, C. M., P. Jutavijittum, J. M. Hubschen, A. Yousukh, B. Samountry, T. Thammavong, K. Toriyama, and C. P. Muller.** 2008. Possible new hepatitis B virus genotype, southeast Asia. *Emerg. Infect. Dis.* **14**:1777-1780.
16. **Tatematsu, K., Y. Tanaka, F. Kurbanov, F. Sugauchi, S. Mano, T. Maeshiro, T. Nakayoshi, M. Wakuta, Y. Miyakawa, and M. Mizokami.** 2009. A Genetic Variant of Hepatitis B Virus Divergent from Known Human and Ape Genotypes Isolated from a Japanese Patient and Provisionally Assigned to New Genotype J. *J. Virol.*
17. **Tanaka, Y. and M. Mizokami.** 2007. Genetic diversity of hepatitis B virus as an important factor associated with differences in clinical outcomes. *J. Infect. Dis.* **195**:1-4.
18. **Palumbo, E.** 2007. Hepatitis B genotypes and response to antiviral therapy: a review. *Am. J. Ther.* **14**:306-309.
19. **Liu, C. J., J. H. Kao, and D. S. Chen.** 2005. Therapeutic implications of hepatitis B virus genotypes. *Liver Int.* **25**:1097-1107.
20. **Zuckerman, A. J., A. Thornton, C. R. Howard, K. N. Tsiquaye, D. M. Jones, and M. R. Brambell.** 1978. Hepatitis B outbreak among chimpanzees at the London Zoo. *Lancet* **2**:652-654.
21. **Hu, X., H. S. Margolis, R. H. Purcell, J. Ebert, and B. H. Robertson.** 2000. Identification of hepatitis B virus indigenous to chimpanzees. *Proc. Natl. Acad. Sci. U. S. A* **97**:1661-1664.
22. **Thornton, S. M., S. Walker, and J. N. Zuckerman.** 2001. Management of hepatitis B virus infections in two gibbons and a western lowland gorilla in a zoological collection. *Vet. Rec.* **149**:113-115.
23. **Verschoor, E. J., K. S. Warren, S. Langenhuijzen, Heriyanto, R. A. Swan, and J. L. Heeney.** 2001. Analysis of two genomic variants of orang-utan hepadnavirus and their relationship to other primate hepatitis B-like viruses. *J. Gen. Virol.* **82**:893-897.
24. **Locarnini, S.** 2004. Molecular virology of hepatitis B virus. *Semin. Liver Dis.* **24 Suppl 1**:3-10.
25. **Schaefer, S.** 2007. Hepatitis B virus taxonomy and hepatitis B virus genotypes. *World J. Gastroenterol.* **13**:14-21.
26. **Dane, D. S., C. H. Cameron, and M. Briggs.** 1970. Virus-like particles in serum of patients with Australia-antigen-associated hepatitis. *Lancet* **1**:695-698.
27. **Albin, C. and W. S. Robinson.** 1980. Protein kinase activity in hepatitis B virus. *J. Virol.* **34**:297-302.
28. **Heermann, K. H., F. Kruse, M. Seifer, and W. H. Gerlich.** 1987. Immunogenicity of the gene S and Pre-S domains in hepatitis B virions and HBsAg filaments. *Intervirology* **28**:14-25.

29. **Gripon, P., S. J. Le, S. Rumin, and C. Guguen-Guillouzo.** 1995. Myristylation of the hepatitis B virus large surface protein is essential for viral infectivity. *Virology* **213**:292-299.
30. **Lambert, C. and R. Prange.** 2001. Dual topology of the hepatitis B virus large envelope protein: determinants influencing post-translational pre-S translocation. *J. Biol. Chem.* **276**:22265-22272.
31. **Lutwick, L. I. and W. S. Robinson.** 1977. DNA synthesized in the hepatitis B Dane particle DNA polymerase reaction. *J. Virol.* **21**:96-104.
32. **Summers, J., A. O'Connell, and I. Millman.** 1975. Genome of hepatitis B virus: restriction enzyme cleavage and structure of DNA extracted from Dane particles. *Proc. Natl. Acad. Sci. U. S. A* **72**:4597-4601.
33. **Staprans, S., D. D. Loeb, and D. Ganem.** 1991. Mutations affecting hepadnavirus plus-strand DNA synthesis dissociate primer cleavage from translocation and reveal the origin of linear viral DNA. *J. Virol.* **65**:1255-1262.
34. **Yang, W., W. S. Mason, and J. Summers.** 1996. Covalently closed circular viral DNA formed from two types of linear DNA in woodchuck hepatitis virus-infected liver. *J. Virol.* **70**:4567-4575.
35. **Yang, W. and J. Summers.** 1998. Infection of ducklings with virus particles containing linear double-stranded duck hepatitis B virus DNA: illegitimate replication and reversion. *J. Virol.* **72**:8710-8717.
36. **Flint, S. J. E. L. W. R. V. R. S. A.** 2004. *Principles of Virology: Molecular Biology, Pathogenesis, and Control of Animal Viruses.* ASM Press, Washington, DC.
37. **Haywood, A. M.** 1994. Virus receptors: binding, adhesion strengthening, and changes in viral structure. *J. Virol.* **68**:1-5.
38. **Paran, N., B. Geiger, and Y. Shaul.** 2001. HBV infection of cell culture: evidence for multivalent and cooperative attachment. *EMBO J.* **20**:4443-4453.
39. **Patel, M., M. Yanagishita, G. Roderiquez, D. C. Bou-Habib, T. Oravec, V. C. Hascall, and M. A. Norcross.** 1993. Cell-surface heparan sulfate proteoglycan mediates HIV-1 infection of T-cell lines. *AIDS Res. Hum. Retroviruses* **9**:167-174.
40. **WuDunn, D. and P. G. Spear.** 1989. Initial interaction of herpes simplex virus with cells is binding to heparan sulfate. *J. Virol.* **63**:52-58.
41. **Barth, H., C. Schafer, M. I. Adah, F. Zhang, R. J. Linhardt, H. Toyoda, A. Kinoshita-Toyoda, T. Toida, T. H. Van Kuppevelt, E. Depla, W. F. von, H. E. Blum, and T. F. Baumert.** 2003. Cellular binding of hepatitis C virus envelope glycoprotein E2 requires cell surface heparan sulfate. *J. Biol. Chem.* **278**:41003-41012.
42. **Schulze, A., P. Gripon, and S. Urban.** 2007. Hepatitis B virus infection initiates with a large surface protein-dependent binding to heparan sulfate proteoglycans. *Hepatology* **46**:1759-1768.

43. **Abou-Jaoude, G. and C. Sureau.** 2007. Entry of hepatitis delta virus requires the conserved cysteine residues of the hepatitis B virus envelope protein antigenic loop and is blocked by inhibitors of thiol-disulfide exchange. *J. Virol.* **81**:13057-13066.
44. **Glebe, D. and S. Urban.** 2007. Viral and cellular determinants involved in hepadnaviral entry. *World J. Gastroenterol.* **13**:22-38.
45. **Neurath, A. R., S. B. Kent, N. Strick, and K. Parker.** 1986. Identification and chemical synthesis of a host cell receptor binding site on hepatitis B virus. *Cell* **46**:429-436.
46. **Pontisso, P., M. G. Ruvoletto, W. H. Gerlich, K. H. Heermann, R. Bardini, and A. Alberti.** 1989. Identification of an attachment site for human liver plasma membranes on hepatitis B virus particles. *Virology* **173**:522-530.
47. **Neurath, A. R., N. Strick, P. Sproul, H. E. Ralph, and J. Valinsky.** 1990. Detection of receptors for hepatitis B virus on cells of extrahepatic origin. *Virology* **176**:448-457.
48. **Neurath, A. R. and N. Strick.** 1990. Antigenic mimicry of an immunoglobulin A epitope by a hepatitis B virus cell attachment site. *Virology* **178**:631-634.
49. **Pontisso, P., M. G. Ruvoletto, C. Tiribelli, W. H. Gerlich, A. Ruol, and A. Alberti.** 1992. The preS1 domain of hepatitis B virus and IgA cross-react in their binding to the hepatocyte surface. *J. Gen. Virol.* **73 (Pt 8)**:2041-2045.
50. **Dash, S., K. V. Rao, and S. K. Panda.** 1992. Receptor for pre-S1(21-47) component of hepatitis B virus on the liver cell: role in virus cell interaction. *J. Med. Virol.* **37**:116-121.
51. **Neurath, A. R., N. Strick, and P. Sproul.** 1992. Search for hepatitis B virus cell receptors reveals binding sites for interleukin 6 on the virus envelope protein. *J. Exp. Med.* **175**:461-469.
52. **Neurath, A. R., N. Strick, and Y. Y. Li.** 1992. Cells transfected with human interleukin 6 cDNA acquire binding sites for the hepatitis B virus envelope protein. *J. Exp. Med.* **176**:1561-1569.
53. **De, F. S., M. G. Ruvoletto, A. Verdoliva, M. Ruvo, A. Raucci, M. Marino, S. Senatore, G. Cassani, A. Alberti, P. Pontisso, and G. Fassina.** 2001. Cloning and expression of a novel hepatitis B virus-binding protein from HepG2 cells. *J. Biol. Chem.* **276**:36613-36623.
54. **Ryu, C. J., D. Y. Cho, P. Gripon, H. S. Kim, C. Guguen-Guillouzo, and H. J. Hong.** 2000. An 80-kilodalton protein that binds to the pre-S1 domain of hepatitis B virus. *J. Virol.* **74**:110-116.
55. **Petit, M. A., F. Capel, S. Dubanchet, and H. Mabit.** 1992. PreS1-specific binding proteins as potential receptors for hepatitis B virus in human hepatocytes. *Virology* **187**:211-222.

56. **Duclos-Vallee, J. C., F. Capel, H. Mabit, and M. A. Petit.** 1998. Phosphorylation of the hepatitis B virus core protein by glyceraldehyde-3-phosphate dehydrogenase protein kinase activity. *J. Gen. Virol.* **79 (Pt 7)**:1665-1670.
57. **Budkowska, A., C. Quan, F. Groh, P. Bedossa, P. Dubreuil, J. P. Bouvet, and J. Pillot.** 1993. Hepatitis B virus (HBV) binding factor in human serum: candidate for a soluble form of hepatocyte HBV receptor. *J. Virol.* **67**:4316-4322.
58. **Harvey, T. J., T. B. Macnaughton, D. S. Park, and E. J. Gowans.** 1999. A cellular protein which binds hepatitis B virus but not hepatitis B surface antigen. *J. Gen. Virol.* **80 (Pt 3)**:607-615.
59. **Li, D., X. Z. Wang, J. Ding, and J. P. Yu.** 2005. NACA as a potential cellular target of hepatitis B virus preS1 protein. *Dig. Dis. Sci.* **50**:1156-1160.
60. **Treichel, U., K. H. Meyer zum Buschenfelde, R. J. Stockert, T. Poralla, and G. Gerken.** 1994. The asialoglycoprotein receptor mediates hepatic binding and uptake of natural hepatitis B virus particles derived from viraemic carriers. *J. Gen. Virol.* **75 (Pt 11)**:3021-3029.
61. **Treichel, U., K. H. Meyer zum Buschenfelde, H. P. Dienes, and G. Gerken.** 1997. Receptor-mediated entry of hepatitis B virus particles into liver cells. *Arch. Virol.* **142**:493-498.
62. **Glebe, D. and W. H. Gerlich.** 2004. Study of the endocytosis and intracellular localization of subviral particles of hepatitis B virus in primary hepatocytes. *Methods Mol. Med.* **96**:143-151.
63. **Owada, T., K. Matsubayashi, H. Sakata, H. Ihara, S. Sato, K. Ikebuchi, T. Kato, H. Azuma, and H. Ikeda.** 2006. Interaction between desialylated hepatitis B virus and asialoglycoprotein receptor on hepatocytes may be indispensable for viral binding and entry. *J. Viral Hepat.* **13**:11-18.
64. **Miyauchi, K., Y. Kim, O. Latinovic, V. Morozov, and G. B. Melikyan.** 2009. HIV enters cells via endocytosis and dynamin-dependent fusion with endosomes. *Cell* **137**:433-444.
65. **Kock, J., E. M. Borst, and H. J. Schlicht.** 1996. Uptake of duck hepatitis B virus into hepatocytes occurs by endocytosis but does not require passage of the virus through an acidic intracellular compartment. *J. Virol.* **70**:5827-5831.
66. **Breiner, K. M. and H. Schaller.** 2000. Cellular receptor traffic is essential for productive duck hepatitis B virus infection. *J. Virol.* **74**:2203-2209.
67. **Pugh, J. C. and J. W. Summers.** 1989. Infection and uptake of duck hepatitis B virus by duck hepatocytes maintained in the presence of dimethyl sulfoxide. *Virology* **172**:564-572.
68. **Grgacic, E. V. and H. Schaller.** 2000. A metastable form of the large envelope protein of duck hepatitis B virus: low-pH release results in a transition to a hydrophobic, potentially fusogenic conformation. *J. Virol.* **74**:5116-5122.

69. **Kann, M., A. Bischof, and W. H. Gerlich.** 1997. In vitro model for the nuclear transport of the hepadnavirus genome. *J. Virol.* **71**:1310-1316.
70. **Rabe, B., D. Glebe, and M. Kann.** 2006. Lipid-mediated introduction of hepatitis B virus capsids into nonsusceptible cells allows highly efficient replication and facilitates the study of early infection events. *J. Virol.* **80**:5465-5473.
71. **Bock, C. T., S. Schwinn, C. H. Schroder, I. Velhagen, and H. Zentgraf.** 1996. Localization of hepatitis B virus core protein and viral DNA at the nuclear membrane. *Virus Genes* **12**:53-63.
72. **Kann, M., B. Sodeik, A. Vlachou, W. H. Gerlich, and A. Helenius.** 1999. Phosphorylation-dependent binding of hepatitis B virus core particles to the nuclear pore complex. *J. Cell Biol.* **145**:45-55.
73. **Chatterji, U., M. D. Bobardt, P. Gaskill, D. Sheeter, H. Fox, and P. A. Gallay.** 2006. Trim5alpha accelerates degradation of cytosolic capsid associated with productive HIV-1 entry. *J. Biol. Chem.* **281**:37025-37033.
74. **Sinzger, C.** 2008. Entry route of HCMV into endothelial cells. *J. Clin. Virol.* **41**:174-179.
75. **Qiao, M., C. A. Scougall, A. Duszynski, and C. J. Burrell.** 1999. Kinetics of early molecular events in duck hepatitis B virus replication in primary duck hepatocytes. *J. Gen. Virol.* **80** (Pt 8):2127-2135.
76. **Kock, J. and H. J. Schlicht.** 1993. Analysis of the earliest steps of hepadnavirus replication: genome repair after infectious entry into hepatocytes does not depend on viral polymerase activity. *J. Virol.* **67**:4867-4874.
77. **Cattaneo, R., H. Will, and H. Schaller.** 1984. Hepatitis B virus transcription in the infected liver. *EMBO J.* **3**:2191-2196.
78. **Treinin, M. and O. Laub.** 1987. Identification of a promoter element located upstream from the hepatitis B virus X gene. *Mol. Cell Biol.* **7**:545-548.
79. **Gough, N. M.** 1983. Core and E antigen synthesis in rodent cells transformed with hepatitis B virus DNA is associated with greater than genome length viral messenger RNAs. *J. Mol. Biol.* **165**:683-699.
80. **Saito, I., Y. Oya, K. Yamamoto, T. Yuasa, and H. Shimojo.** 1985. Construction of nondefective adenovirus type 5 bearing a 2.8-kilobase hepatitis B virus DNA near the right end of its genome. *J. Virol.* **54**:711-719.
81. **David M.Knipe and Peter M.Howley.** 2007. *Fields Virology*, 5th Edition. Lippincott Williams & Wilkins.
82. **Yaginuma, K., I. Nakamura, S. Takada, and K. Koike.** 1993. A transcription initiation site for the hepatitis B virus X gene is directed by the promoter-binding protein. *J. Virol.* **67**:2559-2565.

83. **Will, H., W. Reiser, T. Weimer, E. Pfaff, M. Buscher, R. Sprengel, R. Cattaneo, and H. Schaller.** 1987. Replication strategy of human hepatitis B virus. *J. Virol.* **61**:904-911.
84. **Sen, N., F. Cao, and J. E. Tavis.** 2004. Translation of duck hepatitis B virus reverse transcriptase by ribosomal shunting. *J. Virol.* **78**:11751-11757.
85. **Ou, J. H., O. Laub, and W. J. Rutter.** 1986. Hepatitis B virus gene function: the precore region targets the core antigen to cellular membranes and causes the secretion of the e antigen. *Proc. Natl. Acad. Sci. U. S. A* **83**:1578-1582.
86. **Garcia, P. D., J. H. Ou, W. J. Rutter, and P. Walter.** 1988. Targeting of the hepatitis B virus precore protein to the endoplasmic reticulum membrane: after signal peptide cleavage translocation can be aborted and the product released into the cytoplasm. *J. Cell Biol.* **106**:1093-1104.
87. **Standring, D. N., J. H. Ou, F. R. Masiarz, and W. J. Rutter.** 1988. A signal peptide encoded within the precore region of hepatitis B virus directs the secretion of a heterogeneous population of e antigens in *Xenopus* oocytes. *Proc. Natl. Acad. Sci. U. S. A* **85**:8405-8409.
88. **Bruss, V. and W. H. Gerlich.** 1988. Formation of transmembraneous hepatitis B e-antigen by cotranslational in vitro processing of the viral precore protein. *Virology* **163**:268-275.
89. **Ou, J. H., C. T. Yeh, and T. S. Yen.** 1989. Transport of hepatitis B virus precore protein into the nucleus after cleavage of its signal peptide. *J. Virol.* **63**:5238-5243.
90. **Macrae, D. R., V. Bruss, and D. Ganem.** 1991. Myristylation of a duck hepatitis B virus envelope protein is essential for infectivity but not for virus assembly. *Virology* **181**:359-363.
91. **Loffler-Mary, H., M. Werr, and R. Prange.** 1997. Sequence-specific repression of cotranslational translocation of the hepatitis B virus envelope proteins coincides with binding of heat shock protein Hsc70. *Virology* **235**:144-152.
92. **Pollack, J. R. and D. Ganem.** 1993. An RNA stem-loop structure directs hepatitis B virus genomic RNA encapsidation. *J. Virol.* **67**:3254-3263.
93. **Wang, G. H., F. Zoulim, E. H. Leber, J. Kitson, and C. Seeger.** 1994. Role of RNA in enzymatic activity of the reverse transcriptase of hepatitis B viruses. *J. Virol.* **68**:8437-8442.
94. **Bruss, V.** 1997. A short linear sequence in the pre-S domain of the large hepatitis B virus envelope protein required for virion formation. *J. Virol.* **71**:9350-9357.
95. **Loffler-Mary, H., J. Dumortier, C. Klentsch-Zimmer, and R. Prange.** 2000. Hepatitis B virus assembly is sensitive to changes in the cytosolic S loop of the envelope proteins. *Virology* **270**:358-367.

96. **Poisson, F., A. Severac, C. Hourieux, A. Goudeau, and P. Roingeard.** 1997. Both pre-S1 and S domains of hepatitis B virus envelope proteins interact with the core particle. *Virology* **228**:115-120.
97. **Bruss, V.** 2007. Hepatitis B virus morphogenesis. *World J. Gastroenterol.* **13**:65-73.
98. **Patient, R., C. Hourieux, P. Y. Sizaret, S. Trassard, C. Sureau, and P. Roingeard.** 2007. Hepatitis B virus subviral envelope particle morphogenesis and intracellular trafficking. *J. Virol.* **81**:3842-3851.
99. **Watanabe, T., E. M. Sorensen, A. Naito, M. Schott, S. Kim, and P. Ahlquist.** 2007. Involvement of host cellular multivesicular body functions in hepatitis B virus budding. *Proc. Natl. Acad. Sci. U. S. A* **104**:10205-10210.
100. **Mhamdi, M., A. Funk, H. Hohenberg, H. Will, and H. Sirma.** 2007. Assembly and budding of a hepatitis B virus is mediated by a novel type of intracellular vesicles. *Hepatology* **46**:95-106.
101. **Lambert, C., T. Doring, and R. Prange.** 2007. Hepatitis B virus maturation is sensitive to functional inhibition of ESCRT-III, Vps4, and gamma 2-adaptin. *J. Virol.* **81**:9050-9060.
102. **Urban, S., A. Schulze, M. Dandri, and J. Petersen.** 2009. The replication cycle of hepatitis B virus. *J. Hepatol.*
103. HBF Drug Watch. Hepatitis B foundation . 2009.
Ref Type: Electronic Citation
104. **Schulze, A., A. Schieck, Y. Ni, W. Mier, and S. Urban.** 2010. Fine mapping of pre-S sequence requirements for hepatitis B virus large envelope protein-mediated receptor interaction. *J. Virol.* **84**:1989-2000.
105. **Chouteau, P., S. J. Le, I. Cannie, M. Nassal, C. Guguen-Guillouzo, and P. Gripon.** 2001. A short N-proximal region in the large envelope protein harbors a determinant that contributes to the species specificity of human hepatitis B virus. *J. Virol.* **75**:11565-11572.
106. **Nicoll, A. J., P. W. Angus, S. T. Chou, C. A. Luscombe, R. A. Smallwood, and S. A. Locarnini.** 1997. Demonstration of duck hepatitis B virus in bile duct epithelial cells: implications for pathogenesis and persistent infection. *Hepatology* **25**:463-469.
107. **Lee, J. Y., J. G. Culvenor, P. Angus, R. Smallwood, A. Nicoll, and S. Locarnini.** 2001. Duck hepatitis B virus replication in primary bile duct epithelial cells. *J. Virol.* **75**:7651-7661.
108. **Halpern, M. S., J. M. England, D. T. Deery, D. J. Petcu, W. S. Mason, and K. L. Molnar-Kimber.** 1983. Viral nucleic acid synthesis and antigen accumulation in pancreas and kidney of Pekin ducks infected with duck hepatitis B virus. *Proc. Natl. Acad. Sci. U. S. A* **80**:4865-4869.

109. **Korba, B. E., P. J. Cote, and J. L. Gerin.** 1988. Mitogen-induced replication of woodchuck hepatitis virus in cultured peripheral blood lymphocytes. *Science* **241**:1213-1216.
110. **Korba, B. E., P. J. Cote, M. Shapiro, R. H. Purcell, and J. L. Gerin.** 1989. In vitro production of infectious woodchuck hepatitis virus by lipopolysaccharide-stimulated peripheral blood lymphocytes. *J. Infect. Dis.* **160**:572-576.
111. **Glebe, D.** 2006. Attachment sites and neutralising epitopes of hepatitis B virus. *Minerva Gastroenterol. Dietol.* **52**:3-21.
112. **Glebe, D., S. Urban, E. V. Knoop, N. Cag, P. Krass, S. Grun, A. Bulavaite, K. Sasnauskas, and W. H. Gerlich.** 2005. Mapping of the hepatitis B virus attachment site by use of infection-inhibiting preS1 lipopeptides and tupaia hepatocytes. *Gastroenterology* **129**:234-245.
113. **Ying, C., J. F. Van Pelt, L. A. Van, R. M. Van, P. Leyssen, C. E. De, and J. Neyts.** 2002. Sulphated and sulphonated polymers inhibit the initial interaction of hepatitis B virus with hepatocytes. *Antivir. Chem. Chemother.* **13**:157-164.
114. **Zahn, A. and J. P. Allain.** 2005. Hepatitis C virus and hepatitis B virus bind to heparin: purification of largely IgG-free virions from infected plasma by heparin chromatography. *J. Gen. Virol.* **86**:677-685.
115. **Leistner, C. M., S. Gruen-Bernhard, and D. Glebe.** 2008. Role of glycosaminoglycans for binding and infection of hepatitis B virus. *Cell Microbiol.* **10**:122-133.
116. **Futamura, M., P. Dhanasekaran, T. Handa, M. C. Phillips, S. Lund-Katz, and H. Saito.** 2005. Two-step mechanism of binding of apolipoprotein E to heparin: implications for the kinetics of apolipoprotein E-heparan sulfate proteoglycan complex formation on cell surfaces. *J. Biol. Chem.* **280**:5414-5422.
117. **Gripon, P., I. Cannie, and S. Urban.** 2005. Efficient inhibition of hepatitis B virus infection by acylated peptides derived from the large viral surface protein. *J. Virol.* **79**:1613-1622.
118. **Sominskaya, I., P. Pushko, D. Dreilina, T. Kozlovskaya, and P. Pumpen.** 1992. Determination of the minimal length of preS1 epitope recognized by a monoclonal antibody which inhibits attachment of hepatitis B virus to hepatocytes. *Med. Microbiol. Immunol.* **181**:215-226.
119. **Maeng, C. Y., C. J. Ryu, P. Gripon, C. Guguen-Guillouzo, and H. J. Hong.** 2000. Fine mapping of virus-neutralizing epitopes on hepatitis B virus PreS1. *Virology* **270**:9-16.
120. **Hong, H. J., C. J. Ryu, H. Hur, S. Kim, H. K. Oh, M. S. Oh, and S. Y. Park.** 2004. In vivo neutralization of hepatitis B virus infection by an anti-preS1 humanized antibody in chimpanzees. *Virology* **318**:134-141.

121. **Le, S. J., P. Chouteau, I. Cannie, C. Guguen-Guillouzo, and P. Gripon.** 1999. Infection process of the hepatitis B virus depends on the presence of a defined sequence in the pre-S1 domain. *J. Virol.* **73**:2052-2057.
122. **Blanchet, M. and C. Sureau.** 2007. Infectivity determinants of the hepatitis B virus pre-S domain are confined to the N-terminal 75 amino acid residues. *J. Virol.* **81**:5841-5849.
123. **Le, S. J., P. Chouteau, I. Cannie, C. Guguen-Guillouzo, and P. Gripon.** 1998. Role of the pre-S2 domain of the large envelope protein in hepatitis B virus assembly and infectivity. *J. Virol.* **72**:5573-5578.
124. **Gudima, S., A. Meier, R. Dunbrack, J. Taylor, and V. Bruss.** 2007. Two potentially important elements of the hepatitis B virus large envelope protein are dispensable for the infectivity of hepatitis delta virus. *J. Virol.* **81**:4343-4347.
125. **Fernholz, D., P. R. Galle, M. Stemler, M. Brunetto, F. Bonino, and H. Will.** 1993. Infectious hepatitis B virus variant defective in pre-S2 protein expression in a chronic carrier. *Virology* **194**:137-148.
126. **Blanchet, M. and C. Sureau.** 2006. Analysis of the cytosolic domains of the hepatitis B virus envelope proteins for their function in viral particle assembly and infectivity. *J. Virol.* **80**:11935-11945.
127. **Iwarson, S., E. Tabor, H. C. Thomas, A. Goodall, J. Waters, P. Snoy, J. W. Shih, and R. J. Gerety.** 1985. Neutralization of hepatitis B virus infectivity by a murine monoclonal antibody: an experimental study in the chimpanzee. *J. Med. Virol.* **16**:89-96.
128. **Ogata, N., P. J. Cote, A. R. Zanetti, R. H. Miller, M. Shapiro, J. Gerin, and R. H. Purcell.** 1999. Licensed recombinant hepatitis B vaccines protect chimpanzees against infection with the prototype surface gene mutant of hepatitis B virus. *Hepatology* **30**:779-786.
129. **Shearer, M. H., C. Sureau, B. Dunbar, and R. C. Kennedy.** 1998. Structural characterization of viral neutralizing monoclonal antibodies to hepatitis B surface antigen. *Mol. Immunol.* **35**:1149-1160.
130. **Carman, W. F., A. R. Zanetti, P. Karayiannis, J. Waters, G. Manzillo, E. Tanzi, A. J. Zuckerman, and H. C. Thomas.** 1990. Vaccine-induced escape mutant of hepatitis B virus. *Lancet* **336**:325-329.
131. **Waters, J. A., M. Kennedy, P. Voet, P. Hauser, J. Petre, W. Carman, and H. C. Thomas.** 1992. Loss of the common "A" determinant of hepatitis B surface antigen by a vaccine-induced escape mutant. *J. Clin. Invest* **90**:2543-2547.
132. **Yamamoto, K., M. Horikita, F. Tsuda, K. Itoh, Y. Akahane, S. Yotsumoto, H. Okamoto, Y. Miyakawa, and M. Mayumi.** 1994. Naturally occurring escape mutants of hepatitis B virus with various mutations in the S gene in carriers seropositive for antibody to hepatitis B surface antigen. *J. Virol.* **68**:2671-2676.

133. **Cooreman, M. P., G. Leroux-Roels, and W. P. Paulij.** 2001. Vaccine- and hepatitis B immune globulin-induced escape mutations of hepatitis B virus surface antigen. *J. Biomed. Sci.* **8**:237-247.
134. **Nainan, O. V., M. L. Khristova, K. Byun, G. Xia, P. E. Taylor, C. E. Stevens, and H. S. Margolis.** 2002. Genetic variation of hepatitis B surface antigen coding region among infants with chronic hepatitis B virus infection. *J. Med. Virol.* **68**:319-327.
135. **Ni, F., D. Fang, R. Gan, Z. Li, S. Duan, and Z. Xu.** 1995. A new immune escape mutant of hepatitis B virus with an Asp to Ala substitution in aa144 of the envelope major protein. *Res. Virol.* **146**:397-407.
136. **Jaoude, G. A. and C. Sureau.** 2005. Role of the antigenic loop of the hepatitis B virus envelope proteins in infectivity of hepatitis delta virus. *J. Virol.* **79**:10460-10466.
137. **Schelhaas, M., J. Malmstrom, L. Pelkmans, J. Haugstetter, L. Ellgaard, K. Grunewald, and A. Helenius.** 2007. Simian Virus 40 depends on ER protein folding and quality control factors for entry into host cells. *Cell* **131**:516-529.
138. **Wallin, M., M. Ekstrom, and H. Garoff.** 2004. Isomerization of the intersubunit disulphide-bond in Env controls retrovirus fusion. *EMBO J.* **23**:54-65.
139. **Wallin, M., M. Ekstrom, and H. Garoff.** 2005. The fusion-controlling disulfide bond isomerase in retrovirus Env is triggered by protein destabilization. *J. Virol.* **79**:1678-1685.
140. **Berting, A., C. Fischer, S. Schaefer, W. Garten, H. D. Klenk, and W. H. Gerlich.** 2000. Hemifusion activity of a chimeric influenza virus hemagglutinin with a putative fusion peptide from hepatitis B virus. *Virus Res.* **68**:35-49.
141. **Chojnacki, J., D. A. Anderson, and E. V. Grgacic.** 2005. A hydrophobic domain in the large envelope protein is essential for fusion of duck hepatitis B virus at the late endosome. *J. Virol.* **79**:14945-14955.
142. **Oess, S. and E. Hildt.** 2000. Novel cell permeable motif derived from the PreS2-domain of hepatitis-B virus surface antigens. *Gene Ther.* **7**:750-758.
143. **Stoeckl, L., A. Funk, A. Kopitzki, B. Brandenburg, S. Oess, H. Will, H. Sirma, and E. Hildt.** 2006. Identification of a structural motif crucial for infectivity of hepatitis B viruses. *Proc. Natl. Acad. Sci. U. S. A* **103**:6730-6734.
144. **Shouval, D., P. R. Chakraborty, N. Ruiz-Opazo, S. Baum, I. Spigland, E. Muchmore, M. A. Gerber, S. N. Thung, H. Popper, and D. A. Shafritz.** 1980. Chronic hepatitis in chimpanzee carriers of hepatitis B virus: morphologic, immunologic, and viral DNA studies. *Proc. Natl. Acad. Sci. U. S. A* **77**:6147-6151.
145. **Eichberg, J. W., L. B. Seeff, D. L. Lawlor, Z. Buskell-Bales, K. Ishak, J. H. Hoofnagle, A. L. Goldstein, and J. M. Langloss.** 1987. Effect of thymosin immunostimulation with and without corticosteroid immunosuppression on chimpanzee hepatitis B carriers. *J. Med. Virol.* **21**:25-37.

146. **Thimme, R., S. Wieland, C. Steiger, J. Ghrayeb, K. A. Reimann, R. H. Purcell, and F. V. Chisari.** 2003. CD8(+) T cells mediate viral clearance and disease pathogenesis during acute hepatitis B virus infection. *J. Virol.* **77**:68-76.
147. **Wieland, S., R. Thimme, R. H. Purcell, and F. V. Chisari.** 2004. Genomic analysis of the host response to hepatitis B virus infection. *Proc. Natl. Acad. Sci. U. S. A* **101**:6669-6674.
148. **Wieland, S. F., H. C. Spangenberg, R. Thimme, R. H. Purcell, and F. V. Chisari.** 2004. Expansion and contraction of the hepatitis B virus transcriptional template in infected chimpanzees. *Proc. Natl. Acad. Sci. U. S. A* **101**:2129-2134.
149. **Chisari, F. V.** 1996. Hepatitis B virus transgenic mice: models of viral immunobiology and pathogenesis. *Curr. Top. Microbiol. Immunol.* **206**:149-173.
150. **Ladner, S. K., M. J. Otto, C. S. Barker, K. Zaifert, G. H. Wang, J. T. Guo, C. Seeger, and R. W. King.** 1997. Inducible expression of human hepatitis B virus (HBV) in stably transfected hepatoblastoma cells: a novel system for screening potential inhibitors of HBV replication. *Antimicrob. Agents Chemother.* **41**:1715-1720.
151. **Zhou, T., H. Guo, J. T. Guo, A. Cuconati, A. Mehta, and T. M. Block.** 2006. Hepatitis B virus e antigen production is dependent upon covalently closed circular (ccc) DNA in HepAD38 cell cultures and may serve as a cccDNA surrogate in antiviral screening assays. *Antiviral Res.* **72**:116-124.
152. **Guidotti, L. G., B. Matzke, H. Schaller, and F. V. Chisari.** 1995. High-level hepatitis B virus replication in transgenic mice. *J. Virol.* **69**:6158-6169.
153. **Isogawa, M., M. D. Robek, Y. Furuichi, and F. V. Chisari.** 2005. Toll-like receptor signaling inhibits hepatitis B virus replication in vivo. *J. Virol.* **79**:7269-7272.
154. **Kakimi, K., L. G. Guidotti, Y. Koezuka, and F. V. Chisari.** 2000. Natural killer T cell activation inhibits hepatitis B virus replication in vivo. *J. Exp. Med.* **192**:921-930.
155. **Kimura, K., K. Kakimi, S. Wieland, L. G. Guidotti, and F. V. Chisari.** 2002. Activated intrahepatic antigen-presenting cells inhibit hepatitis B virus replication in the liver of transgenic mice. *J. Immunol.* **169**:5188-5195.
156. **Reifenberg, K., J. Lohler, H. P. Pudollek, E. Schmitteckert, G. Spindler, J. Kock, and H. J. Schlicht.** 1997. Long-term expression of the hepatitis B virus core-e- and X-proteins does not cause pathologic changes in transgenic mice. *J. Hepatol.* **26**:119-130.
157. **Kim, C. M., K. Koike, I. Saito, T. Miyamura, and G. Jay.** 1991. HBx gene of hepatitis B virus induces liver cancer in transgenic mice. *Nature* **351**:317-320.
158. **Dandri, M., M. R. Burda, E. Torok, J. M. Pollok, A. Iwanska, G. Sommer, X. Rogiers, C. E. Rogler, S. Gupta, H. Will, H. Greten, and J. Petersen.** 2001. Repopulation of mouse liver with human hepatocytes and in vivo infection with hepatitis B virus. *Hepatology* **33**:981-988.

159. **Petersen, J., M. Dandri, S. Gupta, and C. E. Rogler.** 1998. Liver repopulation with xenogenic hepatocytes in B and T cell-deficient mice leads to chronic hepadnavirus infection and clonal growth of hepatocellular carcinoma. *Proc. Natl. Acad. Sci. U. S. A* **95**:310-315.
160. **Dandri, M., M. R. Burda, D. M. Zuckerman, K. Wurstthorn, U. Matschl, J. M. Pollok, X. Rogiers, A. Gocht, J. Kock, H. E. Blum, W. F. von, and J. Petersen.** 2005. Chronic infection with hepatitis B viruses and antiviral drug evaluation in uPA mice after liver repopulation with tupaia hepatocytes. *J. Hepatol.* **42**:54-60.
161. **Dandri, M., M. R. Burda, A. Gocht, E. Torok, J. M. Pollok, C. E. Rogler, H. Will, and J. Petersen.** 2001. Woodchuck hepatocytes remain permissive for hepadnavirus infection and mouse liver repopulation after cryopreservation. *Hepatology* **34**:824-833.
162. **Petersen, J., M. Dandri, W. Mier, M. Lutgehetmann, T. Volz, W. F. von, U. Haberkorn, L. Fischer, J. M. Pollok, B. Erbes, S. Seitz, and S. Urban.** 2008. Prevention of hepatitis B virus infection in vivo by entry inhibitors derived from the large envelope protein. *Nat. Biotechnol.* **26**:335-341.
163. **Sells, M. A., M. L. Chen, and G. Acs.** 1987. Production of hepatitis B virus particles in Hep G2 cells transfected with cloned hepatitis B virus DNA. *Proc. Natl. Acad. Sci. U. S. A* **84**:1005-1009.
164. **Glebe, D., M. Aliakbari, P. Krass, E. V. Knoop, K. P. Valerius, and W. H. Gerlich.** 2003. Pre-s1 antigen-dependent infection of Tupaia hepatocyte cultures with human hepatitis B virus. *J. Virol.* **77**:9511-9521.
165. **Shimizu, Y., S. Nambu, T. Kojima, and H. Sasaki.** 1986. Replication of hepatitis B virus in culture systems with adult human hepatocytes. *J. Med. Virol.* **20**:313-327.
166. **Ochiya, T., T. Tsurimoto, K. Ueda, K. Okubo, M. Shiozawa, and K. Matsubara.** 1989. An in vitro system for infection with hepatitis B virus that uses primary human fetal hepatocytes. *Proc. Natl. Acad. Sci. U. S. A* **86**:1875-1879.
167. **Rijntjes, P. J., H. J. Moshage, and S. H. Yap.** 1988. In vitro infection of primary cultures of cryopreserved adult human hepatocytes with hepatitis B virus. *Virus Res.* **10**:95-109.
168. **Gripon, P., C. Diot, N. Theze, I. Fourel, O. Loreal, C. Brechot, and C. Guguen-Guillouzo.** 1988. Hepatitis B virus infection of adult human hepatocytes cultured in the presence of dimethyl sulfoxide. *J. Virol.* **62**:4136-4143.
169. **Galle, P. R., H. J. Schlicht, C. Kuhn, and H. Schaller.** 1989. Replication of duck hepatitis B virus in primary duck hepatocytes and its dependence on the state of differentiation of the host cell. *Hepatology* **10**:459-465.
170. **Gripon, P., C. Diot, and C. Guguen-Guillouzo.** 1993. Reproducible high level infection of cultured adult human hepatocytes by hepatitis B virus: effect of polyethylene glycol on adsorption and penetration. *Virology* **192**:534-540.

171. **Gripon, P., S. Rumin, S. Urban, S. J. Le, D. Glaise, I. Cannie, C. Guyomard, J. Lucas, C. Trepo, and C. Guguen-Guillouzo.** 2002. Infection of a human hepatoma cell line by hepatitis B virus. *Proc. Natl. Acad. Sci. U. S. A* **99**:15655-15660.
172. **Cerec, V., D. Glaise, D. Garnier, S. Morosan, B. Turlin, B. Drenou, P. Gripon, D. Kremsdorf, C. Guguen-Guillouzo, and A. Corlu.** 2007. Transdifferentiation of hepatocyte-like cells from the human hepatoma HepaRG cell line through bipotent progenitor. *Hepatology* **45**:957-967.
173. **Guillouzo, A., A. Corlu, C. Aninat, D. Glaise, F. Morel, and C. Guguen-Guillouzo.** 2007. The human hepatoma HepaRG cells: a highly differentiated model for studies of liver metabolism and toxicity of xenobiotics. *Chem. Biol. Interact.* **168**:66-73.
174. **Quasdorff, M., M. Hosel, M. Odenthal, U. Zedler, F. Bohne, P. Gripon, H. P. Dienes, U. Drebber, D. Stippel, T. Goeser, and U. Protzer.** 2008. A concerted action of HNF4alpha and HNF1alpha links hepatitis B virus replication to hepatocyte differentiation. *Cell Microbiol.* **10**:1478-1490.
175. **Kock, J., M. Nassal, S. MacNelly, T. F. Baumert, H. E. Blum, and W. F. von.** 2001. Efficient infection of primary tupaia hepatocytes with purified human and woolly monkey hepatitis B virus. *J. Virol.* **75**:5084-5089.
176. **Baumert, T. F., C. Yang, P. Schurmann, J. Kock, C. Ziegler, C. Grulich, M. Nassal, T. J. Liang, H. E. Blum, and W. F. von.** 2005. Hepatitis B virus mutations associated with fulminant hepatitis induce apoptosis in primary Tupaia hepatocytes. *Hepatology* **41**:247-256.
177. **Nassal, M.** 1992. The arginine-rich domain of the hepatitis B virus core protein is required for pregenome encapsidation and productive viral positive-strand DNA synthesis but not for virus assembly. *J. Virol.* **66**:4107-4116.
178. **Nemeckova, S., D. Kunke, M. Press, V. Nemecek, and L. Kutinova.** 1994. A carboxy-terminal portion of the preS1 domain of hepatitis B virus (HBV) occasioned retention in endoplasmic reticulum of HBV envelope proteins expressed by recombinant vaccinia viruses. *Virology* **202**:1024-1027.
179. **Bahnson, A. B., J. T. Dunigan, B. E. Baysal, T. Mohny, R. W. Atchison, M. T. Nimgaonkar, E. D. Ball, and J. A. Barranger.** 1995. Centrifugal enhancement of retroviral mediated gene transfer. *J. Virol. Methods* **54**:131-143.
180. **Josse, R., C. Aninat, D. Glaise, J. Dumont, V. Fessard, F. Morel, J. M. Poul, C. Guguen-Guillouzo, and A. Guillouzo.** 2008. Long-term functional stability of human HepaRG hepatocytes and use for chronic toxicity and genotoxicity studies. *Drug Metab Dispos.* **36**:1111-1118.
181. **Gerk, P. M. and M. Vore.** 2002. Regulation of expression of the multidrug resistance-associated protein 2 (MRP2) and its role in drug disposition. *J. Pharmacol. Exp. Ther.* **302**:407-415.

182. **Johnson, D. R., R. S. Bhatnagar, L. J. Knoll, and J. I. Gordon.** 1994. Genetic and biochemical studies of protein N-myristoylation. *Annu. Rev. Biochem.* **63**:869-914.
183. **Martin-Belmonte, F., J. A. Lopez-Guerrero, L. Carrasco, and M. A. Alonso.** 2000. The amino-terminal nine amino acid sequence of poliovirus capsid VP4 protein is sufficient to confer N-myristoylation and targeting to detergent-insoluble membranes. *Biochemistry* **39**:1083-1090.
184. **Bijlmakers, M. J. and M. Marsh.** 2003. The on-off story of protein palmitoylation. *Trends Cell Biol.* **13**:32-42.
185. **Schrempf, S., M. Froeschke, T. Giroglou, L. D. von, and B. Dobberstein.** 2007. Signal peptide requirements for lymphocytic choriomeningitis virus glycoprotein C maturation and virus infectivity. *J. Virol.* **81**:12515-12524.
186. **Sugauchi, F., M. Mizokami, E. Orito, T. Ohno, H. Kato, S. Suzuki, Y. Kimura, R. Ueda, L. A. Butterworth, and W. G. Cooksley.** 2001. A novel variant genotype C of hepatitis B virus identified in isolates from Australian Aborigines: complete genome sequence and phylogenetic relatedness. *J. Gen. Virol.* **82**:883-892.
187. **Chi, S. W., D. H. Kim, S. H. Lee, I. Chang, and K. H. Han.** 2007. Pre-structured motifs in the natively unstructured preS1 surface antigen of hepatitis B virus. *Protein Sci.* **16**:2108-2117.
188. **Engelke, M., K. Mills, S. Seitz, P. Simon, P. Gripon, M. Schnolzer, and S. Urban.** 2006. Characterization of a hepatitis B and hepatitis delta virus receptor binding site. *Hepatology* **43**:750-760.
189. **Maurer-Stroh, S. and F. Eisenhaber.** 2004. Myristoylation of viral and bacterial proteins. *Trends Microbiol.* **12**:178-185.
190. **Brideau, A. D., B. W. Banfield, and L. W. Enquist.** 1998. The Us9 gene product of pseudorabies virus, an alphaherpesvirus, is a phosphorylated, tail-anchored type II membrane protein. *J. Virol.* **72**:4560-4570.
191. **Lyman, M. G., D. Curanovic, A. D. Brideau, and L. W. Enquist.** 2008. Fusion of enhanced green fluorescent protein to the pseudorabies virus axonal sorting protein Us9 blocks anterograde spread of infection in mammalian neurons. *J. Virol.* **82**:10308-10311.
192. **Brideau, A. D., J. P. Card, and L. W. Enquist.** 2000. Role of pseudorabies virus Us9, a type II membrane protein, in infection of tissue culture cells and the rat nervous system. *J. Virol.* **74**:834-845.
193. **Santantonio, T., M. C. Jung, R. Schneider, D. Fernholz, M. Milella, L. Monno, G. Pastore, G. R. Pape, and H. Will.** 1992. Hepatitis B virus genomes that cannot synthesize pre-S2 proteins occur frequently and as dominant virus populations in chronic carriers in Italy. *Virology* **188**:948-952.
194. **Lepere, C., M. Regeard, S. J. Le, and P. Gripon.** 2007. The translocation motif of hepatitis B virus envelope proteins is dispensable for infectivity. *J. Virol.* **81**:7816-7818.

195. **Mangold, C. M., F. Unckell, M. Werr, and R. E. Streeck.** 1995. Secretion and antigenicity of hepatitis B virus small envelope proteins lacking cysteines in the major antigenic region. *Virology* **211**:535-543.
196. **Mangold, C. M. and R. E. Streeck.** 1993. Mutational analysis of the cysteine residues in the hepatitis B virus small envelope protein. *J. Virol.* **67**:4588-4597.
197. **Wounderlich, G. and V. Bruss.** 1996. Characterization of early hepatitis B virus surface protein oligomers. *Arch. Virol.* **141**:1191-1205.
198. **Prange, R. and R. E. Streeck.** 1995. Novel transmembrane topology of the hepatitis B virus envelope proteins. *EMBO J.* **14**:247-256.
199. **Lupberger, J., A. Mund, J. Kock, and E. Hildt.** 2006. Cultivation of HepG2.2.15 on Cytodex-3: higher yield of hepatitis B virus and less subviral particles compared to conventional culture methods. *J. Hepatol.* **45**:547-552.
200. **Glebe, D., A. Berting, S. Broehl, H. Naumann, R. Schuster, N. Fiedler, T. K. Tolle, S. Nitsche, M. Seifer, W. H. Gerlich, and S. Schaefer.** 2001. Optimised conditions for the production of hepatitis B virus from cell culture. *Intervirology* **44**:370-378.
201. **Lepere-Douard, C., M. Trotard, S. J. Le, and P. Gripon.** 2009. The first transmembrane domain of the hepatitis B virus large envelope protein is crucial for infectivity. *J. Virol.* **83**:11819-11829.
202. **Gripon, P., C. Diot, A. Corlu, and C. Guguen-Guillouzo.** 1989. Regulation by dimethylsulfoxide, insulin, and corticosteroids of hepatitis B virus replication in a transfected human hepatoma cell line. *J. Med. Virol.* **28**:193-199.
203. **Heermann, K. H., U. Goldmann, W. Schwartz, T. Seyffarth, H. Baumgarten, and W. H. Gerlich.** 1984. Large surface proteins of hepatitis B virus containing the pre-S sequence. *J. Virol.* **52**:396-402.
204. **Budkowska, A., P. Bedossa, F. Groh, A. Louise, and J. Pillot.** 1995. Fibronectin of human liver sinusoids binds hepatitis B virus: identification by an anti-idiotypic antibody bearing the internal image of the pre-S2 domain. *J. Virol.* **69**:840-848.
205. **Bruss, V., J. Hagelstein, E. Gerhardt, and P. R. Galle.** 1996. Myristylation of the large surface protein is required for hepatitis B virus in vitro infectivity. *Virology* **218**:396-399.
206. **Roeth, J. F. and K. L. Collins.** 2006. Human immunodeficiency virus type 1 Nef: adapting to intracellular trafficking pathways. *Microbiol. Mol. Biol. Rev.* **70**:548-563.
207. **Hildinger, M., M. T. Dittmar, P. Schult-Dietrich, B. Fehse, B. S. Schnierle, S. Thaler, G. Stiegler, R. Welker, and L. D. von.** 2001. Membrane-anchored peptide inhibits human immunodeficiency virus entry. *J. Virol.* **75**:3038-3042.
208. **Egelhofer, M., G. Brandenburg, H. Martinius, P. Schult-Dietrich, G. Melikyan, R. Kunert, C. Baum, I. Choi, A. Alexandrov, and L. D. von.** 2004. Inhibition of

- human immunodeficiency virus type 1 entry in cells expressing gp41-derived peptides. *J. Virol.* **78**:568-575.
209. **Melikyan, G. B., M. Egelhofer, and L. D. von.** 2006. Membrane-anchored inhibitory peptides capture human immunodeficiency virus type 1 gp41 conformations that engage the target membrane prior to fusion. *J. Virol.* **80**:3249-3258.
210. **Taylor, J. A., L. Vojtech, I. Bahner, D. B. Kohn, D. V. Laer, D. W. Russell, and R. E. Richard.** 2008. Foamy virus vectors expressing anti-HIV transgenes efficiently block HIV-1 replication. *Mol. Ther.* **16**:46-51.
211. **Peitzsch, R. M. and S. McLaughlin.** 1993. Binding of acylated peptides and fatty acids to phospholipid vesicles: pertinence to myristoylated proteins. *Biochemistry* **32**:10436-10443.
212. **Valentine, K. G., M. F. Mesleh, S. J. Opella, M. Ikura, and J. B. Ames.** 2003. Structure, topology, and dynamics of myristoylated recoverin bound to phospholipid bilayers. *Biochemistry* **42**:6333-6340.
213. **Ames, J. B., R. Ishima, T. Tanaka, J. I. Gordon, L. Stryer, and M. Ikura.** 1997. Molecular mechanics of calcium-myristoyl switches. *Nature* **389**:198-202.
214. **Tanaka, T., J. B. Ames, T. S. Harvey, L. Stryer, and M. Ikura.** 1995. Sequestration of the membrane-targeting myristoyl group of recoverin in the calcium-free state. *Nature* **376**:444-447.
215. **Goldberg, J.** 1998. Structural basis for activation of ARF GTPase: mechanisms of guanine nucleotide exchange and GTP-myristoyl switching. *Cell* **95**:237-248.
216. **Nagar, B., O. Hantschel, M. A. Young, K. Scheffzek, D. Veach, W. Bornmann, B. Clarkson, G. Superti-Furga, and J. Kuriyan.** 2003. Structural basis for the autoinhibition of c-Abl tyrosine kinase. *Cell* **112**:859-871.
217. **Tang, C., E. Loeliger, P. Luncsford, I. Kinde, D. Beckett, and M. F. Summers.** 2004. Entropic switch regulates myristate exposure in the HIV-1 matrix protein. *Proc. Natl. Acad. Sci. U. S. A* **101**:517-522.
218. **Breitenlechner, C., R. A. Engh, R. Huber, V. Kinzel, D. Bossemeyer, and M. Gassel.** 2004. The typically disordered N-terminus of PKA can fold as a helix and project the myristoylation site into solution. *Biochemistry* **43**:7743-7749.
219. **Chen, B., M. Lian, S. Xu, M. Luo, and X. Zheng.** 2008. A chemical lipid modification of recombinant preS antigen to study the mechanism of HBV attachment to the host cell. *J. Biotechnol.* **137**:8-13.
220. **Rodriguez-Crespo, I., J. Gomez-Gutierrez, M. Nieto, D. L. Peterson, and F. Gavilanes.** 1994. Prediction of a putative fusion peptide in the S protein of hepatitis B virus. *J. Gen. Virol.* **75 (Pt 3)**:637-639.
221. **Rodriguez-Crespo, I., E. Nunez, J. Gomez-Gutierrez, B. Yelamos, J. P. Albar, D. L. Peterson, and F. Gavilanes.** 1995. Phospholipid interactions of the putative fusion

- peptide of hepatitis B virus surface antigen S protein. *J. Gen. Virol.* **76** (Pt 2):301-308.
222. **Nunez, E., B. Yelamos, C. Delgado, J. Gomez-Gutierrez, D. L. Peterson, and F. Gavilanes.** 2009. Interaction of preS domains of hepatitis B virus with phospholipid vesicles. *Biochim. Biophys. Acta* **1788**:417-424.
223. **Kielian, M. and F. A. Rey.** 2006. Virus membrane-fusion proteins: more than one way to make a hairpin. *Nat. Rev. Microbiol.* **4**:67-76.
224. **Lev, N. and Y. Shai.** 2007. Fatty acids can substitute the HIV fusion peptide in lipid merging and fusion: an analogy between viral and palmitoylated eukaryotic fusion proteins. *J. Mol. Biol.* **374**:220-230.
225. **Corcoran, J. A., R. Syvitski, D. Top, R. M. Epand, R. F. Epand, D. Jakeman, and R. Duncan.** 2004. Myristoylation, a protruding loop, and structural plasticity are essential features of a nonenveloped virus fusion peptide motif. *J. Biol. Chem.* **279**:51386-51394.
226. **Zahn, R.** 2003. The octapeptide repeats in mammalian prion protein constitute a pH-dependent folding and aggregation site. *J. Mol. Biol.* **334**:477-488.
227. **Kato, J., K. Hasegawa, N. Torii, K. Yamauchi, and N. Hayashi.** 1996. A molecular analysis of viral persistence in surface antigen-negative chronic hepatitis B. *Hepatology* **23**:389-395.
228. **Pollicino, T., S. Campo, and G. Raimondo.** 1995. PreS and core gene heterogeneity in hepatitis B virus (HBV) genomes isolated from patients with long-lasting HBV chronic infection. *Virology* **208**:672-677.
229. **Raimondo, G., L. Costantino, G. Caccamo, T. Pollicino, G. Squadrito, I. Cacciola, and S. Brancatelli.** 2004. Non-sequencing molecular approaches to identify preS2-defective hepatitis B virus variants proved to be associated with severe liver diseases. *J. Hepatol.* **40**:515-519.
230. **Hileman, R. E., J. R. Fromm, J. M. Weiler, and R. J. Linhardt.** 1998. Glycosaminoglycan-protein interactions: definition of consensus sites in glycosaminoglycan binding proteins. *Bioessays* **20**:156-167.
231. **Chen, Y., T. Maguire, R. E. Hileman, J. R. Fromm, J. D. Esko, R. J. Linhardt, and R. M. Marks.** 1997. Dengue virus infectivity depends on envelope protein binding to target cell heparan sulfate. *Nat. Med.* **3**:866-871.
232. **Hulst, M. M., H. G. van Gennip, and R. J. Moormann.** 2000. Passage of classical swine fever virus in cultured swine kidney cells selects virus variants that bind to heparan sulfate due to a single amino acid change in envelope protein E(rns). *J. Virol.* **74**:9553-9561.
233. **Klimstra, W. B., K. D. Ryman, and R. E. Johnston.** 1998. Adaptation of Sindbis virus to BHK cells selects for use of heparan sulfate as an attachment receptor. *J. Virol.* **72**:7357-7366.

234. **Mandl, C. W., H. Kroschewski, S. L. Allison, R. Kofler, H. Holzmann, T. Meixner, and F. X. Heinz.** 2001. Adaptation of tick-borne encephalitis virus to BHK-21 cells results in the formation of multiple heparan sulfate binding sites in the envelope protein and attenuation in vivo. *J. Virol.* **75**:5627-5637.
235. **Opie, S. R., K. H. Warrington, Jr., M. gbandje-McKenna, S. Zolotukhin, and N. Muzyczka.** 2003. Identification of amino acid residues in the capsid proteins of adeno-associated virus type 2 that contribute to heparan sulfate proteoglycan binding. *J. Virol.* **77**:6995-7006.
236. **Vives, R. R., E. Crublet, J. P. Andrieu, J. Gagnon, P. Rousselle, and H. Lortat-Jacob.** 2004. A novel strategy for defining critical amino acid residues involved in protein/glycosaminoglycan interactions. *J. Biol. Chem.* **279**:54327-54333.
237. **Crublet, E., J. P. Andrieu, R. R. Vives, and H. Lortat-Jacob.** 2008. The HIV-1 envelope glycoprotein gp120 features four heparan sulfate binding domains, including the co-receptor binding site. *J. Biol. Chem.* **283**:15193-15200.
238. **Raman, S., T. H. Hsu, S. L. Ashley, and K. R. Spindler.** 2009. Usage of integrin and heparan sulfate as receptors for mouse adenovirus type 1. *J. Virol.* **83**:2831-2838.
239. **Nakabayashi, H., K. Taketa, K. Miyano, T. Yamane, and J. Sato.** 1982. Growth of human hepatoma cells lines with differentiated functions in chemically defined medium. *Cancer Res.* **42**:3858-3863.
240. **Hanahan, D.** 1983. Studies on transformation of *Escherichia coli* with plasmids. *J. Mol. Biol.* **166**:557-580.
241. **Boussif, O., F. Lezoualc'h, M. A. Zanta, M. D. Mergny, D. Scherman, B. Demeneix, and J. P. Behr.** 1995. A versatile vector for gene and oligonucleotide transfer into cells in culture and in vivo: polyethylenimine. *Proc. Natl. Acad. Sci. U. S. A* **92**:7297-7301.
242. **Kalajzic, I., M. L. Stover, P. Liu, Z. Kalajzic, D. W. Rowe, and A. C. Lichtler.** 2001. Use of VSV-G pseudotyped retroviral vectors to target murine osteoprogenitor cells. *Virology* **284**:37-45.
243. **Dull, T., R. Zufferey, M. Kelly, R. J. Mandel, M. Nguyen, D. Trono, and L. Naldini.** 1998. A third-generation lentivirus vector with a conditional packaging system. *J. Virol.* **72**:8463-8471.
244. **Pham, H. M., E. R. Arganaraz, B. Groschel, D. Trono, and J. Lama.** 2004. Lentiviral vectors interfering with virus-induced CD4 down-modulation potently block human immunodeficiency virus type 1 replication in primary lymphocytes. *J. Virol.* **78**:13072-13081.

Abbreviations

°C	degree Celsius
µg	microgram
µl	microlitre
µM	micromolar
aa	amino acid
Ag	Antigen
Ab	Antibody
AGL	Antigenic loop
b	base
bp	base pairs
C	HBV core
cccDNA	covalently closed circular DNA
CsCl	Caesium chloride
CMV	Cytomegalovirus
CYL-I	Cytosolic loop-I
DAPI	4'6' - Diamidino-2'phenylindole-dihydrochloride
dNTP	Deoxyribonucleoside triphosphate
Delta (Δ)	Deletion
DMEM	Dulbecco's Modified Eagle Medium
DMSO	Dimethyl sulfoxide
DNA	Deoxyribonucleic acid
DR	Direct repeat
ds	double-stranded
DTT	Dithiothreitol
<i>E.coli</i>	<i>Escherichia coli</i>
EDTA	Ethylenediaminetetraacetic acid
Enh	Enhancer
ER	Endoplasmic reticulum
ERGIC	ER Golgi intermediate compartments
<i>et al.</i>	<i>et alii, at aliae, et alia</i>
FCS	Fetal calf serum
g	gram
GAG	Glycosaminoglycan
GE	Genome equivalents
h	hour
HB	Hepatitis B
HBcAg	Hepatitis B core antigen
HBeAg	Hepatitis B e antigen
HBs	Hepatitis B surface protein
HBsAg	Hepatitis B surface antigen
HBV	Hepatitis B virus

HBx	Hepatitis B virus X protein
HCC	Hepatoma cellular carcinoma
Hsc or Hsp	Heat-shock cytoplasm or protein
HCV	Hepatitis C virus
HSPG	Heparan sulfate proteoglycans
IF	Immunofluorescence
Kb	kilo base pairs
kD	kilo dalton
L-protein	HBV large surface protein
M-protein	HBV middle surface protein
Mab	Monoclonal antibody
MCS	Multiple cloning site
MEIA	microparticle enzyme immunoassays
mg	milligram
min	minute
ml	millilitre
mM	millimolar
mRNA	messenger RNA
Myr	myristoyl
N-	amino-
nm	nanometer
NP-40	Nonidet-40
nt	nucleotide
OD	Optical density
ORF	Open reading frame
P	HBV polymerase
PAGE	Polyacrylamide gel electrophoresis
PBS	Phosphate buffered saline
PCR	Polymerase chain reaction
PDI	Protein disulfide isomerase
PEG	Polyethylene glycol
PEI	Polyethylenimine
PFA	Paraformaldehyde
pgRNA	pregenomic RNA
pH	<i>pondus hydrogenii</i>
PHH	Primary human hepatocytes
p.i.	post-infection
p.t.	post-transfection
PTH	Primary <i>tupaia</i> hepatocytes
rcDNA	relaxed circular DNA
RNA	Ribonucleic acid
RNase	Ribonuclease

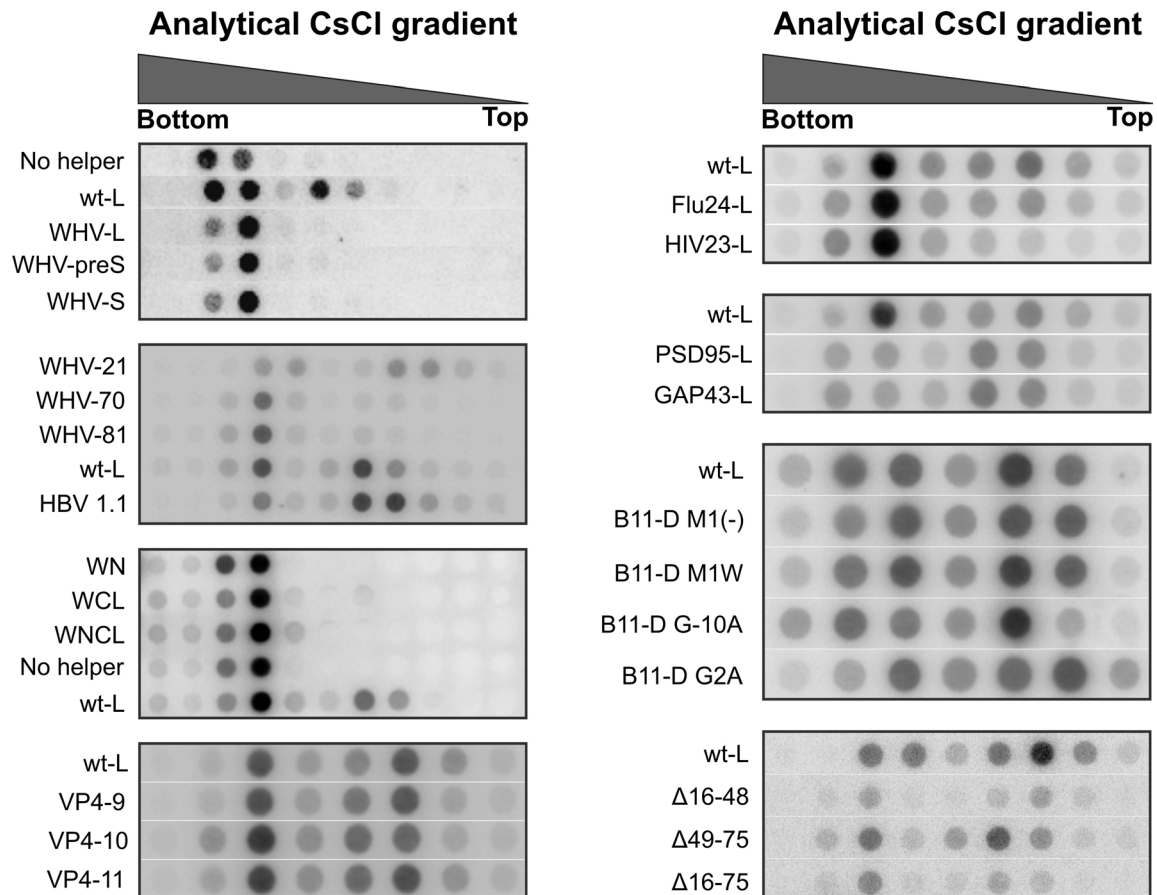
rpm	revolution per minute
RT	Room temperature or Real-time
S-protein	HBV small surface protein
S/N	Signal-to-noise-ratio
S/Co	Signal-to-control-ratio
ss	single-stranded
sec	seconds
SDS	Sodium dodecyl sulfate
SSC	Standard saline citrate
SVPs	Subviral particles
TBS	Tris buffered saline
TEMED	N,N,N',N',-tetramethylethylenediamine
temp	temperature
TM	Transmembrane
TP	Terminal protein
Tris	Tris(hydroxymethyl)-aminomethane
U	Unit
V	Volt

Supplemental

L proteins	21 aa	preS1 107 aa	preS2 55 aa	S 226 aa	Assembly	Infectivity
wt-L					+++	+
WHV-L					-	N.D.
WHV-preS					-	N.D.
WHV-S					-	N.D.
WHV-21					++	-
WHV-70					-	N.D.
WHV-81					-	N.D.
WN					-	N.D.
WCL					-	N.D.
WNCL					-	N.D.
Δ114-123					++++	+
Δ114-173					-	N.D.
Δ114-183					-	N.D.
Δ114-193					-	N.D.
Δ114-203					-	N.D.
Δ114-213					-	N.D.
Δ114-223					-	N.D.
Δ114-233					-	N.D.
Δ114-243					-	N.D.
Δ114-253					-	N.D.
LG11/12MN		MN			+++	-
LG11/12RE		RE			+++	-
Δ16-48					+	-
Δ49-75					++	-
Δ16-75					+	-
Δ11-15					+++	-
Δ41-45					+++	-
Δ71-75					+++	-
G2A/L11R		A R			+++	-
G2A/L11R/ΔTM1		A R			+++	-
Flu24-L					++	-
HIV23-L					+/-	N.D.
psd95-L					+++	-
Gap43-L					+++	-
VP4-9					+++	-
VP4-10					+++	-
VP4-11					+++	-
B11-D M1W		W			+++	-
B11-D M1(-)					+++	-
B11-D G-10A		A			+++	-
B11-D G2A		A			+++	-

FIG. S1. Schematic illustration of other mutant L proteins

The listed mutant L proteins were characterized with respect to virus assembly and infectivity, but not described in the main text of the present PhD thesis. The L proteins from genotype D are shown in black bar, while those from woodchuck hepatitis virus (WHV) are shown in green bar. Note that the fusion peptide from Influenza virus was fused to the N-terminus of L protein (Flu24-L), as well as the fusion peptide of HIV (HIV23-L), palmitoylation motif of psd95 (psd95-L) and Gap43 (Gap43-L). The assembly and infectivity of virus with these L proteins are summarized at the right.

**FIG. S2. Assembly competence of a part of mutant L-proteins listed in FIG. S1**

HBV-DNA specific Dot-blot of fractions of an analytical CsCl density gradient was obtained from supernatants of transfected HuH-7 cells, which was transfected with a mixture of genomic construct (HBV L-) and helper construct (wt-L), or mutant L-protein expression construct.

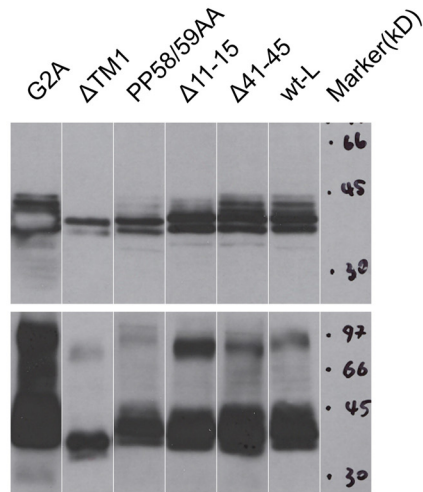
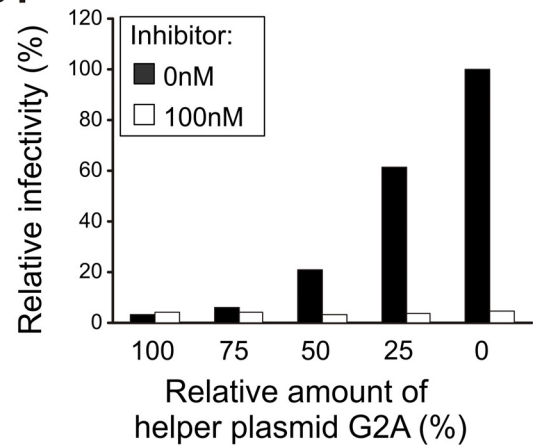
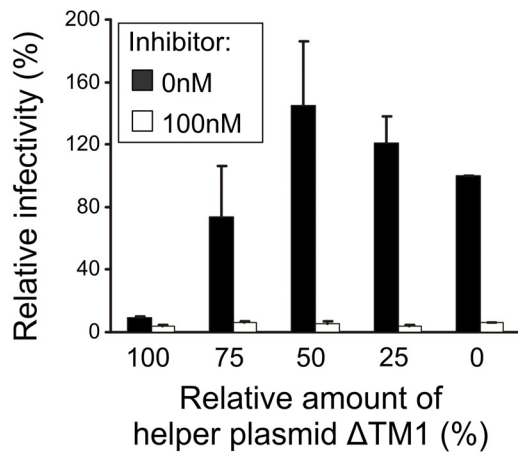
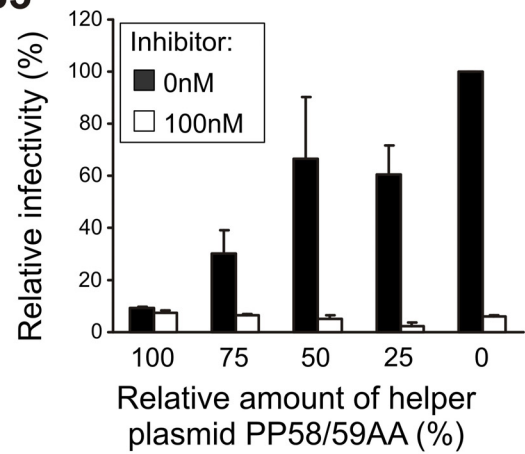
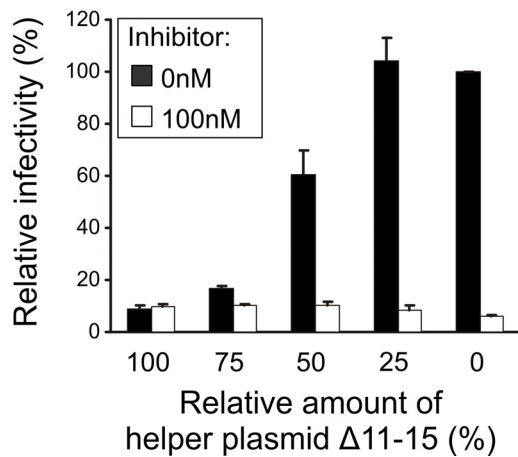
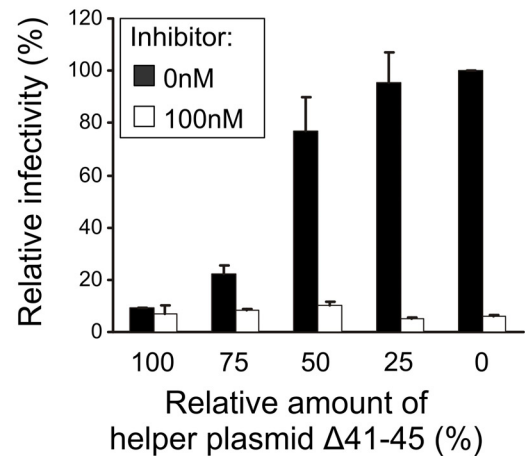
A**B1****B2****B3****B4****B5**

FIG. S3. Dominant negative effect of mutant L protein on virus infectivity was not observed.

A. Western blot of cellular extracts of HuH-7 cells 2 days post-transfection with the wild-type L expression constructs (wt-L), or mutant L protein devoid of myristoylation (G2A), with deleted putative fusion peptide (Δ TM1), with substituted prolines at aa 58-59 (PP58/59AA), with deletion in the essential binding site (Δ 11-15), or with deletion Δ 41-45. Markers with indicated molecular mass are shown in the right.

B1-5. Relative amount of HBsAg secreted from day 8-13 following infection of HepaRG cells by the virus bearing a mixture of wild-type and mutant L-proteins G2A (B1), Δ TM1 (B2), PP58/59AA (B3), Δ 11-15 (B4), Δ 41-45 (B5). For virus production, HuH-7 cells were transfected, in addition to genomic construct (HBV L₊), with a mixture of mutant helper constructs and wild-type helper construct at different ratio resulting in percentage of mutants from 100% to 0%. To test their sensitivity to the inhibitory peptide, virus inoculation was performed in the absence (black bars) or presence of 100 nM (white bars) HBVpreS/2-48^{myr}.

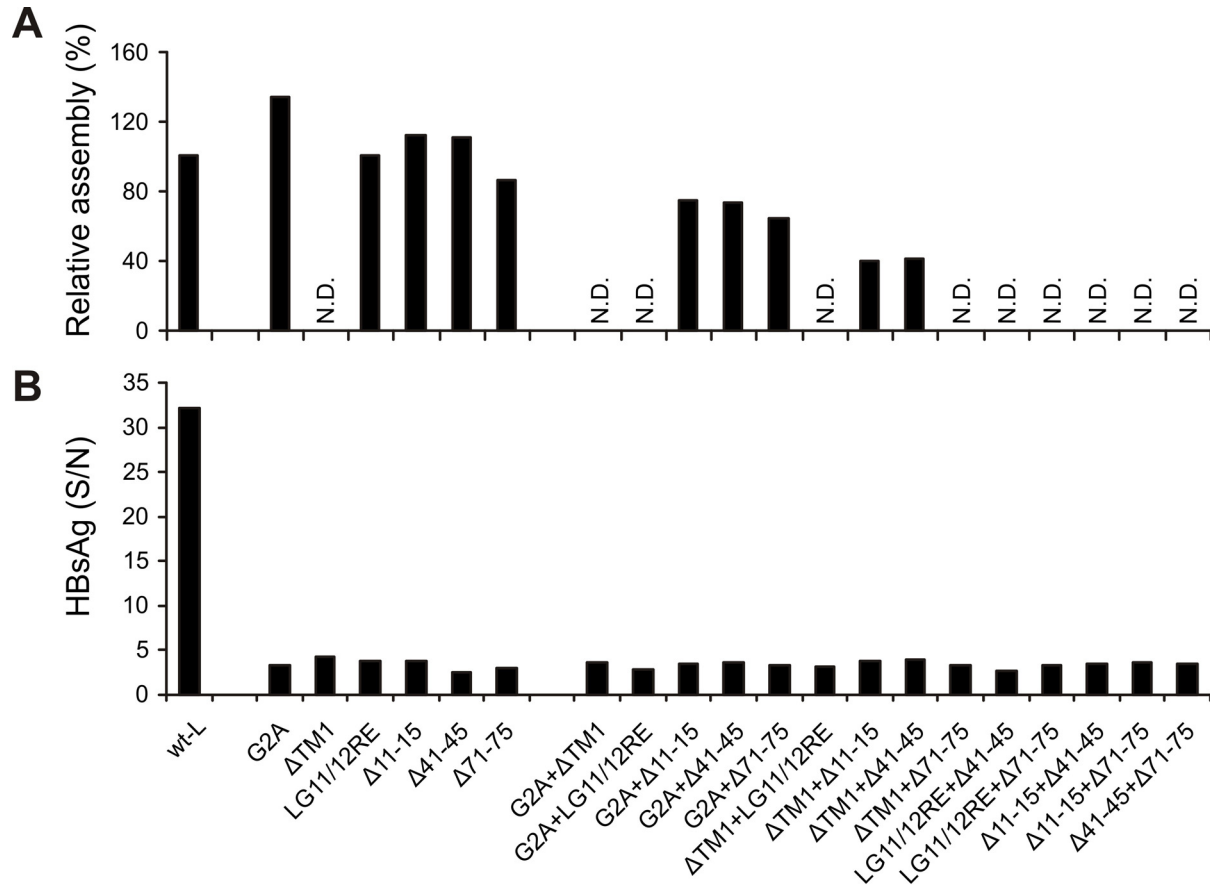


FIG. S4. Infectivity determinants in the same molecule of L protein can not be separated.

A. Mixture of two assembly-competent L-proteins still allows virus production. HuH-7 cells were transfected with a mixture of the genomic construct HBV L₊, and helper constructs expressing wide-type L-protein (wt-L), or helper construct expressing mutant L protein devoid of myristoylation (G2A), the deleted putative fusion peptide (Δ TM1), points mutation at aa 11-12 (LG11/12 RE), a deletion within the essential binding site (Δ 11-15), deletions Δ 41-45 and Δ 71-75, or an equal mixture of two mutant helper as indicated. HBV-DNA specific Dot-blot of fractions of an analytical CsCl density gradient was obtained from supernatants of HuH-7 cells and calculated for the relative assembly compared to wide-type L-protein. N.D., not determined.

B. Infection of HepaRG-cells using concentrated virus preparation obtained from co-transfected HuH-7 cells as described in (A). HBsAg secreted between days 7-11 post-infection was determined (black bars).

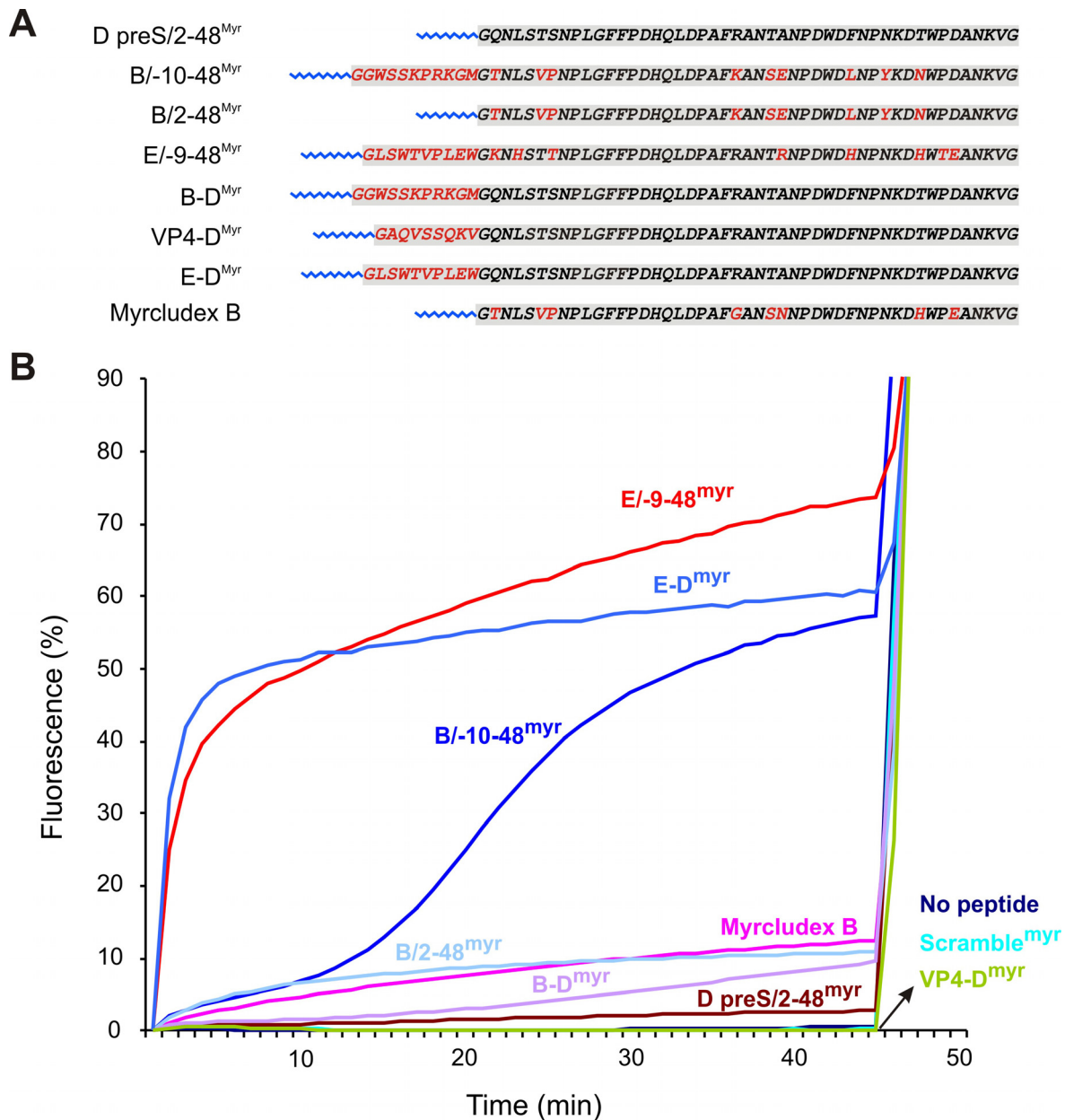


FIG. S5. lipid-leakage assay of wild-type and mutant peptides

A. Schematic illustration of the sequence of peptides used for the lipid-leakage assay. The letters in red indicate the amino acids that differ from the genotype D sequence. All the peptides are myristoylated (blue wave line) at the N-terminus.

B. 50 μ M of the various myristoylated peptides, a scrambled version of Myrcludex B (Scramble^{myr}), and a nonmyristoylated version of Myrcludex B (Myrcludex B Myr(-)), all dissolved in Buffer A (5% Glycerol, 50mM KCl, and 12.5mM HEPES, 50% DMSO), were added to ~12mM liposome containing fluorescence dye (HPTS/DPX). The leakage was assayed by Fluoroskan Ascent FL (Thermo). The results are expressed as the percent of total lipid leakage that occurred when dodecylmaltoside was added to the liposomes. The control (no peptide) represents buffer A alone.

Assurance of research

This thesis was written in the Department of Molecular Virology of the Hygienic Institute at the University of Heidelberg in the period of 08.06.2006 to 19.03.2010 under supervision of Prof. Dr. Stephan Urban.

I herewith declare that I wrote this PhD thesis independently under supervision and used no other sources and aids than those indicated.

Date

Signature

Curriculum Vitae

Yi Ni (倪翼)

Kastellweg 6

69120 Heidelberg

Phone: 06221-6520964

E-mail: yi.ni@med.uni-heidelberg.de

Research Experience:

Jan. 2006 – now

PhD Student

University of Heidelberg

Supervisor: *Prof. Stephan Urban*

- **To investigate the role of envelope proteins during HBV infection.**

Sept. 2003 – Sept. 2005

Product Specialist

Roche Diagnostics

- To take part in application and operation training related to PCR based technology in Roche Diagnostics
- To train internal colleagues, distributors and some key customers about quantitative and qualitative PCR principles and instruments

Feb. 2001 – July. 2003

Medical College of FUDAN UNIVERSITY

Supervisor: *Prof. Sidong Xiong*

- **Master Thesis:** Preparation and characterization of anti-HBV M protein monoclonal antibody by gene immunization
- Involved in the project “HER-2/neu-based Vaccines for Immune Contraception”
- To construct antibody repertoire targeting CDR by random mutagenesis PCR
- Express a chemokine (SDF-1) in yeast system

Aug. 1997 – Mar. 1998

XIAMEN UNIVERSITY

Supervisor: *Prof. Yueying Liu*

- **Bachelor Thesis:** Identify a bacterial strain HA-002 and determine its ability to deoxidize metal ion

Publication

- **Yi Ni**, Jessika Sonnabend, Stefan Seitz, Stephan Urban. The preS2-domain of the Hepatitis B Virus (HBV) is dispensable for infectivity but serves a spacer function for L-protein-connected virus assembly. *J. Virol.* 2010 Feb 3. [Epub ahead of print]
- Andreas Schulze, Alexa Schieck, **Yi Ni**, Walter Mier, and Stephan Urban. Fine mapping of the preS-sequence requirements for Hepatitis B Virus (HBV) large envelope protein mediated receptor interaction. *J. Virol.* 2010, 84(4): 1989
- Do-Hyoung Kim⁺, **Yi Ni**⁺, Si-Hyung Lee, Stephan Urban and Kyou-Hoon Han. An anti-viral peptide derived from the preS1 surface protein of hepatitis B virus. *BMB reports.* 2008, 41(9):640. ⁺*These authors contributed equally to this work.*

Acknowledgement

First of all, I would like to thank Prof. Stephan Urban, for giving me a great opportunity to work here, showing me how much fun I can make out of science.

There is a special thank to Stefan Seitz for his guidance in the beginning of my PhD life. He showed me the way to start a project, gave valuable technical support, and put great effort in reviewing my publications.

I have to thank Jessika Sonnabend for her work during her practical-time, which eventually contributes to finish the preS2 story.

I would also like to extend my gratitude to Christina Kaufman for the reviewing of my thesis and helpful suggestion.

Thank Steffi for translating the summary into German, and thank Dr. Stefan Mehrle for the reviewing of manuscript and the scientific discussions. Thanks to Andreas, Berit, Anja, Caro, Martina, and all former and present members of our lab for their help and friendship.

Thank Prof. Barbara Müller, Prof. Jürgen Kleinschmidt, Prof. Oliver Fackler and Prof. Ursula Klingmüller for reviewing my work and being in my PhD committee.

Thank Prof. Stefan Schaefer for kindly providing the constructs for different HBV genotypes.

During the experimental time, I was supported by the whole group of department of molecular virology at the Hygiene Institutes. I have to thank them all, especially Ralf Bartenschlager, and Volker Lohmann, for the discussions in the seminars and the friendly atmosphere inside the department.

For text corrections I also want to thank my friends, especially Weibin Liu and Yang Zhao.

Finally, I owe a very special thanks to my wife Jing Ni, for her constant support and checking my thesis word by word and I would like to thank my family in Germany and China. The life I spend in Heidelberg would have been absolutely impossible without their encouragement, provided by my mother, Meiyang Lin, father, Kongbao Ni, and my older brother Yan Ni.